Imperial College London

The preparation of new multimetallic materials and the functionalisation of nanoparticles with transition metal units

Saira Naeem

Imperial College London, Department of Chemistry, South Kensington.

A thesis submitted for the degree of Doctor of Philosophy and the Diploma of Imperial College London

Statement of Copyright

Declaration

I declare that the work described in this thesis was carried out in accordance with the regulations of Imperial College London. The work is my own except where indicated in the text and no part of the thesis was submitted previously for a degree at this, or any other university.

Abstract

A range of functionalised dithiocarbamates have been prepared and shown to successfully coordinate to a series of transition metal complexes which can then be used as a starting point for further chemistry. The potential to change the physical properties of these dithiocarbamate (DTC) complexes as a whole has been exploited through protonation of amine-terminated compounds. As well as rendering the complexes moderately soluble in water, the protonated terminal amine groups on the pendant arms can serve as protecting groups for acid-sensitive co-ligands from cleavage or unwanted reaction during transformations in the presence of acids.

An array of diallyl- and methylallyl-terminated DTC complexes have also been formed. The successful ring-closing metathesis of the diallyl units again demonstrates that the additional centre of reactivity on the pendent arms of the DTC ligand can be utilised, allowing further transformations to be carried out without affecting the rest of the complex. Furthermore, the methodology has been extended to nanoparticles where diallyl DTC units have been shown to stabilise the surface of gold nanoparticles.

The study was also expanded to include dithiocarboxylate ligands. Few dithiocarboxylate complexes are known in literature, thus a comparison with the analogous dithiocarbamate species is provided in this report. The first examples of gold(I) complexes of this class of ligand (derived from N-heterocyclic carbenes) have been prepared. The synthesis and characterisation of ruthenium-alkenyl complexes bearing this ligand have also been presented and evidence of a remarkable rearrangement caused by their steric effect has been demonstrated. In addition, it has been shown that imidazolium-2-dithiocarboxylate betaines can be used to form monolayers on the surface of gold nanoparticles.

The synthesis and characterisation of the first ruthenium vinyl complexes bearing the related dialkyldithiophosphate ligand, $[S_2P(OR)_2]^-$ are reported here. The resulting compounds demonstrate reactivity which differs significantly from that displayed by the analogous dithiocarbamate and xanthate compounds.

Following on from the successful investigations of 1,1-dithio ligands, the scope of these explorations was broadened to explore non-sulphur based linkers. These were employed to prepare multimetallic compounds through the inherent affinity of certain donor combinations for particular metals. Isonicotinic acid was employed to link different metal units to generate heteronuclear bi- and trimetallic systems based on careful consideration of their donor properties towards various transition metals (Ru, Rh, Pd, Pt, Ag and Au). In most cases, the first metal was shown to preferentially bind to the carboxylate moiety, and then the nitrogen of the pyridine ring was used in attempts to coordinate further metals. The synthesis of pentametallic complexes using the isonicotinic ligand (based on a rhodium core) is also presented, including the successful coordination of ruthenium metal units to the carboxylate moiety. The design was extended to explore the palladated tetraphenylporphyrin, [(Pd-

TPP)(*p*-$CO_2H)_4$], which illustrated that not only can these metallo-porphyrins be used as a scaffold for the addition of peripheral metal units, but also that further functional group transformations can be carried out on the terminal units.

Lastly, having explored the utility of these nitrogen-oxygen mixed-donor ligands in the formation of multimetallic compounds, this approach was extended to the surface functionalisation of silver nanoparticles. The nitrogen donor groups of these ligands were shown to readily bind to the surface of silver colloids, allowing the straightforward attachment of metal units to the surface of these materials.

بِسْمِ اللَّهِ الرَّحْمَٰنِ الرَّحِيمِ

(In the Name of God, The Most Beneficent, The Most Merciful)

Acknowledgements

First and above all, I thank Almighty God. It is only by His grace and bounty I am able to complete this thesis: *He gives you of all that you ask Him; and if you reckon the bounties of God, you can never count them*… (Quran: 14:34).

I owe sincere and earnest thanks to my supervisor, Dr. James Wilton-Ely, who gave me the opportunity to carry out this PhD. Throughout my time of research and writing of this thesis, if it was not for his guidance, encouragement and support, I would never have been able to reach the finishing line! Words can not express my gratitude.

I would like to thank the JWE group, both past and present, for providing such enjoyable and memorable times in the lab. In particular I would like to thank Ellie Ogilvie, Payel Patel and Angela Ribes for their help with the work on dithiocarbamate, dialkyldithiophosphate and mixed-donor ligand chemistry, respectively. I have been very fortunate to have worked with such enthusiastic and hardworking people who made all those publications possible!

I wish to express my sincere thanks to the following people, whose input in this research have made it possible to produce this thesis:
Dr. Graeme Hogarth (University College London): collaboration on dithiocarbamate chemistry.
Prof. Lionel Delaude (University of Liège): collaboration on dithiocarboxylate chemistry.
Dr. Steve Firth (University College London): TEM images.
Dr. Mahmoud Ardakani, (Imperial Collge): TEM/EDX.
Dr. Andrew White (Imperial College): Crystallography.
Dr. Peter Haycock and Dr. Dick Shepherd (Imperial College): NMR spectroscopy.
Prof. Andrea Sella (University College London): assistance with molecular mass determinations.
Dr. Katherine Holt and Muhammed Haque (University College London): CV experiments.

I thank EPSRC for funding this research project and gratefully acknowledge the support and facilities provided by the Department of Chemistry, Imperial College London.

Thanks to all my friends who have been steadfast in their support: Noor Din, Niraku Ahmad, Helna Patel, Fatma Dogan, Sara Ferdousi, Hanan Kamel and Rasha Osman - listening patiently when I spoke about my research, trying their best to sound interested!

Finally, I wish to extend my warmest thanks to my family, especially to my parents for their continual support, understanding and words of encouragement throughout my PhD and for their invaluable prayers.

Publications

- **The functionalisation of ruthenium(II) and osmium(II) alkenyl complexes with amine- and alkoxy-terminated dithiocarbamates.**
  S. Naeem, E. Ogilvie, A. J. P. White, G. Hogarth and J. D. E. T. Wilton-Ely, *Dalton Trans.*, 2010, **39**, 4080-4089.

- **Multifunctional dithiocarbamates: Synthesis and ring-closing metathesis of diallyldithiocarbamate complexes.**
  S. Naeem, A. J. P. White, G. Hogarth and J. D. E. T. Wilton-Ely, *Organometallics*, 2010, **29**, 2547-2556.

- **Non-innocent behaviour of dithiocarboxylate ligands based on N-heterocyclic carbenes.**
  S. Naeem, A. L. Thompson, L. Delaude and J. D. E. T. Wilton-Ely, *Chem. Eur. J.*, 2010, **16**, 10971-10974.

- **The use of imidazolium-2-dithiocarboxylates in the formation of gold(I) complexes and gold nanoparticles.**
  S. Naeem, L. Delaude, A. J. P. White and J. D. E. T. Wilton-Ely, *Inorg. Chem.*, 2010, **49**, 1784-1793.

- **Dithiocarboxylate complexes of ruthenium(II) and osmium(II).**
  S. Naeem, A. L. Thompson, A. J. P. White, L. Delaude and J. D. E. T. Wilton-Ely, *Dalton Trans.*, 2011, **40**, 3737-3747.

- **Synthesis and reactivity of dialkyldithiophosphate complexes of ruthenium(II).**
  P. Patel, S. Naeem, A. J. P. White and J. D. E. T. Wilton-Ely, *RSC Adv.*, 2012, **2**, 999-1008.

Table of Contents

Chapter 1: Introduction

1. Chapter 1: Introduction

1.1. Multimetallic complexes based on 1,1-dithio ligands

1.1.1. Dithiocarbamates

Dithiocarbamates (DTCs) have been widely used for over a century as chelating ligands in coordination chemistry as the sulphur lone pairs show a great affinity for metal centres and thereby form complexes with them.[1, 2]

Preparation of the DTC ligand involves the rapid reaction of secondary amines with carbon disulphide (CS_2), often in the presence of a base (e.g. potassium hydroxide). Since free DTCs can be somewhat unstable in their acidic form (dithiocarbamic acid), they are usually prepared as metal salts under strongly basic conditions. Reactions are carried out in water, methanol or ethanol and typically at room temperature (*Fig. 1*).

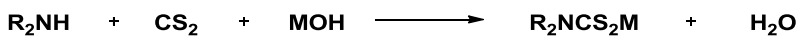

Figure 1.

Although primary and secondary amines can both be used to prepare DTCs, significant differences in their reactivities and product stabilities are observed. DTCs generated from primary amines are generally less stable than their secondary amine counterparts, and can decompose to give the corresponding isothiocyanate (*Fig. 2*).

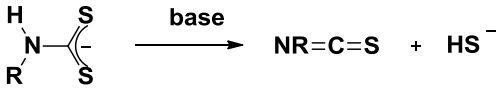

Figure 2.

The huge interest in DTC ligands can partly be attributed to the ability of this ligand class to stabilise varied oxidation states. This property can be traced to the contribution of the resonance forms of the DTC ligand; whereby the dithiocarbamate and thioureide versions stabilise low and high oxidation state metals respectively. In the latter form, the nitrogen carries a positive charge and both sulphur atoms carry a negative charge. This allows the ligand to complex strongly to metals in high oxidation states (*Fig. 3*). This can also explain why, in comparison, xanthates[3] are not as good at stabilising high oxidation state metals, as a positive charge on the electronegative oxygen would be

unfavourable. A further characteristic of DTC ligands is the multiple bond nature the thioureide form confers on the nitrogen-carbon bond, resulting in restricted rotation.

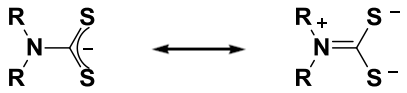

Figure 3. Resonance forms of the dithiocarbamate ligand

Additionally, the above resonance forms can also explain why DTCs can act as strong- and weak- field ligands. If the dithiocarbamate resonance dominates, then the ligand shows strong-field characteristics, whereas, if the thioureide contribution is more significant, then weak-field ligand behaviour results.[1]

Numerous binding modes of DTCs have been observed with transition metals (*Fig. 4*), however the most common of these is the simple chelating mode (**A**), which is found with most transition metals. Here, the two metal-sulphur interactions are roughly equal and the ligand can be considered as a net three-electron donor.

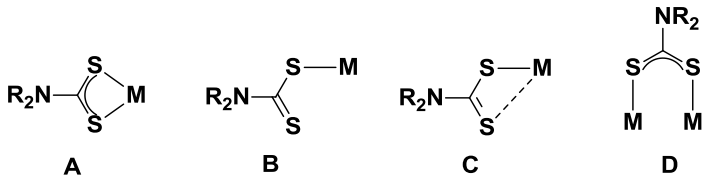

Figure 4. Binding modes of DTCs

DTCs also adopt a monodentate binding mode (**B**). In cases where the co-ligands are sterically bulky, their spatial demands force monodentate coordination of the DTC ligand. Crystallographic evidence has shown that this mode of binding is commonly seen in gold DTC complexes, though this is rarely a steric consequence, but rather due to the preferred linear coordination in Au(I).[4]

An intermediate situation, when the binding of the DTC ligand to the metal centre is highly asymmetric, is termed *anisobidentate* (**C**). This mode is relatively common at gold and mercury centres that favour a linear two-coordinate geometry.[5]

Dithiocarbamates can also bridge two metal atoms via mode **D**. Each sulphur atom binds to a single metal centre in a μ^2 fashion. This mode of bonding is seen in gold(I) and gold(III) centres.[6]

Due to their properties, DTCs and their transition metal complexes have found considerable use in the analysis of metals.[7] They have also been employed in the separation of different metal ions

by high-performance liquid chromatography (HPLC)[8, 9] and capillary gas chromatography (GC).[10, 11] In addition, they have found use as rubber vulcanization accelerators[12], fungicides[13] and pesticides.[14] For a ligand class which has existed for over 150 years, relatively few applications have been unearthed. However one recent application for which dithiocarbamate complexes are currently being researched, is in the field of medicine as anti-cancer drugs. Gold(III) DTC derivatives have proved to be promising candidates for the treatment of cancer, revealing greater cytotoxic behaviour towards human tumour cell lines than the well-known cisplatin complex.[15]

Even though a plethora of DTC ligands and their complexes are known, the potential of the NR_2 substituents has often not been fully exploited. Early studies of DTC transition metal complexes revealed insoluble behaviour in an aqueous medium. Work by Jones *et al* addressed this problem and demonstrated the water solubility of DTC metal complexes with polar end groups (such as hydroxy and carboxy functional groups) on the DTC ligands. Since this early work on water solubility, little further development has been attempted.[16]

The first example of a transition metal complexed by a DTC was related by Delépine in a report in which he prepared a range of aliphatic DTCs.[17] Since then, examples of all d-block metals have been prepared and their electrochemical and structural properties investigated.[18]

Systems in which several metal centres are incorporated into the framework allow the properties of the different metal centres to be exploited within the same system. Some fascinating work on the development of multidentate DTC ligands for the synthesis of multimetallic arrays of this type has been reported.[19] The stepwise construction of these arrays was achieved by extending one end of a diamine selectively upon reaction with CS_2, and complexing this with a transition metal. The new compound was then able to react again with base and CS_2 before complexing a further transition metal, resulting in hetero- and homo-multimetallic compounds (*Fig. 5*).

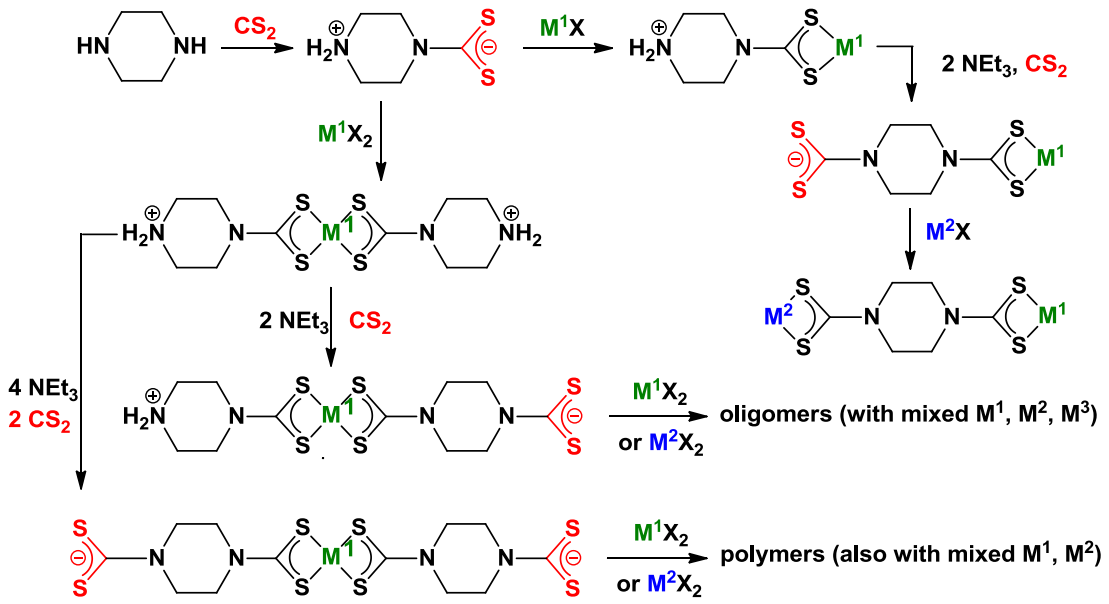

Figure 5. Multimetallic assemblies based on piperazine.[19]

An example is shown below (*Fig. 6*), in which the bis(dithiocarbamate) ligand bridges two different metal centres. The first metal was introduced before the second dithiocarbamate donor had been generated, as shown in *Figure 5*.[20]

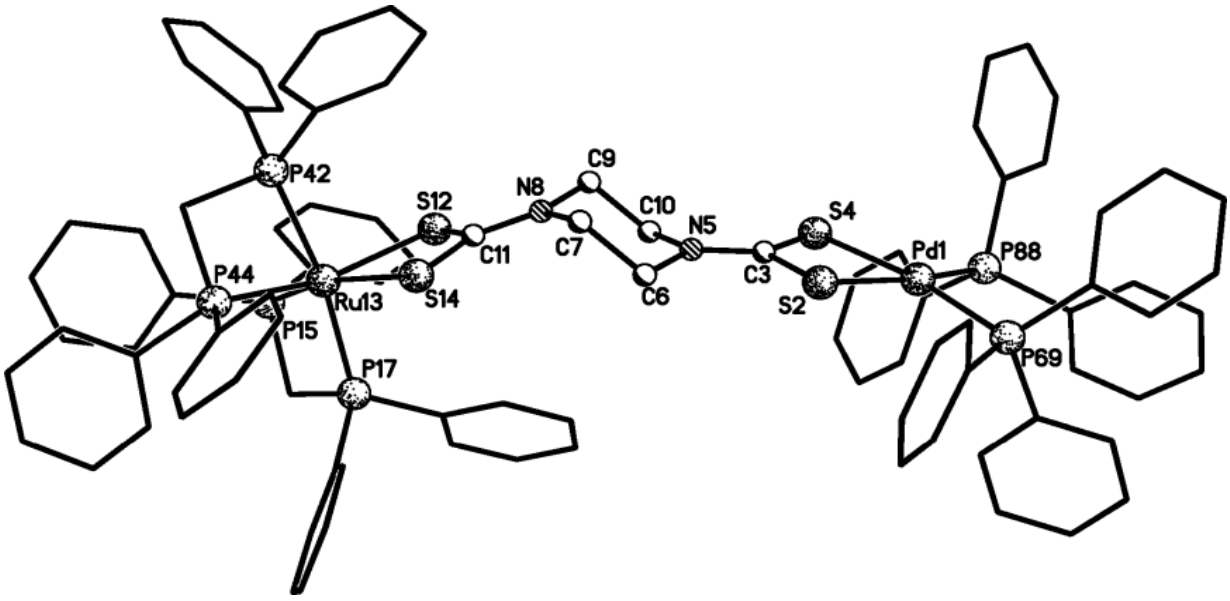

Figure 6. Heterobimetallic complex of ruthenium and palladium.[20]

A further example in which multi-functionalised DTC ligands have been exploited in this area of metal-directed self-assembly, is in the development of novel supramolecular architectures. Beer has reported the synthesis of a range of macrocyclic and macrobicyclic complexes of varying dimensions.[21] These structures were formed by the coordination of transition metals with an appropriate bis-DTC salt (*Fig. 7*). The resultant dinuclear macrocycle can bind organic and inorganic guest species, and the internal dimensions of the cyclic complex can be tuned by varying the spacer group to accommodate the host. The authors also report the construction of a range of interlocked catenane structures which can be prepared easily due to the labile nature of the metal sulphur bonds.

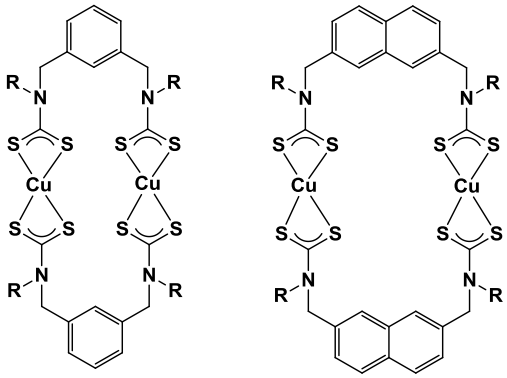

Figure 7. Examples of macrocyclic complexes with differing cavity dimensions.[21]

1.1.2. Dithiocarboxylates

Dithiocarboxylate metal complexes (L_nMS_2CR, where R is a carbon-based substituent) are less well known in the literature than DTC complexes and those with xanthate ligands (*Fig. 8*).[1-3] Relatively few examples are known and this can perhaps be explained due to the more demanding synthesis of the ligand, compared to addition of an amine or alkoxide to carbon disulphide.

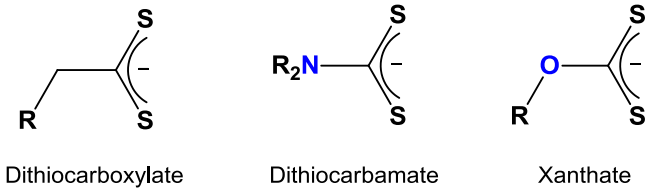

Figure 8.

N-heterocyclic carbenes (NHCs, *Fig. 9*, **A**), have attracted great interest and have been investigated extensively since their isolation in 1991.[22] These divalent carbon ligands are excellent alternatives to phosphines and their derivatives have been widely used in catalysis as they offer a number of valuable attributes suited to catalysis. In addition to its lack of lability, the electronic and steric properties of the NHC can be tuned by simply changing the substituents on the heterocycle and, as a result, a range of tailored catalysts can be produced. A well-known example of the role played by NHCs as ancillary ligands is provided by the second-generation Grubbs' alkene metathesis catalyst, $[Ru(=CHPh)(NHC)Cl_2(PCy_3)]$ (**B**).[23, 24]

Since NHC ligands exhibit remarkable electron-donating properties, they form strong sigma bonds to metal centres. They have been shown to successfully complex not only to ruthenium, but also to other transitions metals, such as gold (**C**).[25]

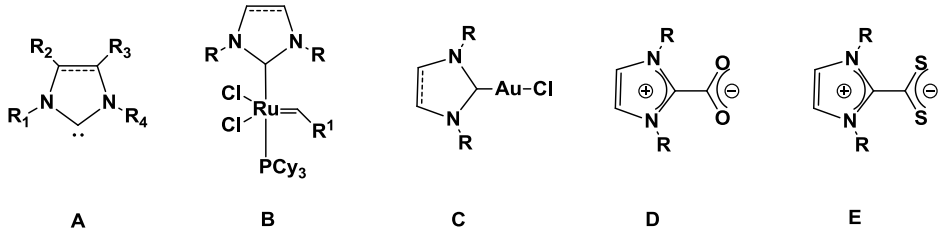

Figure 9.

In a more recent development in the field, it was shown that NHCs react with carbon dioxide to generate zwitterions (**D**) which could subsequently be used to introduce NHCs to metal centres for use in catalysis without the need to generate the free carbene. These zwitterionic NHC•CO_2 adducts can easily be stored and manipulated unlike the oxygen and moisture-sensitive free carbene species.[26]

Recently this strategy has been expanded to include adducts of NHCs with CS_2, giving rise to zwitterionic imidazolium-2-dithiocarboxylate betaines, (**E**). These NHC•CS_2 zwitterions have the potential to act as good donors for transition metals. In contrast to their carboxylate analogues, they do not eliminate carbon disulphide upon reaction with the metals. Furthermore, they are more thermally stable in the solid state and less labile in solution than their carboxylate analogues.[27]

Delaude *et al* carried out preliminary investigations on the coordination behaviour of NHC•CS_2 with ruthenium compounds and examples of these complexes were published recently in 2009.[27, 28] Only one example of NHC•CS_2 complexation with gold(III) has been reported (poorly characterised),[29] but no examples with gold(I) centres.

1.1.3. Dialkyldithiophosphates

Another related member of the 1,1-dithio family, is the dialkyldithiophosphate ligand class.[30-32] These compounds are related to dithiophosphinates[33, 34] (*Fig. 10*) and differ from the other 1,1-dithio ligands discussed here by the presence of a PS_2 moiety rather than a CS_2 unit. A number of metal complexes of this ligand class have been reported.[35]

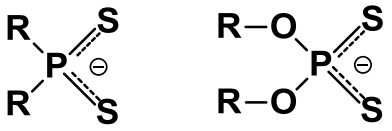

Figure 10. Members of the 1,1-dithio ligand family bearing the PS_2 moiety: dithiophosphinate (left) and dithiophosphate (right)

A key feature of these ligands is that the substituents which give rise to the steric profile of the ligand, are attached directly to the PS_2 unit (c.f. $R_2NCS_2^-$ or $ROCS_2^-$). Since many applications of donor chelates benefit from or require the use of sterically demanding substituents, this attribute differentiates dialkyldithiophosphates from dithiocarbamates or xanthates. It is well known that bulky ligands can be used to control the steric profile of a metal centre and can therefore influence the selectivity of metal catalysts; they can be used to prevent the binding of additional ligands to metal centres (i.e. bulky ligands can be employed to form steric protection); bulky ligands can also be used to stabilise reactive intermediates (stabilisation of unusual coordination numbers, geometries) etc.

The applications associated with the dialkyldithiophosphate ligand, $[S_2P(OR)_2]$, are significant in the literature. They have found use as antioxidants (zinc dialkyldithiophosphates, ZDDP) and oil additives.[36] As with dithiocarbamates, early reports highlight their use as analytical reagents[37] and chelates for extraction.[38-40] Ruthenium compounds containing dialkyldithiophosphate units (including other 1,1-dithio ligands) have recently been investigated in a medical setting as nitric oxide scavengers and to modulate metalloproteinase activity.[41]

The coordination chemistry of dialkyldithiophosphate ligands has been explored intermittently and a few examples of metal complexes are known. Ruthenium dialkyldithiophosphate complexes in various oxidation states have been reported, including a Ru(0) example.[42] Since dialkyldithiophosphates are 'soft' donors, they are expected to stabilise lower oxidation states to a greater extent; hence most examples are of divalent ruthenium.[30-32, 43] Ru(III) compounds have also been reported[44], including homoleptic examples, $[Ru\{S_2P(OR)_2\}_3]$.[45] Only in 2007 did Leong and Goh describe tetravalent ruthenium compounds bearing the dialkyldithiophosphate ligand for the first time.[46]

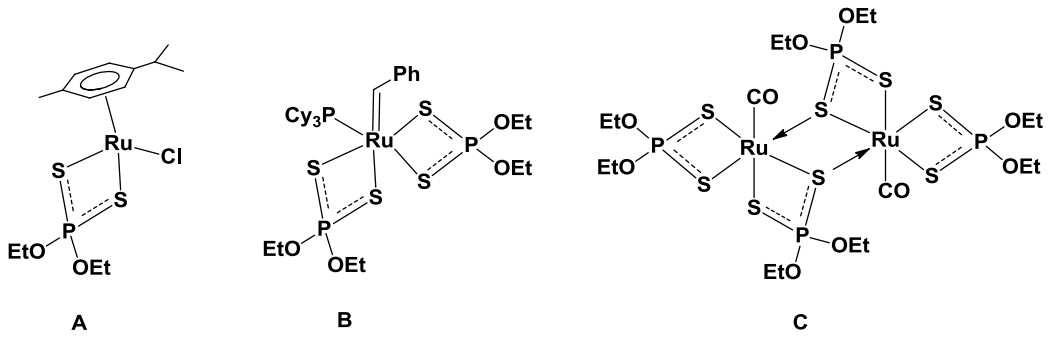

Figure 11. Examples of ruthenium dialkyldithiophosphate compounds.

A few organometallic complexes have also been reported and *Figure 11* (**A** and **B**) illustrates some representative ruthenium examples. The first complex, $[RuCl\{\kappa^2\text{-}S_2P(OEt)_2\}(\eta^6\text{-}p\text{-cymene})]$ (**A**), was obtained by addition of $NH_4[S_2P(OEt)_2]$ to the dimer, $[RuCl_2(\eta^6\text{-}p\text{-cymene})]_2$,[30] while the second (**B**) is derived from the reaction of the Grubbs' metathesis catalyst, $[Ru(=CHPh)Cl_2(PCy_3)_2]$ with two equivalents of $KS_2P(OEt)_2$.[31] The third complex (**C**), isolated by Hogarth and Deeming[47], demonstrates a bridging mode for the dialkoxydithiophosphate ligand. The crystal structure of the dinuclear ruthenium complex reveals a *cis* disposition of the dithiophosphate units and this can be compared to the analogous dithiocarbamate dimer, which adopts a *trans* arrangement of the ligands (*Fig. 12*). The difference in the geometrical orientations of the 1,1-dithio ligands is most probably steric in nature.

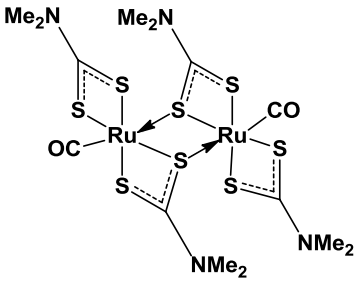

Figure 12. The dinuclear ruthenium dithiocarbamate dimer adopting a *trans* disposition.

1.2. Gold Nanoparticles and surface functionalisation with sulphur units

1.2.1. Historical perspective

Gold nanoparticles (NPs) are key building blocks in the field of nanotechnology in the 21st century. However the interest in gold colloids can be traced as far back as the ancient Egyptians who believed these materials to have curative powers.[49] Colloidal gold was used by the Romans towards the Middle Ages for decorative purposes in colouring ceramics and for staining glass. One of the most well-known examples is the Lycurgus Cup, made in 4th century AD, which contains gold colloids, causing the cup to change colour from green, in reflected light, to ruby red in transmitted light (*Fig. 13*).

Figure 13. The Lycurgus Cup: The opaque green cup turns to a glowing translucent red when light is shone through it.[48]

Gold colloids found many uses in medicine until the Middle Ages. They were used for treatment of various diseases such as heart and venereal problems, epilepsy and tumours. They were also used to diagnose syphilis. This test was used up until the 20th century when its reliability was questioned and the method was eventually abandoned![50]

It was not until the mid-19th century that serious study on gold colloids was started by Michael Faraday.[51] He determined the presence of these colloids when he noticed the formation of deep-red solutions of colloidal gold when aqueous tetrachloroaurate ($AuCl_4^-$) was reduced using phosphorus in CS_2. Faraday investigated these gold colloids further and provided the first description, in scientific terms, of their optical properties. He observed the reversible colour changes of gold colloidal films upon mechanical compression (from blue/purple to green upon compression).[52]

1.2.2. Modern Uses

The most popular method of synthesising gold nanoparticles is by that reported by Turkevitch *et al* involving the citrate reduction of $HAuCl_4$ in water, which gives NPs of 20 nm in size.[53] Later, attempts to control the size of the NPs led to a method in which the ratio between the trisodium citrate and gold was varied.[54] This was used as a precursor to more versatile NPs, since the weakly bound citrate shell around the gold colloid could easily be displaced with other ligands. A recent example in which this method has been employed is the preparation of sodium 3-mercaptopropionate-stabilized gold NPs.[55] Here, the simultaneous addition of the citrate salt and the mercaptopropionate ligand results in formation of the more stabilised mercaptopropionate passivated NP. The size of the particle can be controlled by varying the ligand/gold ratio (*Fig. 14*).

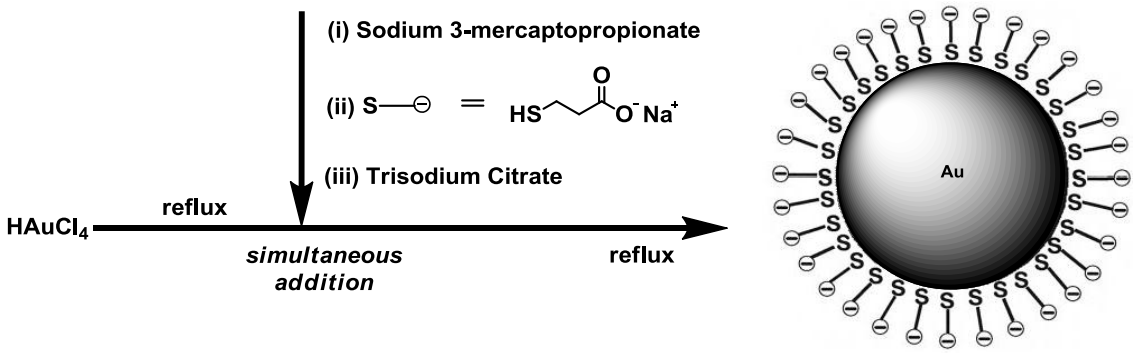

Figure 14. Preparation procedure of anionic mecapto-ligand-stabilised gold NPs in water.[55]

The functionalisation of gold surfaces with sulphur-based organic ligands is an area of research which has led to great interest in the fields of surface science and nanomaterials chemistry. Pioneering work by Ulman[56] on the preparation and investigation of two-dimensional self-assembled monolayers (SAMs) led to the exploration of three-dimensional SAMs, comprising of thiol encapsulated gold NPs.[49]

The first examples of gold NPs passivated with alkanethiols of varying chain lengths, were reported by Mulvaney and Giersig in the mid 1990s.[57] Shortly afterwards, the Brust-Schiffrin method for gold NP synthesis was introduced.[58] This one-pot method was far simpler and produced thermally and air-stable NPs of reduced dispersity with good control over the size of the particles. The great advantage of these NPs was that they could easily be handled and characterised in the same way as organic compounds. Furthermore, the NPs could also be stored in air for several months at room temperature without any adverse effects.

The two-phase synthesis of this technique was similar to that of Faraday's method and exploited the strong binding ability of the thiol unit to the gold through the soft nature of both gold and sulphur atoms. Tetraoctylammonium bromide (TOAB) was used as the phase-transfer reagent to transfer $AuCl_4^-$ into toluene. Next, $AuCl_4^-$ was reduced by sodium borohydride ($NaBH_4$) in the presence of the thiol. An instant colour change of the organic phase, from orange to deep brown, was observed upon addition of the reducing agent, indicating the formation of gold colloids (*Fig. 15*).

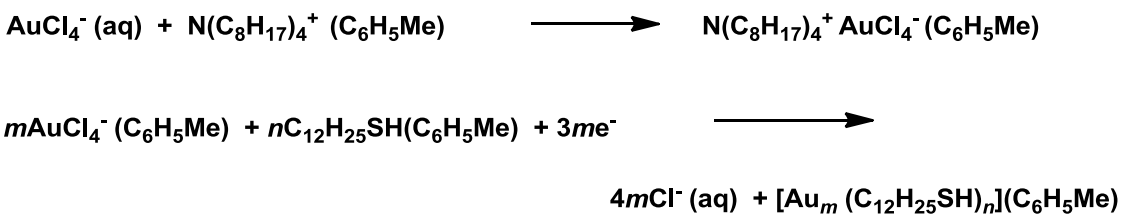

Figure 15. Reduction of Au(III) to Au(0).[58]

It was reported that the thiol:gold ratio controlled the size of the gold NPs with larger thiol to gold mole ratios giving smaller gold core sizes. For example, a 1:6 ratio led to an average NP diameter of 5.2 nm while diameter of around 3 nm are obtained using a 1:2 ratio. Further investigation revealed the fast addition of the reducing agent and cooled solutions produced smaller, more monodisperse particles.

Brust and co-workers then expanded this synthetic route and demonstrated the stabilisation of gold NPs by tethering the bifunctional thiol unit, *p*-mercaptophenol, to the colloid in a single-phase system.[59] A variety of other functionalised thiol surface units were also introduced to demonstrate that they too could be used to stabilise gold NPs. Using this approach, it was shown that it was possible to synthesise NP lattices by attaching NPs to one another via the functionalities tethered on their outer shell, building linked multi-dimensional structures.[60]

Mixed-monolayer systems greatly enhance the versatility of NPs, allowing multiple functionalities to be appended onto the outer layer. Murray *et al* demonstrated the controlled exchange of thiols using a range of functionalised thiol units in a stepwise fashion.[61] These thiol-exchange materials can then undergo further reactions.[62] (*Fig. 16*).

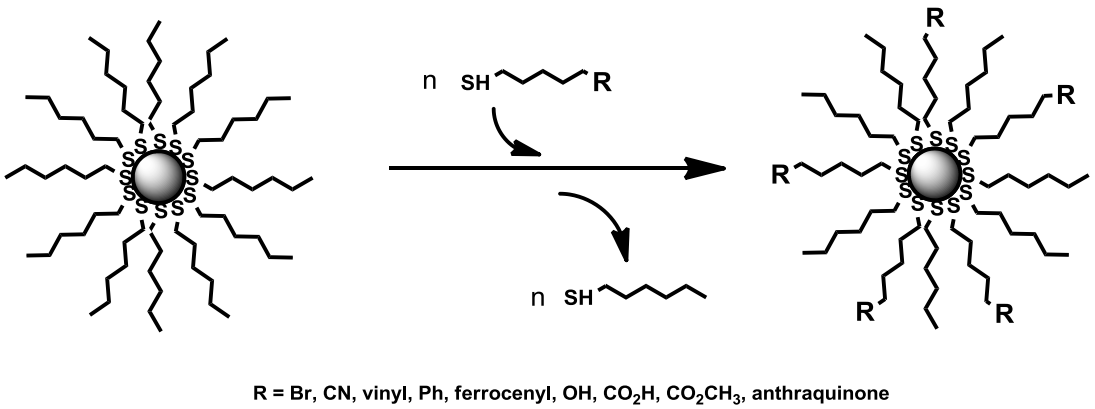

Figure 16. Scheme for the thiol-exchange reaction between alkanethiols and various other functionalised thiols.[49]

1.2.2.1. Functionalisation of the gold surface using metal units

A growing field in which thiols have been heavily utilised is in the functionalisation of gold nanoparticles with metal units. Transition metals have been placed on the outer surface of NPs in order to tailor the properties of the surfaces towards specific applications. This has attracted attention from researchers working on a wide range of applications such as nanoelectronics[63], sensors[64], catalysis[65] and biomedicine.[66]

Catalysis

Nanoparticles passivated with metal units offer many attractive properties which make them highly suitable as catalysts. For example, the catalyst nanoparticles can easily be separated from the organic products using simple techniques such as precipitation or filtration and then be re-used. Also, since the chemisorbed layer of thiols is relatively well-ordered, the environment and density of the surface can easily be modified, making these NPs highly versatile. These species involve relatively simple synthetic preparation and characterisation, which can be contrasted to other methods of immobilisation. An early report of a catalytic gold NP with tethered metal complexes, was that of thiols with ruthenium dimer complexes passivating the surface of the nanoparticle. This catalyst was successfully employed to explore the ring-opening metathesis polymerization of norbornene (*Fig. 17*).[65]

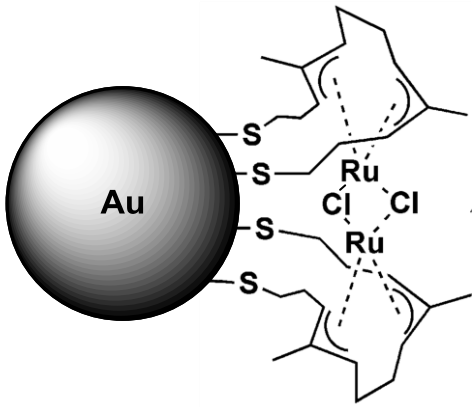

Figure 17. A chloro-bridged ruthenium dimer immobilised on the surface of a AuNP. [65]

Another more recent example is that of a gold NP with a mixed surface of polar or apolar groups surrounding the embedded metal NP.[67] This catalyst was used to hydrogenate methyl α-acetamidocinnamate enantioselectively. The topographic surface was found to direct the reaction selectivity and the apolar end groups gave better reaction conversions than their polar counterparts. Furthermore, it was suggested by the authors that this idea could be expanded and "pockets" could be created around the NP in which catalysis could be performed on selectively orientated substrates – imitating enzymatic action. This could be achieved by constructing a mixed surface of varying alkanethiol chain lengths and surrounding the shorter chain lengths with the catalytic metal units and attaching the longer chain lengths to the gold surface, resulting in the formation of the pockets (*Fig.18*).

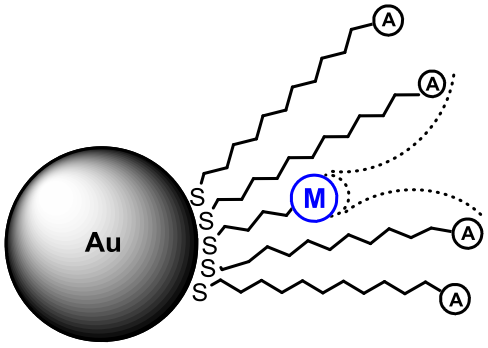

Figure 18. Formation of 'pockets', creating a specific binding site for the substrate.

Sensors

Functionalised NPs exhibit many attributes which make them ideal candidates for use in the design of sensing systems. Properties such as their large surface area and immobilisation of active surface sites can be utilized in this area of study. Another great advantage is the pre-organisation of the surface units which all point outwards. Much work is being done on the design and synthesis of receptors which can selectively recognise and sense anionic guest species. Methods are being developed whereby redox-active anion receptors or specific molecular recognition elements can be incorporated into NP systems to form highly selective sensors. Astruc and co-workers were the first to implement this idea by introducing ferrocene units on the surface of gold NPs using the Brust-Schiffrin method.[64] Since ferrocene moieties possess exceptional redox properties, the selective recognition and binding of oxo anions to them could be sensed electrochemically. The Astruc group extended these studies and synthesized, through partial exchange reactions, a series of gold nanoparticles with different concentrations of amidoferrocene units (of variable chain lengths) upon a dodecane thiol covered surface (*Fig. 19*).[68]

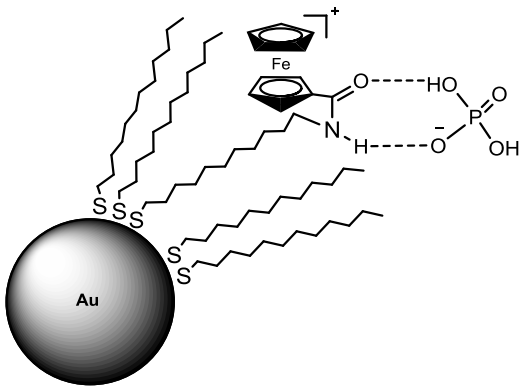

Figure 19. Complexation of amido ferrocene on a gold NP surface and binding of the anion to the ferrocene moiety.

Cyclic voltammetry experiments were performed on the NPs to study their electrochemical properties. It was found that the voltammetric wave due to the electrochemical oxidation of the ferrocene units was superseded by a second wave (at less positive potential) on addition of the $H_2PO_4^-$ anion. Saturation of all of the ferrocene units with the anion eventually led to complete disappearance of the original ferrocene oxidation wave. The strong binding of the anion with the ferrocene moiety can be explained by the additional hydrogen-bonding involved between the $H_2PO_4^-$ anion and the amido groups adjacent to the ferrocene. The substitution of one of the ferrocene rings with C_5Me_5 unsurprisingly inhibited this behaviour as no hydrogen bonding between the oxoanion and amido group was present.

Metalloporphyrins have also recently been investigated in this area of study. Recently Beer and Davis demonstrated that redox-active zinc metalloporphyrins behave as anion receptors and complex strongly to $H_2PO_4^-$ and Cl^-.[69] Thiolate coated gold NPs were modified to possess dithiol tethers. The anions were found to bind through the Lewis acid zinc centre and hydrogen bonding to the amide component (*Fig. 20*). It was noted that enhanced binding affinities towards anions were observed when the metal units were placed on the gold nanoparticle surface in contrast to the free metalloporphyrins.

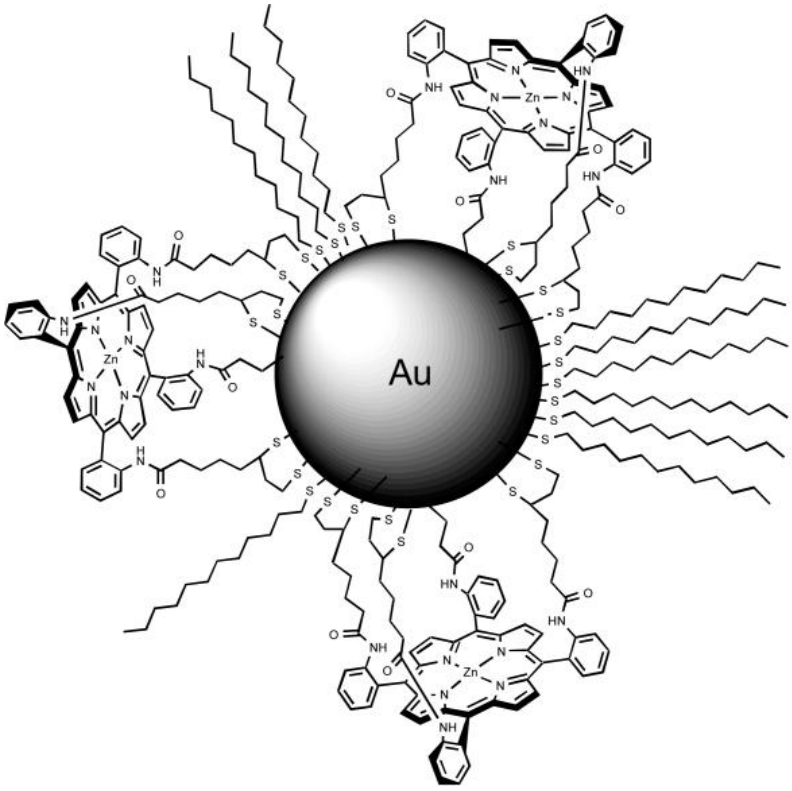

Figure 20. Partial exchange of alkanethiols with metalloporphyrin thiol ligands on a gold NP surface.[69]

Pyridine-based ligands, such as terpyridyl ligands with thiol end groups, have been attached to gold nanoparticles.[70] The nitrogen donors allow the facile coordination of metals to these ligands. An example of divalent ruthenium coordinated to the surface of gold colloids through these polydentate ligands (and thiol units) has been prepared and its behaviour probed.

Lanthanoid metals have also been employed to functionalise gold NPs to produce phosphorescent colloids which can be used in sensing applications.[71] Eu (III)/Tb(III) ions were complexed to 2,2'-dipyridine units attached to the surface of gold NPs by thiols. Their luminescence properties were studied and they were shown to form phosphorescent nanomaterials with no effect on their luminescence behaviour (i.e. emission time).

Certain biological functions require a balance in the concentration of various metal ions such as Ca^{2+} and Mg^{2+} (for example, Ca^{2+} regulates the contraction of cardiac and smooth muscles), however, their determination in complex biological systems is quite difficult because they are present in specific locations with a concentration gradient (calcium channels). The gold NPs bearing lanthanide complexes described above, have been shown to permit easy substitution with alkaline earth metal ions such as Ca^{2+}, resulting in an immediate decrease in the luminescence observed

though no change was detected upon addition of Na^+ and K^+ ions. Thus, these NPs are ideal as high-affinity sensors for the detection of biologically important cations in specific sites, and have opened up the scope to understand the properties and functions of various biological processes.

Functionalisation of nanoparticles using dithio surface units

Very recently an interest in other surface units has directed research towards xanthates,[72] dithiocarbamates and dithiocarboxylates, as these sulphur-containing ligands are an attractive alternative to thiols (and disulphides[73]).

Although much work has been done on the coordination chemistry of dithiocarbamates (DTCs), only recently has attention turned to their application in self assembly on gold. DTCs have great potential in this field due to their ease of synthesis compared to that of thiols. Wei *et al* demonstrated that dithiocarbamate units stabilise gold NPs against desorption and other environmental stress to a much greater degree than thiols.[74] Since they feature a CS_2 group, they thus exhibit enhanced chemisorption to gold surfaces owing to the two points of contact. In addition, the intramolecular S-S distance of the CS_2 group is almost equal to that of adjacent bonding sites on Au surfaces, resulting in adsorption in an ordered manner (*Fig. 21*).

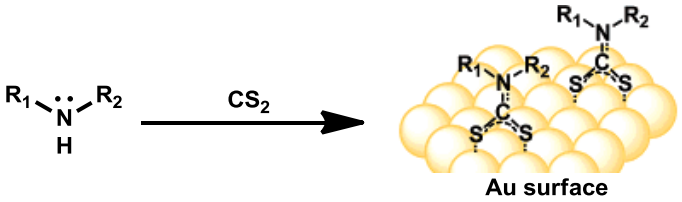

Figure 21. Dithiocarbamate-anchored monolayers by *in situ* condensation of amines and CS_2.[74]

The stability of DTC units on gold NP surfaces compared to thiols is further highlighted by Sharma *et al*. The authors generated DTCs with DNA conjugates which were then functionalised to attach to the surface of AuNPs.[75] The stability of the material was tested by displacement reactions and it was found that due to the strong binding of bidentate DTC units towards AuNP surfaces, displacement was prevented. In contrast, thiolated oligonucleotides have been shown to readily undergo displacement.[76]

The optical and electronic properties of DTC and thiol protected NPs has also been compared. Wessels and co-workers prepared films of AuNPs interlinked by various organic dithiol and bis-DTC derivatives.[77] Their charge transfer propertites were compared and it was found the DTC linker molecules displayed significantly enhanced optoelectronic properties.

Beer and co-workers have exploited the preparation of bipyridine-derived DTC ligands in one of the earliest studies, introducing the functionalised DTCs onto gold NPs.[78] The authors report the synthesis and characterisation of ruthenium(II) tris-bipyridyl DTC-capped nanoparticles made from the corresponding Ru(II) DTC complex (*Fig. 22*).

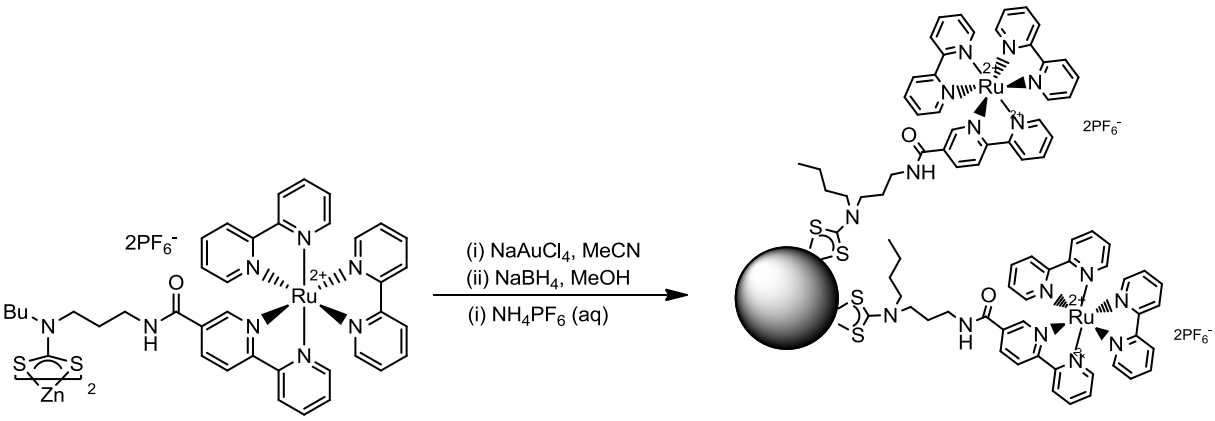

Figure 22. Synthesis of ruthenium(II) tris-bipyridyl DTC capped Au nanoparticles.[78]

More recently a zwitterionic piperazine dithiocarbamate, $S_2CNC_4H_8NH_2$, has been prepared and utilized as a precursor for the synthesis of gold nanoparticles with metal surface units.[19, 20, 79] The metalla-dithiocarbamate complexes, $L_2Ni(S_2CNC_4H_8NCS_2)$ (L_2 = dppe, dppf) were used to functionalise the surface of AuNPs by the displacement of a citrate shell to produce Ni and FeNi NPs (*Fig. 23*).

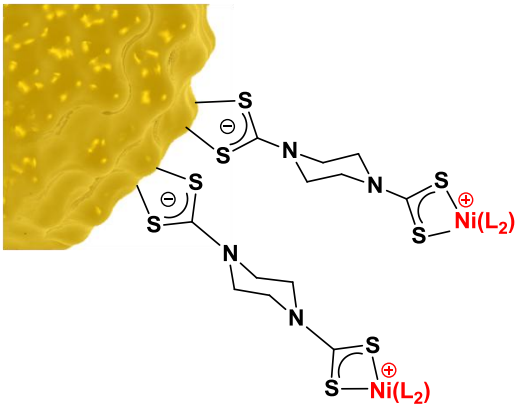

Figure 23. AuNPs stabilised by Ni DTC complexes.[79]

The synthetic challenges of thiol group functionalisation can be contrasted to the relative synthetic ease by which DTC units can be incorporated onto the the surface of nanoparticles, producing novel modified surface NP materials. These NPs offer great potential for the development of nanoscale electronic devices, sensor and catalysts.

1.3. Multimetallic complexes based on mixed-donor ligands

1.3.1. Metal centres linked by oxygen and nitrogen donors

The incorporation of more than one metal unit within the same coordination framework offers many benefits, especially if the properties of different metals are combined. Many ligands other than the 1,1-dithio species discussed already are known to generate multimetallic systems. For example multimetallic complexes based on dicarboxylic acids and bipyridines are well established in the literature. Such linkers have been used in the construction of coordination polymers[80, 81] and metal-organic frameworks (MOFs).[82-84] Most examples of these networks are based on symmetrical linkages, forming homopolymetallic complexes.[85-87] Only one group has recently reported a hetreopolymetallic motif based on an isonicotinic acid framework.[88] The preparation of multimetallic networks featuring two different metal centres has proved to be considerably challenging. To overcome this difficulty either a protection/deprotection strategy must be employed, or the donor combinations of the linker must be carefully tailored to each metal centre. As mentioned earlier (*Section 1.1.1, Fig. 5*), one end of a piperazine molecule can be converted into a dithiocarbamate while protecting the other end as an ammonium unit in the zwitterion $H_2NC_4H_8NCS_2$. This protecting approach has allowed the successful preparation of heteromultimetallic compounds bearing 2-6 metal units.[19]

Mixed donor ligands are particularly useful for generating heteromultimetallic compounds. They contain at least two different donor groups capable of chelating to metal ions. Such multifunctional ligands fulfil the same role as the 1,1-dithio unit, but use the innate affinity of certain donor combinations for particular metals rather than a protection strategy.

Herein some background information on carboxylates and pyridine ligands is provided since these ligands are commonly used to generate homopolymetallic systems. The possibilities which arise from combining the two can be exploited in mixed-donor ligands and will be discussed subsequently in the Results and Discussion section.

1.3.1.1. Carboxylates and pyridines as linkers

The wide array of coordination modes of the carboxylate anion coupled with its high affinity for metals ions, gives rise to metal carboxylate complexes with rich structural chemistry. Some examples of their coordination modes are shown below using the benzoate ligand (*Fig. 24*).

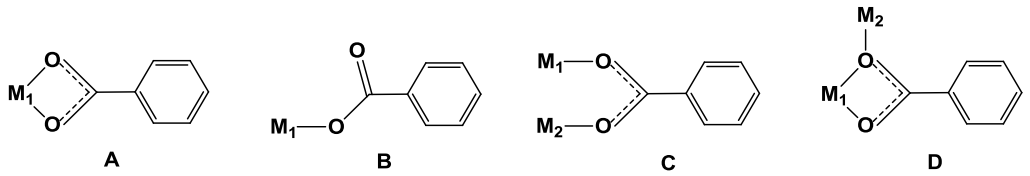

Figure 24. Binding modes of carboxylates.

Although many carboxylate complexes are known, one of the most interesting classes is one in which two metal centres are bridged by four carboxylate ligands. These have come to be known as 'paddlewheel' complexes (PWCs) through analogy to boats with a paddlewheel (*Fig. 25*).[89] This type of linkage of dicarboxylate units leads to well-ordered lattice structures and the framework often allows multiple bonds between the metals and the ordered linkage. The tuneability of the ligands and the (often) coordinatively-unsaturated nature of the metal centre make them good candidates for catalysis.[90]

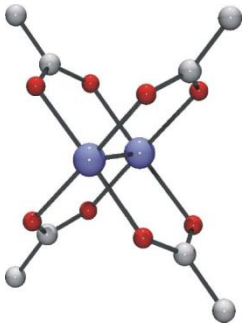

Figure 25. Molecular structure of molybdenum acetate with the paddlewheel motif Mo (blue), O (red) and C (grey).[89]

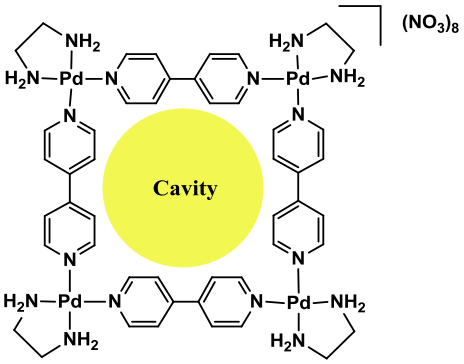

Figure 26. An iconic example of a multimetallic compound based on pyridyl bridging ligands, generating a molecular square with a central cavity.

The ligand 4,4'-bipyridine (4,4'-bipy) is an ideal linker between different transition metal centres for the propagation of coordination networks. It has two potential binding sites which are arranged in an opposite (*exo*) fashion. In principle, the pyridyl groups of 4,4'-bipy can rotate along a

central C–C bond; however the rotation does not affect the mutual orientation of the two lone pairs. Therefore 4,4'-bipy can be regarded as a rigid and classical bridging ligand. Its length and inflexible structure facilitates the construction of networks with metal atoms, which results in the formation of cavities of molecular dimensions (*Fig. 26*). The 4,4'-bipy ligand forms a variety of networks ranging from one-dimensional to three-dimensional with several transition metal salts. The geometry of the architectures depends on several factors such as the coordination geometry of the metal atom, the presence of guest molecules, ligand and transition metal ratios and anions.[91]

1.3.1.2. Metal Organic Framework (MOF) complexes

Countless research efforts have concentrated in recent years on a wide variety of coordination polymers.[92] The most recent, high-profile setting for carboxylate linkers is found in metal-organic frameworks (MOFs). This field originated from work on zeolites and many synthetic routes are similar. MOFs are materials which are formed by the coordination of metals to polydentate linkers, leading to porous materials. The internal cavities between the linked metal units provide a huge internal surface area, making them suitable for storage of gases, in particular. (*Fig. 27*).[82-84] MOFs can not only store hydrogen molecules,[93] but also carbon dioxide,[94] carbon monoxide,[95] methane,[96] and oxygen have been reported.[97] For this reason, MOFs have become an important class of functional materials. The most common types of connectors used in MOFs are dicarboxylate ligands (oxalate, terephthlalate etc.) and recently research into using molecular PWCs as building blocks for the synthesis of MOFs has even been reported.[89]

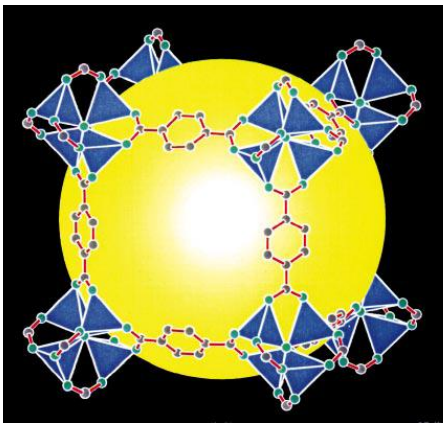

Figure 27. Depictions of a Metal Organic Framework (MOF) formed by polycarboxylate ligands. The yellow sphere illustrates the cavity created.[82]

A key requirement of the bridging ligands in MOFs is the ability of the ligands to form bonds reversibly so that a thermodynamic product can be achieved. Carboxylate ligands serve MOF formation very well in this respect.[98]

MOFs have found use in many applications other than storage. They can be used in gas purification as strong chemisorption can take place between unwanted molecules (such as amines, phosphines, oxygenates, alcohols, water, or sulphur-containing molecules) and the framework. This allows the desired gas to pass through the MOF, leaving behind the unwanted molecules. Gas separation can be also performed with MOFs because they allow certain molecules to pass through

their pores based on their size. This is particularly important for separating out harmful gases such as carbon dioxide.

MOFs are also used in catalysis because of their shape, size selectivity and their large volume.[99] The fine structure and nature of the active site can be controlled and it is possible to have a homogeneous distribution of one or more active sites.

1.3.2. Mixed-donor ligands derived from carboxylate and pyridine units

Mixed donor ligands in which both the dicarboxylate and bipyridine ligands are combined offer great potential in the construction of hetero-multimetallic arrays. Isonicotinic acid (IUPAC name: pyridine-4-carboxylic acid) is a pyridine variant with a carboxylic acid unit in the 4-position (*Fig. 28*). It is the simplest combination of pyridine and carboxylic acid functional groups and is an isomer of nicotinic acid (also known as niacin and vitamin B_3) which differs by the fact that the carboxylic acid side chain is present at the 3-position.

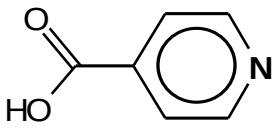

Figure 28. Isonicotinic acid

Nicotinic acid is an essential human nutrient and acts to reduce cholesterol and triglycerides in the blood. It has also been shown to reduce cardiovascular problems. Isonicotinic acid itself is mainly used in antituberculosis drugs such as isoniazid (isonicotinic acid hydrazide). Isonicotinic acid and its derivatives are also employed in manufacturing pharmaceuticals and agrochemicals.

Since isonicotinic acid contains both oxygen and nitrogen donors and monodentate and (potentially) bidentate functionality at either end, under the right conditions these differences can be exploited to link different metal units to create heterobimetallic compounds. This is in contrast to dicarboxylic acids or 4,4'-bipyridine, which result in homobimetallic compounds.

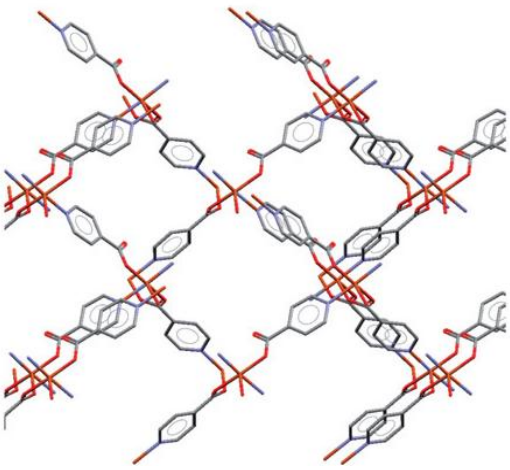

Figure 29. MOF based on a copper-isonicotinate framework.[100]

The coordination chemistry of isonicotinic acid and its derivatives are varied and they have been used in a number of contexts, including as a structural element in MOFs. For example, Pichon *et al* described the construction of a 3-

dimensional motif based on an isonicotinate framework in a recent paper involving a solvent-free preparation process (Fig. 29).[100] This bifunctional ligand has shown to have great potential in the assembly of MOFs and some further examples of such architectures can be found in literature.[101, 102]

A recent report employed isonicotinic acid to bond to rhodium(III) metal centres. It was found that the ligands coordinated through the nitrogen donors and that the protonated/deprotonated forms could be controlled by adjusting the pH (*Fig. 30*).[103] However, under the right conditions the isonicotinic acid ligand can coordinate through either one or both oxygen donors. An example of the former coordination mode (monodentate) is shown in *Fig. 31*.[104]

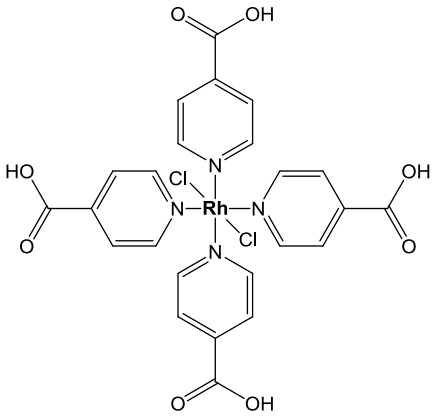

Figure 30. Structure of $[RhCl_2(isonicH)_4]^+$.[103]

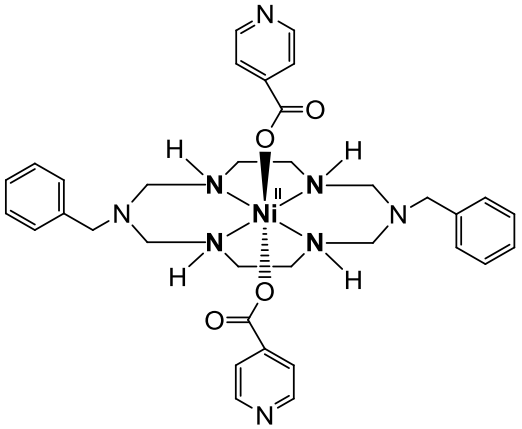

Figure 31. Structure of $[Ni(isonic)(C_{22}H_{34}N_6)]$ showing monodentate coordination of the isonicotinate ligands.[104]

These examples aside, surprisingly little has been achieved in coordination chemistry using isonicotinic acid or similar bifunctional linkers.

2. Chapter 2: Aims

Although there are many complexes of 1,1'-dithio ligands, there is still much unexplored potential for such ligands when functionalised with units capable of further reactivity. Dithiocarboxylates are relatively neglected members of the 1,1'-dithio ligand class yet the reaction of N-heterocyclic carbenes with carbon disulfide provides a route to a sterically-tuneable family of zwitterionic dithiocarboxylates. These observations led to the following aims:

- to explore the reactivity of functionalised dithiocarbamate ligands after coordination
- to investigate the coordination chemistry of dithiocarboxylates based on N-heterocyclic carbenes

Given the difficulties associated with preparing heteromultimetallic compounds using conventional symmetrical linkers (e.g., 4,4'-bipyridine, terephthalate), new methods of preparing such species are needed if the properties of different metals are to be utilised within the same system. Accordingly, another aim of the project was:

- the development of nitrogen-oxygen mixed-donor ligands to achieve the formation of di-, tri- and pentametallic heteronuclear compounds

It was recognised that the methodologies developed to address the aims outlined above would also be applicable to the attachment of functionality to the surface of metal nanoparticles. This led to the aim:

- to functionalise gold and silver nanoparticles with functional surface units, including transition metals

Chapter 3: Transition metal dithiocarbamate (DTC) complexes of group 8 and 10 metals

3. Chapter 3: Transition metal dithiocarbamate (DTC) complexes of group 8 and 10 metals

As described in *Section 1.1.1*, most DTCs are prepared in a simple manner from secondary amines, however the potential of exploiting the substituents on these amines has not been extensively investigated. DTC ligands, $[S_2CNR_2]^-$, where R is either a methyl or ethyl group, are commercially available. It is somewhat surprising that so many reports are limited to the methyl or ethyl variants since a more adventurous approach allows the facile incorporation of additional functionality into the molecule.

The work described here (which has now been published[105, 106]), focuses on exploiting the NR_2 substituents chemically by preparing complexes bearing functionalised DTCs. In this chapter the initial incorporation of amine and methoxy functionality[107, 108] into the DTC framework is presented. This has proven to be an efficient means to further functionalise the molecule, and to change the physical properties of the entire complex. The range of functionality has also been extended by introducing diallyl and methylallyl groups to the terminal amine units, permitting the investigation of the reactivity of coordinated functionalised DTC ligands towards alkene metathesis.

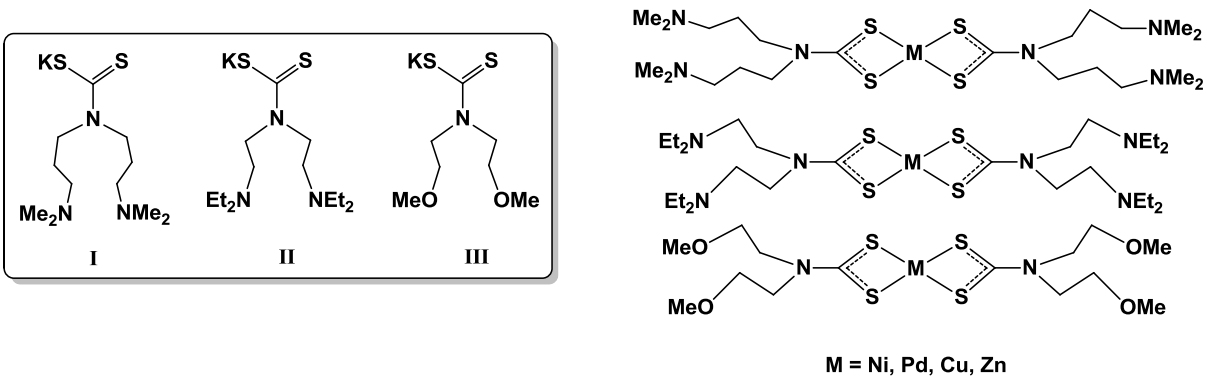

Figure 32. The three functionalised dithiocarbamate ligands used in this work and homoleptic examples of previous complexes prepared using them (M = Ni, Cu, Zn).[108]

3.1. Amine- and methoxy-terminated DTCs

3.1.1. Synthesis of amine- and methoxy-DTCs

Ruthenium bis(diphenylphosphino)methane complexes

One of the most versatile ruthenium starting materials for introducing bidentate ligands[19, 109, 110] is the compound *cis*-[$RuCl_2(dppm)_2$] (dppm = 1,1-bis(diphenylphosphino)methane).[111] Removal of the chloride ligands can readily generate a pair of active sites without affecting the stability of the remaining coordination sphere, due to the inertness of the dppm ligands. In addition, the dppm ligands display diagnostic resonances in both the ^{1}H and ^{31}P NMR spectra. Because of these attractive properties, this compound has been employed in the preparation of DTC transition metal complexes in previous work in this area.[19, 112]

The ligand $KS_2CN(CH_2CH_2CH_2NMe_2)_2$ (**I**) was prepared *in situ* by treating a methanol solution of 3,3′-iminobis(*N*,*N*-dimethylpropylamine) with CS_2 in the presence of potassium hydroxide. Addition of a slight excess of the ligand to *cis*-[$RuCl_2(dppm)_2$], in the presence of NH_4PF_6, produced the colourless cation [$Ru\{S_2CN(CH_2CH_2CH_2NMe_2)_2\}(dppm)_2]PF_6$ (**1**) in 82% yield (*Scheme 1*). The dppm ligands were evident by the two new pseudotriplets observed in the ^{31}P NMR spectrum at –15.5 and –2.1 ppm, showing a coupling of 34.1 Hz. Furthermore, the multiplet resonances for the methylene protons at 4.42 and 4.97 ppm in the ^{1}H NMR spectrum also confirmed the retention of the dppm ligand. The presence of the propylene arms of the DTC unit was established by the observation of pairs of multiplets at 1.32, 1.40 ppm and 3.12, 3.64 ppm as well as a further broad multiplet at 1.87 ppm. The methyl protons gave rise to distinct resonances at 1.95 ppm, integrating to 12 protons, as expected. The overall structure of **1** was also confirmed by a molecular ion in the electrospray mass spectrum (+ve mode) at *m/z* 1132 and good agreement of elemental analysis with calculated values.

The ligand $KS_2CN(CH_2CH_2NEt_2)_2$ (**II**) was also prepared, bearing shorter and less flexible pendant arms than **I**. Following the same approach, ligand **II** was generated *in situ* and treated with *cis*-[$RuCl_2(dppm)_2$] and NH_4PF_6 to yield [$Ru\{S_2CN(CH_2CH_2NEt_2)_2\}(dppm)_2]PF_6$ (**2**). Multiplets in the ^{1}H NMR spectrum at 2.40, 3.28 and 3.81 ppm were observed for the shorter ethylene bridge of the ligand. The ethyl substituents displayed resonances at 1.05 and 2.57 ppm, showing mutual J_{HH} coupling of 7.1 Hz. The formulation of **2** was further confirmed by the molecular ion at *m/z* 1160, observed in 100% abundance in the mass spectrum (ES +ve).

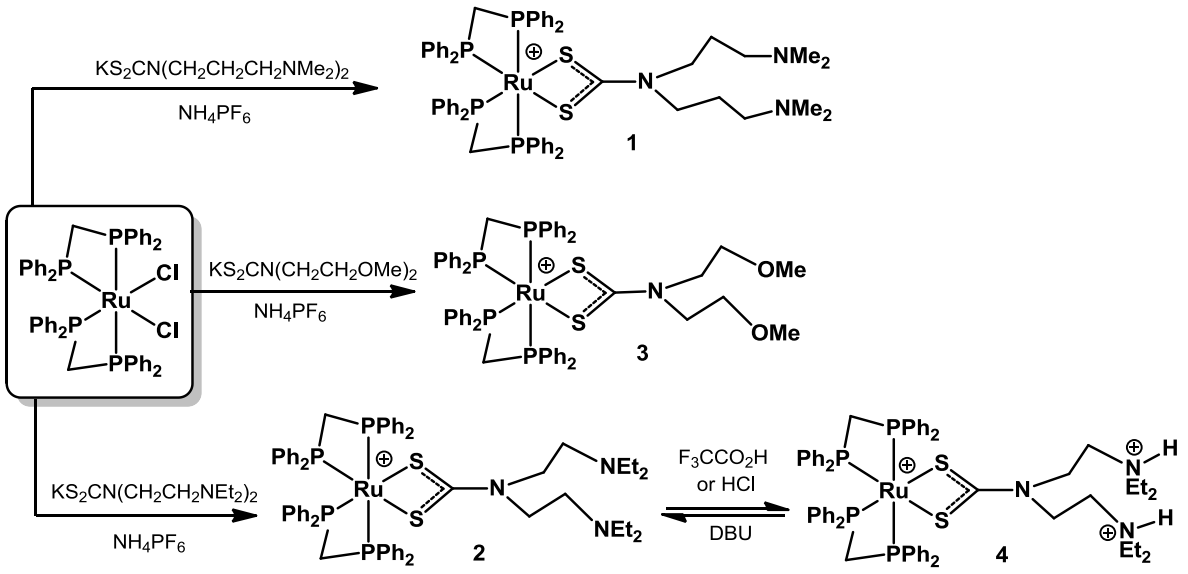

Scheme 1. Preparation of dithiocarbamate complexes from *cis*-[$RuCl_2(dppm)_2$].

The DTC ligand with methoxy-terminated pendant functional groups, $KS_2CN(CH_2CH_2OMe)_2$ (**III**)[108, 113] was subsequently employed in the investigation. This ligand was treated with *cis*-[$RuCl_2(dppm)_2$] and NH_4PF_6 to yield the compound [$Ru\{S_2CN(CH_2CH_2OMe)_2\}(dppm)_2]PF_6$ (**3**) (*Scheme 1*). Unlike the amino-terminated dithiocarbamate ligands, pairs of resonances were not observed in the ^1H NMR spectrum, instead the methyl protons gave rise to a singlet at 3.38 ppm and a multiplet was seen at 3.51 ppm for the methylene protons adjacent to the methoxy group. An additional resonance was observed at 3.79 ppm for the remaining methylene protons. Single crystals of **3** were grown by slow diffusion of ethanol into a dichloromethane solution of **3** and the structure was determined by X-ray diffraction (see *Fig. 36* and *Structural Discussion, 2.3*).

Ruthenium and osmium alkenyl complexes

Since the three DTC ligands **I - III** coordinated smoothly with the $Ru(dppm)_2$ unit, attention turned towards the coordination of the same ligands with group 8 alkenyl complexes.[114] The insertion of alkynes into the ruthenium–hydride bond of [$RuHCl(CO)(PPh_3)_3$] has been shown to be a convenient route for the generation of the corresponding alkenyl species, [$Ru(CR^1{=}CHR^2)Cl(CO)(PPh_3)_2$].[115] Since its discovery, this approach has been widely embraced as a versatile entry point into ruthenium vinyl chemistry.[116-118]

It was decided that the most suitable triphenylphosphine-based vinyl species to use as a starting point would be the compounds [$Ru(CR^1{=}CHR^2)Cl(CO)(PPh_3)_2$][115] and [$Ru(CR^1{=}CHR^2)Cl(CO)(BTD)(PPh_3)_2$][119], in which BTD (2,1,3- benzothiadiazole) is present as a labile ligand. BTD confers greater crystallinity to the materials and also competes efficiently with

PPh_3 to avoid contamination with tris(phosphine) byproducts[114, 120]. These ruthenium vinyl compounds display reactivity at the metal centre but also have the potential to undergo reaction at the vinyl ligand itself, as will be demonstrated here (γ-hydroxy variants).

It should be noted that although many ruthenium (and to a lesser extent osmium) DTC complexes are known, no example has been reported with the amine- or methoxy-terminated ligands used here.

A slight excess of $KS_2CN(CH_2CH_2CH_2NMe_2)_2$ (**I**) was added to $[Ru(CH{=}CHBu^t)Cl(CO)(BTD)(PPh_3)_2]$, producing a pale yellow microcrystalline solid. This product gave rise to a new singlet in the ^{31}P NMR spectrum at 39.5 ppm. Retention of the alkenyl ligand was confirmed by a singlet at 0.40 ppm (^tBu) in the ^1H NMR spectrum and alkenyl resonances at 4.60 and 6.30 ppm, showing mutual coupling of 16.4 Hz. The alkenyl signal which appeared further downfield, displayed coupling to the mutually *trans* phosphine ligands (J_{HP} = 2.7 Hz) and was thus assigned as Hα. Resonances for the methyl protons for the terminal NMe_2 units (singlets) appeared at 2.12 and 2.14 ppm and the pair of multiplets observed in the region 1.09 to 3.19 ppm were assigned to the propylene chain. The ^{13}C NMR spectrum showed a singlet resonance at 206.1 ppm which was assigned to the CS_2 unit of the DTC ligand. The pairs of resonances observed between 57.1 - 24.9 ppm, were due to carbons of the $(CH_2)_3$ units while the methyl carbons of the *tert*-butyl unit resonated at a slightly more downfield value of 45.5 ppm. Infrared data displayed characteristic features for the DTC (ν_{CN} at 1457 cm^{-1}) and triphenylphosphine ligands. An intense absorption at 1905 cm^{-1} was also observed due to the carbonyl ligand. Analysis by electrospray (+ve ion) mass spectrum displayed an abundant molecular ion at *m/z* 1000, confirming the overall composition of complex to be $[Ru(CH{=}CHBu^t)\{S_2CN(CH_2CH_2CH_2NMe_2)_2\}(CO)(PPh_3)_2]$ (**5**). Elemental analysis results showed good agreement with calculated values and further corroborated the formulation of compound **5** (*Scheme 2*).

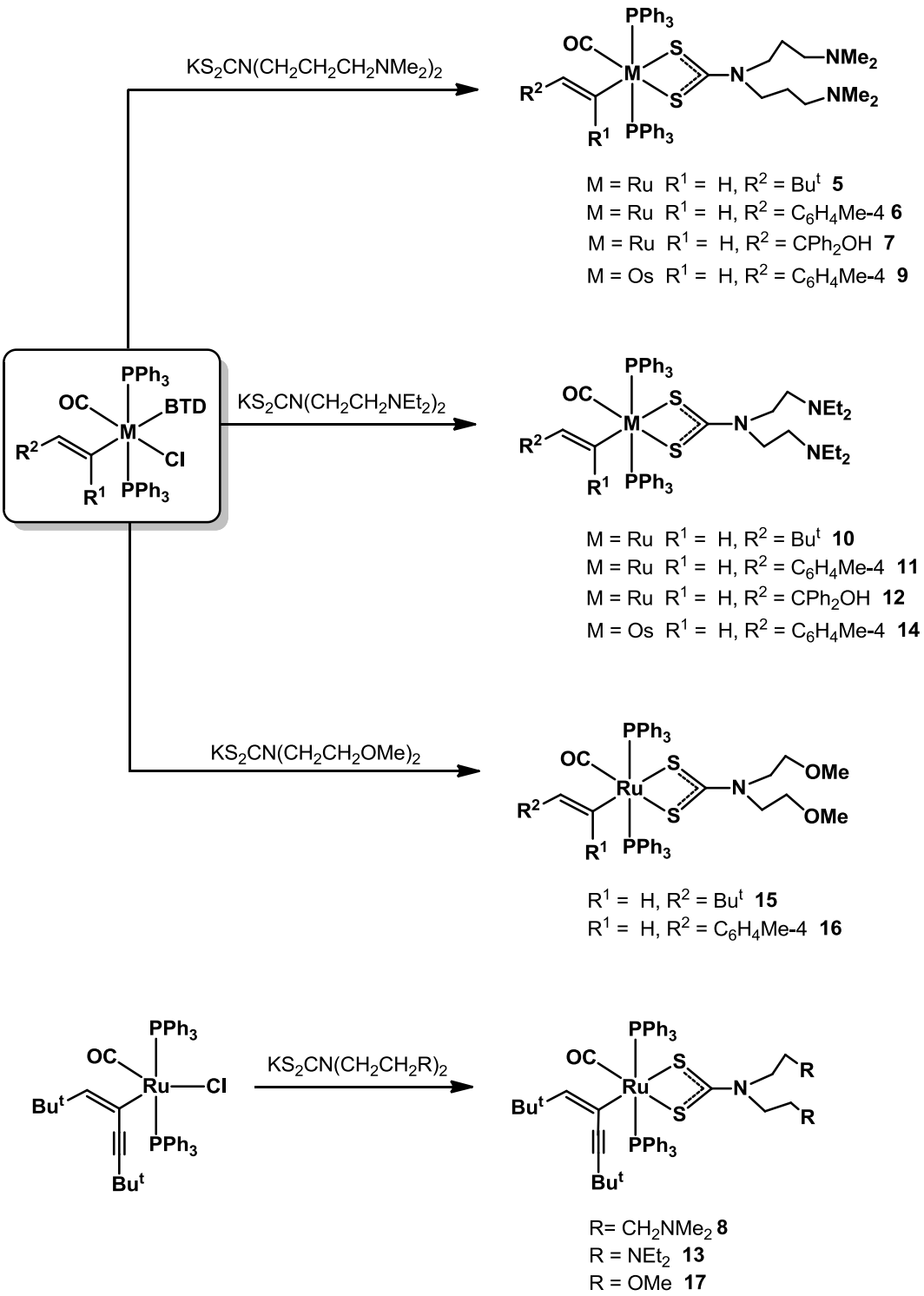

Scheme 2. Preparation of alkenyl dithiocarbamate complexes.

Two additional ruthenium examples bearing ligand **I** were prepared. These complexes contained either an aromatic or a γ-hydroxy substituted alkenyl ligand, giving rise to complexes $[Ru(CH{=}CHC_6H_4Me\text{-}4)\{S_2CN(CH_2CH_2CH_2NMe_2)_2\}(CO)(PPh_3)_2]$ (**6**) and

[Ru(CH=CHCPh$_2$OH){S$_2$CN(CH$_2$CH$_2$CH$_2$NMe$_2$)$_2$}(CO)(PPh$_3$)$_2$] (**7**) respectively. These compounds were prepared following the same procedure as for **5**, and both displayed typical spectroscopic features for the ligands. The retention of the hydroxy group in **7** was evidenced by the resonance at 2.60 ppm. The disubstituted enynyl derivative [Ru(C(C≡CBu^t)=CHBu^t){S$_2$CN(CH$_2$CH$_2$CH$_2$NMe$_2$)$_2$}(CO)(PPh$_3$)$_2$] (**8**) was also synthesised using the same approach from pentacoordinate [Ru(C(C≡CBu^t)=CHBu^t)Cl(CO)(PPh$_3$)$_2$]. The ^{1}H NMR spectrum showed no remarkable difference to features for the DTC ligand compared to the previous examples other than the more closely spaced multiplet resonances attributed to the amine arms of the dithiocarbamate ligand. A singlet was observed at 5.19 ppm for the alkenyl proton.

In order to confirm that an analogous reaction proceeded between DTC ligands and alkenyl complexes of osmium, [Os(CH=CHC$_6$H$_4$Me-4){S$_2$CN(CH$_2$CH$_2$CH$_2$NMe$_2$)$_2$}(CO)(PPh$_3$)$_2$] (**9**), was prepared from [Os(CH=CHC$_6$H$_4$Me-4)Cl(CO)(BTD)(PPh$_3$)$_2$]. Spectroscopic characterisation revealed little spectroscopic difference to **6**, apart from the lower frequency of the ν_{CO} absorption at 1894 cm^{-1} in the solid state infrared spectrum, as expected for the more electron-rich osmium complex.

The analogous diethylamino ligand, KS$_2$CN(CH$_2$CH$_2$NEt$_2$)$_2$ (**II**), was used to prepare [Ru(CH=CHBu^t){S$_2$CN(CH$_2$CH$_2$NEt$_2$)$_2$}(CO)(PPh$_3$)$_2$] (**10**) from [Ru(CH=CHBu^t)Cl(CO)(BTD)(PPh$_3$)$_2$] in the same manner. Features attributed to the alkenyl, phosphine and carbonyl ligands were found to be similar to those observed for **5**. In order to confirm the generality of the coordination chemistry shown by [S$_2$CN(CH$_2$CH$_2$NEt$_2$)$_2$]$^-$ with the alkenyl precursors and to increase the options for structural determination through X-ray diffraction, the complexes [Ru(CH=CHC$_6$H$_4$Me-4){S$_2$CN(CH$_2$CH$_2$NEt$_2$)$_2$}(CO)(PPh$_3$)$_2$] (**11**), [Ru(CH=CHCPh$_2$OH){S$_2$CN(CH$_2$CH$_2$NEt$_2$)$_2$}(CO)(PPh$_3$)$_2$] (**12**), [Ru(C(C≡C^{t}Bu)=CH^{t}Bu){S$_2$CN(CH$_2$CH$_2$NEt$_2$)$_2$}(CO)(PPh$_3$)$_2$] (**13**) and [Os(CH=CHC$_6$H$_4$Me-4){S$_2$CN(CH$_2$CH$_2$NEt$_2$)$_2$}(CO)(PPh$_3$)$_2$] (**14**) were also generated (*Scheme 2*).

A methanolic solution of the ligand, KS$_2$CN(CH$_2$CH$_2$OMe)$_2$ (**III**) (generated *in situ*), was added to the alkenyl complexes [Ru(alkenyl)Cl(CO)(BTD)(PPh$_3$)$_2$]. The ^{31}P NMR spectrum gave rise to two closely spaced resonances, indicating that two products had been formed. Further evidence for this was given by the ^{1}H NMR spectrum, which showed two sets of alkenyl resonances. A crystallographic investigation (not reported here) revealed that a complex with the methyl xanthate ligand, [S$_2$COMe]$^-$, had also been formed. This can be traced to the reaction of methanol with excess carbon disulphide. In order to confirm the proposed route to this byproduct, the complex [Ru(CH=CHBu^t)(S$_2$COMe)(CO)(PPh$_3$)$_2$] was prepared in the same manner as the known isopropyl xanthate analogue.[121] ^{1}H NMR analysis revealed the resonances seen in the initial product mixture (e.g. S$_2$COMe resonance at 3.20 ppm in the ^{1}H NMR spectra).

The experimental procedures were modified and methanol was eliminated from both ligand preparation (i.e. an aqueous solution of **III** was prepared) and work up of the complex. Complexes

[Ru(alkenyl){$S_2CN(CH_2CH_2OMe)_2$}(CO)(PPh_3)$_2$] (alkenyl = CH=CHBu^t, **15**; CH=CH_6H_4Me-4, **16**; C(C≡CBu^t)=CHBu^t), **17**) were smoothly prepared in high yields. The ^{1}H NMR spectrum of complex **15** revealed two singlets for the methoxy protons at 3.19 and 3.20 ppm as well as triplets for the protons of the pendant arms at 2.85, 3.07, 3.18 and 3.48 ppm (all showing coupling of around 6 Hz). Typical features for the alkenyl ligands were also observed. Similar spectroscopic and analytical data were obtained for **16** and **17** (*Scheme 2*). Single crystals of [Ru(CH=CH_6H_4Me-4){$S_2CN(CH_2CH_2OMe)_2$}(CO)(PPh_3)$_2$] (**16**) were grown and the molecular structure determined by X-ray diffraction (see *Fig. 37* and *Structural Discussion, 2.3*)

3.1.2. Protonation studies

The project was then extended to investigate the reactivity of the amine terminated DTC complexes. The complexes were treated with acid with the aim of forming ammonium functionalised metal compounds.

The complex [Ru{$S_2CN(CH_2CH_2NEt_2)_2$}(dppm)$_2$]PF_6 (**2**) was chosen for the initial protonation study due to the robustness conferred by the dppm moiety. Addition of two equivalents of trifluoroacetic acid to a dichloromethane solution of **2** resulted in no colour change. After work up, the isolated solid was studied by ^{1}H NMR, revealing the chemical shifts of the resonances for the ethyl substituents of the DTC ligand had moved and had broadened considerably. The multiplet resonances assigned to the ethylene units had also shifted. The solid state infrared spectrum revealed a new intense band at 1670 cm^{-1} for the trifluoroacetate counteranions as well as a ν_{PF} absorption at 833 cm^{-1} for the hexafluorophosphate anion. These data suggested that the complex [Ru{$S_2CN(CH_2CH_2NHEt_2)_2$}(dppm)$_2$](PF_6)(O_2CCF_3)$_2$ (**4**) had been produced (*Scheme 1*). It appears that the PF_6^-counteranion has a relatively strong interaction with the ammonium units as both NMR and IR data showed retention of the anion. Unsuccessful attempts to obtain NMR data for the compound in D_2O reflected its low solubility. However, treatment of **2** with two equivalents of dry HCl afforded **4** as the chloride salt, which showed modest water solubility in comparison. It is plausible to assume that the aqueous solubility of the compound may be improved further if more than one dithiocarbamate unit were attached to the metal centre.

It was anticipated that treatment of the alkenyl complexes, [Ru(CR=CHR)(DTC-amine)(CO)(PPh_3)$_2$], would not result in straightforward protonation of the amine functionality since the σ-organyl ligand is prone to cleavage by acids such as HCl. However, this was found not to be the case. After treatment of [Ru(CH=CHBu^t){$S_2CN(CH_2CH_2CH_2NMe_2)_2$}(CO)($PPh_3$)$_2$] (**5**) with two equivalents of trifluoroacetic acid, little difference was observed in the chemical shift of the ^{31}P NMR resonance. The ^{1}H NMR spectrum showed considerable shifts in the resonances for the methyl (2.66

and 2.72 ppm) and propylene (1.42 - 3.51 ppm) protons which compared well with the values for **5**. This clearly indicated that protonation had occurred at the amine units. The alkenyl and phosphine resonances in the same spectrum showed insignificant differences in the shifts, indicating that the co-ligands had been unaffected by the transformation. The IR spectrum displayed a new peak at 1674 cm^{-1}, which was assigned to the trifluoroacetate counteranions, and a peak at 1915 cm^{-1} attributed to the ν_{CO} absorption. Mass spectrometry and elemental analysis further confirmed the formulation as $[Ru(CH{=}CH^tBu)\{S_2CN(CH_2CH_2CH_2NHMe_2)_2\}(CO)(PPh_3)_2](O_2CCF_3)_2$ (**18**) (*Scheme 3*). Addition of DBU (1,8-Diazabicyclo[5.4.0]undec-7-ene) was found to reverse this protonation, which regenerated **5**.

Protonation of the γ-hydroxy alkenyl complex, $[Ru(CH{=}CHCPh_2OH)\{S_2CN(CH_2CH_2CH_2NMe_2)_2\}(CO)(PPh_3)_2]$ (**7**), did not proceed in the same manner as the *tert*-butyl alkenyl complex **5**. Treatment of **7** with an excess of trifluoroacetic acid, caused an instant colour change from colourless to intense red, indicating the generation of a new chromophore in the molecule. This observation could be compared to the protonation of **5** which did not display any noticeable colour change.

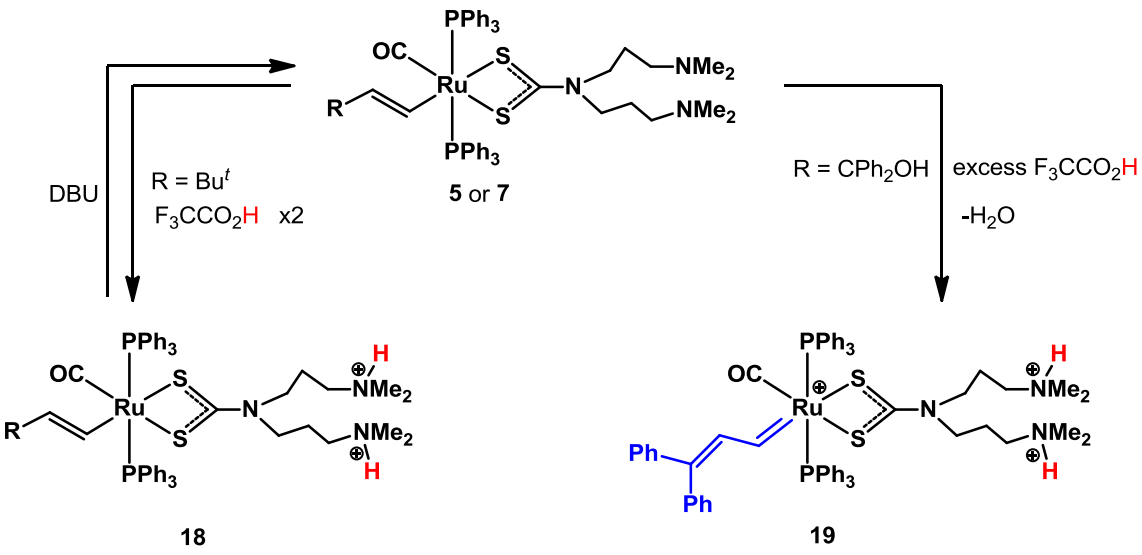

Scheme 3. Protonation reactions of alkenyl complexes **5** (R = Bu^t) and **7** (R = CPh_2OH).
DBU = (1,8-Diazabicyclo[5.4.0]undec-7-ene).

The ^{31}P NMR spectrum showed a significant shift of the singlet observed in the precursor **7** (39.9 ppm), to 32.0 ppm, indicating a new compound had formed. Further evidence was seen in the ^1H NMR spectrum, which displayed two new downfield doublets at 8.10 and 14.68 ppm, showing a mutual coupling of 14.0 Hz, the latter typical of the chemical shift of a carbene proton. The resonances due to the protons of the methyl substituents of the DTC ligand had also shifted from the

original resonances observed for **7**, providing further evidence for the protonation at the nitrogen lone pairs. The remaining protons of this ligand were apparent only as two broad multiplets centred at 1.41 and 2.98 ppm. IR data presented a shift in frequency of the ν_{CO} absorption from 1913 cm^{-1} in **7** to 1952 cm^{-1} in **19**. This implied decrease in electron density at the metal centre, suggests the formation of a cation. Further confirmation of the formulation of $[Ru(=CHCH=CPh_2)\{S_2CN(CH_2CH_2CH_2NHMe_2)_2\}(CO)(PPh_3)_2](O_2CCF_3)_3$ (**19**) was provided by ^{13}C NMR spectroscopy (310.5 ppm, RuCH, J_{CP} = 8.6 Hz), mass spectrometry (molecular ion at *m/z* 1108 and a peak for fragmentation of the vinylcarbene unit at *m/z* 916) and elemental analysis. (*Scheme 3*).

From the successful formation of **18** and **19**, it is apparent that dithiocarbamate ligands can be used in the development of molecules in which the protection of acid-sensitive functionality (within the system) is required. Preferential attack at the amine moiety occurs on addition of small amounts of acid (leaving the rest of the molecule unaffected). This is also demonstrated when **7** is treated with one equivalent of trifluoroacetic acid. Initially a slight red colouration is observed, however ^{1}H NMR analysis reveals protonation of the amine groups rather than formation of the vinylcarbene, **19**. The carbene is only generated when more than two equivalents of acid are added.

3.2. Allyl- and methylallyl- terminated DTCs

It was decided to further explore the potential for reactivity of functionalised DTC metal complexes. Through the incorporation of diallyl functionality into the pendent amine substituents of the DTC unit, Gladysz and co-workers have demonstrated that ring-closing metathesis (RCM) can be performed on allyl substituted phosphines within the coordination sphere of a metal, resulting in new ligand architectures.[122]

Very few examples of complexes bearing the diallyldithiocarbamate ligand (*Fig. 33*) have been reported (mostly in the 1970s). Thus far only homoleptic examples using simple metal salt precursors of iron[123, 124], cobalt, nickel[125], copper[126], silver[127] and gold[128] have been made.

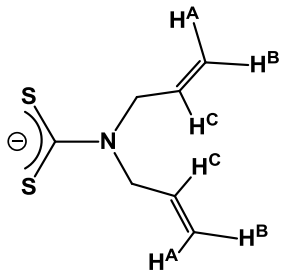

Figure 33. The diallyldithiocarbamate ligand employed in this work, showing the numbering scheme used for spectroscopic purposes.

In the context of alkene metathesis, substrates such as amines are problematic due to the interaction of the amine lone pair with the catalyst. However, in the dithiocarbamate shown in *Figure 33*, the nitrogen lone pair contributes to the partial multiple bond nature of the C–N bond. This renders the nitrogen non-basic and thus enables metathesis to occur. Herein this potential is explored, demonstrating that once the DTC diallyl ligand is coordinated to the metal centre, the diallyl functionality can enter into simple organic transformations (such as alkene metathesis. See *Chapter 3.2.1.1*).

3.2.1. Synthesis of diallyl DTC complexes

Treatment of an aqueous solution of diallylamine with CS_2, in the presence of KOH, generated the diallyl ligand $KS_2CN(CH_2CH{=}CH_2)_2$ *in situ*. An excess of this ligand was added to *cis*-$[RuCl_2(dppm)_2]$ in the presence of NH_4PF_6. After work up, the pale yellow cation $[Ru\{S_2CN(CH_2CH{=}CH_2)_2\}(dppm)_2]PF_6$ (**20**) was generated in 69% yield (*Scheme 4*). The ^{31}P NMR spectrum showed two new pseudotriplets at –18.4 and –5.3 ppm, with a coupling of 34.3 Hz, indicating the retention of the dppm ligands. In addition, the multiplet resonances for the methylene protons at 4.50 and 4.94 ppm in the ^{1}H NMR spectrum provided confirmation of this. The dithiocarbamate unit gave rise to a multiplet at 4.09 ppm for the NCH_2 moiety, and resonances for the the alkene protons were observed to lower field at 5.24 ($=CH^A$), 5.31 ($=CH^B$) and 5.61 ($=CH^C$) ppm. Further confirmation of the formulation of **20** was provided by a molecular ion in the electrospray mass spectrum (+ve mode) at *m/z* 1042 and the values obtained for elemental analysis, which were in good agreement with calculated values.

Having demonstrated that complexation to a 'Ru$(dppm)_2$' unit was facile, the coordination of the diallyl-DTC ligand to group 8 alkenyl complexes was explored. Although many ruthenium dithiocarbamate compounds are known, no examples have been reported with the allyl-terminated ligands used here.

An orange solution of $[Ru(CH{=}CHBu^t)Cl(CO)(BTD)(PPh_3)_2]$ in dichloromethane was treated with a slight excess of $KS_2CN(CH_2CH{=}CH_2)_2$. On addition, a rapid decolourisation occurred and a pale yellow solution was formed which, after work up, produced a pale yellow solid. The ^{31}P NMR spectrum showed a new singlet at 39.7 ppm and retention of the alkenyl ligand was apparent by a singlet at 0.39 ppm in the ^{1}H NMR spectrum (^{t}Bu). Resonances for the alkenyl protons at 4.58 (J_{HP} = 1.8 Hz) and 6.30 (J_{HP} = 2.7 Hz) ppm, showing mutual coupling of 16.4 Hz as well as coupling to the phosphorus nuclei were also observed. Additionally, the inequivalent NCH_2 protons gave rise to doublets at 3.31 and 3.79 ppm, while doublets for the allylic protons were observed at 4.74 (1H), 4.87

(1H), 5.01 (2H) ppm as well as a multiplet for the =CH^C protons at 5.37 (2H) ppm. Analysis by infrared spectroscopy showed typical features for dithiocarbamate (ν_{CN} at 1479 cm^{-1}) and triphenylphosphine ligands, as well as an intense absorption at 1901 cm^{-1} for the carbonyl ligand. The overall composition was established as [Ru(CH=CHBu^t){S_2CN(CH_2CH=CH_2)$_2$}(CO)(PPh_3)$_2$] (**21**). This was further confirmed by an abundant molecular ion in the electrospray (+ve ion) mass spectrum at *m/z* 909 and good agreement of elemental analysis with calculated values (*Scheme 4*).

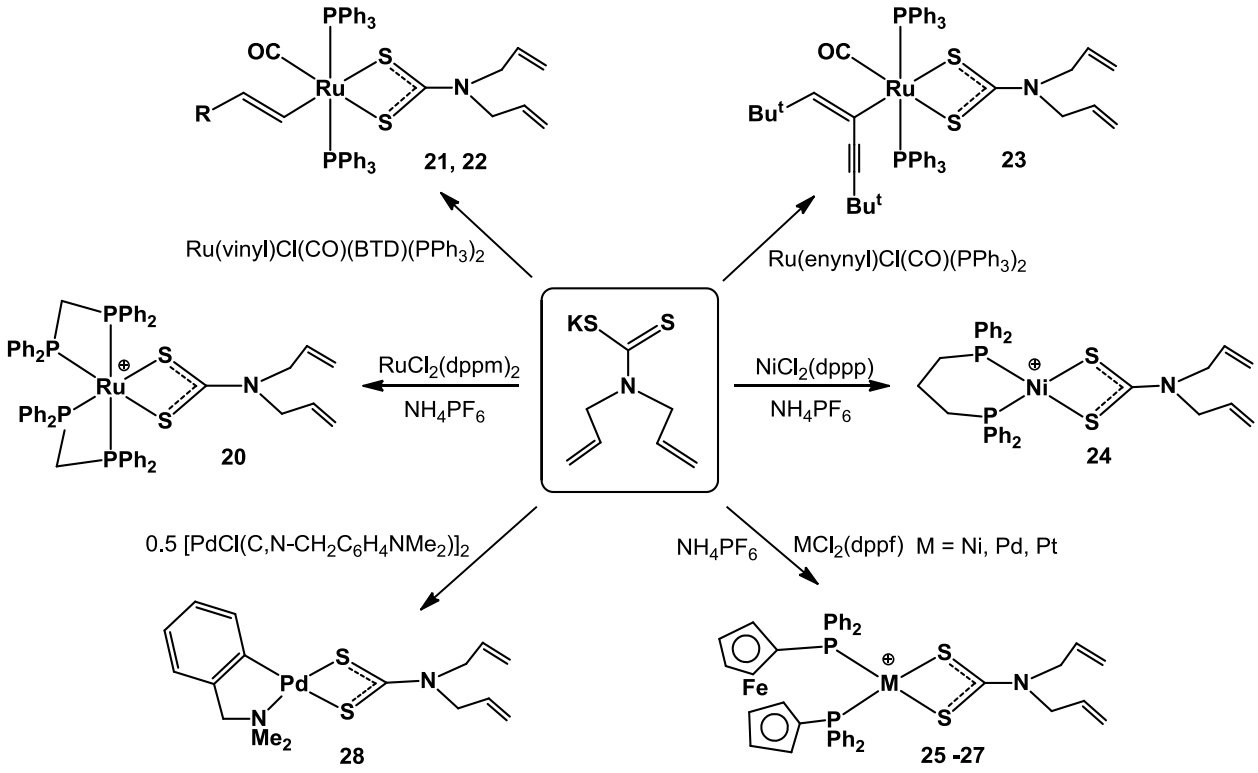

Scheme 4. Preparation of diallyldithiocarbamate complexes, R = Bu^t (**21**), C_6H_4Me-4 (**22**); BTD = 2,1,3-benzothiadiazole.

Compounds [Ru(CH=CHC$_6$H$_4$Me-4){S_2CN(CH_2CH=CH_2)$_2$}(CO)(PPh_3)$_2$] (**22**) and [Ru(C(C≡CBu^t)=CHBu^t){S_2CN(CH_2CH=CH_2)$_2$}(CO)(PPh_3)$_2$] (**23**) were prepared using a similar approach, in moderate yields. Their formulation was confirmed by spectroscopic and analytical data. Single crystals of **22** were grown and studied by X-ray crystallography (see *Fig. 38* and *Structural Discussion, 3.3*).

The investigation of other metal units with different coordination geometries was subsequently attempted in order to provide a comparison so a range of group 10 compounds was chosen for reaction with the diallyl-DTC ligand. An excess of $KS_2CN(CH_2CH=CH_2)_2$ was added to

the square planar nickel complex [$NiCl_2$(dppp)] (dppp = 1,3-bis(diphenylphosphino)propane) in the presence of NH_4PF_6 to afford an orange complex. This was formulated as [Ni{$S_2CN(CH_2CH=CH_2)_2$}(dppp)]PF_6 (**24**) after analysis by NMR spectroscopy. The diphosphine ligand gave rise to two multiplets in the ^{1}H NMR spectrum at 2.18 and 2.68 ppm along with doublets at 4.15 ppm (J_{HH} = 6.2 Hz), 5.23 (J_{HH} = 17.1 Hz), 5.33 (J_{HH} = 10.2 Hz) and 5.67 ppm (multiplet) for the diallyldithiocarbamate ligand. The overall formulation was supported by a molecular ion at *m/z* 642 and good agreement of elemental analysis with calculated values (*Scheme 4*). Single crystals of **24** were grown and a structural investigation undertaken (see *Fig. 40* and *Structural Discussion, 3.3*).

Complexes bearing the dppf ligand (1,1'-bis(diphenylphosphino)ferrocene) were prepared in a similar fashion. The compounds [MCl_2(dppf)], were used to produce compounds of all three metals of group 10, namely [M{$S_2CN(CH_2CH=CH_2)_2$}(dppf)]PF_6 (M = Ni, **25**; M = Pd, **26**; M = Pt, **27**). As expected, the complexes displayed similar spectroscopic features with the cyclopentadienyl protons resonances appearing at 4.59 and 4.69 ppm as two broad singlets in each case. In addition, compound **27** displayed a characteristic J_{PtP} coupling of 3367 Hz in the ^{31}P NMR spectrum.

A further palladium example was synthesised from the [Pd(*C*,*N*-$C_6H_4NCH_2Me_2$)Cl]$_2$ dimer. The resulting organometallic complex [Pd(*C*,*N*-$C_6H_4NCH_2Me_2$){$S_2CN(CH_2CH=CH_2)_2$}] (**28**), showed typical resonances for the [$S_2CN(CH_2CH=CH_2)_2$]$^-$ ligand in the ^{1}H NMR spectrum. In addition, resonances for the cyclometallated ligand were also observed; two singlets at 2.93 and 4.02 ppm corresponding to the methyl and methylene groups respectively, along with a multiplet for the aromatic protons (*Scheme 4*).

3.2.1.1. Ring-closing metathesis reactions of diallyl DTCs complexes

As highlighted earlier, the interest in introducing functionality into the pendant arms of DTCs was aimed at utilizing this additional centre of reactivity within the complex. The next stage of the investigation was to probe the chemistry of the pendant allyl units of coordinated diallyl dithiocarbamate using ring-closing metathesis.

Ring-closing alkene metathesis (or RCM) is a powerful tool used extensively in the area of natural product synthesis for the straightforward preparation of small and medium sized rings and heterocycles.[129] This well-established method involves the use of coordinatively unsaturated precatalysts. The 16-electron nature of these precatalysts can prove problematic in the metathesis of olefin molecules bearing unprotected amines. The amine lone pair and and alkene moiety are found to compete for the coordination of the catalyst metal centre. In order to prevent this, electron-withdrawing

substituents can be introduced to the amine in order to favour alkene coordination.[130] Another approach is to coordinate the amine lone pair to a Lewis acid such as $Ti(OPr^i)_4$ before metathesis is carried out.[131] However, this issue is not encountered in DTCs formed from olefinic amines as the nitrogen lone pair is delocalised and involved in bonding within the DTC unit (double bond character is observed in the N-C bond), thus the reactivity is directed solely towards the pendent alkene moiety.

A further factor which could affect RCM of the complexes described here is that the C-N double bond character of the DTC unit prevents free rotation about this bond. However in this study it was found that a wide range of metal complexes of the diallyldithiocarbamate ligand easily undergo ring-closing metathesis catalysed by $[Ru(=CHPh)Cl_2(SIMes)(PCy_3)]$ (SIMes = 1,3-bis(2,4,6-trimethylphenyl)imidazolium-2-ylidene), including ones bearing surprisingly sterically bulky co-ligands.[106] *Figure 34* provides a comparison of the steric attributes of the co-ligands investigated in this study (excluding the diallyl DTC ligand).

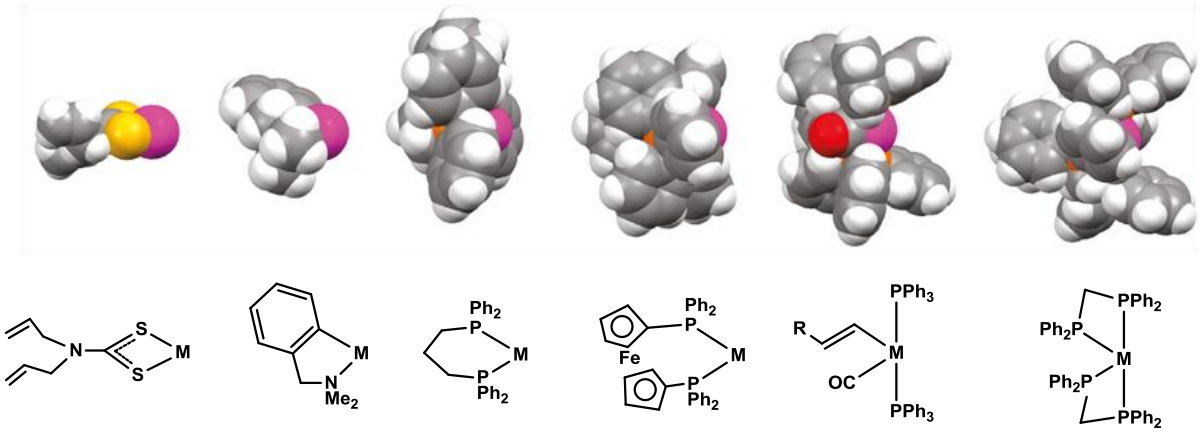

Figure 34. Steric profiles of co-ligand sets in the complexes chosen to investigate ring-closing metathesis; R = C_6H_4Me-4.[106]

At first, the simple homoleptic compounds, $[Ni\{S_2CN(CH_2CH{=}CH_2)_2\}_2]$ (**34**) and $[Co\{S_2CN(CH_2CH{=}CH_2)_2\}_3]$ (**35**), were investigated. These compounds were prepared by literature methods (and hitherto unavailable NMR data recorded).[124] All RCM reactions were carried out under nitrogen. Complex **34** was treated with 5 mol % of the catalyst $[Ru(=CHPh)Cl_2(SIMes)(PCy_3)]$ per dithiocarbamate ligand (10 mol % overall) in dry, degassed dichloromethane. After two hours, the ^1H NMR spectrum showed that only negligible amounts of the starting material had remained, and instead the spectrum displayed two singlet resonances at 4.36 and 5.91 ppm. These could be attributed to the methylene and alkene protons, respectively, since these values agreed well with those found in the literature for the $[S_2CNC_4H_6]^-$ ligand.[132] The mass spectrum (ES +ve) did not display a molecular

ion but instead exhibited a peak for $2[M]^+$ at *m/z* 696. However, elemental analysis results confirmed that the 3-pyrroline DTC complex, $[Ni(S_2CNC_4H_6)_2]$ (**36**) had indeed been formed (*Scheme 5*).

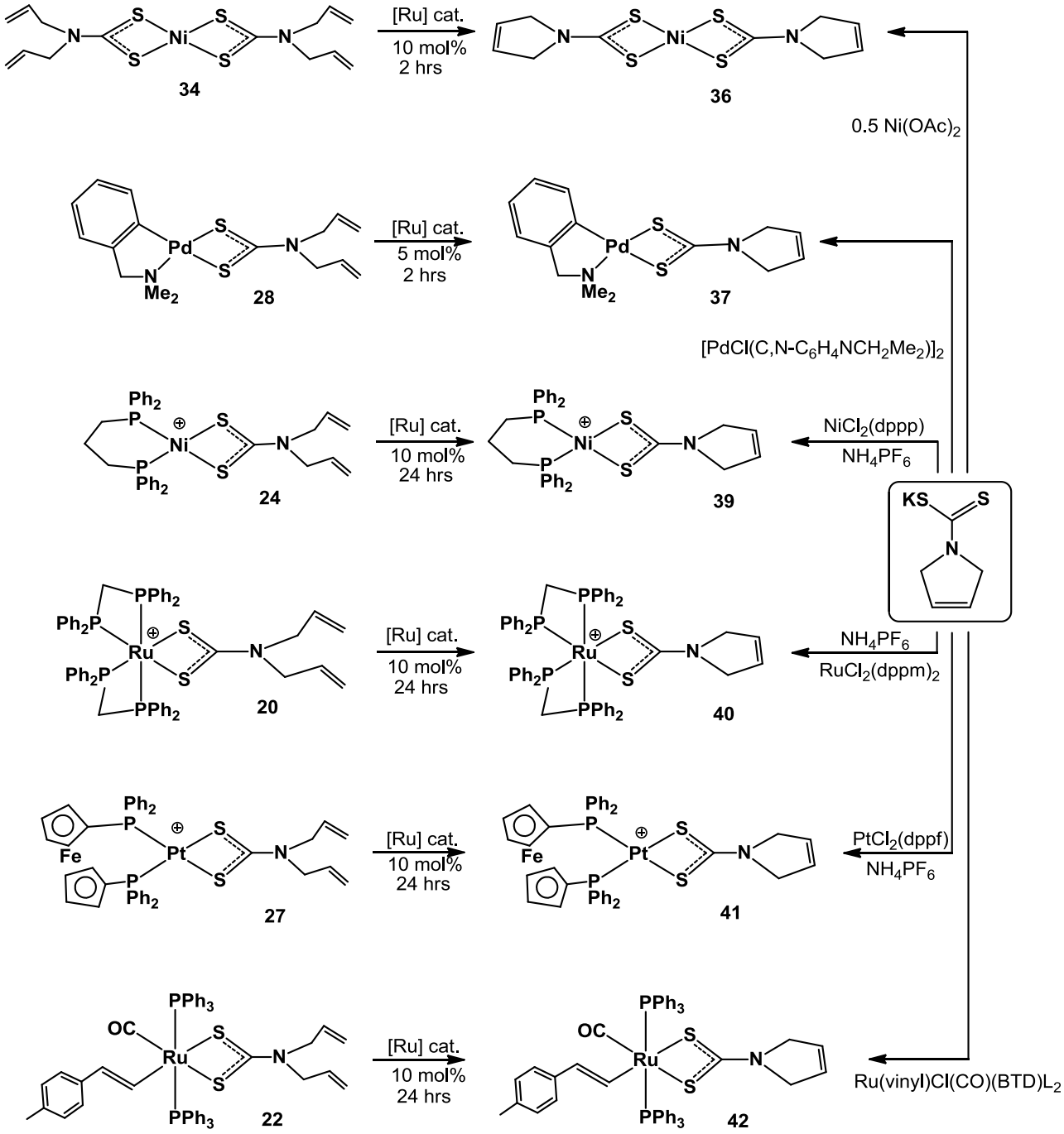

Scheme 5. Ring-closing metathesis and direct routes to 3-pyrroline-dithiocarbamate complexes. [Ru] cat. = $[Ru(=CHPh)Cl_2(SIMes)(PCy_3)]$; BTD = 2,1,3-benzothiadiazole; L = PPh_3.

Preparation of **36** by an alternative route further confirmed its formulation; thus the direct reaction of $Ni(OAc)_2$ with two equivalents of the pre-formed $KS_2CNC_4H_6$[132] resulted in identical data.

Treatment of [Pd(*C*,*N*-$C_6H_4NCH_2Me_2$){$S_2CN(CH_2CH=CH_2)_2$}] (**28**) in the same manner resulted in complete conversion to the ring-closed product [Pd(*C*,*N*-$C_6H_4NCH_2Me_2$)($S_2CNC_4H_6$)] (**37**). A doublet and a multiplet at 4.56 (J_{HH} = 13.5 Hz) and 5.97 ppm were observed in the ^{1}H NMR spectrum for the NCH_2 and alkene protons, respectively, in addition to the resonances for the cyclometallated ligand. Further confirmation of the formation of **37** was provided by the observation of a molecular ion in the mass spectrum (ES +ve) at 385. The same product was also prepared using the direct method described above (*Scheme 5*).

Since both of these successful reactions involved sterically undemanding square planar substrates, the focus of attention turned to the octahedral cobalt complex, [Co{$S_2CN(CH_2CH=CH_2)_2$}$_3$] (**35**), and ring-closing of three diallyl DTC units was attempted. After two hours, no reaction was observed and this remained the case even after 24 hours. Higher catalytic loadings did not affect the reaction either so in order to test whether the product suffered from some sort of instability, [Co($S_2CNC_4H_6$)$_3$] (**38**) was prepared directly from cobalt acetate and $KS_2CNC_4H_6$ (*Scheme 6*). ^{1}H NMR analysis indicated the product was viable as resonances for the 3-pyrroline DTC ligand were observed at 4.48 and 5.91 ppm, similar to those observed for the other complexes of this ligand prepared in this work. Furthermore, mass spectrometry and elemental analysis data confirmed the formulation. Thus, it appears that the octahedral arrangement of the sterically crowded diallyl DTC ligands prevents coordination and subsequent metathesis of the alkene units by the ruthenium alkylidene catalyst in the RCM reaction.

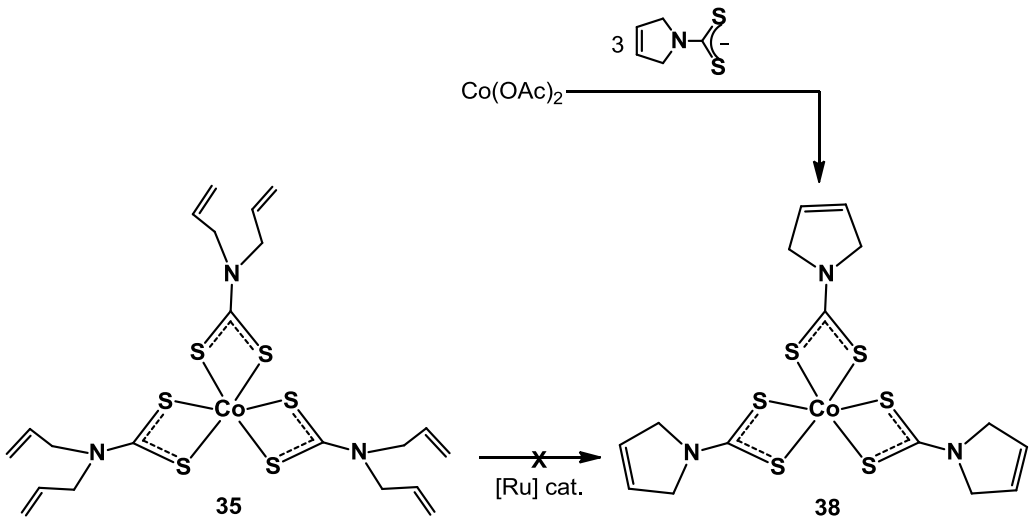

Scheme 6.

After 2 hours, no clear changes in the ^{31}P and ^{1}H NMR spectra were observed in the attempted ring- closing metathesis of [Ni{$S_2CN(CH_2CH=CH_2)_2$}(dppp)]PF_6 (**24**) with 10 mol % of the catalyst. However, after 24 hours the spectroscopic data revealed the formation of [Ni($S_2CNC_4H_6$)(dppp)]PF_6 (**39**). Mass spectrometry and elemental analysis data also agreed with this

formulation. Single crystals of this compound were grown (*Fig. 41*) and the structure determined. The significant structural features of the main cation are discussed in *Structural Discussion, 3.3*. Thus, proof was obtained that metathesis of the coordinated diallyl DTC ligand was possible despite the steric hindrance introduced by the dppp ligand.

The same pattern of reactivity was found with $[Pt\{S_2CN(CH_2CH=CH_2)_2\}(dppf)]PF_6$ (**27**), which underwent ring-closing metathesis with 10 mol % $[Ru(=CHPh)Cl_2(SIMes)(PCy_3)]$ after 24 hours to yield $[Pt(S_2CNC_4H_6)(dppf)]PF_6$ (**41**) in 89% yield. These results illustrate that there seems to be no difference between the reactivity of first and third row transition metal complexes as both seem to undergo metathesis with relative ease.

After 2 hours, under the same reaction condiditions, the bis(dppm) complex $[Ru\{S_2CN(CH_2CH=CH_2)_2\}(dppm)_2]PF_6$ (**20**) did not show any sign of conversion. It was assumed that the sterically demanding nature of the dppm ligand would prove problematic for metathesis, however after 24 hours, conversion to $[Ru(S_2CNC_4H_6)(dppm)_2]PF_6$ (**40**) was shown to be complete. These results indicate that steric factors may slow the reaction but need not prevent RCM from taking place.

Following the successful RCM of complexes bearing robust bidentate chelates (diphosphines and cyclometallated ligands), attention turned to the metathesis reaction of the less robust vinyl complex, $[Ru(CH=CHC_6H_4Me\text{-}4)\{S_2CN(CH_2CH=CH_2)_2\}(CO)(PPh_3)_2]$ (**22**), which comprises a monodentate ligand and additional alkenyl functionality. After 24 hours the transformation was found to be complete and $[Ru(CH=CHC_6H_4Me\text{-}4)(S_2CNC_4H_6)(CO)(PPh_3)_2]$ (**42**) was formed. Due to the lack of symmetry in this molecule, the ^1H NMR spectrum was slightly more complicated than that observed for the other cyclised examples. The NCH_2 protons were identified as two broadened singlets at 3.50 and 3.77 ppm, while the protons of the *E*-alkene gave rise to a singlet resonance at 5.62 ppm. Further confirmation was given by the infrared data which displayed an absorption at 1912 cm^{-1} corresponding to the ν_{CO} stretch. The molecular ion observed in the (ES +ve) mass spectrum at *m/z* 915 was also consistent with the formulation.

In order to confirm the nature of compounds **36** – **42**, they were all prepared directly from 3-pyrroline DTC and the appropriate precursors. Spectroscopic data validated their structures. It is worth noting that the RCM method is significantly cheaper (3-pyrroline is relatively expensive), and therefore this route would be more cost effective if the cyclised products were to be prepared on a larger scale.

3.2.2. Synthesis of methylallyl DTC complexes

An analogous series of DTC complexes bearing both methyl and allyl functionality were also prepared and their spectroscopic features determined (*Scheme 7*). Since these complexes provide only a single site of reactivity on the pendent arms of the DTC unit (in contrast to the the diallyl DTC complexes), they were explored in the investigation of cross metathesis reactions (see *Chapter 3.2.2.1*).

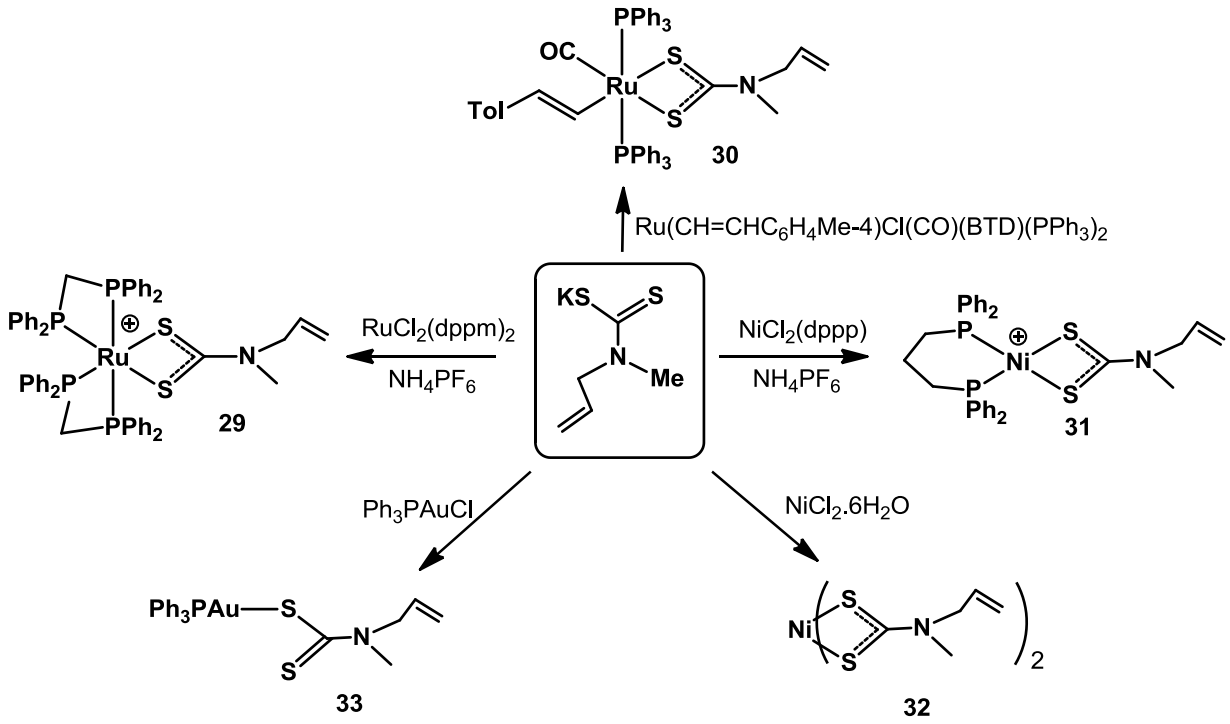

Scheme 7. Preparation of methyallyl dithiocarbamate complexes.

An aqueous solution of the $KS_2CN(CH_2CH{=}CH_2)Me$ ligand was prepared (following the same procedure as for the diallyl ligand preparation).[124] Addition of an excess of this ligand to *cis*-$[RuCl_2(dppm)_2]$ in the presence of NH_4PF_6 provided the pale yellow cation $[Ru\{S_2CN(CH_2CH{=}CH_2)Me\}(dppm)_2]PF_6$ (**29**) in 95% yield (*Scheme 7*). Typical resonances for the dppm ligand in the ^{31}P NMR and ^{1}H NMR were clearly observed. The presence of the dithiocarbamate unit was confirmed by a singlet at 2.93 ppm, corresponding to the NMe protons and a multiplet at 4.06 ppm for the NCH_2 moiety. The alkene protons were observed as resonances to lower field at 5.30 ($=CH^{A,B}$) and 5.58 ($=CH^{C}$) ppm (see *Fig.33* for notation). The overall composition was supported by a molecular ion in the electrospray mass spectrum (+ve mode) at *m/z* 1016 and good agreement of elemental analysis with calculated values.

The alkenyl complex, [Ru(CH=CHC$_6$H$_4$Me-4){S$_2$CN(CH$_2$CH=CH$_2$)Me}(CO)(PPh$_3$)$_2$] (**30**) was generated in a similar fashion. Addition of a slight excess of KS$_2$CN(CH$_2$CH=CH$_2$)Me to [Ru(CH=CHC$_6$H$_4$Me-4)Cl(CO)(BTD)(PPh$_3$)$_2$] in acetone and dichloromethane yielded a pale yellow product after work up. Both ^{31}P NMR and ^{1}H NMR confirmed the formulation of **30**. Interestingly, the ^{1}H NMR spectrum revealed that two isomers of **30** had been generated. Restricted rotation about the N-C bond, due to its partial double bond character, is likely to be the cause of these two isomers:

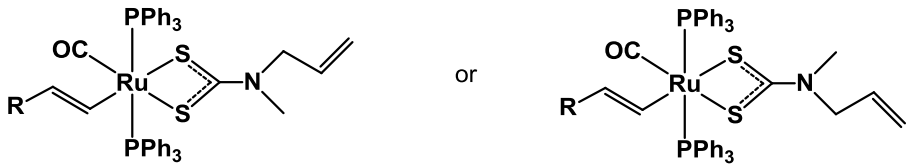

Figure 35. Two isomers of [Ru(CH=CHC$_6$H$_4$Me-4){S$_2$CN(CH$_2$CH=CH$_2$)Me}(CO)(PPh$_3$)$_2$] (**30**).

The isomers were apparent due to the two singlets observed for the NMe protons at 2.40 and 2.60 ppm, and two resonances for the doublets of the NCH$_2$ protons seen at 3.48 and 3.78 ppm. All these resonances integrated to half the expected values compared to the PPh$_3$ resonances. Resonances for the allylic protons further suggested formation of an isomeric mixture. Two doublets at 4.82 and 4.85 ppm were observed for =CH^A and two multiplet resonances at 5.24, 5.32 for =CH^C. A doublet of doublets at 5.01 ppm for the =CH^B protons, integrating to two protons, again suggested two isomers. The overall formulation of **30** was confirmed by an abundant molecular ion in the electrospray (+ve ion) mass spectrum at *m/z* 917 and good agreement of elemental analysis with calculated values (*Scheme 7*). Single crystals of **30** were grown (*Fig. 39*) and a structural study undertaken the results of which are discussed further in *Structural Discussion, 3.3*.

In a similar manner, complexes [Ni{S$_2$CN(CH$_2$CH=CH$_2$)Me}(dppp)]PF$_6$ (**31**), [Ni{S$_2$CN(CH$_2$CH=CH$_2$)Me}$_2$] (**32**) and [Au{S$_2$CN(CH$_2$CH=CH$_2$)Me}(PPh$_3$)] (**33**) were prepared by treatment of the methylallyl DTC ligand with the corresponding starting materials (*Scheme 7*). The NMR data for **31** showed similar features to that of **24**, along with an additional characteristic methyl singlet (at 3.12 ppm) in the ^{1}H NMR spectrum. As expected, isomers were not observed in the spectrum due to the symmetry of the dppp unit. The bis (DTC) nickel complex **32**, did not display doubling of the resonances, which would indicate isomeric mixtures. The ^{1}H NMR spectrum displayed a singlet at 3.14 ppm (NMe), doublet at 4.20 ppm (NCH$_2$) and resonances for the vinyl moiety (5.30 ppm for =CH^{A,B} and 5.77 ppm for =CH^C), confirming the formulation of **32**. Further support was given by the mass spectrum and elemental analysis.

The ^{1}H NMR spectrum of **33** displayed the expected resonances for the methylallyl DTC unit (singlet at 3.45 ppm for NMe, doublet at 4.62 ppm for NCH$_2$, two multiplets at 5.26, 5.29 ppm for =CH^{A,B} and a multiplet at 5.96 ppm for =CH^C). In addition, multiplet resonances in the lower field region were assigned to the phenyl protons of the PPh$_3$ ligand. The overall formulation of **33** was

confirmed by an abundant molecular ion in the electrospray (+ve ion) mass spectrum at *m/z* 606 and good agreement of elemental analysis with calculated values (*Scheme 7*).

3.2.2.1. Cross-metathesis reactions of methylallyl DTCs

Given the success of the RCM reactions and the preparation of both diallyl and methylallyl DTC complexes, efforts were made to cross metathesise the terminal alkene moiety. Cross metathesis of the diallyl DTC complex, $[Ru\{S_2CN(CH_2CH=CH_2)_2\}(dppm)_2]PF_6$ (**20**), with methyl acrylate and 10 mol % of the catalyst $[Ru(=CHPh)(SIMes)Cl_2(PCy_3)]$, were unsuccessful as ^1H NMR data revealed the ring closured product, **40**, had been generated instead. Clearly, the close proximity of the pendent allyl units favoured RCM over cross metathesis. Therefore, the reaction was repeated with the methylallyl DTC complex, $[Ni\{S_2CN(CH_2CH=CH_2)Me\}(dppp)]PF_6$ (**31**) in order to avoid this problem. However the cross metathesis reaction was again unsuccessful. An attempt to cross metathesise the less bulky homoleptic complex $[Ni\{S_2CN(CH_2CH=CH_2)Me\}_2]$ (**32**) (which offers two sites of reaction), with higher catalyst loadings, also failed. Experiments with large excess of methyl acrylate also failed to give the desired product. It is likely that further modification of the reaction conditions may need to be implemented as well as employing a metathesis catalyst which favours cross-metathesis.

3.3. Structural Discussion

Compound	**M-S** (Å)	**C-S** (Å)	**C(2)-N(4)** (°)	**S(1)-M-S(3)** (°)	**S(1)-C-S(3)** (°)
3	2.4237(5) 2.4351(5)	1.704(2) 1.717(2)	1.340(3)	71.444(19)	112.03(12)
16	2.4936(4) 2.4661(4)	1.7105(19) 1.7066(19)	1.337(2)	70.346(15)	113.47(10)
22	2.4999(5) 2.4619(4)	1.713(2) 1.707(2)	1.328(3)	70.296(16)	113.29(11)
30	2.4471(4) 2.5229(4)	1.7134(17) 1.7011(18)	1.334(2)	70.124(14)	113.51(9)
24	2.2089 (17) 2.2097(17)	1.723(7) 1.728(7)	1.314(8)	79.24(6)	109.5(4)
39	2.2158(7) 2.2300(7) 2.2286(7) 2.2277(7)	1.722(3) 1.721(3) 1.716(3) 1.717(3)	1.300(3) 1.309(3)	79.45(3) 79.21(3)	111.22(14) 111.65(15)
Vinyl *(Literature)*	*2.466(1)* *2.508(1)*	*1.707(5)* *1.697(6)*	*1.354(7)*	*70.33(4)*	*114.6(3)*

Table 1. Tabulated bond lengths (Å) and bond angles (°) of compounds **3**, **16**, **22**, **24**, **30** and **39**

Vinyl = $[Ru(C(C{\equiv}CPh){=}CHPh)(S_2CNC_4H_8NH_2)(CO)(PPh_3)_2]Cl$

Single crystals of dithiocarbamate compounds **3**, **16**, **22**, **24**, **30** and **39** were grown and structural studies undertaken. The structures are shown in *Figures 36-41*. Only selected protons are shown and all hexafluorophosphate anions are omitted.

A distorted octahedral geometry is observed in the crystal structure of **3**, with the *cis*-interligand angles appearing between the range 71.444(19) to 103.630(19)° (*Fig. 36).* The Ru–S distances, S(1)–C(2)–S(3) and S(1)–Ru–S(3) angles (*Table 1*), all correlate well with the bimetallic complex $[\{(dppm)_2Ru\}_2(S_2CNC_4H_8NCS_2)]^{2+}$.[109] The C–S and C(2)–N(4) distances both suggest considerable multiple bond character, and in the latter case, can be traced back to the contribution of the thioureide resonance form of the DTC ligand (*Fig. 3*). Delocalisation throughout the S_2CN unit also gives rise to the planar geometry observed.

Similar features were found in **16** (*Fig. 37*). However, the Ru–S distances were longer than those found in complex **3**, reflecting the greater *trans* influence of the carbonyl and alkenyl ligands compared to the phosphorus donors of the dppm ligands. Moreover, the Ru-S(1) distance was elongated significantly more than the Ru-S(3) distance, reflecting the greater *trans* influence of the

alkenyl ligand over that of the carbonyl ligand. A similar elongation of the Ru–S distance opposite the alkenyl ligand over that *trans* to the carbonyl is also found in the other two ruthenium vinyl examples (**22** and **30**) as well as the vinyl literature complex $[Ru(C(C{\equiv}CPh){=}CHPh)(S_2CNC_4H_8NH_2)(CO)(PPh_3)_2]Cl$.[133]

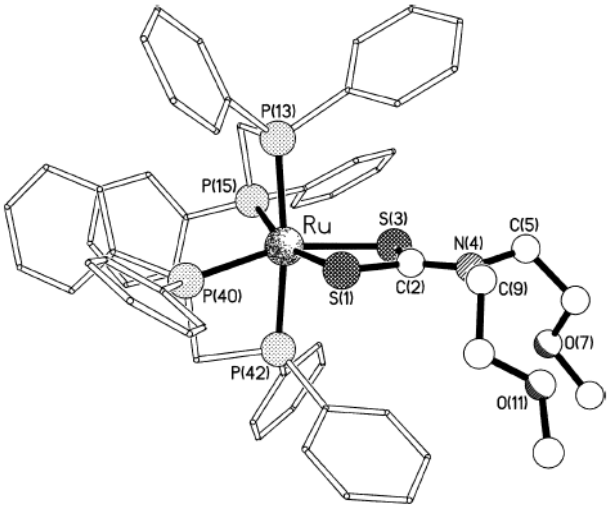

Figure 36. The molecular structure of the cation in $[Ru\{S_2CN(CH_2CH_2OMe)_2\}(dppm)_2]PF_6$ **(3)**. Selected bond lengths (Å) and angles (°); Ru–S(1) 2.4237(5), Ru–S(3) 2.4351(5), Ru–P(13) 2.3541(5), Ru–P(15) 2.3344(5), Ru–P(40) 2.3207(5), Ru–P(42) 2.3233(5), S(1)–C(2) 1.704(2), C(2)–S(3) 1.717(2), C(2)–N(4) 1.340(3), S(1)–Ru–S(3) 71.444(19), S(1)–C(2)–S(3) 112.03(12).

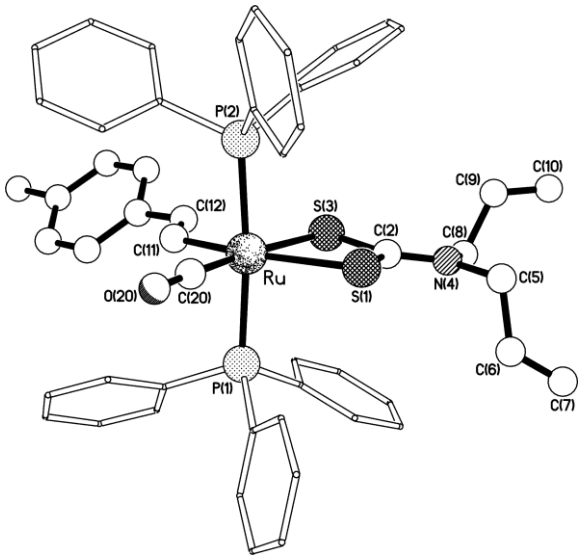

Figure 37. The molecular structure of $[Ru(CH{=}CHC_6H_4Me\text{-}4)\{S_2CN(CH_2CH_2OMe)_2\}(CO)(PPh_3)_2]$ (**16**). Selected bond lengths (Å) and angles (°): Ru–S(1) 2.4999(5), Ru–S(3) 2.4619(4), Ru–P(1) 2.3689(5), Ru–P(2) 2.3607(5), Ru–C(11) 2.088(2), Ru–C(20) 1.845(2), S(1)–C(2) 1.713(2), C(2)–N(4) 1.328(3), C(2)–S(3) 1.707(2), C(6)–C(7) 1.311(5), C(9)–C(10) 1.308(4), C(11)–C(12) 1.336(3), S(1)–Ru–S(3) 70.296(16), P(1)–Ru–P(2) 174.402(17), S(1)–C(2)–S(3) 113.29(11), Ru–C(11)–C(12) 125.77(15).

The crystal structures of **22** and **30** showed very similar features to those in the structure of **16** (all three are vinyl complexes). Again, the characteristically longer Ru-S(1) bond *trans* to the alkenyl group observed in both cases, reflects the greater *trans* influence of the alkenyl ligand over that of the carbonyl (*Fig. 38 and 39*). Other bond data associated with the complex are unremarkable. It is worth noting that although the ^{1}H NMR spectroscopy data revealed that two isomers of **30** had been generated, only a single isomer was found in the crystal selected.

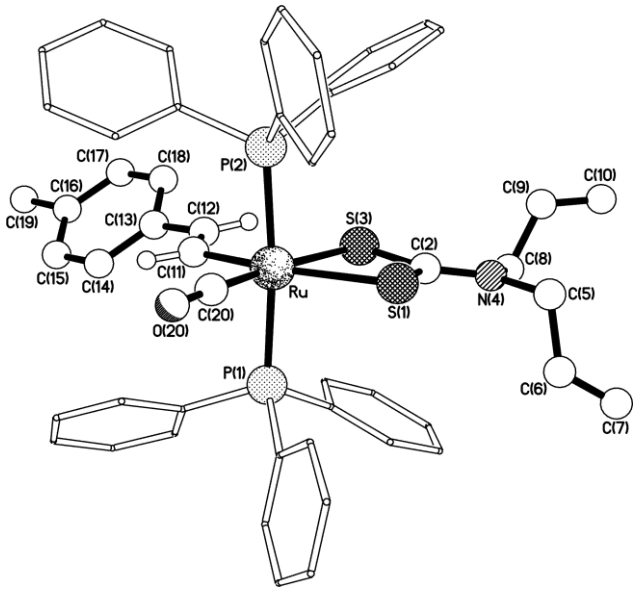

Figure 38. The molecular structure of [Ru(CH=CHC$_6$H$_4$Me-4){S$_2$CN(CH$_2$CH=CH$_2$)$_2$}(CO)(PPh$_3$)$_2$] (**22**). Selected bond lengths (Å) and angles (°): Ru–S(1) 2.4999(5), Ru–S(3) 2.4619(4), Ru–P(1) 2.3689(5), Ru–P(2) 2.3607(5), Ru–C(11) 2.088(2), Ru–C(20) 1.845(2), S(1)–C(2) 1.713(2), C(2)–N(4) 1.328(3), C(2)–S(3) 1.707(2), C(6)–C(7) 1.311(5), C(9)–C(10) 1.308(4), C(11)–C(12) 1.336(3), S(1)–Ru–S(3) 70.296(16), P(1)–Ru–P(2) 174.402(17), S(1)–C(2)–S(3) 113.29(11), Ru–C(11)–C(12) 125.77(15).

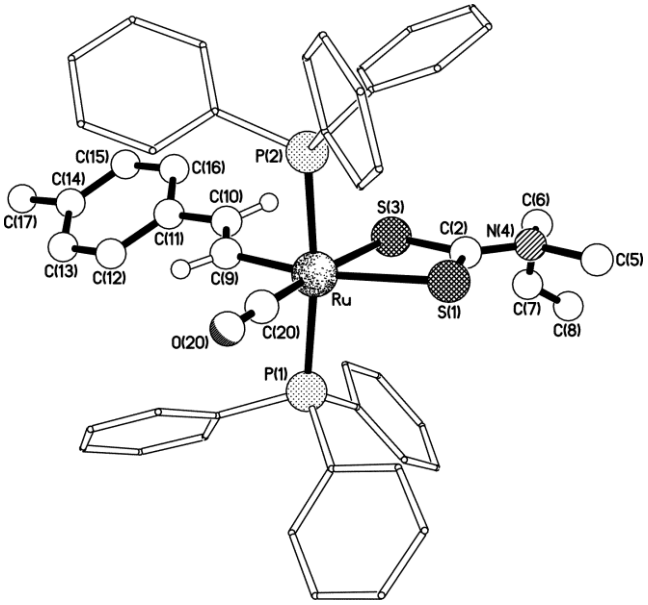

Figure 39. The molecular structure of [Ru(CH=CHC$_6$H$_4$Me-4){S$_2$CN(CH$_2$CH=CH$_2$)(Me)}(CO)(PPh$_3$)$_2$] (**30**). Selected bond data (distances in Å and angles in degrees): Ru–C(9) 2.0763(16), Ru–S(3) 2.4471(4), Ru–S(1) 2.5229(4), S(1)–C(2) 1.7134(17), C(2)–N(4) 1.334(2), C(2)–S(3) 1.7011(18), C(9)–C(10) 1.338(2), P(2)–Ru–P(1) 172.988(15), S(3) –Ru–S(1) 70.124(14), C(10)–C(9)–Ru 127.29 (12), S(3)–C(2)–S(1) 113.51(9).

The geometry at the nickel centre in the structures of both [Ni{S$_2$CN(CH$_2$CH=CH$_2$)$_2$}(dppp)]PF$_6$ (**24**) and [Ni(S$_2$CNC$_4$H$_6$)(dppp)]PF$_6$ (**39**) is distorted square planar, and thus the steric bulk of the phosphine ligand is not in close proximity to the DTC moiety (in contrast to the structures of the octahedral complexes **3**, **16, 22** and **30**). Other data associated with the dppp ligands are similar to those recorded for previous examples of nickel dithiocarbamate compounds in the literature, such as [Ni(S$_2$CNC$_4$H$_8$NH$_2$)(dppp)]$^{2+}$.[19] (*Fig. 40*). Two independent cations are found in the crystal structure of [Ni(S$_2$CNC$_4$H$_6$)(dppp)]PF$_6$ (**39**). The crystal structure of cation A is shown in *Fig. 41* (the crystal structure of cation B can be found in the *Supplementary Information*, *10.1.3*, *Fig. S1*). Unsurprisingly the geometry at the nickel centre is distorted square planar in a similar fashion to that found for the diallyl nickel complex **24**. The C(6)–C(7) distances are consistent with the presence of a double bond in the pyrroline ring and all other features compare well with those found in **24** and the literature complex. The bond angles and bond distances of cations A and B are the same with the exception of the two Ni–S bonds which are the same in cation B [2.2286(7) and 2.277(7) Å], but significantly (statistically) different in A [2.22158(7) and 2.2300(7)Å]. For bond angles and distances of cations A and B, see *Supplementary Information*, *10.1.3*.

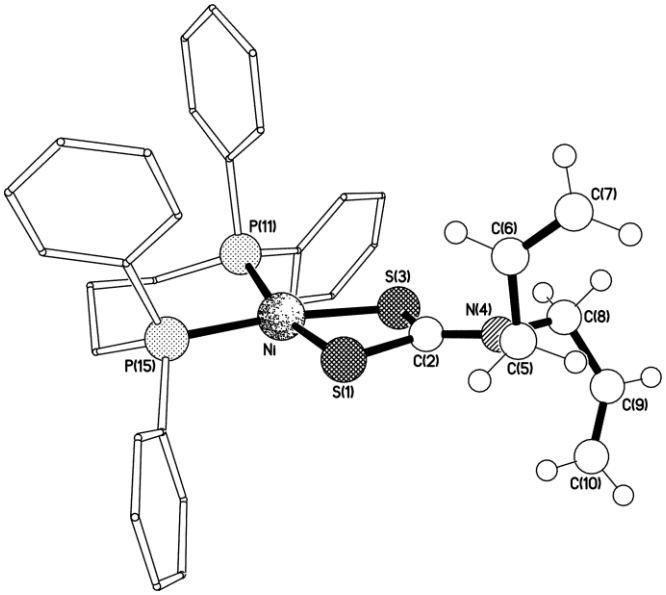

Figure 40. Molecular structure of the cation in [Ni{$S_2CN(CH_2CH{=}CH_2)_2$}(dppp)]PF_6 (**24**)**.** Selected bond data (distances in Å and angles in degrees): Ni–S(1) 2.2089(17), Ni–S(3) 2.2097(17), Ni–P(11) 2.1747(17), Ni–P(15) 2.1788(17), S(1)–C(2) 1.723(7), C(2)–N(4) 1.314(8), C(2)–S(3) 1.728(7), C(6)–C(7) 1.304(11), C(9)–C(10) 1.271(15), S(1)–Ni–S(3) 79.24(6), P(11)–Ni–P(15) 94.56(6), S(1)–C(2)–S(3) 109.5(4).

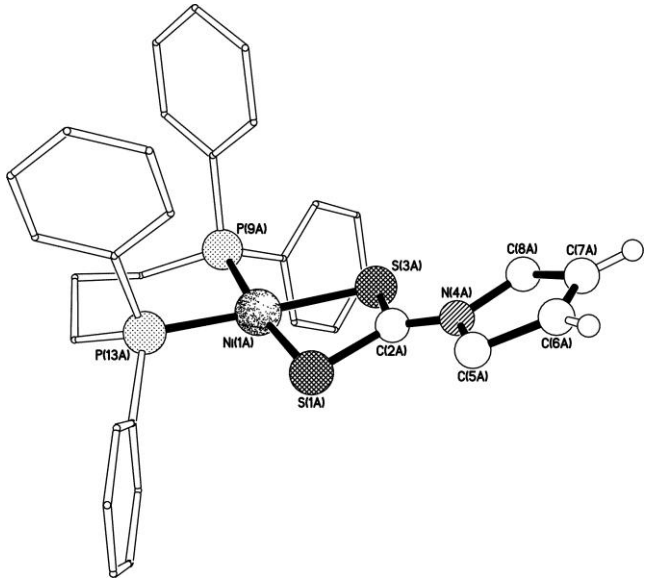

Figure 41. The molecular structure of one (A) of the two crystallographically independent cationic complexes present in the crystals of [Ni($S_2CNC_4H_6$)(dppp)]PF_6 (**39**). Selected bond data (distances in Å and angles in degrees): Ni(1A)–P(13A) 2.1654(7), Ni(1A)–P(9A) 2.1740(7), Ni(1A)–S(1A) 2.2158(7), Ni(1A)–S(3A) 2.2300(7), S(1A)–C(2A) 1.722(3), C(2A)–N(4A) 1.300(3), C(6A)–C(7A) 1.305(5), P(13A)–Ni(1A)–P(9A) 93.81(3), P(13A)–Ni(1A)–S(1A) 92.47(3), P(9A)–Ni(1A)–S(3A) 93.81(3), S(1A)–Ni(1A)–S(3A) 79.45(3), S(3A)–C(2A)–S(1A) 111.22(14).

3.4. Summary

The complexes discussed here represent the first examples of ruthenium and osmium complexes with amine- or methoxy-terminated 'smart' dithiocarbamate ligands ($[S_2CN(CH_2CH_2CH_2NMe_2)_2]^-$, $[S_2CN(CH_2CH_2NEt_2)_2]^-$ and $[S_2CN(CH_2CH_2OMe)_2]^-$). The coordinatively-saturated complexes generated can then be used as a starting point for further chemistry.

Under mildly acidic conditions, the amine-terminated compounds undergo protonation which results in the clean formation of ammonium units. Under acidic conditions, the protonated complexes are rendered more water soluble than their completely insoluble precursors. Because of the commercial availability and low cost of the amines, and the simple preparation of the corresponding dithiocarbamates, these ligands offer an attractive method of introducing additional pendant functionality into a metal complex. The amine units can also be used as protecting groups to shield acid-sensitive co-ligands from cleavage or unwanted reaction during transformations in the presence of acid.

The diallyl dithiocarbamate ligand provides another example of the ability of dithiocarbamates to introduce further functionality into metal complexes. Formerly, only simple, homoleptic compounds of the diallyl dithiocarbamate ligand had been reported, however in this study the ligand has been shown to coordinate successfully to ruthenium σ-alkenyl and bis(dppm) compounds as well as examples of all three group 10 metals.

The pendant allyl groups can act as a site of further reactivity in order to transform the compound as a whole by undergoing ring-closing metathesis to generate cyclic complexes *in situ*. This has been demonstrated by metathesis of a range of diallyl DTCs, which proceeded cleanly (and in some cases rapidly) under mild conditions. Surprisingly the steric environment of the diallyl complexes was shown to have only a modest influence on this reaction.

Chapter 4: Gold(I) dithiocarbamate complexes

4. Chapter 4: Gold(I) dithiocarbamate complexes

Gold dithiocarbamate complexes are known for mono-, di-, and trivalent gold. However, the majority of these reports do not look beyond the commercially available dithiocarbamate ligands. Where this is not the case[134, 135], much interesting chemistry has been uncovered. Shifting the focus from group 8 and 10 transition metal diallyl DTCs, the investigation of the coordination and subsequent reactivity (RCM) of the diallydithiocarbamate ligand was extended to gold(I) complexes. In doing so, the chemistry of these complexes is shown to depart significantly from that found for complexes with metals earlier in the transition series. Through these investigations it was discovered that some of these compounds provide access to gold nanoparticles from molecular dithiocarbamate precursors.

4.1. Synthesis of gold diallyldithiocarbamate complexes

The diallydithiocarbamate ligand, $KS_2CN(CH_2CH=CH_2)_2$, was generated as before from diallylamine and a slight excess of KOH and carbon disulphide. This solution was used in all subsequent reactions and was used immediately before any precipitation of the ligand could occur. An acetone solution of $[(Ph_3P)AuCl]$ was treated with 1.5 equivalents of $KS_2CN(CH_2CH=CH_2)_2$ to yield a yellow product in very high yield. Mass spectrometry (molecular ion at *m/z* 632) and elemental analysis supported the formation of the complex $[(Ph_3P)Au\{S_2CN(CH_2CH=CH_2)_2\}]$ (**43**), formed through displacement of the chloride ligand by a sulphur donor of the dithiocarbamate ligand (*Scheme 8*). ^{31}P NMR spectrum displayed a new singlet at 36.3 ppm, while analysis by ^{1}H NMR spectroscopy showed three multiplet resonances not present in the precursor at 4.59 ppm (NCH_2 protons), 5.25 ppm ($H^{A,B}$) and 5.98 ppm (H^{C}) – for assignments, see *Figure 33*. In this example, discrete couplings could not be reliably identified. To complete the characterization of this molecule, single crystals were grown by vapour diffusion of diethyl ether onto a solution of **43** in dichloromethane and a suitable crystal used for a structural study (see *Fig. 43* and *Structural Discussion, 4.3* for further details).

Complexes bearing phosphines with greater and smaller steric bulk than triphenylphosphine, $[(Cy_3P)Au\{S_2CN(CH_2CH=CH_2)_2\}]$ (**44**) and $[(Me_3P)Au\{S_2CN(CH_2CH=CH_2)_2\}]$ (**45**), respectively, were also prepared. In contrast to the case for **43**, the couplings between the allyl protons in the ^{1}H NMR spectrum were observed clearly in complex **44** with the NCH_2 protons resonating at 4.54 ppm as a doublet (J_{HH} = 5.8 Hz). The doublets of doublets at 5.22 and 5.25 ppm were attributed to the terminal olefinic protons H^{A} (J_{HAHC} = 15.9 Hz) and H^{B} (J_{HBHC} = 8.8 Hz), respectively, and showed a mutual coupling of 1.4 Hz. The remaining allyl proton (H^{C}) was observed as a multiplet at 5.97 ppm. Similar spectroscopic features were observed in the ^{1}H NMR spectrum of

[$(Me_3P)Au\{S_2CN(CH_2CH=CH_2)_2\}$] (**45**) along with a doublet for the protons of the trimethylphosphine ligand (J_{HP} = 11.0 Hz).

The investigation was then broadened to include ligands other than phosphines. Although phosphine ligands are the most common non-sulphur donors in gold(I) chemistry, isocyanide ligands have also been shown to act as good ligands in many examples. A series of complexes bearing these ligands has been shown to display interesting structural diversity, which can be traced to the favourable conditions created for aurophilic contacts due to their relatively slim steric profile (^{t}BuNC, ^{i}PrNC etc.).[136-139] With this in mind, the compound [(^{t}BuNC)$Au\{S_2CN(CH_2CH=CH_2)_2\}$] (**46**) was prepared from [(^{t}BuNC)AuCl] and $KS_2CN(CH_2CH=CH_2)_2$. The isocyanide ligand was identified from the ν_{CN} absorption at 2203 cm^{-1} in the solid state IR spectrum and a singlet at 0.53 ppm (^{t}Bu) in the ^{1}H NMR spectrum, in addition to typical resonances for the dithiocarbamate ligand. No molecular ion was observed in either electrospray or FAB mass spectra, although a fragmentation was observed in the latter for [M –CN^{t}Bu]$^+$ at *m/z* 369. While care must be taken when correlating reactivity with the fragmentations observed in the high-energy environment of a mass spectrometer, loss of isocyanide is also apparent in solution. Over a period of hours in solution, an orange precipitate was observed which was subsequently identified as the homoleptic complex [$Au_2\{S_2CN(CH_2CH=CH_2)_2\}_2$] (**51**), described later. Consequently, good agreement of elemental analysis with calculated values proved impossible.

In order to broaden the range of co-ligands investigated, in particular from a steric viewpoint (metathesis studies), the NHC complex [(IDip)$Au\{S_2CN(CH_2CH=CH_2)_2\}$] (**47**) was prepared in good yield from [(IDip)AuCl] (IDip = 1,3-bis(2,6-diisopropylphenyl)imidazium-2-ylidene) using the same method. Typical resonances for the dithiocarbamate ligand were observed in the ^{1}H NMR spectrum alongside doublets (1.25, 1.41 ppm) and a septet (2.74 ppm) for the isopropyl substituents of the IDip ligand. Resonances for the aromatic protons were also observed at 7.38 and 7.53 ppm, while the HC=CH unit gave rise to a singlet resonance at 7.77 ppm. The overall formulation was confirmed by elemental analysis and mass spectrometry (FAB, +ve mode).

Having demonstrated the facile preparation of monogold species, attempts were made to synthesise a number of digold complexes with the diallydithiocarbamate ligand. [dppa$(AuCl)_2$] (dppa = 1,2-bis(diphenylphosphino)acetylene) is an ideal species for the preparation of linear digold complexes. Because of the rigid nature of the (dppa) ligand, intramolecular Au...Au contacts are unfavourable and therefore a linear geometry is likely to be adopted. This is the case for the bright yellow compound, [(dppa)$\{AuS_2CN(CH_2CH=CH_2)_2\}_2$] (**48**), formed by treatment of [dppa$(AuCl)_2$] with two equivalents of the diallyldithiocarbamate ligand (*Scheme 8*). Spectroscopic data for the dithiocarbamate ligand were found to be similar to those reported for the complexes discussed above,

while the presence of two '$AuS_2CN(CH_2CH{=}CH_2)_2$' units was confirmed by mass spectrometry (molecular ion at *m/z* 1133) and excellent agreement of elemental analysis with calculated values.

Reaction between [(dppf)$(AuCl)_2$] and 2.2 equivalents of $KS_2CN(CH_2CH{=}CH_2)_2$ yielded a pale yellow compound in 80% yield. In contrast to **48**, the flexibility afforded by the ferrocenyl unit suggested the possibility of a metallacyclic species, $[(dppf)Au_2(\mu\text{-}S_2CN(CH_2CH{=}CH_2)_2]^+$, which was supported by the major peak in the FAB mass spectrum at *m/z* 1120. However, integration of the resonances for the protons of the cyclopentadienyl rings at 4.49 and 4.92 ppm in the ^{1}H NMR spectrum with those attributed to the diallyldithiocarbamate ligands ruled this possibility out, as did the elemental analysis values. Thus, the product was formulated as $[(dppf)\{AuS_2CN(CH_2CH{=}CH_2)_2\}_2]$ (**49**, *Scheme 8*). A metallacyclic species was however successfully obtained from [(dppm)$(AuCl)_2$]. The resulting product was initially isolated in poor yield from direct reaction of one equivalent of the dithiocarbamate with this precursor. This synthesis was replaced by an improved one in which the chloride ligands were abstracted with silver triflate prior to addition of $KS_2CN(CH_2CH{=}CH_2)_2$. The product $[(dppm)Au_2\{S_2CN(CH_2CH{=}CH_2)_2\}]OTf$ (**50**) gave rise to similar spectroscopic features as found in the previous complexes apart from a multiplet at 4.74 ppm for the PCH_2P protons. Unfortunately, none of these complexes proved sufficiently crystalline for an X-ray diffraction study to be undertaken.

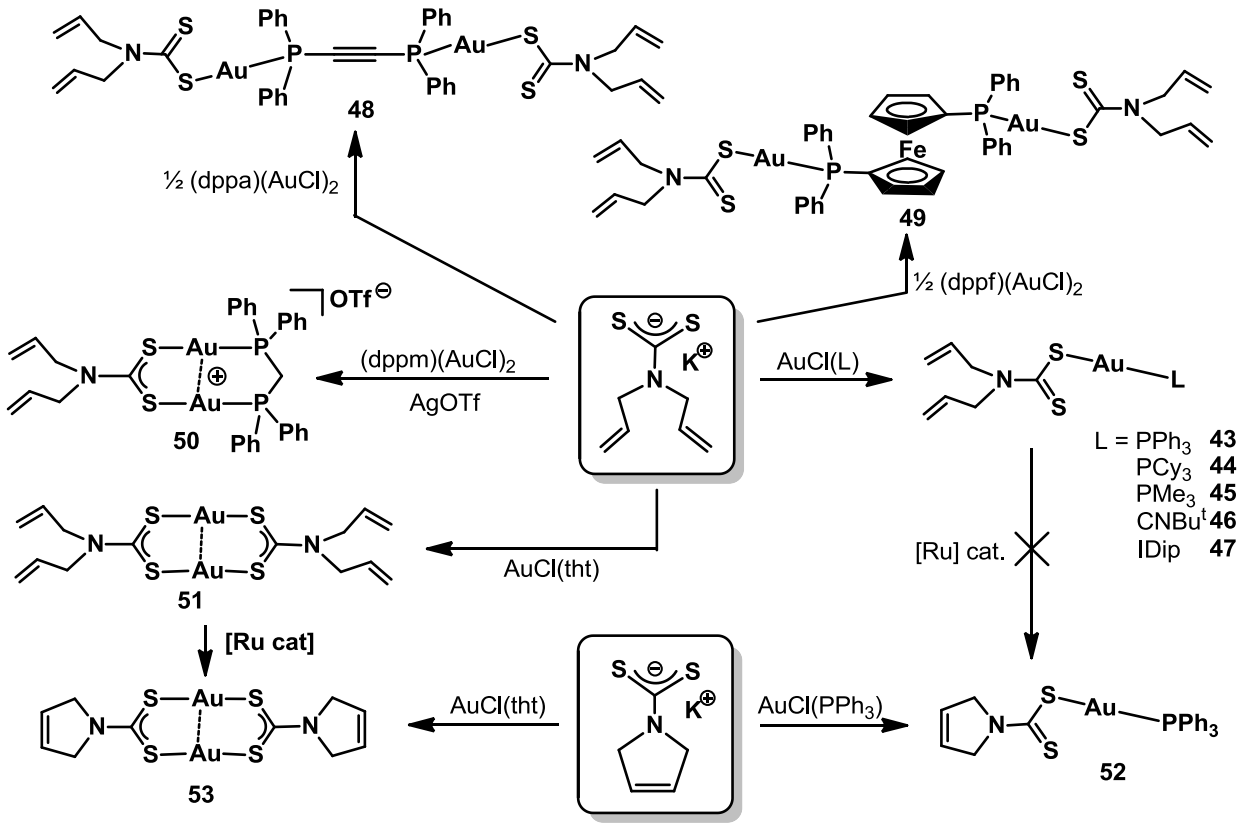

Scheme 8. [Ru] cat. = 10 mol% [$Ru(=CHPh)Cl_2(SIMes)(PCy_3)$]; IDip = 1,3-bis(2,6-diisopropylphenyl)imidazol-2-ylidene)

As mentioned earlier, the complex [(^{t}BuNC)Au{$S_2CN(CH_2CH=CH_2)_2$}] (**46**) spontaneously loses the isocyanide ligand in solution to form the homoleptic species [Au_2{$S_2CN(CH_2CH=CH_2)_2$}$_2$] (**51**). A more direct synthesis of **51** is afforded by reaction of equimolar quantities of [(tht)AuCl] and $KS_2CN(CH_2CH=CH_2)_2$ (*Scheme 8*). The spectroscopic and analytical data for this compound were found to be unremarkable but confirmed the identity of the product. In order to explore the properties of this compound further, single crystals were grown by vapour diffusion of diethyl ether into a dichloromethane solution of the complex and a structural determination was undertaken (see *Fig. 44* and *Structural Discussion, 4.3*).

4.1.1. Ring-closing metathesis reactions

Having demonstrated (*Chapter 3*) for the first time that coordinated dithiocarbamate ligands could be ring-closed even in sterically encumbered environments,[106] the ring-closing metathesis of the gold(I) complexes prepared here were explored. Their linear geometry renders them very open to the approach of the Grubbs second generation metathesis catalyst, [Ru(=CHPh)Cl_2(SIMes)(PCy_3)], however, after stirring [(Ph_3P)Au{$S_2CN(CH_2CH=CH_2)_2$}] (**43**) with 10 mol% of the catalyst for hours and then days under nitrogen, the gold complex appeared unchanged. In order to ascertain whether there was some inherent instability in the ring-closed product, [(Ph_3P)Au($S_2CNC_4H_6$)] (**52**), this was prepared directly from a solution of 3-pyrrolinedithiocarbamate. The ^{1}H NMR displayed singlet resonances at 4.49 (NCH_2) and 5.96 ppm (CH=CH) in addition to aromatic peaks for the coordinated triphenylphosphine. Mass spectrometry and elemental analysis data were also in agreement with the formulation. Establishing that the product was viable, attention returned to the ring-closing metathesis reaction. It was a possibility that the PPh_3 unit could be liberated from **43** and coordinate to the catalyst (causing deactivation, as [Ru(=CHPh)Cl_2(SIMes)(PPh_3)] is known to be far less active), however, no reaction was observed either with [(Cy_3P)Au{$S_2CN(CH_2CH=CH_2)_2$}] (**44**). Eliminating phosphines from the gold substrate entirely with [(^{t}BuNC)Au{$S_2CN(CH_2CH=CH_2)_2$}] (**46**) had no beneficial effect, but did result in deposition of gold metal on the glassware (even under nitrogen).

It appeared that complex **43** was having some deactivating effect on the catalyst, so in order to test this hypothesis, the ring-closing of [Ni{$S_2CN(CH_2CH=CH_2)_2$}] to [Ni($S_2CNC_4H_6$)$_2$] using 10 mol% [Ru(=CHPh)Cl_2(SIMes)(PCy_3)] was attempted. This reaction is known to proceed cleanly in 1-2 hours. However, before the nickel complex was introduced, 10 mol% of **43** was added to the solution of the catalyst in dichloromethane (all under N_2). The reaction of the nickel complex is normally complete after 1 hour. After 1 hour no more **43** was discernible by ^{31}P NMR spectroscopy (d^6-acetone) but two new resonances at 54.9 (major) and 42.4 ppm (minor) were observed (as well as some of the catalyst at 28.8 ppm). In the ^{1}H NMR spectrum, only 8% conversion to the ring closed

nickel product was observed. After 3 days, 58% conversion had been achieved, this remained essentially the same thereafter. After 4 days a third additional, yet significant, peak was seen in the ^{31}P NMR spectrum at 25 ppm (likely to be $O=PPh_3$). In the conventional reaction of $[Ni\{S_2CN(CH_2CH=CH_2)_2\}]$ without any gold complex, the only resonances in the ^{31}P NMR spectrum were at 28.8 (pre-catalyst) and 22.5 (possibly a solvent stabilized catalyst species) ppm. Therefore, it is possible to suggest that a weak adduct is formed between $[Ru(=CHPh)Cl_2(SIMes)(PCy_3)]$ and $[(Ph_3P)Au\{S_2CN(CH_2CH=CH_2)_2\}]$ (**43**) which gives rise to a peak at 54.9 ppm (negligible PCy_3 or $O=PCy_3$ were observed in the spectra). Attempts to isolate this species were unsuccessful with only mixtures of the two components retrieved.

A clear difference in the ring-closing activity seen in the diallyldithiocarbamate complexes of groups 8-10, is that these all examples contained bidentate dithiocarbamate ligands, whereas the same ligand exhibits a monodentate mode in complexes **43** – **47**. Preferential coordination of a lone pair on the pendant sulphur to the vacant site at the ruthenium centre could lead to deactivation of the catalyst towards alkenes. To test this, $[Au_2\{S_2CN(CH_2CH=CH_2)_2\}_2]$ (**51**), in which both sulphurs are coordinated, was treated with 10 mol% $[Ru(=CHPh)Cl_2(SIMes)(PCy_3)]$ in dichloromethane under nitrogen. After 2 hours, analysis of the product revealed no resonances for **51**, instead two new peaks were observed at 4.52 and 6.00 ppm, corresponding to the NCH_2 and CH=CH protons of the ring closed product, $[Au_2(S_2CNC_4H_6)_2]$ (**53**). The nature of this product was confirmed by mass spectrometry (ES +ve mode) and elemental analysis (*Scheme 8*). Furthermore, **53** was also prepared directly from [(tht)AuCl] and 3-pyrrolinedithiocarbamate.

4.2. Functionalised gold nanoparticles

The reduction of well-defined gold(I) precursors containing phosphine,[140] amine[141] and most recently, carbene[142] ligands has been shown to yield surface-stabilised gold nanoparticles. Very recently, Selvam and Chi reported the thermal preparation (140 °C) of thiol-coated gold nanoparticles from molecular gold(I) precursors in the presence of thiol surfactants.[143] This illustrated that molecular gold(I) precursors could be used in nanoparticle preparation rather than *in situ* reduction of gold(III) salts.

Dithiocarbamate ligands have been shown to make excellent surface units for gold nanoparticles. [74, 75, 77, 78, 144, 145] Accordingly it was decided to explore the preparation of nanoparticles from $[Au_2\{S_2CN(CH_2CH{=}CH_2)_2\}_2]$ (**51**) using aqueous sodium borohydride as the reducing agent (*Scheme 9*). On addition of this reagent to an acetone solution of **51**, an immediate darkening occurred, leading to precipitation of a black solid. After purification, the material was analyzed by solid state infrared spectroscopy to show absorptions similar to those observed for the dithiocarbamate ligand in the precursor. However, the ^{1}H NMR spectrum revealed resonances characteristic of the diallyldithiocarbamate ligand at 4.06, 4.94, 4.99 and 5.53 ppm, shifted from the positions found in **51**. Transmission Electron Microscopy (TEM) showed nanoparticles of $Au@S_2CN(CH_2CH{=}CH_2)_2$ (**NP1**) (*Fig. 42a*) of diameter 4.8 nm (± 0.7 nm). The size distribution is similar to that found for previous preparations of dithiocarbamate passivated nanoparticles using the Brust-Schiffrin method (*in situ* reduction of gold(III) in the presence of a phase transfer agent and thiol).

In contrast to the work by Selvam and Chi,[143] the size of the nanoparticles is surprisingly small for the low ratio of gold to surface unit dictated by the stoichiometry of the $[Au_2(DTC)_2]$ compound. Normally, this would lead to larger nanoparticles as seen for $Au(CH_3)(PPh_3)$/thiol (2:1 ratio, 15.7 nm ± 1.3 nm). This discrepancy may well be due to differences between the mechanism of nanoparticle growth in the presence of thiolate and dithiocarbamate surface units.

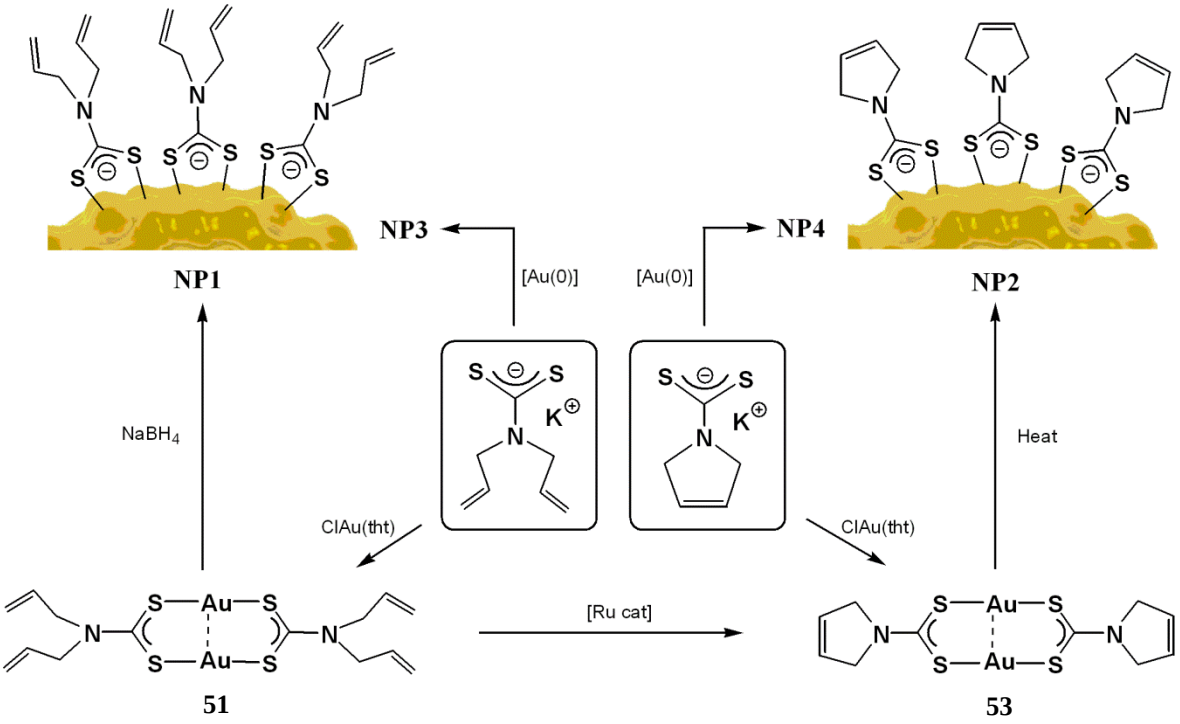

Scheme 9. [Ru cat] = 10 mol% [Ru(=CHPh)Cl_2(SIMes)(PCy_3)]; tht = tetrahydrothiophene.

It was found that a solution of [$Au_2(S_2CNC_4H_6)_2$] (**53**) (formed by ring-closing of **51**), spontaneously converted to gold nanoparticles on gentle warming. The process was complete after 30 mins and analysis of the black material by IR and ^{1}H NMR spectroscopy revealed it to be Au@$S_2CNC_4H_6$ (**NP2**). The TEM image of this material (*Fig. 42b*) showed dispersed nanoparticles of diameter 4.0 nm (± 0.7 nm). This result complements that involving the thermolysis of Au(CH_3)(PPh_3) in the presenceof thiol surfactants, but under much milder conditions than the 140 °C used previously.

The citrate reduction of $HAuCl_4$ is a well known method used to prepare nanoparticles in the 15-20 nm diameter range.[146] In earlier work, it has been demonstrated that the citrate shell can be successfully displaced by dithiocarbamate units prepared in situ.[20, 79, 145] Using this approach, Au@$S_2CN(CH_2CH{=}CH_2)_2$ (**NP3**) nanoparticles of diameter 13.7 nm (± 3.6 nm) were prepared (*Fig. 42c*). After repeated washing with water to remove citrate and uncoordinated dithiocarbamate, analysis by infrared and ^{1}H NMR spectroscopy revealed the presence of the diallyldithiocarbamate surface units. TEM imaging showed a surprisingly large size distribution. Using the same citrate reduction approach, Au@$S_2CNC_4H_6$ (**NP4**) nanoparticles were also prepared (*Fig. 42d*), which showed a much narrower range of diameters (15.0 ± 1.8 nm). Again, the presence of the 3-pyrroline-dithiocarbamate surface units was confirmed by ^{1}H NMR and infrared spectroscopy.

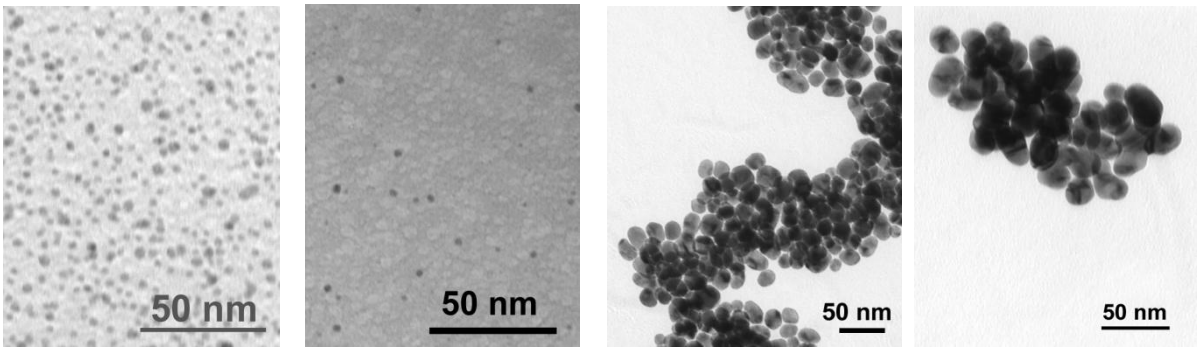

a) **NP1** (4.8 ± 0.7 nm) b) **NP2** (4.0 ± 0.7 nm) c) **NP3** (13.7 ± 3.6 nm) d) **NP4** (15.0 ± 1.8 nm)

Figure 42. TEM of Au@$S_2CN(CH_2CH{=}CH_2)_2$ (**NP1**) and Au@$S_2CNC_4H_6$ (**NP2**) nanoparticles prepared directly and Au@$S_2CN(CH_2CH{=}CH_2)_2$ (**NP3**) and Au@$S_2CNC_4H_6$ (**NP4**) nanoparticles prepared *via* a citrate stabilised intermediate.

Under similar conditions, heating **43** or **44** (or treating with $NaBH_4$) only led to deposition of gold metal rather than formation of nanoparticles. This suggests that there is an advantage possessed by the metallacyclic compounds (**51** and **53**) in this process. It is tempting to imagine that the existence of the $Au_2(DTC)_2$ metallacycle provides a degree of pre-organisation which favours the formation of the nanoparticle material. This phenomenon has been postulated to play a role in the formation of gold nanowires from [(oleylamine)AuCl] complexes.[141]

In a similar way in which the fate of the thiol proton is unclear in many thiol/thiolate-capped gold nanoparticles[147, 148], the nature of the interaction between the dithiocarbamate and the gold surface has not been elucidated in detail. Energy Dispersive X-ray Spectroscopy (EDX) analysis failed to reveal the presence of sodium (**NP1**) or potassium ions (**NP3**, **NP4**) acting as countercations to the anionic dithiocarbamate. **NP2** was obtained directly and spontaneously from heating the $[Au_2(S_2CNC_4H_6)_2]$ (**53**) precursor in the absence of sodium borohydride. In this case, it was initially postulated that electroneutrality in this material could be provided by $[H_2N(C_4H_6)]^+$ cations formed from the decomposition of excess surface units, however, no evidence for these units (e.g., IR, ^{1}H NMR spectroscopy) has been found.

Once nanoparticles of different sizes bearing both $[S_2CN(CH_2CH{=}CH_2)_2]^-$ and $[S_2CNC_4H_6]^-$ surface units had been prepared, investigations took place to attempt to ring-close nanoparticles **NP1** and **NP3** to generate **NP2** and **NP4**, respectively. The approximate coverage of the nanoparticles with the surface units was calculated based on a 70% coverage using a 'footprint' of the ligand estimated from the crystal structure of compound **51**. This allowed a rough concentration to be ascertained.[149] The diallydithiocarbamate-capped nanoparticles were stirred for 2 days with 10 mol% $[Ru(=CHPh)Cl_2(SIMes)(PCy_3)]$ under nitrogen, however, no reaction was apparent. Higher loadings also failed to improve the situation and it is possible that deactivation of the catalyst could be

occurring due to similar interactions as described earlier (interaction of the ruthenium centre with lone pairs on the sulphur donors).

4.3. Structural Discussion

The structural study carried out for complex [(Ph_3P)Au{$S_2CN(CH_2CH=CH_2)_2$}] (**43**) reveals the expected linear geometry at the gold(I) centre [174.980(16) Å]. The bonding mode of the diallyldithiocarbamate ligand is best described as anisobidentate with the Au–S(1) length of 2.3456(4) Å being much shorter than the distance between the gold and the other sulphur donor [S(3)], which is 3.0020(5) Å. The sum of the van der Waals radii for gold and sulphur is 3.46 Å.[150] The difference in the S(1)–C(2) and C(2)–S(3) distances is significant at 1.7436(17) and 1.6971(17) Å, respectively, indicating substantial multiple bond character in the non-coordinating arm of the dithiocarbamate ligand. The C(2)–N(4) length of 1.341(2) Å suggests modest multiple bond character. The other bond lengths of the 1,1-dithio ligand are unremarkable.

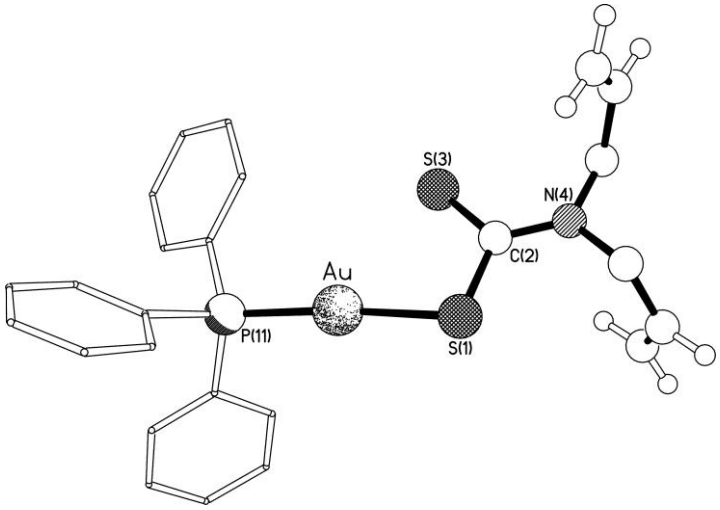

Figure 43. The molecular structure of [(Ph_3P)Au{$S_2CN(CH_2CH=CH_2)_2$}] (**43**). Selected bond lengths (Å) and angles (°); Au–S(1) 2.3456(4), Au–P(11) 2.2517(4), S(1)–C(2) 1.7436(17), C(2)–S(3) 1.6971(17), C(2)–N(4) 1.341(2), S(1)–Au–P(11) 174.980(16), S(1)–C(2)–S(3) 119.97(10).

In contrast to compound **43**, the dithiocarbamate ligands are coordinated in a bridging fashion in the structure of the metallacyclic complex [Au_2{$S_2CN(CH_2CH=CH_2)_2$}$_2$] (**51**). The bonding patterns of the two unique dithiocarbamate ligands are very similar, the Au-S and S-C bond lengths,

and the S-C-S angles all being nearly identical, with the symmetric C-S bond lengths indicating evenly distributed multiple bond character in the CS_2 units, in contrast to compound **43**. The contribution of the thioureide resonance form is observable in the short C(2)–N(4) and C(12)–N(14) distances of 1.338(4) and 1.330(4) Å, respectively.

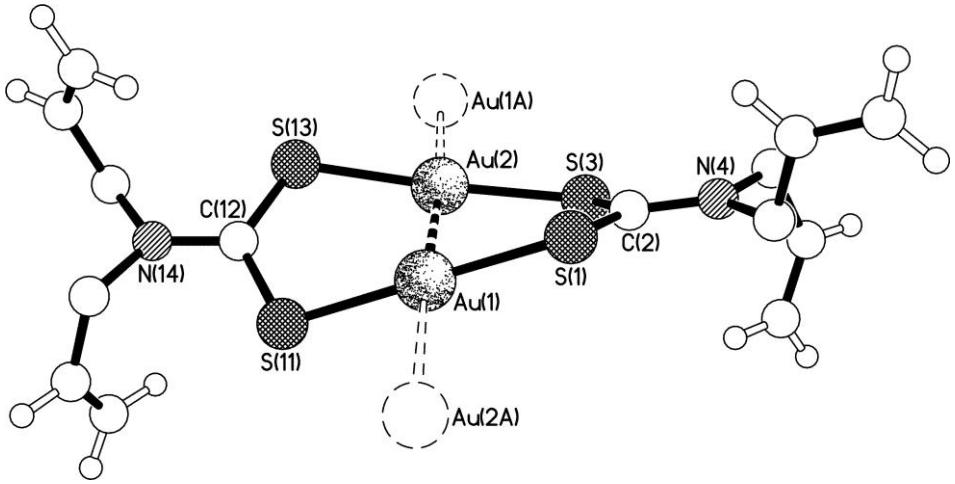

Figure 44. The molecular structure of $[Au_2\{S_2CN(CH_2CH{=}CH_2)_2\}_2]$ (**51**). Selected bond lengths (Å) and angles (°); Au(1)–S(1) 2.2913(8), Au(1)–S(11) 2.2967(8), Au(2)–S(3) 2.2958(9), Au(2)–S(13) 2.2950(9), S(1)–C(2) 1.728(3), C(2)–S(3) 1.731(3), C(2)–N(4) 1.338(4), S(11)–C(12) 1.734(3), C(12)–S(13) 1.727(3), C(12)–N(14) 1.330(4), Au(1)···Au(2) 2.79030(15), Au(1)···Au(2A) 2.98997(15), Au(2)···Au(1A) 2.98997(15), S(1)–Au(1)–S(11) 177.10(3), S(3)–Au(2)–S(13) 176.41(3), S(1)–C(2)–S(3) 127.1(2), S(11)–C(12)–S(13) 126.5(2).

In such metallacycles, it is common to observe the contribution of aurophilic interactions in the short intramolecular Au···Au distances observed.[151] In complex **51**, a very short Au(1)···Au(2) distance of 2.79030(15) Å is seen. This is shorter than the distance of 2.9617(7) Å found in $[Au_2\{S_2CN(C_5H_{11})_2\}_2]$[152] and substantially below the sum of the van der Waals radii of 3.32 Å.[142] Although the S–Au–S angles are both very close to linear [176.41(3) and 177.10(3)°], on closer inspection, it can be seen the gold(I) centres deviate slightly towards each other, showing that their close proximity is not solely due to the requirements of the bridging ligands. In addition to these intramolecular interactions, surprisingly short intermolecular contacts of 2.98997(15) Å are also observed (*Fig. 45*). This is only slightly longer than the 2.9617(7) Å found in $[Au_2\{S_2CN(C_5H_{11})_2\}_2]$ and a search of the crystallographic literature reveals that the distance in **51** is among the shortest 20% of intermolecular distances observed between gold(I) centres.[153]

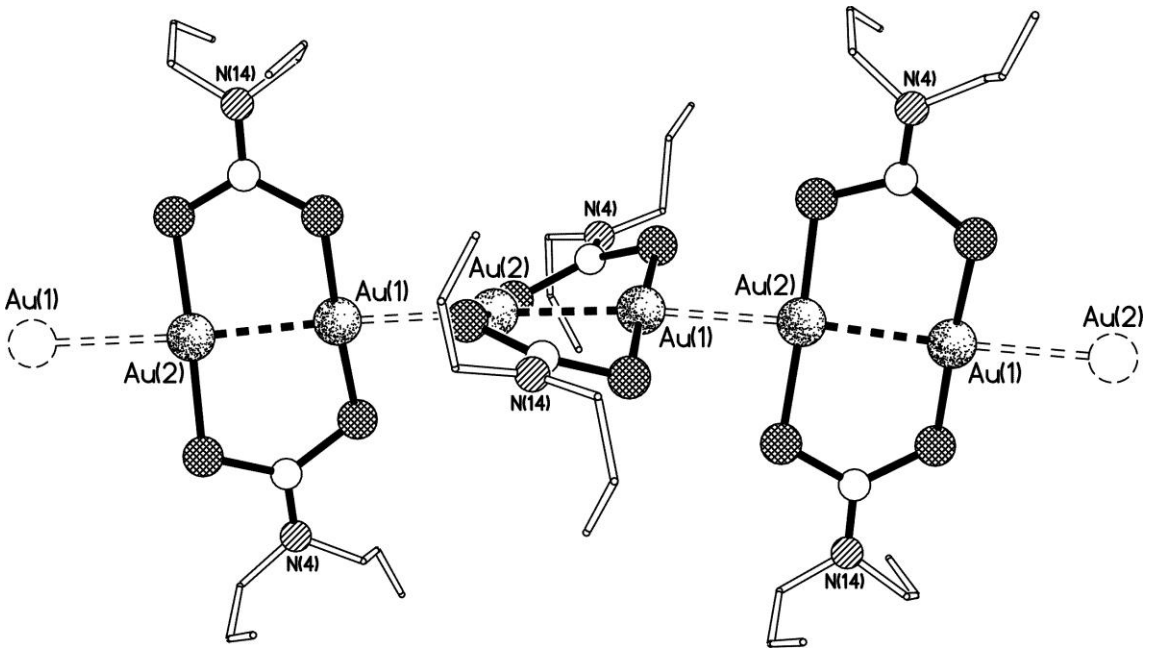

Figure 45. Part of one of the chains of 4_1-screw related molecules that extend along the crystallographic c axis direction present in the structure of **51**. The intra- and intermolecular Au···Au separations are 2.79030(15) and 2.98997(15) Å respectively.

Given that compound **51** forms gold nanoparticles on gentle warming, it is tempting to suggest that the aurophilic contacts[151] present in the precursor may influence the formation of nanoparticles, as it has been postulated in the formation of gold nanowires from [(oleylamine)AuCl] complexes.[141]

4.4. Summary

The diallyl dithiocarbamate ligand is again shown to form a series of stable complexes with gold(I) precursors, bearing phosphine, carbene and isocyanide co-ligands. However the results presented in this chapter illustrate the issues which arise from employing ring-closing metathesis within the coordination environment of gold(I) dithiocarbamate complexes. However, once both sulphur donors have been incorporated into metal-based bonding, ring-closure can take place. For the first time, molecular dithiocarbamate precursors have been used to generate functionalized gold nanoparticles –in one case simply by gentle heating.

Chapter 5: Dithiocarboxylate complexes

5. Chapter 5: Dithiocarboxylate complexes

This chapter demonstrates that imidazol(in)ium-2-dithiocarboxylate ligands have significant, hitherto untapped potential in the field of coordination chemistry. NHCs have been found to be unsuitable ligands for the stabilisation of complexes with high-valent metal centres. Reactions of NHCs with CS_2 yields a versatile ligand class (NHC•CS_2), which combines the attributes of other 1,1-dithio ligands with a variable steric influence on the metal centre.

Exploration of the coordination chemistry of NHC dithiocarboxylate (NHC•CS_2) adducts dates back to 1986 when Borer *et al* showed that 1,3-dimethylimidazolium-2-dithiocarboxylate formed stable complexes with a number of transition metal halides or nitrates.[29, 154] Limited characterisation of these compounds (lack of NMR and structural studies) has contributed to the ambiguous understanding of their structural properties which may be why they have been somewhat overlooked for over twenty years. A recent report in 2009 by Delaude *et al*, described in detail the investigation of ruthenium–arene complexes bearing NHC•CS_2 ligands and compounds with the generic formula [RuCl(S_2C•NHC)(*p*-cymene)]PF_6 (*p*-cymene = 1-isopropyl-4-methylbenzene), which were thoroughly characterised.[28] The study presented in this chapter further investigates the complexation of ruthenium (and osmium) compounds with NHC•CS_2 ligands. The work described here has been published.[155, 156]

Additionally, the reactivity of these betaines with gold(I) systems is also explored. Around the same period, the Wilton-Ely group were investigating the stepwise construction of multimetallic arrays, utilizing zwitterionic dithiocarbamates based on piperazine ($S_2CNC_4H_8NH_2$), whereby the incorporation of gold(I) complexes into multimetallic systems was shown.[19, 20, 79, 109, 145] This work on zwitterions has thus prompted the further study of NHC•CS_2 betaines with gold(I) complexes. Due to the steric tunability and their stability towards loss of the CS_2 moiety, NHC•CS_2 betaines are an attractive choice of ligand with which to explore gold(I) chemistry. Their ability to behave as excellent ligands for monovalent gold complexes, whether homoleptic or with a range of phosphorus- or carbon-based co-ligands, is demonstrated and herein the first examples of a range of gold(I) NHC•CS_2 compounds are presented. The study is further developed to show their behaviour as stable surface units for gold nanoparticles in a similar manner to that of dithiocarbamates. The work here, on the coordination chemistry of gold(I) with the NHC•CS_2 ligand, has also recently been published.[157]

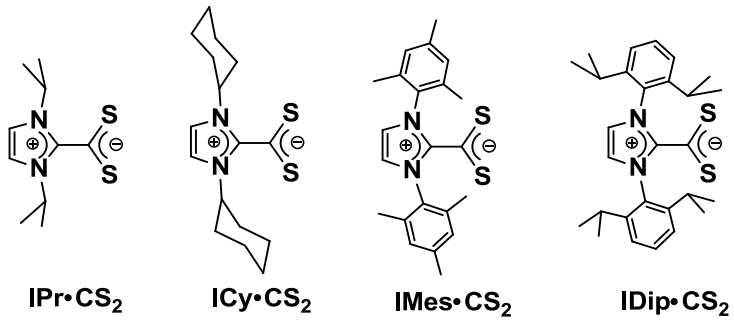

Figure 46. Imidazolium-2-dithiocarboxylate ligands used in this work (made by L. Delaude).

5.1. Ruthenium and osmium dithiocarboxylate complexes

As described previously, compounds of the type $[Ru(CR^1{=}CHR^2)Cl(CO)(BTD)(PPh_3)_2]$ are suitable species to use as starting materials for the introduction of vinyl functionality into complexes. The synthesis and characterisation of a range of ruthenium and osmium vinyl complexes bearing the NHC•CS_2 ligand, with a range of substituents on their nitrogen atoms, are described.

5.1.1. Synthesis of Ru and Os NHC•CS_2 complexes

A bright orange solution of $[Ru(CH{=}CHBu^t)Cl(CO)(BTD)(PPh_3)_2]$ (BTD = 2,1,3-benzothiadiazole) in dichloromethane was treated with IPr•CS_2 (the least bulky dithiocarboxylate betaine used in this work), in the presence of NH_4PF_6. This resulted in a green colouration, and after work-up, the pale green solid obtained was analysed by ^{31}P NMR spectroscopy to be a single new phosphorus-containing compound, giving rise to a singlet resonance at 37.5 ppm. The ^1H NMR spectrum exhibited a singlet at 0.42 ppm (Bu^t) and two doublets of triplets at 4.76 and 6.27 ppm (mutual coupling of 16.8 Hz), confirming the retention of the vinyl ligand. The multiplet resonating at lower field displayed the largest J_{HP} coupling to the mutually *trans* phosphine ligands, which led to the assignment of this resonance to the α-proton of the vinyl group. Resonances were also observed for the imidazolium-2-dithiocarboxylate ligand; a doublet at 1.15 ppm and a septet at 3.49 ppm, both showing a coupling of 6.7 Hz were distinctly identified as the isopropyl substituents. Amid the aromatic resonances, a singlet at 7.29 ppm was observed which was assigned to the imidazolium HC=CH protons. Analysis by (ES) mass spectroscopy (+ve mode) displayed a molecular ion at *m/z* 965 and elemental analysis supported the overall composition of the complex to be $[Ru(CH{=}CHBu^t)(\kappa^2\text{-}S_2C{\bullet}IPr)(CO)(PPh_3)_2]PF_6$ (**54**) (*Scheme 10*).

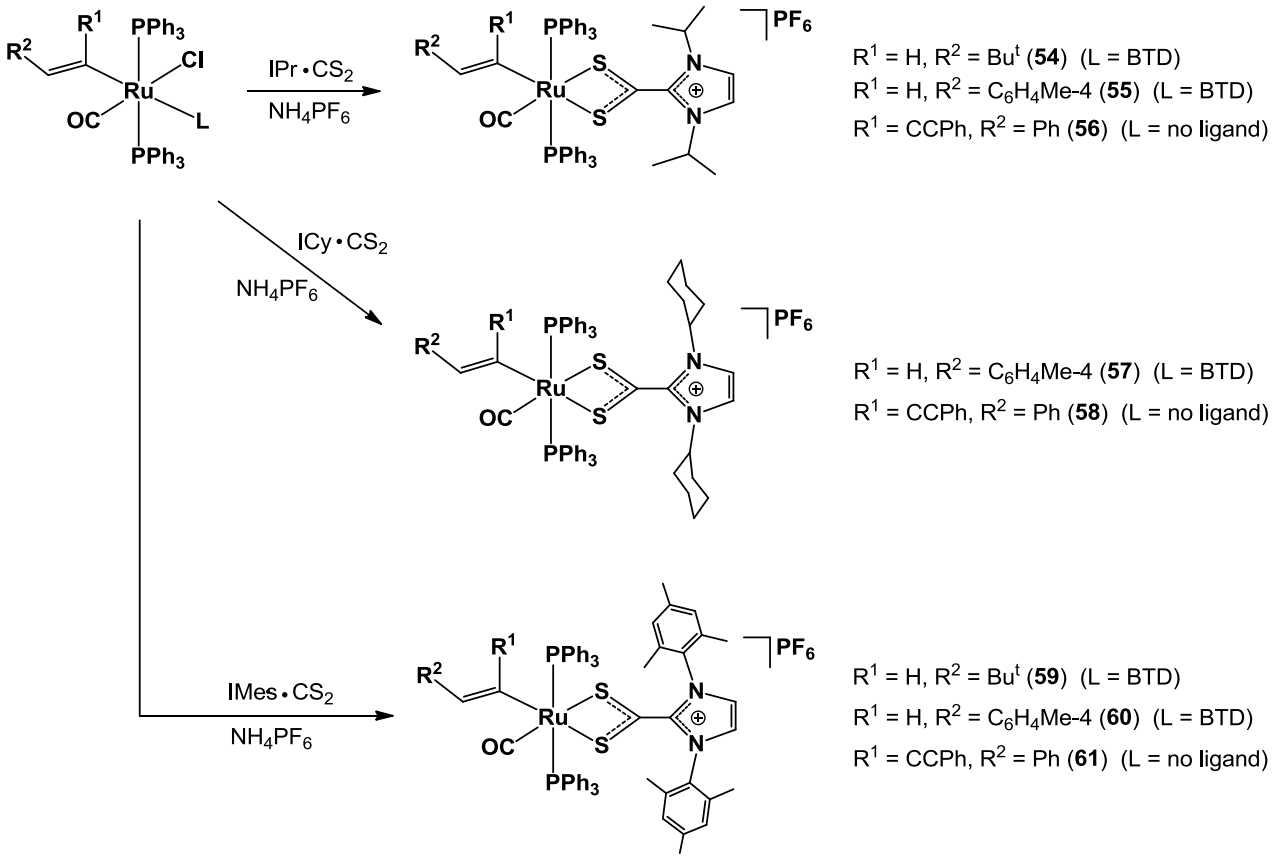

Scheme 10. Formation of ruthenium NHC•CS_2 complexes. BTD = 2,1,3-benzothiadiazole.

[Ru(CH=CHC$_6$H$_4$Me-4)(κ^2-S$_2$C•IPr)(CO)(PPh$_3$)$_2$]PF$_6$ (**55**) was prepared following the same procedure whereby [Ru(CH=CHC$_6$H$_4$Me-4)Cl(CO)(BTD)(PPh$_3$)$_2$] was treated with a slight excess of the IPr•CS_2 ligand and NH_4PF_6 to yield a black crystalline solid in 87% yield (*Scheme 10*). Similar spectroscopic data were exhibited to those found for **54**, the main difference being the presence of resonances for the 4-tolylvinyl substituent. These appeared as a singlet at 2.23 ppm (CH_3) and an AB system at 6.21 and 6.85 ppm (J_{AB} = 8.1 Hz) for the C_6H_4 protons. Further confirmation of the formulation of **55** was given by mass spectrometry and elemental analysis. Characterisation by X-ray crystallography of the single crystals grown, allowed a structural study to be undertaken (see *Fig. 48* and *Structural Discussion, 5.1.2*).

The disubstituted vinyl complex, [Ru(C(C≡CPh)=CHPh)(κ^2-S$_2$C•IPr)(CO)(PPh$_3$)$_2$]PF$_6$ (**56**), was subsequently synthesised by reaction of the five-coordinate enynyl starting material, [Ru(C(C≡CPh)=CHPh)Cl(CO)(PPh$_3$)$_2$], with IPr•CS_2 and NH_4PF_6 (*Scheme 10*). Characterisation by ^{1}H NMR and infrared spectroscopy both clearly confirmed the presence of the enynyl ligand with a singlet at 5.76 ppm (characteristic of the Hβ proton) and an absorption at 2146 cm^{-1} (ν(C≡C)),

respectively. Overall, the reactivity of IPr•CS_2 with the vinyl precursors, was found to be comparable to that of other dithio ligands, such as dithiocarbamates[105, 106, 121, 133, 158] and xanthates.[121, 159]

The coordination chemistry of the more sterically demanding analogue, 1,3-dicyclohexyl-imidazolium-2-dithiocarboxylate, was then investigated. Reaction of [Ru(CH=CHC_6H_4Me-4)Cl(CO)(BTD)(PPh_3)$_2$] with ICy•CS_2 in the presence of NH_4PF_6 (*Scheme 10*) afforded green crystals of [Ru(CH=CHC_6H_4Me-4)(κ^2-S_2C•ICy)(CO)(PPh_3)$_2$]PF_6 (**57**). The ^{1}H NMR spectrum displayed several multiplets between 0.85 and 1.87 ppm, all attributed to the cyclohexyl methylene units, and a deshielded signal at 4.32 ppm was assigned to the NCH protons. Resonances for the vinyl ligand were similar to those observed in **55**. Further characterisation was possible by ^{13}C NMR due to the high solubility of the complex. Two triplet resonances (closely-spaced) at 206.1 (J_{PC} = 4.7 Hz) and 205.2 (J_{PC} = 15.2 Hz) ppm were observed, with the greater coupling resonance assigned to the carbonyl ligand owing its closer proximity to the phosphorus nuclei. The other triplet was assigned to the dithiocarboxylate CS_2 carbon. Lastly, the vinyl α-carbon was identified as the resonance at 145.4 ppm, displaying a characteristically large J_{PC} coupling of 15.3 Hz. Further confirmation was given by standard 2D NMR experiments (HMBC, HMQC). Mass spectrometry and elemental analysis were also used to formulate complex **57**.

In a similar manner, the coordinatively-unsaturated compound [Ru(C(C≡CPh)=CHPh)Cl(CO)(PPh_3)$_2$] was treated with ICy•CS_2 to yield [Ru(C(C≡CPh)=CHPh)(κ^2-S_2C•ICy)(CO)(PPh_3)$_2$]PF_6 (**58**) (*Scheme 10*). Spectral features for the complex were found to be similar to the 4-tolylvinyl derivative (**57**), with the exception that the singlet attributed to the HC=CH protons was clearly visible at 7.09 ppm (as opposed to being obscured by the aromatic protons in **57**).

In order to investigate the effect of the bulky enynyl ligand on the dithiocarboxylate chelate, a structural study was undertaken with crystals grown from **58** (see *Fig. 49* and *Structural Discussion, 5.1.2*).

The effect of steric bulk on the coordination chemistry of dithiocarboxylate betaines was then explored. The percentage of buried volume (%V_{Bur}),[27, 160] is a parameter which indicates the steric properties of NHC betaines.[161] The value of %V_{Bur} increases in the order: IPr•CS_2 < ICy•CS_2 < IMes•CS_2 < IDip•CS_2. Accordingly, the IMes•CS_2 and IDip•CS_2 ligands were chosen as comparisons to ICy•CS_2, due to their increasing steric bulk.

Treatment of [Ru(CH=CHBu^t)Cl(CO)(BTD)(PPh_3)$_2$] with IMes•CS_2 afforded the green complex Ru(CH=CHBu^t)(κ^2-S_2C•IMes)(CO)(PPh_3)$_2$]PF_6 (**59**) (*Scheme 10*). Characterisation by ^{31}P NMR revealed a singlet (at 38.7 ppm) which suggested a mutually *trans* arrangement of the phosphine ligands, while ^{1}H NMR showed distinct resonances for the methyl groups on the mesityl rings (*ortho* at 1.38 ppm and *para* at 2.30 ppm). Using the same approach, complexes [Ru(CH=CHC_6H_4Me-4)(κ^2-S_2C•IMes)(CO)(PPh_3)$_2$]PF_6 (**60**) and [Ru(C(C≡CPh)=CHPh)(κ^2-

S_2C•IMes)(CO)(PPh_3)$_2$]PF_6 (**61**) were also obtained in high yields (*Scheme 10*). Analysis of the spectroscopic data confirmed the presence of the IMes•CS_2 ligand in these complexes and all other data were consistent with the corresponding formulations.

An osmium example was also prepared. The hexacoordinate, purple osmium complex [Os(CH=CHC_6H_4Me-4)Cl(CO)(BTD)(PPh_3)$_2$][162] was treated with a slight excess of IMes•CS_2 and NH_4PF_6, affording the green complex [Os(CH=CHC_6H_4Me-4)(κ^2-S_2C•IMes)(CO)(PPh_3)$_2$]PF_6 (**62**) in high yield (*Scheme 11*). The solid state infrared spectrum of **62** showed a lower ν(CO) frequency absorption compared to its ruthenium analogue **60** (1919 cm^{-1} vs. 1934 cm^{-1}), consistent with the more electron-rich metal centre of osmium. Further confirmation of **62** was given by the molecular ion at *m/z* 1241, found in 100% abundance in the electrospray mass spectrum (+ve mode). Another osmium complex was synthesised containing a disubstituted vinyl ligand. The starting material, [Os(C(C≡CPh)=CHPh)Cl(CO)(BTD)(PPh_3)$_2$], was treated with IMes•CS_2 and NH_4PF_6 in the same manner to give the brown complex, [Os(C(C≡CPh)=CHPh)(κ^2-S_2C•IMes)(CO)(PPh_3)$_2$]PF_6 (**63**) (*Scheme 11*). A broadened singlet, due to long distance coupling to the phosphorus nuclei, was observed in the ^{1}H NMR spectrum at 6.48 ppm for the Hβ proton. The solid-state infrared spectrum displayed a ν(C≡C) absorption at 2143 cm^{-1} which was attributed to the triple bond of the enynyl ligand.

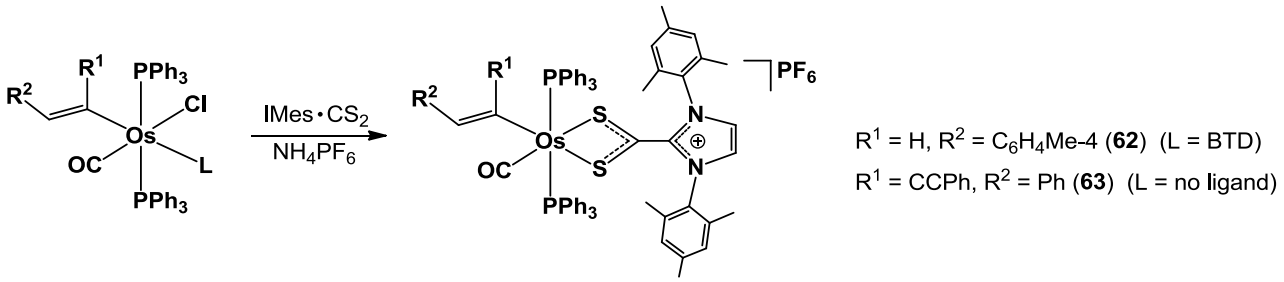

Scheme 11. Formation of osmium complexes.
BTD = 2,1,3-benzothiadiazole.

The bulkiest ligand used in this study, IDip•CS_2, was next explored in order to investigate its effect on the coordination environment of the ruthenium centre. The same experimental method employed for the IPr•CS_2 and ICy•CS_2 reactions was used. Thus, complex [Ru(CH=CHC_6H_4Me-4)Cl(CO)(BTD)(PPh_3)$_2$] reacted with a slight excess of IDip•CS_2 and NH_4PF_6 to afford a pale brown solid in 62% yield (*Scheme 12*). It was immediately obvious from the ^{31}P NMR spectrum that the reaction had proceeded differently to the previous reactions. The phosphorus nuclei were rendered inequivalent as a pair of doublets was observed at 26.7 and 37.1 ppm (with mutual coupling of 20.1 Hz). This (and the magnitude of the coupling constant) suggested a *cis* arrangement of the two phosphine ligands. The solid state IR spectrum revealed the retention of the carbonyl with an intense

ν(CO) absorption observed at 1962 cm^{-1}. The vinyl ligand had also been retained as indicated by the presence of a doublet at 5.04 ppm (J_{HH} = 15.8 Hz) in the ^{1}H NMR spectrum. The other vinyl proton was obscured by the aromatic resonances. Two septets at 2.35 and 2.46 ppm were attributed to the 2,6-diisopropylphenyl substituents and the imidazolium ring (HC=CH unit) was confirmed by a singlet at 7.43 ppm. However, a singlet observed at 6.37 ppm, integrating to a single proton in the ^{1}H NMR spectrum was perplexing. Further characterisation was therefore carried out in order to obtain more information about the product formed.

The electrospray mass spectrum showed an abundant peak at *m/z* 1271, which seemed to be consistent with the formulation [Ru(CH=CHC$_6$H$_4$Me-4)(κ^2-S$_2$C•IDip)(CO)(PPh$_3$)$_2$]Cl (despite the expected elimination of NH_4Cl), whereas elemental analysis seemed to indicate a structure which included both a chloride and a PF_6^- counteranion. To obtain a clearer picture of the elusive product, crystals were grown and a structural study was carried out.[156, 163] This revealed that migration of the vinyl group onto the dithiocarboxylate ligand had taken place, resulting in the formation of [Ru{κ^2-SC(H)S(CH=CHC$_6$H$_4$Me-4)•IDip)}Cl(CO)(PPh$_3$)$_2$]PF$_6$ (**64**, *Fig. 47*). To ensure that solvent effects had not influenced this migration during the crystallisation process, the crystals used for the structural determination were re-dissolved and gave identical NMR spectra to those obtained for the bulk sample.

Two-dimensional NMR experiments (ROESY, COSY, HMBC, HMQC) provided proof that the resonance at 6.37 ppm was indeed due to the proton on the tetrahedral S$_2$CHR unit.[156] Furthermore the ^{13}C NMR spectrum revealed that the resonance for the dithiocarboxylate carbon had significantly shifted upfield from 206.1 ppm in **57** to 59.5 ppm in **64**.

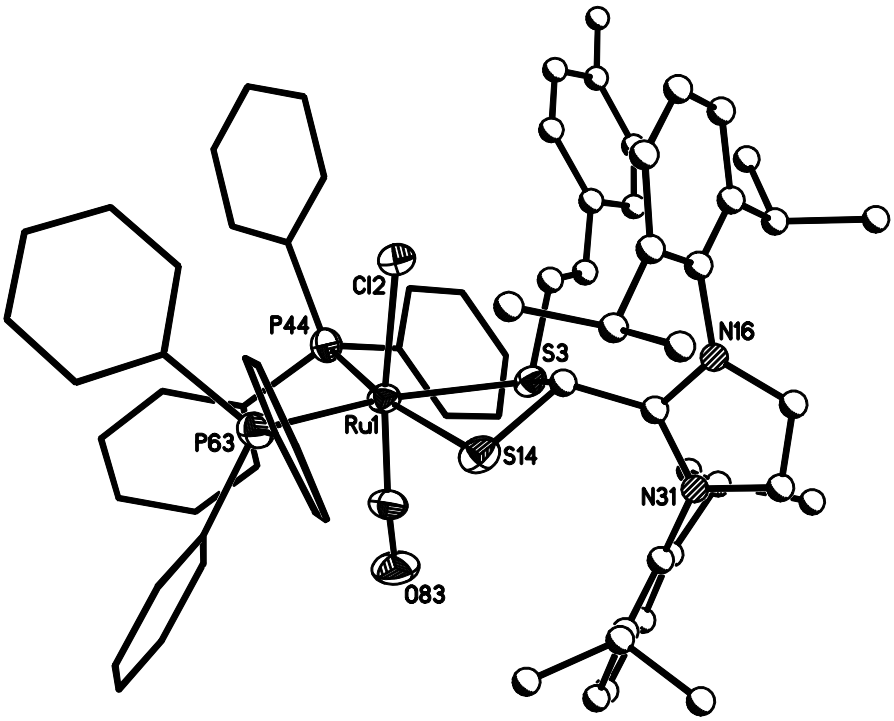

Figure 47. X-ray crystal structure of SC(H)S(CH=CHC$_6$H$_4$Me-4)•IDip)}Cl(CO)(PPh$_3$)$_2$]PF$_6$ (**64**).

Due to the greater steric bulk of the IDip•CS_2 ligand (compared to the isopropyl or cyclohexyl analogues), it is highly probable that the two PPh_3 ligands are forced to adopt a *cis* arrangement, causing the vinyl and dithiocarboxylate ligands to come close in proximity. The presence of an additional proton in **64** is puzzling and can possibly be explained by the mechanistic scheme presented in *Scheme 12*, in which a carbene is formed from the vinyl through protonation by NH_4^+, followed by attack at the α-carbon by the neighbouring sulphur atom. The successive transfer of a proton onto the S_2CR unit and attack of the still-present chloride would then form the observed product.

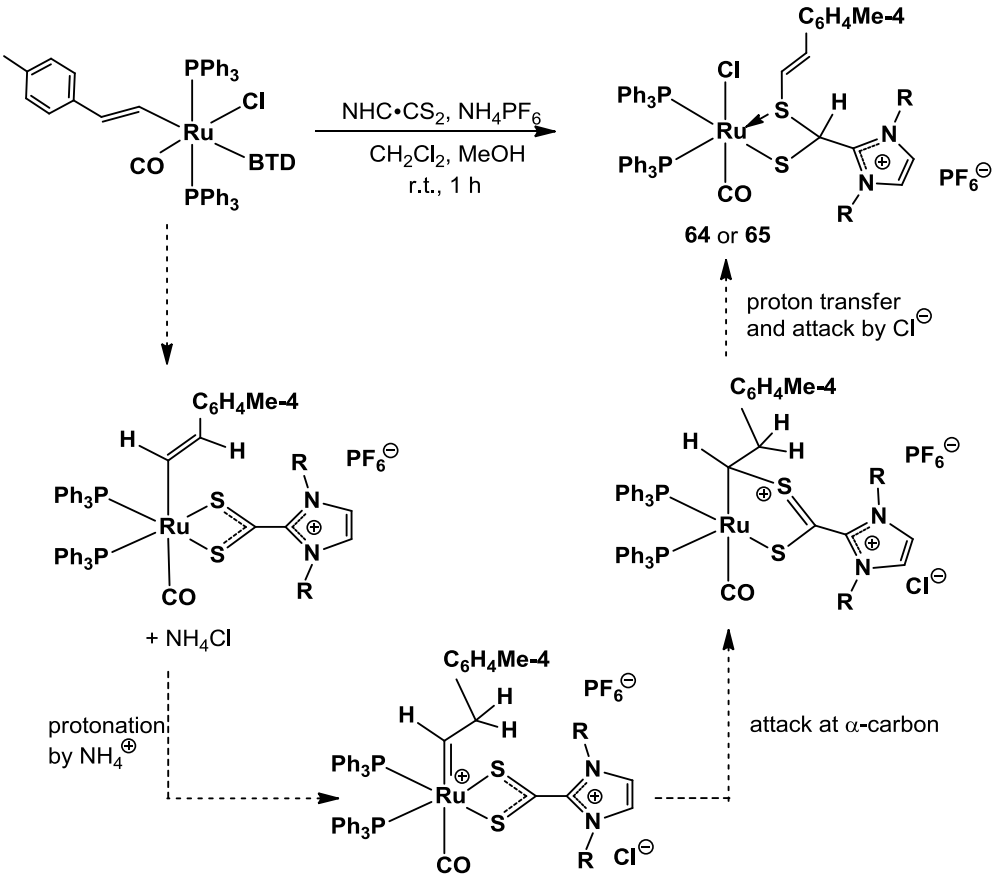

Scheme 12. Formation of complexes **64** (R = 2,6-diisopropylphenyl) and **65** (R = mesityl) with the possible mechanism.

Since this type of coupling of dithiocarbamates and carbene ligands has been reported before (*Scheme 13a*),[164, 165] it is quite probable that the above reaction follows the same course. Further support for the described mechanism was provided when the reaction was performed with KPF_6 instead of NH_4PF_6. This did not lead to compound **64**, but instead gave an intractable mixture of products. Eliminating methanol (and hence dissolved NH_4Cl) from the reaction also failed to produce **64**. The rearrangement observed here correlates closely to the phosphonium-2-dithiocarboxylate (**A**) /

dithiomethylphosphonium (**B**) isomerism described by Hector and Hill when investigating the reaction between [RuHCl(CO)(PPh_3)$_3$] and $Cy_3P{\bullet}CS_2$ (*Scheme 13b*).[166]

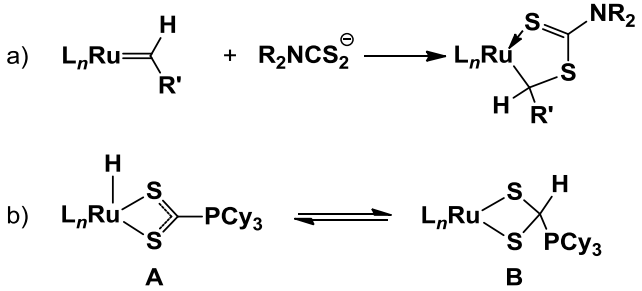

Scheme 13. a) Addition of dithiocarbamates to ruthenium carbene compounds; b) relationship between phosphonium-2-dithiocarboxylate (**A**) and dithiomethylphosphonium ligands (**B**)

Closer examination of the ^{31}P NMR spectra of the crude samples of mesityl-substituted complexes [Ru(CH=CHR)(κ^2-$S_2C{\bullet}$IMes)(CO)(PPh_3)$_2$]PF_6, **59** (R = Bu^t) and **60** (R = C_6H_4Me-4), revealed a pair of doublets, corresponding to small amounts (5–10%) of a byproduct. Furthermore, the ^1H NMR featured singlets which were characteristic of the S_2CH proton. Allowing dichloromethane/methanol solutions of **[**Ru(CH=CHBu^t)Cl(CO)(BTD)(PPh_3)$_2$] and [Ru(CH=CH_6H_4Me-4)Cl(CO)(BTD)(PPh_3)$_2$] to stir overnight in the presence of IMes$\bullet CS_2$ and NH_4PF_6, resulted in the formation of new products, as clearly observed in the ^{31}P NMR spectrum. However, only in the case of the 4-tolyl derivative, was a clean reaction observed and **65** was isolated as the sole product (*Scheme 12*). The ^{31}P NMR spectrum of the product displayed a pair of doublets at 28.1 and 37.9 (J_{PP} = 19.1 Hz) ppm, and the ^1H NMR spectrum displayed a singlet at 6.28 ppm, attributed to the S_2CH proton. Further characterisation by mass spectrometry and elemental analysis formulated the product to be [Ru{κ^2-SC(H)S(CH=CH_6H_4Me-4)$\bullet$IMes)}Cl(CO)(PPh_3)$_2$]PF_6 (**65**). An attempt to heat the reaction mixture (rather than stirring overnight) failed to result in a clean conversion of [Ru(CH=CH_6H_4Me-4)Cl(CO)(BTD)(PPh_3)$_2$] into **65**.

An investigation into the intermediacy of complex Ru(CH=CH_6H_4Me-4)(κ^2-$S_2C{\bullet}$IMes)(CO)(PPh_3)$_2$]PF_6 (**60)** in the formation of **65** was instigated. Overnight treatment of **60** with NH_4Cl afforded **65**, thus indicating the significance of a proton source needed to initiate the migration of the vinyl group. Following this, the reaction of **60** with NH_4Cl in CD_2Cl_2/CD_3OD (3:1 v/v) was studied by ^1H and ^{31}P NMR spectroscopy. After 3 days, with no stirring or aggregation, clean conversion to **65** was observed. It was noted that the S_2CH singlet (6.28 ppm) in the ^1H NMR spectrum of **65** obtained under these conditions, integrated to a value of only 0.3 protons compared to the *ortho*-methyl resonance at 2.02 ppm (6H), the =CHtolyl resonance at 5.41 ppm (1H) and a C_6H_4

resonance at 6.96 ppm (2H). This observation suggested that some deuterium exchange had taken place.

The NMR experiment was performed again, however this time in the absence of NH_4Cl. After two days of monitoring, no sign of reaction was observed. Interestingly, when solid NH_4Cl was added to a CD_2Cl_2 solution of **60** (absence of CD_3OD) and left for days, very slow conversion was observed.

It is evident from the NMR data, that the triphenylphosphine ligands in the final product (**65**) adopt a *cis*-configuration. The mutually *trans* configuration of complex **60** suggests a rearrangement thus takes place. So, in order to ascertain the geometrical nature of compound **60**, with a view to its possible role as an intermediate in the reaction, a NOESY experiment was performed (^{31}P NMR does not distinguish either configuration as both would give rise to singlet resonances due to the symmetry of the molecule). The NOESY experiment performed on **60** failed to show any interaction between Hβ and the protons of the *ortho*-methyl substituents on the IMes•CS_2 ligand (which would be in close proximity if the vinyl and dithiocarboxylate ligands were forced into a *cis*-relationship), suggesting that a mutually *trans* arrangement had been retained. Lastly, the osmium complexes **62** and **63** showed no tendency to rearrange under the same experimental conditions.

5.1.2. Structural Discussion

The *cis*-interligand angles of 70.05(2)–101.62(9)° and 70.10(6)–98.5(2)° for compounds **55** and **58** respectively, suggest both complexes exhibit a distorted octahedral geometry. The S–Ru–S bite angle of the NHC•CS_2 ligand is the smallest of these angles in both complexes. Due to the bulkiness of the isopropyl and cyclohexyl groups, the linear P–Ru–P angle is forced to deviate from linearity to 170.59(2)° in **55** and 174.41(7)° in **58**. A greater *trans* influence of the enynyl ligand over the carbonyl ligand is observed as the Ru–S bond lengths of the ICy•CS_2 chelate differ significantly (2.4773(19) Å and 2.4393(18) Å for Ru–S(2) and Ru–S(4), respectively). This appears not to be as prominent in the structure of **55** as much closer values for the Ru–S(3) [2.4682(7) Å] and Ru–S(1) [2.4713(7) Å] bond lengths are observed. The short C–S distances in **55** [1.675(3) Å and 1.679(3) Å] and **58** [1.690(7) Å and 1.663(7) Å] evidently suggest multiple bond character. Furthermore these distances correspond more to typical C=S double bond lengths (1.67 Å) than to C–S single bonds (1.75 Å),[167] (the two C–S distances are the same in each complex). The S_2C–carbene distance [1.461(4) Å in **55** and 1.472(9) Å in **58**] can be compared to the bond distance of the R_2N–CS_2 bond in dithiocarbamate complexes (which displays significant bond character). The S_2C–carbene distance in these complexes is closer to the single bond lengths observed for the cyclohexyl carbons in **58**, than the vinyl double bond distances of 1.346(3) Å [C(15)–C(16) in **55**] or 1.341(9) Å [C(60)–C(61) in **58**].

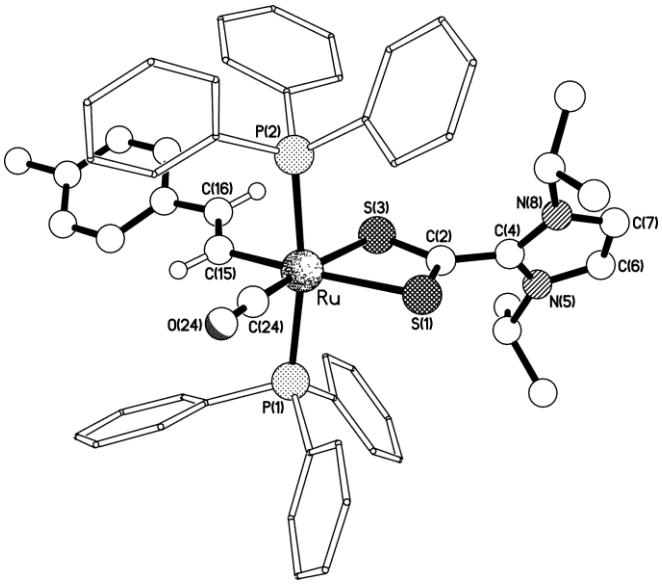

Fig. 48. Structure of the cation in [Ru(CH=CHC_6H_4Me-4)(κ^2-S_2C•IPr)(CO)(PPh_3)$_2$]PF_6 (**55**). Selected bond distances (Å) and angles (°): Ru–C(24) 1.849(3), Ru–C(15) 2.078(2), Ru–S(1) 2.4713(7), Ru–S(3) 2.4682(7), S(1)–C(2) 1.675(3), C(2)–S(3) 1.679(3), C(2)–C(4) 1.461(4), C(15)–C(16) 1.346(3), P(1)–Ru–P(2) 170.59(2), S(3)–Ru–S(1) 70.05(2), C(16)–C(15)–Ru 126.59(19), S(1)–C(2)–S(3) 115.39(15). The hexafluorophosphate anion has been omitted to aid clarity.

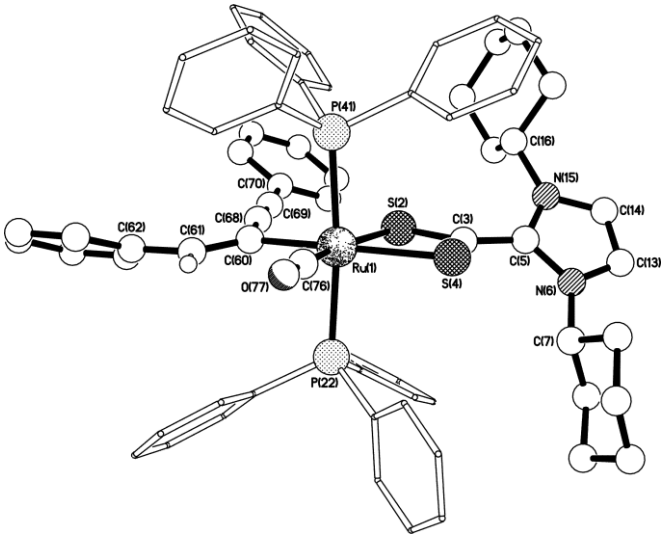

Fig. 49. Structure of the cation in $[Ru(C(C{\equiv}CPh){=}CHPh)(\kappa^2\text{-}S_2C{\bullet}ICy)(CO)(PPh_3)_2]PF_6$ (**58**). Selected bond distances (Å) and angles (°): Ru(1)–S(2) 2.4773(19), Ru(1)–S(4) 2.4393(18), Ru(1)–C(60) 2.114(6), Ru(1)–C(76) 1.844(7), S(2)–C(3) 1.690(7), C(3)–S(4) 1.663(7), C(3)–C(5) 1.472(9), C(5)–N(6) 1.359(9), C(5)–N(15) 1.360(9), C(60)–C(61) 1.341(9), C(68)–C(69) 1.202(9), C(76)–O(77) 1.153(8), S(2)–Ru(1)–S(4) 70.10(6), P(22)–Ru(1)–P(41) 174.41(7), S(2)–C(3)–S(4) 114.7(4), Ru(1)–C(60)–C(61) 126.2(5). The hexafluorophosphate anion has been omitted to aid clarity.

Disorder in the structure of **55** renders the bond data for the imidazolium unit unreliable. However, in complex **58**, rotation around the C(3)–C(5) axis is observed, which results in the imidazolium ring being twisted by 46.4° with respect to the plane of the CS_2 unit. This can be compared to the crystal structure of free dithiocarboxylate betaines, which shows that the carbenium ion plane lies perpendicular to the dithiocarboxylate moiety. This is partly due to steric effects but is due to a large degree to the coulombic interactions between the carbenium ion carbon and the lone pair electrons of the negatively charged chalcogen atoms.[168] The bond lengths of the N_2C^+ motif in **58** [1.360(9) Å and 1.359(9) Å] are the same and indicate significant C=N double bond character due to electronic conjugation. These bond lengths are similar to those observed in the complex $[RuCl(\kappa^2\text{-}S_2C{\bullet}IMes)(p\text{-cymene})]PF_6$.[28] Furthermore, the bond lengths of the enynyl ligand in **58** is comparable to those found in the literature complex, $[Ru(C(C{\equiv}CPh){=}CHPh)(\kappa^2\text{-}S_2CNC_4H_8NH_2)(CO)(PPh_3)_2]PF_6$.[133]

5.2. Gold(I) dithiocarboxylate complexes

5.2.1. Synthesis of gold(I) NHC•CS_2 complexes

In the previous section, the NHC•CS_2 ligand class was investigated as a bidentate chelate. Pairing the same ligands with gold(I) centres allows their chemistry to be explored in monodentate or bridging modes.

A dichloromethane solution of the starting material, [AuCl(PPh_3)], was treated with a slight excess of the least bulky imidazolium-2-dithiocarboxylate ligand used in this study, IPr•CS_2, in the presence of NH_4PF_6. This afforded a pale brown solid in 73% yield (*Scheme 14*). Along with a resonance due to the hexafluorophosphate counteranion, a singlet in the ^{31}P NMR spectrum was observed at 36.0 ppm, indicating the formation of a single new product. ^1H NMR analysis showed a doublet at 1.55 ppm and a septet at 4.87 ppm (mutual coupling of 6.8 Hz), confirming the presence of isopropyl substituents on the dithiocarboxylate ligand. Resonances at lower field were assigned to the PPh_3 ligand and a singlet at 7.36 ppm was attributed to the HC=CH unit of the imidazole ring. The overall composition was formulated as [(Ph_3P)Au(S_2C•IPr)]PF_6 (**66**), based on an abundant molecular ion in the electrospray mass spectrum at *m/z* 687 and good agreement of elemental analysis. Crystals suitable for X-ray diffraction analysis could not be obtained, but linear coordination was assumed with the possibility of an interaction with the other sulphur donor of the dithiocarboxylate ligand (i.e. anisobidentate coordination).

The bulkier IMes•CS_2 betaine was treated with [AuCl(PPh_3)] and NH_4PF_6 under the same experimental conditions to afford [(Ph_3P)Au(S_2C•IMes)]PF_6 (**67**) in 84% yield (*Scheme 14*). The new complex displayed singlets in the ^1H NMR spectrum at 2.25 and 2.37 ppm for the *ortho*- and *para*-methyl substituents of the mesityl groups. The aromatic *meta* protons appeared as a singlet at 7.08 ppm, slightly upfield from the imidazole HC=CH protons at 7.41 ppm. Single crystals of the complex were grown and a structural study undertaken (see *Fig. 50* and *Structural Discussion, 5.2.2*).

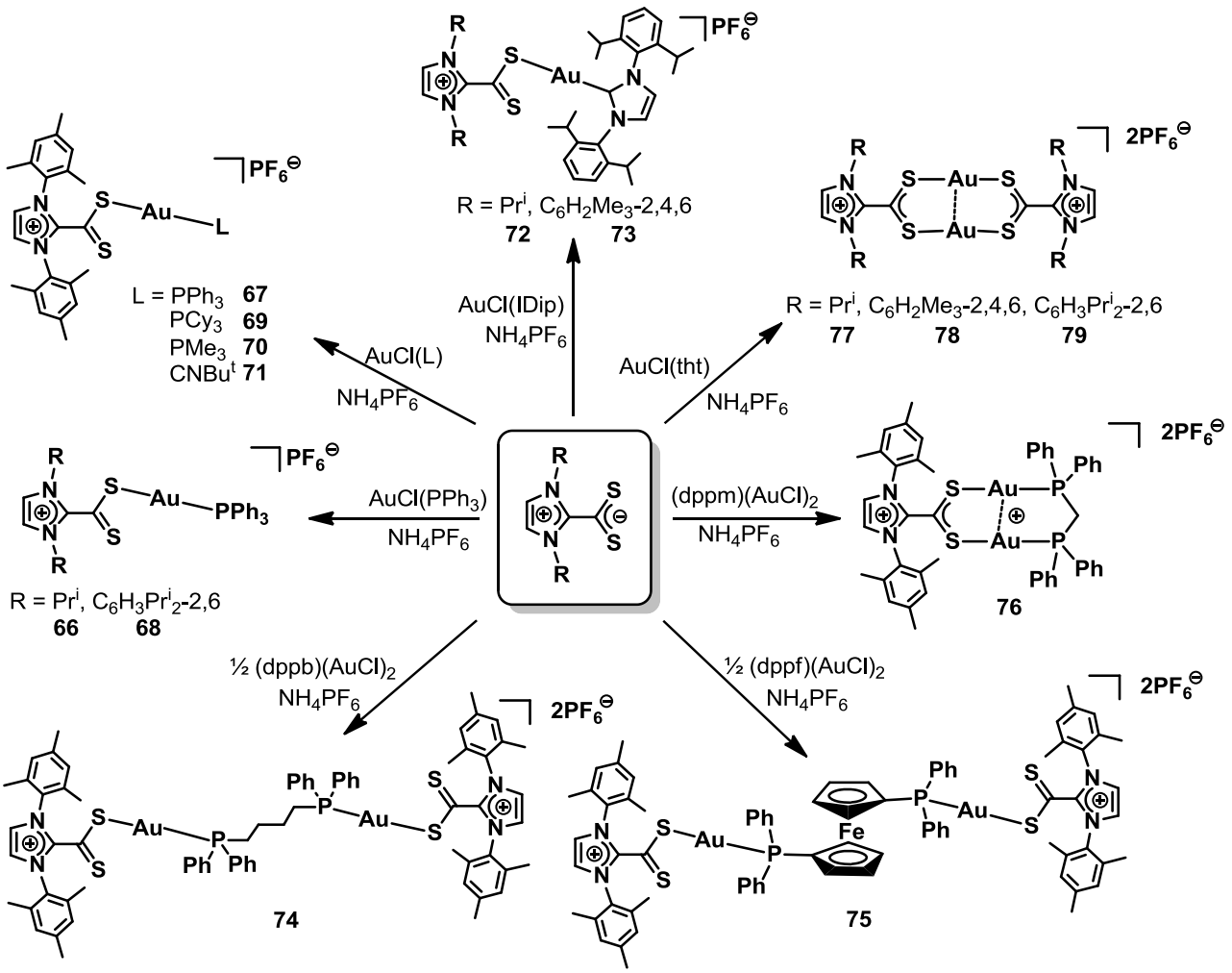

Scheme 14. Preparation of the gold(I) imidazolium-2-dithiocarboxylate complexes.

The most sterically demanding ligand, IDip•CS_2, was allowed to react with [AuCl(PPh_3)] and NH_4PF_6, forming [(Ph_3P)Au(S_2C•IDip)]PF_6 (**68**). ^{1}H NMR analysis revealed doublets at 1.24 (J_{HH} = 7.1 Hz) and 1.36 (J_{HH} = 6.7 Hz) ppm for the methyl groups and the C*H*Me_2 protons were identified as a septet at 2.66 (J_{HH} = 6.8 Hz) ppm. The remaining aromatic resonances of the IDip•CS_2 unit were obscured by the features of the triphenylphosphine ligand. In order to investigate the effect on the structure of increasing the steric bulk from IMes•CS_2 to IDip•CS_2, a structural investigation was also carried out (see *Fig. 51* and *Structural Discussion, 5.2.2*).

Bonding contacts between formally closed-shell d^{10} Au(I) centres (aurophilic interactions)[151], often depend on the steric profile of the attached ligands in these (typically) linear compounds.[151] Therefore, in order to investigate such systems, a series of gold(I) complexes with ligands of varying steric bulk were prepared. The precursor, [AuCl(PPh_3)], was replaced with [AuCl(PCy_3)], [AuCl(PMe_3)] and [AuCl(CN^tBu)] in the subsequent reactions.

[AuCl(PCy_3)] reacted smoothly with IMes•CS_2 to afford [(Cy_3P)Au(S_2C•IMes)]PF_6 (**69**) in 75% yield. Similar spectroscopic features to **67** were observed apart from multiplets assigned to the cyclohexyl protons between 1.24 and 2.08 ppm in the ^{1}H NMR spectrum. In order to provide a contrast to **67**, the precursor [AuCl(PMe_3)], bearing the smallest readily available phosphine was utilised to prepare [(Me_3P)Au(S_2C•IMes)]PF_6 (**70**). The protons of the trimethylphosphine ligand were clearly identified in the ^{1}H NMR spectrum as a doublet at 1.58 ppm with coupling to the phosphorus nucleus (11.2 Hz).

The precursor, [AuCl(CN^{t}Bu)], presents a low level of steric bulk at the gold centre and has been used to generate thiolate complexes with unusual solid state structures.[136-139] Reaction of [AuCl(CN^{t}Bu)] with IMes•CS_2, in the presence of NH_4PF_6, afforded [(^{t}BuNC)Au(S_2C•IMes)]PF_6 (**71**) in 93% yield (*Scheme 14*). The ^{1}H NMR spectrum clearly indicated the retention of the isonitrile ligand by the presence of a singlet at 1.54 ppm for the *tert*-butyl group. Disappointingly, attempts to grow single crystals of complexes **69** – **71** were unsuccessful and thus the effect of the diverse steric profiles of these ligands on potential Au···Au contacts, could not be determined.

Although phosphine-based compounds of the general formula [AuCl(PR_3)], are well-known as precursors in gold(I) chemistry, complexes bearing N-heterocyclic carbenes are rapidly gaining popularity as an alternative choice of ligand to phosphines.[25, 169] [AuCl(IDip)] was treated with the least bulky of the dithiocarboxylate ligands used in this work, IPr•CS_2, to afford [(IDip)Au(S_2C•IPr)]PF_6 (**72**) in 71% yield (*Scheme 14*). The formation of this product was confirmed by ^{1}H NMR analysis. Doublets for the isopropyl methyl groups (1.31 and 1.38 ppm) were observed in addition to other typical resonances of the IPr•CS_2 ligand. Resonances for the metal-bonded IDip ligand were also observed consisting of a septet (2.86 ppm) for the isopropyl groups along with resonances at 7.24 (s, HC=CH), 7.40 (d, J_{HH} = 7.8 Hz, C_6H_3) and 7.62 (t, J_{HH} = 7.8 Hz, C_6H_3) ppm, all confirming the formulation of **72**. An abundant molecular ion at *m/z* 813 in the electrospray spectrum and good agreement of elemental analysis with calculated values also further supported the formulation.

The pale green complex [(IDip)Au(S_2C•IMes)]PF_6 (**73**) was also prepared in a similar fashion (*Scheme 14*). Single crystals of complexes **72** and **73** were grown and their molecular structures determined by X-ray diffraction (*Figs. 52* and *53*). These compounds provide interesting examples of molecular architectures in which the carbene motif is found bonded directly to the metal as well as via an intermediate dithiocarboxylate unit (see *Structural Discussion, 5.2.2*).

Digold complexes of the type [{$Ph_2P(CH_2)_nPPh_2$}($AuCl)_2$] have been shown to exhibit diverse structures in the solid state simply as a result of lengthening the hydrocarbon bridge.[151] For example, the longer bridged complex, [(dppb)($AuCl)_2$] (dppb = 1,4-bis(diphenylphosphino)butane), does not display intramolecular aurophilic interactions, while shorter linkers, especially [(dppm)($AuCl)_2$],

favour 'A-frame' complexes with short contacts between the neighbouring gold centres. Incorporation of this motif in compounds with dithio ligands (e.g., $[(dppm)Au_2(S_2CNR_2)]^+$) has been reported.[170] Taking this as an inspiration, the synthesis of digold compounds bearing the NHC•CS_2 ligands was explored.

The gold complexes, $[(dppb)(AuCl)_2]$ and $[(dppf)(AuCl)_2]$ were each treated with two equivalents of IMes•CS_2. The green, dicationic complexes $[(dppb)\{Au(S_2C•IMes)\}_2](PF_6)_2$ (**74**) and $[(dppf)\{Au(S_2C•IMes)\}_2](PF_6)_2$ (**75**) were formed in high yields (*Scheme 14*). The dppb ligand in complex **74** was identified by the multiplets at 1.62 and 2.37 ppm in the ^{1}H NMR spectrum. In addition, resonances for the IMes•CS_2 unit, which were similar to those observed in the spectra of the monometallic complexes **67**, **69** – **71** and **73** were also observed. In complex **75**, the presence of the ferrocenyl unit was confirmed by two broad singlets at 4.23 and 4.38 ppm in the ^{1}H NMR spectrum. Integration of the spectra for both **74** and **75** clearly indicated that two dithiocarboxylate ligands were present, rather than a single ligand forming a dithiocarboxylate metallacycle.[19, 171, 172] This can be contrasted with the product of IMes•CS_2 with $[(dppm)(AuCl)_2]$, which was formulated as the metallacycle $[(dppm)\{Au_2(S_2C•IMes)\}](PF_6)_2$ (**76**) on the basis of the ratio between the methylene protons at 3.72 (J_{HP} = 12.3 Hz) ppm and the resonances of the IMes•CS_2 ligand. This stoichiometry was further supported by elemental analysis and mass spectrometry data. Unfortunately single crystals of sufficient quality could not be grown in order to investigate the solid state structures of these compounds.

Since many dithio ligands, such as dithiocarbamates,[1] form homoleptic digold complexes of the form $[Au_2(S_2CNR_2)_2]$ (see *Chapter 4*), the investigation was broadened to see whether the dithiocarboxylate ligands would display similar behaviour. [AuCl(tht)] (tht = tetrahydrothiophene, a labile ligand) was treated with one equivalent of each NHC•CS_2 betaine, in the presence of NH_4PF_6, to give the brown digold complexes $[Au_2(S_2C•NHC)_2](PF_6)_2$ (NHC = IPr, **77**; IMes, **78**; IDip, **79**) (*Scheme 14*). Spectroscopic and analytical data confirmed their formulation. The ^{1}H NMR spectra (in CD_2Cl_2) of compound **79** and the free IDip•CS_2 ligand were generally similar, but with a few subtle differences. Complex **79** displayed a broad singlet for the isopropyl $CHMe_2$ protons at 2.52 ppm, rather than the sharp septet seen in the spectrum of the ligand at 2.97 ppm (J_{HH} = 6.8 Hz). A similar broadening was also observed for the HC=CH imidazole protons at 7.46 ppm in contrast to the sharp singlet at 7.07 ppm observed in the spectrum of the free ligand. Related dithiocarbamate compounds, such as $[Au_2(S_2CNEt_2)_2]$[173], are known for the very short gold-gold contacts seen in the solid state, however no crystals suitable for X-ray diffraction could be obtained of complexes **77** – **79** to allow a comparison.

5.2.2. Structural Discussion

Single crystals of compounds **67**, **68**, **72** and **73** were grown and structural studies undertaken. Protons and the hexafluorophosphate counteranions have been omitted for clarity. All four complexes display an almost linear geometry about the metal. The Au-P distances of (**67**) and 2.2595(5) Å (**68**) are comparable to that of 2.2447(10) Å reported for the dithiocarbamate compound [(Ph_3P)Au($S_2CNC_4H_8$)].[174] The Au-C(IDip) bond distances of 2.025(3) Å for **72** and 2.017(4) Å for **73** are significantly greater than that of 1.942(3) Å found in the precursor, [(IDip)AuCl].[169] This suggests that IPr•CS_2 and IMes•CS_2 exert a superior *trans* influence compared to chloride.

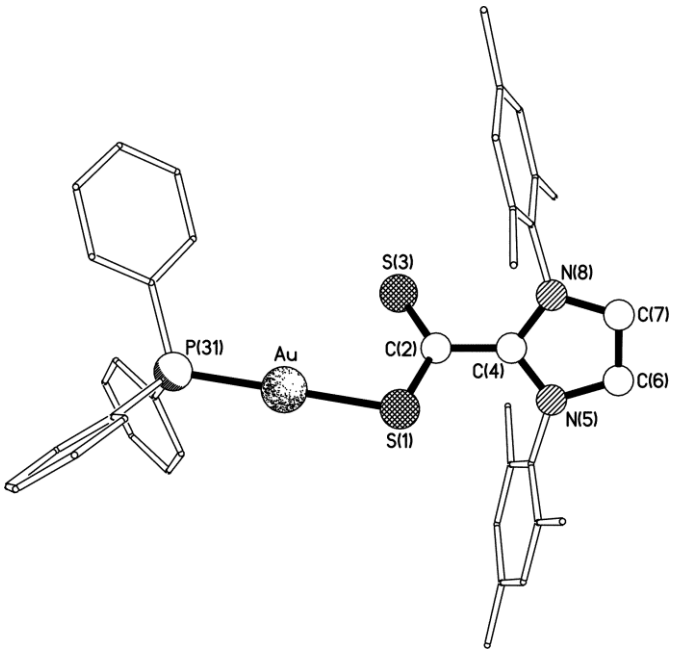

Figure. 50. The molecular structure of [(Ph_3P)Au(S_2C•IMes)](PF_6) (**67**). Selected bond lengths (Å) and angles (°); Au–P(31) 2.2622(7), Au–S(1) 2.3223(7), S(1)–C(2) 1.708(3), C(2)–C(4) 1.487(4), C(2)–S(3) 1.640(3), C(4)–N(5) 1.334(3), C(4)–N(8) 1.337(3), P(31)–Au–S(1) 178.94(3), C(2)–S(1)–Au 102.03(9).

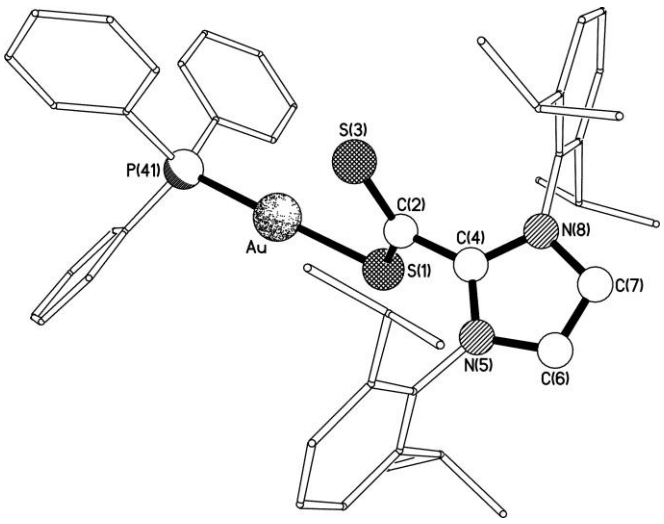

Figure. 51. The molecular structure of [(Ph_3P)Au(S_2C•IDip)](PF_6) (**68**). Selected bond lengths (Å) and angles (°); Au–P(41) 2.2595(5), Au–S(1) 2.3147(5), S(1)–C(2) 1.7027(14), C(2)–C(4) 1.483(2), C(2)–S(3) 1.6420(16), C(4)–N(8) 1.343(2), C(4)–N(5) 1.343(2), P(41)–Au–S(1) 173.63(2), C(2)–S(1)–Au 104.76(6).

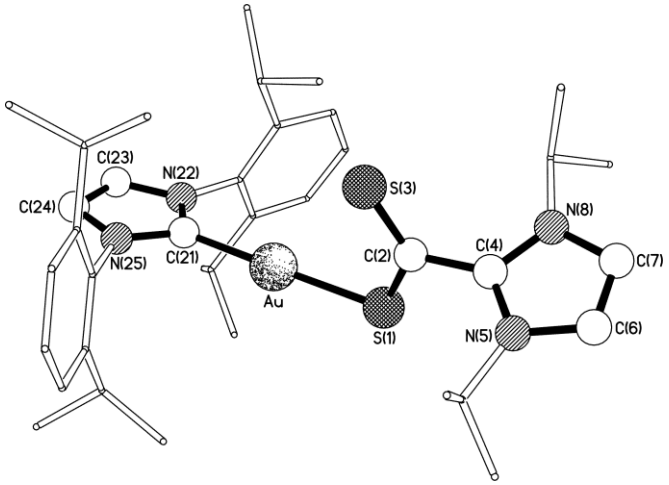

Figure. 52. The molecular structure of [(IDip)Au(S_2C•IPr)](PF_6) (**72**). Selected bond lengths (Å) and angles (°); Au–C(21) 2.025(3), Au–S(1) 2.3047(8), S(1)–C(2) 1.701(4), C(2)–C(4) 1.495(5), C(2)–S(3) 1.639(4), C(4)–N(5) 1.336(5), C(4)–N(8) 1.345(5), C(21)–N(25) 1.341(4), C(21)–N(22) 1.347(4), C(21)–Au–S(1) 175.98(9), C(2)–S(1)–Au 106.99(12).

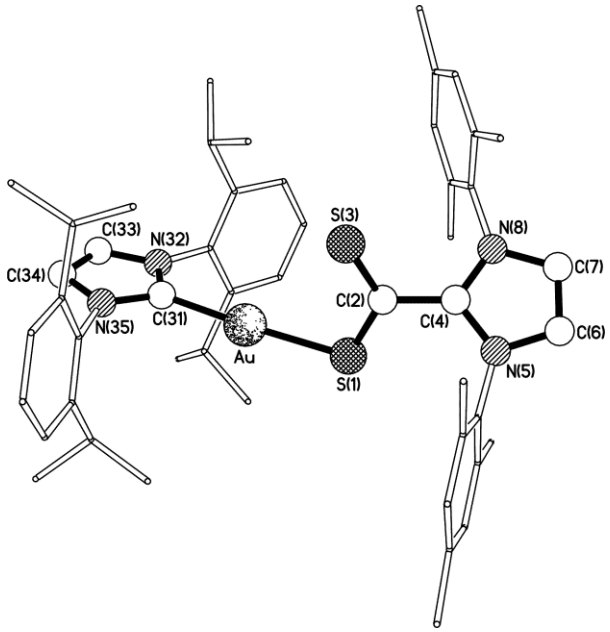

Figure. 53. The molecular structure of [(IDip)Au(S_2C•IMes)](PF_6) (**73**). Selected bond lengths (Å) and angles (°); Au–C(31) 2.017(4), Au–S(1) 2.2912(10), S(1)–C(2) 1.702(5), C(2)–C(4) 1.494(5), C(2)–S(3) 1.643(4), C(4)–N(8) 1.333(6), C(4)–N(5) 1.339(6), C(31)–N(32) 1.341(5), C(31)–N(35) 1.348(5), C(31)–Au–S(1) 169.54(11), C(2)–S(1)–Au 105.30(15).

There are no previously reported examples of gold(I) complexes of NHC•CS_2. The Au–S(1) distances of **67**, **68**, **72** and **73** range between 2.2912 (10) Å and 2.3223 (7) Å which fall between the distances observed for thiolate species, such as [(^{t}BuNC)Au($SC_6H_4CO_2H$-2)] [2.278(5) Å][175] and that

found for the DTC complex [(Ph_3P)Au($S_2CNC_4H_8$)] [2.3334 (11) Å].[174] The C(2)-S(3) bond lengths of 1.640(3), 1.6420(16), 1.639(4) and 1.643(4) Å are all substantially shorter than the C(2)-S(1) bonds (1.708(3), 1.7027(14), 1.701(4) and 1.702(5) Å) of the sulphur atom [S(1)] coordinated directly to the metal indicating some multiple bond character.

The Au–S(3) distance of 3.3549(8) in **67** indicates a weak interaction, however those of 3.4825(5) in **68**, 3.5612(9) in **72** and 3.4817(11) Å in **73** are too long to be considered significant bonding interactions. It is perhaps surprising that there is not more interaction between this arm of the chelate and the metal centre (particularly for **68**), as typically anisobidentate coordination in gold dithiocarbamate compounds is observed – for example, [(Ph_3P)Au($S_2CNC_4H_8$)][174] displays a corresponding Au-S distance of 3.0440(13) Å. Despite the favourable planarity of the heterocyclic unit, the formation of intermolecular Au···Au contacts is prevented by the steric demands of the substituents. The cationic nature of the IMes•CS_2 unit is not reflected in any difference of the C(4)-N(8) or C(4)-N(5) bond lengths in the heterocycle compared to the IDip carbene unit, however, these distances are shorter than 1.374(6) and 1.387(6) Å found for the free ligand.[28]

5.3. Functionalised gold nanoparticles

Having generated gold(I) complexes from the NHC•CS_2 ligands, it was decided to explore the potential of these dithio molecules to act as surface units on gold nanoparticles. Nanoparticles covered with the IMes•CS_2 ligand were prepared by two methods. Citrate-stabilized gold nanoparticles were generated[146] from $HAuCl_4$, and a dichloromethane-methanol solution of IMes•CS_2 was added. An instant darkening of the reaction mixture indicated the displacement of the citrate shell and the formation of IMes•CS_2-stabilized nanoparticles (**NP5**) (*Scheme 15*). These were washed thoroughly with cold dichloromethane to remove unattached IMes•CS_2 units.

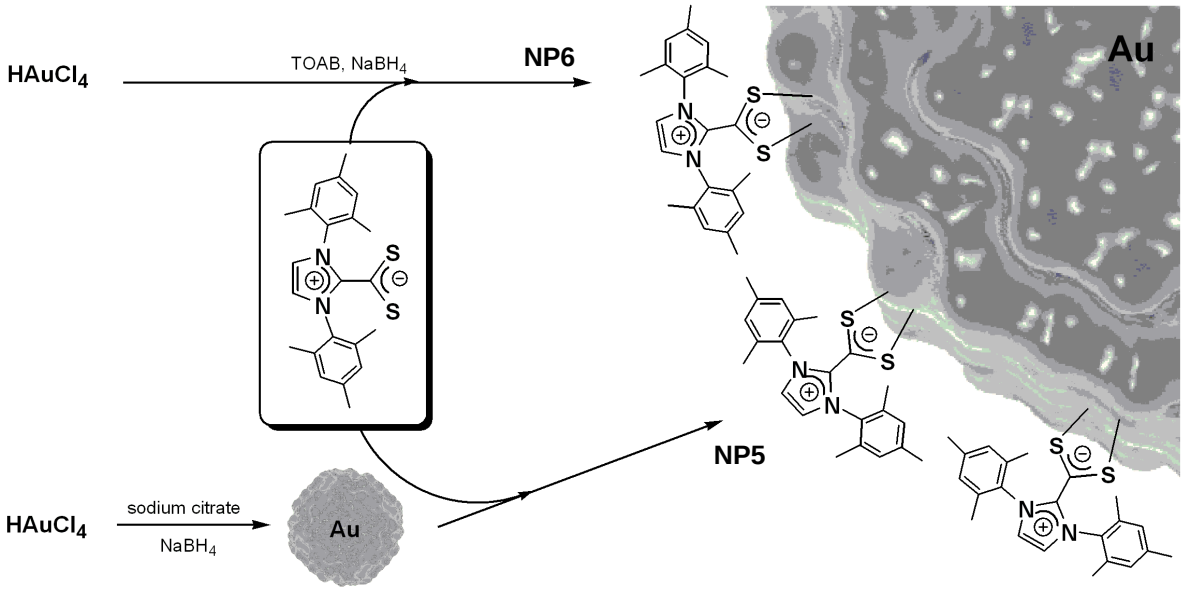

Scheme 15. Preparation of Gold Nanoparticles (**NP5** and **NP6**) with IMes•CS_2 Surface Units

Broadened resonances at chemical shifts similar (but not identical) to those found in free IMes•CS_2 were observed in the ^{1}H NMR spectrum of **NP5**. IR spectroscopy also supported formation of **NP5** as peaks almost identical with those displayed by the ligand itself were observed. Analysis of **NP5** using transmission electron microscopy (TEM) revealed nanoparticles of diameter 11.5 (±1.2) nm, as shown in *Fig. 54*.

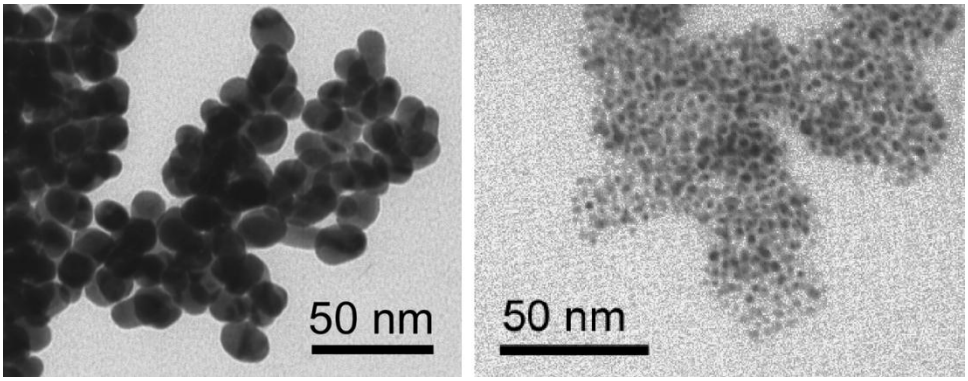

Figure 54. TEM image of (left) **NP5** and (right) **NP6**

The second, more direct method pioneered by Brust *et al*,[58] was used to form **NP6** (*Scheme 15*). These were of much smaller size compared to **NP5**. As with **NP5**, this material was washed thoroughly. However, removal of free IMes•CS_2 proved more problematic because of its similar solubility to the nanoparticle material itself. It was found that warming the nanoparticles in acetonitrile dissolved all of the solid and cooling at -20 °C led to crystallization of the free IMes•CS_2 surface units, which could then be separated. TEM imaging indicated that the nanoparticles of **NP6** were of average diameter 2.6 (±0.3) nm and showed extensive interparticle agglomeration (*Fig. 54*).

Preparation of **NP5** and **NP6** demonstrate that imidazolium-2-dithiocarboxylates can successfully be attached to gold nanoparticles in the same manner as shown for DTCs. These results illustrate the potential of 1,1-dithio ligands other than DTCs to be used as nanoparticle surface units.

5.4. Summary

The ruthenium and osmium organometallic compounds prepared in the earlier part of this study contribute significantly to the small number of group 8 transition metal complexes based on dithiocarboxylate ligands already established in literature. These NHC•CS_2 zwitterions not only display comparable reactivity to conventional 1,1-dithio ligands, but also exhibit unexpected chemistry under the right conditions. Altering the steric profile of the substituents on the heterocyclic ring is shown to influence the course of the reaction, illustrating the potential for modifying the coordination sphere of chelated metal centres through tuning of the NHC substituents. Since changing the substituents on these complexes does not seem to influence the electronic effect of the complexes (i.e. no variation observed in the carbonyl stretching frequency), they could prove useful in situations where only steric tuning is required.

The first examples of monovalent gold complexes of dithiocarboxylate ligands derived from NHCs have also been prepared and characterised. The NHC•CS_2 ligand behaves as an excellent monodentate or bridging donor for a variety of mono- and bimetallic gold complexes with phosphine, carbene and isonitrile co-ligands. In addition, imidazolium-2-dithiocarboxylate betaines can be used to form monolayers on the surface of gold nanoparticles in a similar manner to dithiocarbamates.

Chapter 6: Dialkyldithiophosphate complexes

6. Chapter 6: Dialkyldithiophosphate complexes

The 1,1-dithio ligands explored up to this point, dithiocarbamates and dithiocarboxylates, both complex metal centres through the CS_2 moiety. In order to broaden the investigation, the coordination chemistry of the related dialkyldithiophosphate species, $[(RO)_2PS_2]^-$, was investigated next, providing a comparison with the aforementioned dithio analogues. The following work presented in this study has been published.[176]

6.1. Vinyl dialkyldithiophosphate complexes

The vinyl precursors, $[Ru(CR^1{=}CHR^2)Cl(CO)(PR_3)_2]$ were again employed to synthesise the dialkydithiophosphate complexes described here. In addition, the hydride compounds $[RuHCl(CA)(BTD)(PPh_3)_3]$ (A = O,[119, 177] S[178]), were prepared and the thiocarbonyl variant used to form $[Ru(CPh{=}CHPh)Cl(CS)(BTD)(PPh_3)_2]$ with diphenylacetylene. These were subsequently used in the complexation of the dialkydithiophosphate ligand.

A dichloromethane solution of $[Ru(CH{=}CHC_6H_4Me\text{-}4)Cl(CO)(BTD)(PPh_3)_2]$ and a slight excess of ammonium diethyldithiophosphate, $(NH_4)[S_2P(OEt)_2]$, were stirred for 1 hour at room temperature. The immediate colour change observed (red to yellow), indicated the displacement of the BTD chromophore from the metal centre. After workup, a yellow product was isolated and analysed. The ^{31}P NMR spectrum displayed two singlets at 32.7 and 94.8 ppm, with the higher field resonance shifting from the value observed for the ruthenium precursor (26.0 ppm). Accordingly it was thus attributed to the triphenylphosphine ligand bonded to ruthenium in the product. The lower field resonance was assigned to the diethyldithiophosphate unit, since this value corresponds reasonably closely to the $(NH_4)[S_2P(OEt)_2]$ starting material resonance (at 112.8 ppm). Moreover, the expected deshielding effect of the pentavalent nature of the phosphorus centre further supports this assignment. The ^1H NMR spectrum of the product revealed resonances at 7.48 and 5.25 ppm for the Hα and Hβ proton (both showing mutual J_{HH} coupling of 16.9 Hz), respectively, which are characteristic of the vinyl ligand. The coupling observed for the Hα proton also displayed coupling to the phosphorus nuclei of the phosphine ligands (J_{HP} = 4.1 Hz). This appeared as a doublet of triplets, suggesting a mutually *trans* arrangement. Resonances for the PPh_3 protons were observed between 7.34 – 7.56 ppm, while the AB system of the tolyl substituent displayed resonances at 6.17 and 6.82 ppm (J_{AB} = 8.0 Hz) with the methyl group giving rise to a singlet at 2.22 ppm. Further upfield, resonances for the ethoxy groups of the coordinated $[S_2P(OEt)_2]^-$ ligand were noted, which included a triplet at 0.89 ppm

(J_{HH} = 7.1 Hz) corresponding to the $OCCH_3$ protons and multiplets at 2.93 and 3.18 ppm assigned to the OCH_2 protons. Analysis of the ^{13}C NMR spectrum revealed a triplet at 147.4 ppm (J_{PC} = 14.0 Hz), corresponding to the α-carbon of the vinyl ligand, with the observed coupling traced to the mutually *trans* phosphorus nuclei. In addition, two doublet resonances at 61.7 (J_{PC} = 7.4 Hz) and 15.7 (J_{PC} = 8.8 Hz) ppm were attributed to the dithiophosphate ligand. A triplet at 205.3 ppm (J_{PC} = 14.9 Hz) indicated retention of the carbonyl ligand and further confirmation of this was provided by an absorption at 1916 cm^{-1} in the solid state infrared spectrum. Other intense absorptions in the IR spectrum, namely 1015 and 947 cm^{-1} (not present in the precursor), were assigned to the dithiophosphate ligand. Mass spectroscopy (FAB +ve mode) revealed a molecular ion of m/z 955 and elemental analysis results were found to agree well with calculated values for the formulation $[Ru(CH=CHC_6H_4Me\text{-}4)\{\kappa^2\text{-}S_2P(OEt)_2\}(CO)(PPh_3)_2]$ (**80**).

In a similar manner, reaction of $(NH_4)[S_2P(OEt)_2]$ and $[Ru(CH=CHBu^t)Cl(CO)(BTD)(PPh_3)_2]$ led to the formation of the yellow product, $[Ru(CH=CHBu^t)\{\kappa^2\text{-}S_2P(OEt)_2\}(CO)(PPh_3)_2]$ (**81**), in reasonable yield. Analysis of the ^1H NMR spectroscopic data for this complex revealed them to be comparable to those obtained for complex **80** apart from features related to the tertiary butylvinyl ligand, which displayed a pair of doublets (J_{HH} = 16.1 Hz) at 4.61 (Hβ) and 6.08 (Hα) ppm and a singlet resonance at 0.36 ppm for the methyl groups.

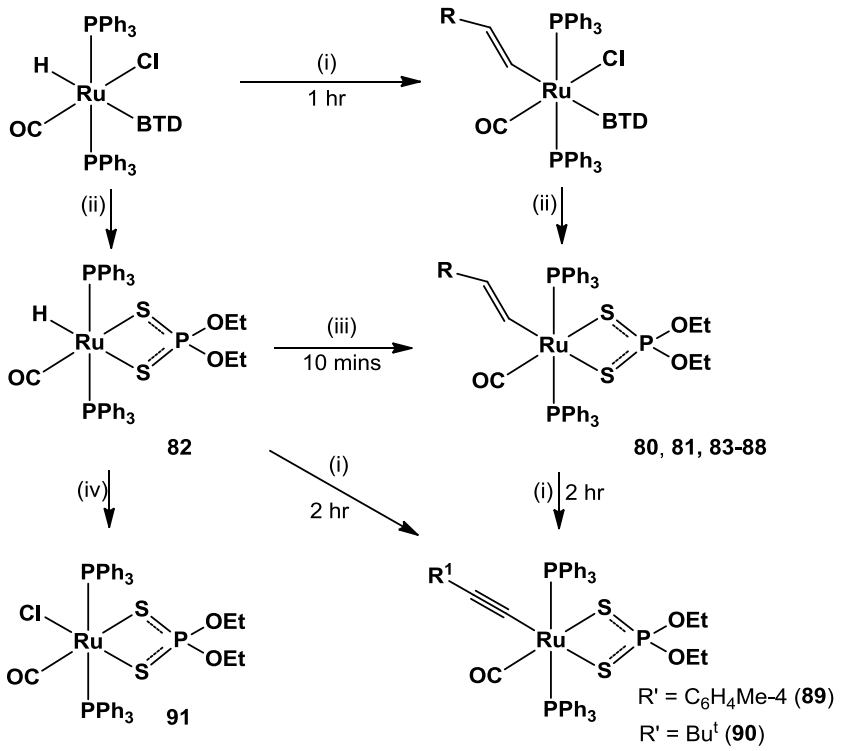

Scheme 16. Formation of ruthenium dithiophosphate complexes.
(i) HC≡CC_6H_4Me-4 or HC≡CBu^t; (ii) $(NH_4)[S_2P(OEt)_2]$; (iii) HC≡CR; (iv) *N*-chlorosuccinimide.
BTD = 2,1,3-benzothiadiazole. R = C_6H_4Me-4 (**80**), Bu^t (**81**), *n*-C_4H_9 (**83**), $CH_2OSi(Bu^t)Me_2$ (**84**), CO_2Me (**85**), Fc (**86**), CPh_2OH (**87**), (HO)C_6H_{10} (**88**).

The starting materials, $[Ru(CH=CHR)Cl(CO)(BTD)(PPh_3)_2]$ (R = C_6H_4Me-4, Bu^t) are both synthesised from the reaction of $[RuHCl(CO)(BTD)(PPh_3)_2]$ with the corresponding alkynes.[119] The same precursor was found to react directly with the diethylthiophosphate ligand to yield $[RuH\{\kappa^2\text{-}S_2P(OEt)_2\}(CO)(PPh_3)_2]$ (**82**).[179] This compound has previously been formed from $[RuHCl(CO)(PPh_3)_3]$, but the yields are similar for both routes (*Scheme 16*). Spectroscopic and analytical data for **82** were found to be consistent with those reported in the literature.[179]

Typically 1,1-dithio chelates such as dithiocarbamates are not labile at room temperature, therefore addition of further ligands to the metal centre once coordinative saturation has been achieved is not possible. However in the case of the coordinatively-saturated complex, $[RuH\{\kappa^2\text{-}S_2P(OEt)_2\}(CO)(PPh_3)_2]$ (**82**), it was discovered in this study that the diethyldithiophosphate ligand exhibits hemilabile behaviour resulting in a vacant coordination site *cis* to the hydride, which can allow the coordination of an alkyne and then subsequent insertion into the Ru-H bond. Thus, stirring a dichloromethane solution of $[RuH\{\kappa^2\text{-}S_2P(OEt)_2\}(CO)(PPh_3)_2]$ (**82**) with an excess of 4-ethynyltoluene for 10 mins at room temperature, afforded $[Ru(CH=CHC_6H_4Me\text{-}4)\{\kappa^2\text{-}$

$S_2P(OEt)_2\}(CO)(PPh_3)_2]$ (**80**). This approach provided a new synthetic route to vinyl complexes bearing the bidentate 1,1-dithio ligand (*Scheme 16*).

This approach was employed in order to investigate the steric effect of the terminal alkynes on the coordination geometry of the complex and a range of alkynes of varying bulkiness were explored. Treatment of **82** with hex-1-yne afforded $[Ru\{CH=CH(n\text{-}C_4H_9)\}\{\kappa^2\text{-}S_2P(OEt)_2(CO)(PPh_3)_2]$ (**83**) after 40 minutes. ^{1}H NMR spectroscopy provided evidence for the generation of the vinyl ligand due to the resonances at 6.13 and 4.37 ppm (α- and β-protons, respectively) and multiplets in the spectral region 0.73 – 1.60 ppm for the *n*-butyl unit.

Reaction of **82** with 1.5 equivalents of the more bulky alkyne, $HC{\equiv}CCH_2OSi(Bu^t)Me_2$, resulted in the formation of $[Ru\{CH=CHCH_2OSi(Bu^t)Me_2\}\{\kappa^2\text{-}S_2P(OEt)_2\}(CO)(PPh_3)_2]$ (**84**). The ^{1}H NMR spectrum displayed characteristic resonances for the dithiophosphate ligand as well as a doublet at 6.51 ppm (J_{HH} = 15.8 Hz) for the α-proton, and a multiplet for the β-proton at 4.53 ppm. This latter resonance displayed coupling to the OCH_2 protons which were observed at 3.44 (d, J_{HH} = 5.2 Hz) ppm. In addition, singlets for the tertiarybutyl (0.86 ppm) and methyl (0.09 ppm) protons were observed. A further example was prepared bearing the methyl propiolate ligand, which reacted in a similar way with **82** to afford $[Ru(CH=CHCO_2Me)\{\kappa^2\text{-}S_2P(OEt)_2\}(CO)(PPh_3)_2]$ (**85**).

Introduction of an additional metal centre to the system was achieved through the use of ethynylferrocene. Reaction of this organometallic ligand with **82**, yielded $[Ru(CH=CHFc)\{\kappa^2\text{-}S_2P(OEt)_2\}(CO)(PPh_3)_2]$ (**86**) within 20 minutes. The presence of the ferrocenyl group was confirmed by the ^{1}H NMR spectrum, displaying resonances at 3.88 (singlet, C_5H_5), 3.84 and 3.39 ppm (broadened triplets, C_5H_4), along with characteristic resonances for the alpha and beta vinyl protons. In all examples presented, both phosphine ligands were retained (mass spectrometry, elemental analysis).

The γ-hydroxyvinyl analogue, $[Ru(CH=CHCPh_2OH)\{\kappa^2\text{-}S_2P(OEt)_2\}(CO)(PPh_3)_2]$ (**87**), was also prepared using the same synthetic method (from reaction of **82** and 1,1-diphenylpropyn-1-ol). The ^{1}H NMR spectrum displayed resonances for the vinyl ligand, with a doublet at 5.40 ppm (J_{HH} = 16.4 Hz) attributed to Hβ (Hα was assumed to be obscured by the aromatic resonances), and a singlet at 0.92 ppm for the OH proton. Single crystals were grown by slow diffusion of ethanol into a dichloromethane solution of **87** and a structural study was undertaken (see *Fig. 55* and *Structural Discussion, 6.3*). This successful structural study followed previous attempts. For example, crystals isolated from analytically pure (NMR spectroscopy) samples of compound **80** were studied by X-ray crystallography but rather than confirming the structure of **80**, the crystals obtained were of the known structure of $[RuH\{\kappa^2\text{-}S_2P(OEt)_2\}(CO)(PPh_3)_2]$ (**82**) instead. This provides clear evidence that insertion into the Ru-H bond is reversible and that β-elimination can occur over longer periods in solution.

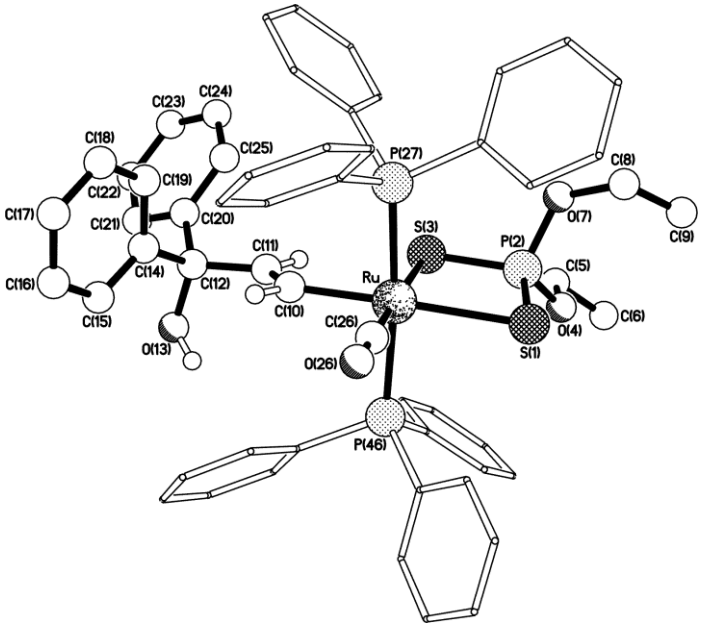

Figure 55. Molecular structure of [Ru(CH=CHCPh$_2$OH){κ^2-S$_2$P(OEt)$_2$}(CO)(PPh$_3$)$_2$] (**87**). Selected bond distances (Å) and angles (°): Ru–C(26) 1.835(3), Ru–C(10) 2.081(2), Ru–P(46) 2.3780(6), Ru–P(27) 2.4125(7), Ru–S(3) 2.5238(6), Ru–S(1) 2.5896(6), S(1)–P(2) 1.9808(9), P(2)–O(4) 1.586(2), P(2)–O(7) 1.592(2), P(2)–S(3) 1.9825(9), C(10)–C(11) 1.329(4), P(46)–Ru–P(27) 173.25(2), S(3)–Ru–S(1) 78.28(2), S(1)–P(2)–S(3) 109.07(4), C(11)–C(10)–Ru 127.7(2).

It has been reported that the treatment of [Ru(CH=CHCPh$_2$OH)(κ^2-*S*,*N*-MI)(CO)(PPh$_3$)$_2$] (MI = 1-methylimidazole-2-thiolate) with HBF$_4$, results in the dehydration of the hydroxyvinyl ligand and formation of the vinylcarbene complex, [Ru(=CH=CPh$_2$)(κ^2-*S*,*N*-MI)(CO)(PPh$_3$)$_2$]BF$_4$.[180] However, the same reaction attempted with compound [Ru(CH=CHCPh$_2$OH){κ^2-S$_2$P(OEt)$_2$}(CO)(PPh$_3$)$_2$] (**87**) gave a mixture of products when treated with one equivalent of HBF$_4$, CF$_3$CO$_2$H or *p*-toluenesulfonic acid. A possible reason for this may be due to some reaction also taking place at the dialkyldithiophosphate ligand as well as at the vinyl moiety.

Another example of a γ-hydroxyvinyl complex was prepared by addition of 1-ethynyl-1-cyclohexanol to [RuH{κ^2-S$_2$P(OEt)$_2$}(CO)(PPh$_3$)$_2$] (**82**) to form [Ru{CH=CH(HO)C$_6$H$_{10}$}{κ^2-S$_2$P(OEt)$_2$}(CO)(PPh$_3$)$_2$] (**88**). The ^{1}H NMR spectrum displayed two doublets for the vinyl protons at 6.58 and 4.79 (J_{HH} = 16.4 Hz) ppm as well as multiplet resonances between 0.78 – 1.34 ppm which were attributed to the cyclohexyl protons. A singlet was observed at 1.61 ppm and assigned to the hydroxy proton on the vinyl ligand. The remaining resonances for the ethoxy substituents of the dialkoxydithiophosphate ligand were similar to those observed for the other complexes.

Reaction of the enynyl compound, [Ru(C(C≡CPh)=CHPh)Cl(CO)(PPh$_3$)$_2$], with (NH$_4$)[S$_2$P(OEt)$_2$] produced a yellow solid. The ^{31}P NMR spectrum of the crude product revealed

significant amounts of free PPh_3 and some $O{=}PPh_3$, in addition to resonances for the S_2P and $RuPPh_3$ nuclei. Analysis by ^1H NMR confirmed the presence of the enynyl ligand (Hβ at 6.39 ppm) and integration of this proton with those in the aromatic region, suggested only one triphenylphosphine ligand was present. Other resonances for the coordinated $[S_2P(OEt)_2]^-$ ligand corroborated well with those observed in the spectra of **80 - 91**. The infrared spectrum (solid state) indicated retention of the carbonyl ligand, and good agreement of calculated values with the elemental analysis results formulated the product to be $[Ru(C(C{\equiv}CPh){=}CHPh)\{\kappa^2\text{-}S_2P(OEt)_2\}(CO)(PPh_3)]$ (**92**) (*Scheme 17*). Three possible structures (*Fig. 56*) are consistent with the spectroscopic (^1H, ^{31}P NMR, IR spectroscopy) and elemental analysis data.

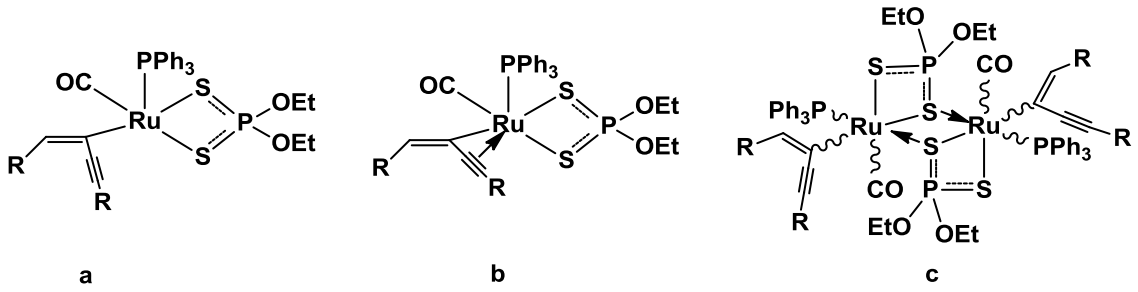

Fig. 56. Possible structures of compound $[Ru(C(C{\equiv}CPh){=}CHPh)\{\kappa^2\text{-}S_2P(OEt)_2\}(CO)(PPh_3)]$ (**92**).

Although the starting material $[Ru(C(C{\equiv}CPh){=}CHPh)Cl(CO)(PPh_3)_2]$ is coordinatively unsaturated,[181] it would be unlikely that the addition of the bidentate donor, $[S_2P(OEt)_2]^-$, would generate another 16-electron species (**a**). If the triple bond were to interact with the metal centre, as shown in the case of (**b**), then coordinative saturation could be achieved. This type of interaction has been reported in literature for the complex, $[Ru(\eta^3\text{-}PhC{\equiv}C\text{-}C{=}CHPh)(CO)_2(PPh_3)_2]PF_6$[182], and if this were the case for (**b**), then the proton decoupled ^{13}C NMR spectrum would show resonances for the carbon nuclei (of the carbon-carbon triple bond) coupling to the phosphorus through the metal centre. However, the region in which resonances for these nuclei typically appear was found to be obscured by features from the aromatic groups.

The mass spectrum (FAB, +ve mode) of **92** featured a molecular ion of *m/z* 740, indicating a mononuclear species; however it is also possible that fragmentation in the mass spectrometer could have occurred so the possibility of the dimeric structure, (**c**), could still not be ruled out. Analysis by infrared spectroscopy failed to show an absorption for the triple bond, typically observed at around 2150 cm^{-1}. This is not unusual as the IR spectrum for the reported compound, $[Ru(\eta^3\text{-}PhC{\equiv}C\text{-}$

C=CHPh)$(CO)_2(PPh_3)_2]PF_6$, also failed to show a clear ν(C≡C) absorption for the coordinated triple bond.[182]

Finally a technique was sought which could determine whether a monomeric or dimeric structure had been adopted. The Signer osmometry method[183] is a technique for measuring molecular weight and is based on the principle that the vapour pressure of a solution depends upon the mole fraction of dissolved solute. A precise amount of compound **92** and the Vaska's complex, $[IrCl(CO)(PPh_3)_2]$ (used as a stable reference compound), were dissolved in a measured volume of dichloromethane, respectively. The two solutions were left to equilibrate in the apparatus (*Supplementary Information, 10.4.2*) under a partial vacuum for two days. After this period the measurements had stabilised to show that the mass calculated from the readings of the apparatus was within 5% of the mass of the monomer, (**b**), which ruled out structure (**c**). Therefore it was concluded the formulation was $[Ru(\eta^3\text{-PhC}\equiv\text{C-C=CHPh})\{\kappa^2\text{-}S_2P(OEt)_2\}(CO)(PPh_3)]$ (**92**) (*Scheme 17*).

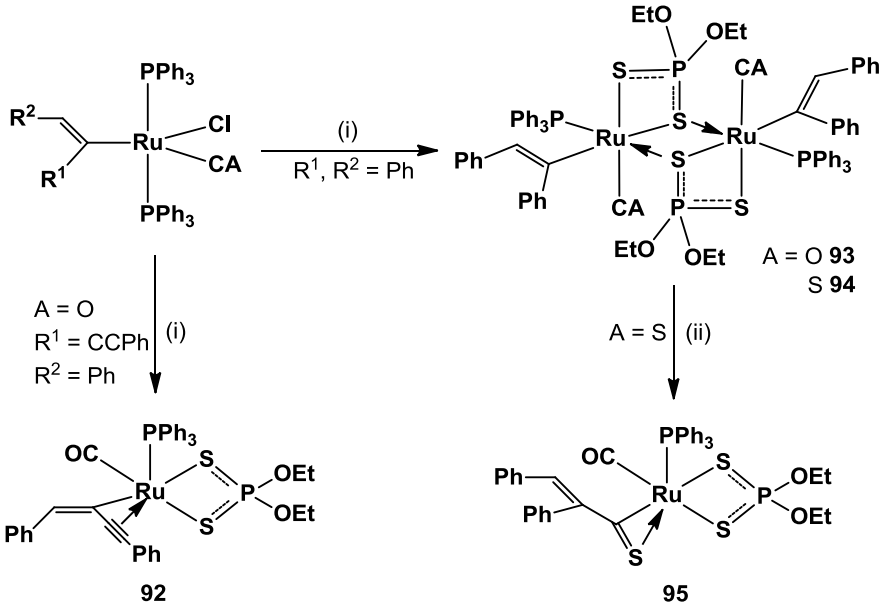

Scheme 17. Formation of ruthenium stilbenyl diethyldithiophosphate complexes.
A = O, S. (i) $(NH_4)[S_2P(OEt)_2]$; (ii) CO.

Reaction of the stilbenyl compound, $[Ru(CPh=CHPh)Cl(CO)(PPh_3)_2]$, with $(NH_4)[S_2P(OEt)_2]$ was also expected to afford a monophosphine compound as observed for **92**. However measurements with the Signer apparatus indicated that the complex was in fact dimeric. This seems plausible as an adjacent alkyne donor is not available, thus preventing a stabilising interaction (as found in **92**) taking place. Therefore the complex was formulated as the dimer $[Ru(CPh=CHPh)\{\mu,\kappa^1,\kappa^2\text{-}S_2P(OEt)_2\}(CO)(PPh_3)]_2$ (**93**) (*Scheme 17*), which is supported by the structurally charaterised literature complex $[Ru(CO)\{\kappa^2\text{-}S_2P(OEt)_2\}\{\mu,\kappa^1,\kappa^2\text{-}S_2P(OEt)_2\}]_2$.[47]

The analogous precursor [Ru(CPh=CHPh)Cl(CS)(PPh_3)$_2$], containing a thiocarbonyl instead of a carbonyl group, was found to react with (NH_4)[$S_2P(OEt)_2$] in the same way to give the corresponding complex, [Ru(CPh=CHPh){μ,κ^1,κ^2-$S_2P(OEt)_2$}(CS)(PPh_3)]$_2$ (**94**) (*Scheme 17*). Spectrocopic data was similar to **93** - the main difference being the intense ν_{CO} (1965 cm^{-1} in **93**) and ν_{CS} (1280 cm^{-1} in **94**) absorptions.

In a recent paper it was reported that thiocarbonyl vinyl species such as [Ru(CR^1=CHR^2)Cl(CS)(PPh_3)$_2$] (R^1 = H, Ph; R^2 = Ph), react with carbon monoxide to undergo migratory insertion of thiocarbonyl and vinyl ligands to form the thioacyl complexes, [Ru(η^2-SCCR^1=CHR^2)Cl(CO)(PPh_3)$_2$].[178] Therefore the possibility for migration to occur in complexes bearing the diethyldithiophosphate ligand was also explored. Carbon monoxide was bubbled through a dichloromethane solution of **94**, causing an immediate colour change from yellow to deep red. The ^{31}P NMR spectrum of the isolated red product revealed two new resonances at 49.7 and 102.7 ppm. Further analysis by ^{1}H NMR spectroscopy revealed a sharp singlet at 7.94 ppm corresponding to the Hβ proton (7.38 ppm reported for [Ru(SCCR^1=CHR^2)Cl(CO)(PPh_3)$_2$]), which showed no coupling to the triphenylphosphine ligands. The infrared spectrum displayed a new band at 1910 cm^{-1}, characteristic for the ν_{CO} absorption and a less intense absorption at 1256 cm^{-1}, which was assigned to ν_{CS} of the thioacyl ligand. Further confirmation that the compound formed was [Ru(η^2-SCCPh=CHPh){κ^2-$S_2P(OEt)_2$}(CO)(PPh_3)] (**95**), was given by results from mass spectrometry (molecular ion at *m/z* 801), Signer measurement and elemental analysis.

An attempt to generate the corresponding acyl complex from the carbonyl analogue (**93**) proved to be unsuccessful. Passing carbon monoxide through a dichloromethane solution of **93**, instead gave incomplete conversion to the hydride **82**, indicating that β-elimination of diphenylacetylene had probably occurred.

As a short digression from the exploration of the dialkyldithiophosphate ligand, the related unsymmetrical diethylthiophosphate ligand, [S(O)$P(OEt)_2$]$^-$ was subsequently investigated. Complexation of this mixed-donor ligand to transition metal centres, provides a useful comparison for the coordination chemistry of its symmetrical analogue. Commercially available K[S(O)$P(OEt)_2$] reacted readily with [Ru(CH=CHC$_6$H$_4$Me-4)Cl(CO)(BTD)(PPh_3)$_2$] to yield a yellow product (*Scheme 18*). In the ^{31}P NMR spectrum, two new resonances were clearly visible at 29.7 and 48.8 ppm. The latter resonance was assigned to the phosphorus nucleus of the diethylthiophosphate ligand (the phosphorus nucleus in the free ligand resonates at 56.4 ppm). The remaining spectroscopic features were found to be similar to those of compound **82** and the compound was assigned as [Ru(CH=CHC$_6$H$_4$Me-4){κ^2-S(O)$P(OEt)_2$}(CO)(PPh_3)$_2$] (**96**).

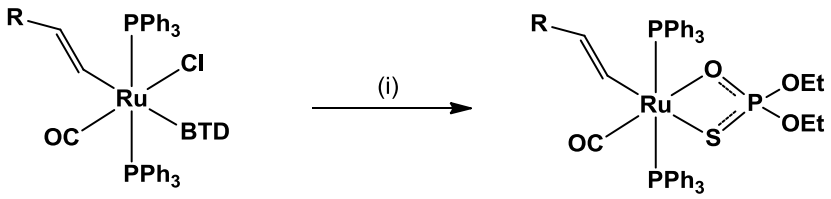

Scheme 18. Formation of ruthenium diethylthiophosphate complex (**96**).
(i) K[S(O)P(OEt)$_2$]; R = C_6H_4Me-4, BTD = 2,1,3-benzothiadiazole.

The sulphur donor is proposed to be arranged in a *trans* fashion to the vinyl moiety (*Scheme 18*). This is based on the regiochemistry observed in the related vinyl complexes chelated by the mixed-donor, 1-methylimidazole-2-thiolate ligand, in [Ru(CR^1=CHR^2)(κ^2-*S*,*N*-MI)(CO)(PPh$_3$)$_2$].[184]

6.2. Acetylide dialkyldithiophosphate complexes

Surprisingly, it was discovered that stirring a dichloromethane solution of [RuH{κ^2-S$_2$P(OEt)$_2$}(CO)(PPh$_3$)$_2$] (**82**) for 3 hours with excess 4-ethynyltoluene, led to clean formation of a new product (^{31}P NMR spectroscopy). After work-up, the ^{1}H NMR spectrum clearly showed the retention of the [S$_2$P(OEt)$_2$]$^-$ ligand. Furthermore, resonances for a tolyl substituent (AB system at 6.44 and 6.83 (J_{AB} = 7.8 Hz) ppm) and methyl group (2.23 ppm) were featured. However, no vinyl protons were apparent. Analysis by solid state infrared spectroscopy revealed a carbonyl peak at 1936 cm^{-1} and a medium intensity absorption at 2105 cm^{-1} which was assigned to a $\nu_{C\equiv C}$ band for an acetylide ligand bonded to the ruthenium centre. On the basis of these data, the product was formulated to be [Ru(C≡CC_6H_4Me-4){κ^2-S$_2$P(OEt)$_2$(CO)(PPh$_3$)$_2$] (**89**) (*Scheme 16*). Further confirmation came from the ^{13}C NMR spectrum, in which the carbon nuclei of the acetylide ligand were found to resonate at 115.8 (s, Cβ) and 108.1 (t, Cα, J_{PC} = 21.0 Hz) ppm. Mass spectrometry (FAB, +ve ion) displayed a molecular ion at *m/z* 954 and elemental analysis further supported the composition of **89**.

The above reaction demonstrated the displacement of the vinyl ligand on addition of excess alkyne. To confirm this, [Ru(CH=CHC$_6H_4$Me-4){κ^2-S$_2$P(OEt)$_2$}(CO)(PPh$_3$)$_2$] (**80**) was treated with an excess of HC≡CC_6H_4Me-4 and refluxed for 10 minutes in toluene. [Ru(C≡CC_6H_4Me-4){κ^2-S$_2$P(OEt)$_2$}(CO)(PPh$_3$)$_2$] (**89**) was formed as the main product, however on closer inspection of the ^{1}H

NMR of the crude product, resonances for a byproduct, namely, $H_2C=C(H)C_6H_4Me$-4, were observed (5.26 ppm, J_{HH} = 10.9 Hz; 5.78 ppm, J_{HH} = 17.6 Hz; 6.77 ppm, J_{HH} = 17.6, 10.9 Hz).

Using the same approach, the compound $[Ru(C{\equiv}CBu^t)\{\kappa^2\text{-}S_2P(OEt)_2\}(CO)(PPh_3)_2]$ (**90**), was formed by heating $[Ru(CH=CHC_6H_4Me\text{-}4)\{\kappa^2\text{-}S_2P(OEt)_2\}(CO)(PPh_3)_2]$ (**80**) with an excess of $HC{\equiv}CBu^t$ in toluene. The tertiary butyl protons were immediately identified by the new singlet resonance at 0.76 ppm, integrating to 9 protons in the ^{1}H NMR spectrum of **90**. A possible mechanistic explanation for the displacement reactions could be that the diethyldithiophosphate chelate opens up, allowing oxidative addition of the alkyne, to give a temporary Ru(IV) hydrido vinyl acetylide species. This intermediate compound then eliminates the vinyl ligand (evident from the alkene resonances observed in the ^{1}H NMR spectrum) (*Scheme 19*). The hemilability of the $[S_2P(OEt)_2]^-$ ligand is quite remarkable as elevated temperatures are required for the analogous vinyl to acetylide transformations in the dithiocarbamate compounds $[Ru(CH=CHC_6H_4Me\text{-}4)\{\kappa^2\text{-}S_2CNR_2\}(CO)(PPh_3)_2]$.[133, 158] Another possibility to consider is that rather than the hemilability of the 1,1-dithio ligand creating the vacant site for the transformation, it is formed by dissociation of a phosphine ligand. However, this proved not to be the case after following the conversion of $[RuH\{\kappa^2\text{-}S_2P(OEt)_2\}(CO)(PPh_3)_2]$ (**82**) to **80** to **89** by ^{31}P NMR in CD_2Cl_2 - no free triphenylphosphine was observed during the course of the reaction.

At first, the transformation of **82** to **90** with excess $HC{\equiv}CBu^t$ was carried out in 1,2-dichloroethane. Spectroscopic data revealed the presence of a side product in very low yield, identified as $[RuCl\{\kappa^2\text{-}S_2P(OEt)_2\}(CO)(PPh_3)_2]$ (**91**). Compound **91** could also be obtained directly from treatment of **82** with *N*-chlorosuccinimide. The transformation of **82** to **90** can avoid contamination with **91** by using a non-chlorinated solvent such as tetrahydrofuran or toluene.

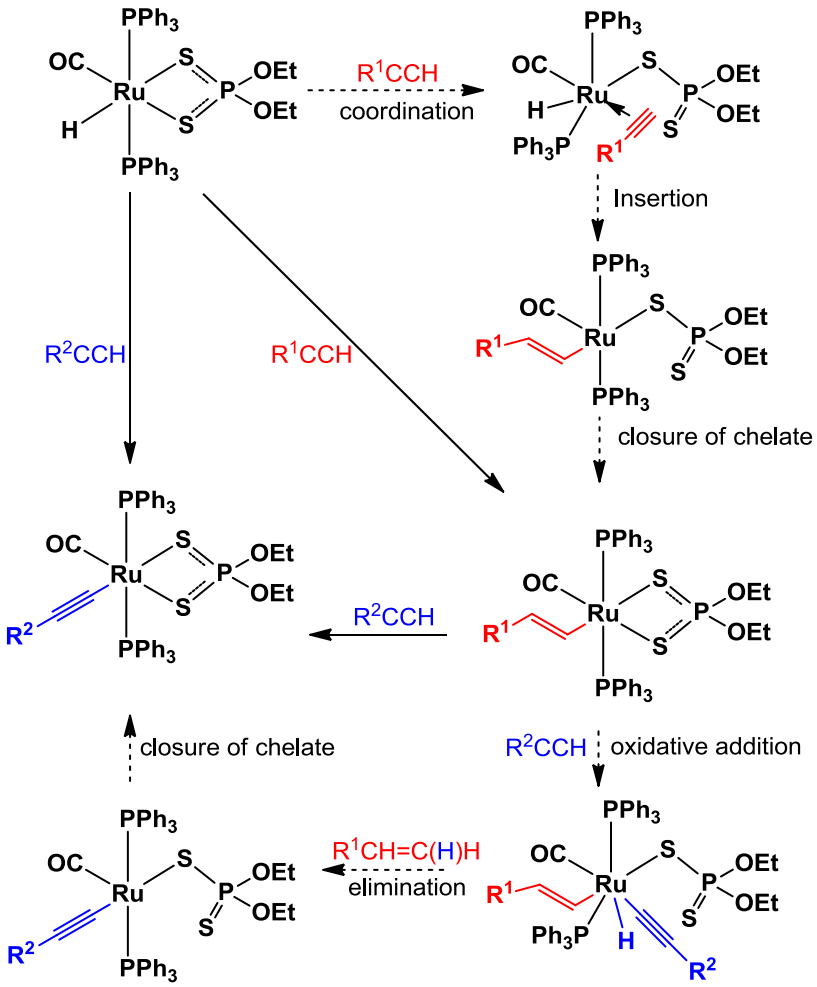

Scheme 19. Possible mechanism of formation of vinyl and acetylide diethyldithiophosphate complexes.

The formation of the acetylide complexes **89** and **90** via the route described above, can be compared to isolation of the only other reported ruthenium dialkyldithiophosphate complex with a σ-organyl ligand, [Ru(C≡CPh){κ^2-$S_2P(OEt)_2$}(η^6-*p*-cymene)]. This was obtained by an unusual method which involved the treatment of [RuCl{κ^2-$S_2P(OEt)_2$}(η^6-*p*-cymene)] with the molybdenum alkynyl transfer agent, [Mo(C≡CPh)(η^3-allyl)$(CO)_2$(bipy)].[32]

6.3. Structural Discussion

Analysis of a single crystal of complex [Ru(CH=CHCPh$_2$OH){κ^2-S$_2$P(OEt)$_2$}(CO)(PPh$_3$)$_2$] (**87**) exhibited a distorted octahedral structure with *cis*-angles at the metal centre in the range 78.28(2) – 100.03(8)°, the smallest of which is the S(3)–Ru–S(1) angle. This angle in the diethyldithiophosphate ligand is found to be larger than that of other 1,1,-dithio ligands such as dithiocarbamates and xanthates. The S(1)–P(2)–S(3) angle [109.07(4)°] of the diethyldithiophosphate ligand in **87**, corresponds closely to that found in the structure of [RuH{κ^2-S$_2$P(OEt)$_2$}(CO)(PPh$_3$)$_2$] (**82**).[179] The pentavalent phosphorus reveals a tetrahedral geometry, with P(2)–S(3) and S(1)–P(2) distances of 1.9825(9) and 1.9808(9) Å, respectively, being the same. Although the steric effect of the ethoxy substituent is clear (indicated by ready loss of a phosphine ligand), little deviation of the P(46)-Ru–P(27) angle is observed (173.25(2)°) in this structure. The superior *trans* influence of the vinyl ligand is evident by the longer Ru–S(1) bond (2.5896(6) Å) compared to the Ru–S(3) bond distance of 2.5238(6) Å. The structural data associated with the vinyl ligand are unremarkable.

6.4. Summary

The coordination chemistry of dialkyldithiophosphate ligands reported in the literature is usually found to be comparable to that of the related 1,1-dithio ligands, dithiocarbamates and xanthates. However on closer investigation, it is apparent that these ligands can demonstrate markedly different behaviour, which can partly be explained due to the greater steric influence of the ligand on the coordination environment of the metal. The spontaneous loss of a phosphine when disubstituted vinyl complexes are prepared, illustrates the steric effect of the dialkyldithiophosphate ligand. Moreover the hemilability of coordinated [S$_2$P(OEt)$_2$]$^-$ at room temperature is also greater than that noted for other 1,1-dithio chelates. Thus, the insertion of alkynes to form vinyl ligands, the displacement of vinyl ligands to form acetylides, and the coordination of carbon monoxide to induce migratory insertion and thioacyl formation is rendered facile. These properties may have significant potential for exploitation in a catalytic context.

Chapter 7: Multimetallic complexes based on nitrogen-oxygen mixed-donor ligands

7. Chapter 7: Multimetallic complexes based on nitrogen-oxygen mixed-donor ligands

With the aim of generating multimetallic architectures from simple, commercially available ligands with donor groups other than sulphur, mixed-donor ligands were explored next. In particular, ligands containing both oxygen and nitrogen functionalities were employed in the study. As discussed in *Chapter 1*, the preparation of multimetallic networks featuring two different metal centres has proved to be a challenging task. Thus, the remainder of this thesis explores bifunctional ligands, to generate heteromultimetallic systems by exploiting the donor properties of their terminal functionalities towards certain metal centres. In addition, the surface stabilisation of silver nanoparticles with the same ligands is also demonstrated.

7.1. Bi- and trimetallic complexes

The vinyl species [Ru(CR^1=CHR^2)Cl(CO)(BTD)(PPh_3)$_2$] were employed as starting points for the formation of the multimetallic compounds as they possess ligands with diagnostic spectroscopic properties (^{1}H, ^{13}C, ^{31}P NMR and IR spectroscopy). The vinyl ligand, in particular, allows the introduction of spectroscopic 'tags' (e.g., ^{19}F NMR active units) to aid in the analysis. However, the sensitivity of the vinyl ligand towards acidic conditions and the lability of the phosphines can sometimes prove a disadvantage. In these situations, the more robust starting material, *cis*-[$RuCl_2$(dppm)$_2$] is preferred, which also possesses useful spectroscopic properties (NMR spectroscopy) due to the phosphorus nuclei and the protons of the methylene groups.

7.1.1. Isonicotinate complexes

Isonicotinic acid (pyridine-4-carboxylic acid) was treated with a slight excess of sodium methoxide and the mixture added to a dichloromethane solution of [Ru(CH=CHC_6H_4Me-4)Cl(CO)(BTD)(PPh_3)$_2$]. An immediate colour change was observed from red to yellow. After work up, the yellow product was analysed by ^{31}P NMR spectroscopy to reveal a new singlet at 38.1 ppm. ^{1}H NMR analysis revealed typical resonances for the vinyl ligand at 7.76 and 5.36 ppm for Hα and Hβ protons (showing mutual J_{HH} coupling of 15.3 Hz), respectively. The lower field resonance also

showed coupling (doublet of triplets) to the phosphorus nuclei of the phosphine ligands (J_{HP} = 2.6 Hz) suggesting a mutually *trans* arrangement for the phosphines. An AB system at 6.83 and 6.88 ppm (J_{AB} = 7.9 Hz) was observed for the tolyl substituent along with a singlet at 2.24 ppm for the methyl group. A doublet resonance at 8.31 ppm (J_{HH} = 5.6 Hz) was assigned to the protons in positions 2 and 6 (closest to the nitrogen) of the pyridinecarboxylate ligand. The remaining protons of the ligand were found to resonate at 6.33 (J_{HH} = 5.6 Hz). The retention of the carbonyl ligand was supported by an intense absorption at 1912 cm^{-1} in the infrared spectrum along with a band at 1515 cm^{-1} attributed to the coordinated carboxylate group. Although no molecular ion was observed in the mass spectrum (FAB +ve mode), an abundant fragmentation was noted at *m/z* 631 for loss of phosphine. These data, in conjunction with good agreement of elemental analysis with calculated values, confirmed the overall formulation (*Scheme 20*) to be [Ru(CH=CHC_6H_4Me-4){κ^2-$O_2CC_5H_4N$)(CO)(PPh_3)$_2$] (**97**).

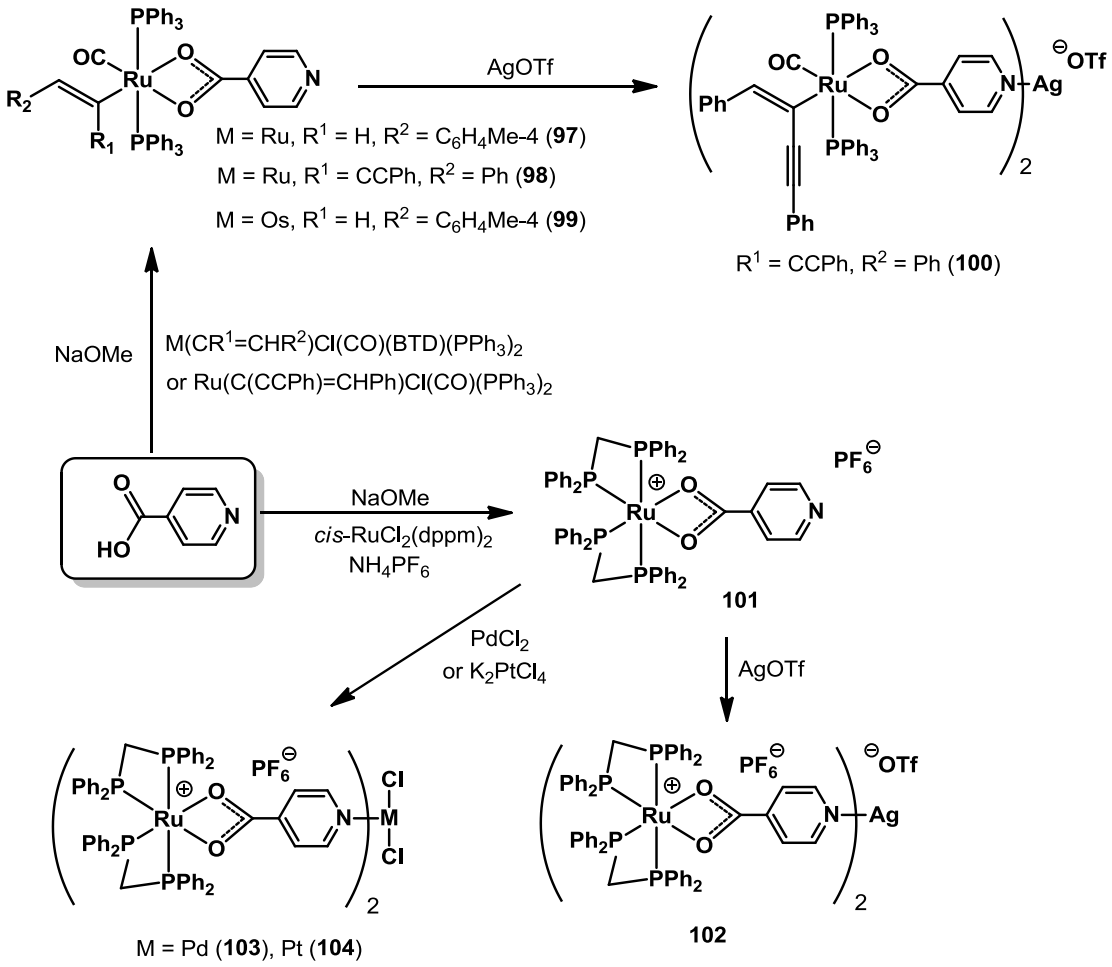

Scheme 20. Formation of heterotrimetallic complexes.

A similar reaction resulted between $HO_2CC_5H_4N$ and [Ru(C(C≡CPh)=CHPh)Cl(CO)$(PPh_3)_2$] in the presence of NaOMe to yield [Ru(C(C≡CPh)=CHPh)(κ^2-$O_2CC_5H_4N$)(CO)$(PPh_3)_2$] (**98**). The presence of the enynyl ligand was confirmed by an absorption at 2159 cm^{-1} in the solid state infrared spectrum and a singlet resonance at 5.72 ppm in the ^{1}H NMR spectrum for Hβ. Single crystals of the compound were obtained by slow diffusion of a dichloromethane solution of the complex into ethanol. An X-ray diffraction study revealed the structure shown in *Fig. 57* (see *Structural Discussion, 7.1.1.1* for more details).

An osmium analogue of compound **97**, [Os(CH=CHC_6H_4Me-4){κ^2-$O_2CC_5H_4N$)(CO)$(PPh_3)_2$] (**99**), was prepared in an identical manner. Spectroscopic features were found to be very similar to those observed for **97** apart from the characteristically lower frequency shift of the ν_{CO} absorption in the infrared spectrum at 1900 cm^{-1}.

Treatment of **98** with half an equivalent of AgOTf led to linking of the pyridine units to form the heterotrimetallic complex, [{Ru(C(C≡CPh)=CHPh)(CO)$(PPh_3)_2$(κ^2-$O_2CC_5H_4N$)}$_2$Ag]OTf (**100**). Little difference was observed in the ^{31}P NMR spectrum to that of **98**, however, a small shift in the resonance of the protons in the 2,6-positions of the pyridine ring was observed in the ^{1}H spectrum to 8.44 ppm. While a molecular ion was not observed in the mass spectrum (FAB or ES), a large peak was noted for the loss of the 'Ru(C(C≡CPh)=CHPh)(CO)$(PPh_3)_2$(κ^2-$O_2CC_5H_4N$)' fragment. The formulation was further supported by good agreement of elemental analysis with calculated values.

The compound *cis*-[$RuCl_2$(dppm)$_2$] was allowed to react with isonicotinic acid in the presence of base and NH_4PF_6 to yield the new compound, [Ru(κ^2-$O_2CC_5H_4N$)(dppm)$_2$]PF_6 (**101**) in 79 % yield. The resonance displayed by this compound in the ^{1}H NMR spectrum at 8.79 ppm (J_{HH} = 4.9 Hz) was attributed to the pyridylcarboxylate ligand, while the remaining resonances were obscured by those for the dppm ligands. The presence of the carboxylate unit was confirmed by an absorption at 1513 cm^{-1} in the infrared spectrum and a resonance at 180.3 ppm in the ^{13}C NMR spectrum. Further features in the same spectrum at 150.6, 139.5 and 121.9 ppm were assigned to the pyridinecarboxylate ligand. Compound **101** provided the second starting material for subsequent transformations, allowing harsher conditions to be employed without loss of the more robust bis(dppm) metal unit.

Reaction with silver triflate led to isolation of the complex [{Ru(dppm)$_2$(κ^2-$O_2CC_5H_4N$)}$_2$Ag]$(PF_6)_2$(OTf) (**102**) in 75% yield. Once again, little change was observed in the ^{31}P NMR spectrum, however, the resonances of the protons next to the pyridine nitrogen were shifted slightly from 8.74 ppm in the precursor to 8.87 (J_{HH} = 6.0 Hz) ppm in **102**. No molecular ion was observed in the FAB mass spectrum (+ve mode) but excellent agreement of elemental analysis with calculated values was obtained.

Some of the most significant compounds of the group 10 metals bear nitrogen-based ligands, such as *cis*-platin.[185] Thus, it was decided to explore the possibility of using the nitrogen donors in **101** to coordinate to palladium and platinum salts. Reaction of two equivalents of **101** with one of $PdCl_2$ led to formation of a dark yellow solid. This was formulated as $[\{Ru(dppm)_2(\kappa^2\text{-}O_2CC_5H_4N)\}_2PdCl_2](PF_6)_2$ (**103**) on the basis of a molecular ion in the FAB mass spectrum at *m/z* 2306 and good agreement of analytical data with calculated values. Again, a small downfield shift was observed in the 2,6-pyridyl resonance at 8.94 (J_{HH} = 6.5 Hz) ppm, compared to the precursor. The same was observed in the platinum analogue, $[\{Ru(dppm)_2(\kappa^2\text{-}O_2CC_5H_4N)\}_2PtCl_2](PF_6)_2$ (**104**) (*Scheme 20*), except that the multiplicity of the resonance was not clearly resolved due to a small J_{PtH} coupling.

The focus of the research then shifted to attempts to introduce a second organometallic centre into the molecule. Gold(I) compounds are known to coordinate readily to nitrogen donors, especially when bearing an electron-withdrawing ligand such as the pentafluorophenyl group. Thus, it was decided to explore the coordination chemistry of $[Au(C_6F_5)(tht)]$ (tht = tetrahydrothiophene) with complexes of the type used in the previous experiments.

In addition to the versatile reactivity at the metal centre shown by the vinyl complexes $[Ru(CR^1{=}CHR^2)Cl(CO)(BTD)(PPh_3)_2]$, a wide range of substituents (R^1 and R^2) can be introduced through their synthesis from ruthenium hydride precursors. This was exploited in order to introduce a fluorinated 'tag' to the vinyl unit. The alkyne, 1-ethynyl-4-fluorobenzene, was used to prepare the new vinyl compound, $[Ru(CH{=}CHC_6H_4F\text{-}4)Cl(CO)(BTD)(PPh_3)_2]$ (**105**), in good yield from $[RuHCl(CO)(BTD)(PPh_3)_2]$ (*Scheme 21*). The ^{19}F NMR spectrum displayed a singlet resonance at -120.1 ppm, while the remaining spectroscopic data were found to be very similar to the other vinyl precursors and thus unremarkable. The same procedure employed to prepare **97** was used to convert **105** into the isonicotinate compound $[Ru(CH{=}CHC_6H_4F\text{-}4)(\kappa^2\text{-}O_2CC_5H_4N)(CO)(PPh_3)_2]$ (**106**). In addition to similar spectroscopic data to those seen for **97**, the ^{19}F nuclear magnetic resonance remained essentially unshifted, at -121.4 ppm. Treatment of equimolar quantities of **106** and $[Au(C_6F_5)(tht)]$ led to the formation of the brown compound, $[Ru(CH{=}CHC_6H_4F\text{-}4)\{\kappa^2\text{-}O_2CC_5H_4N(AuC_6F_5)\}(CO)(PPh_3)_2]$ (**107**). Unsurprisingly, the most diagnostic data came from the ^{19}F NMR spectrum, in which resonances were observed at -163.1, -159.3 and -116.5 ppm for the *meta*-, *para*- and *ortho*-fluorine nuclei of the C_6F_5 ligand, respectively, along with a peak at -121.2 ppm for the vinyl substituent. The integration of these resonances was found to be 2:1:2:1, confirming the formation of the bimetallic complex (*Scheme 21*).

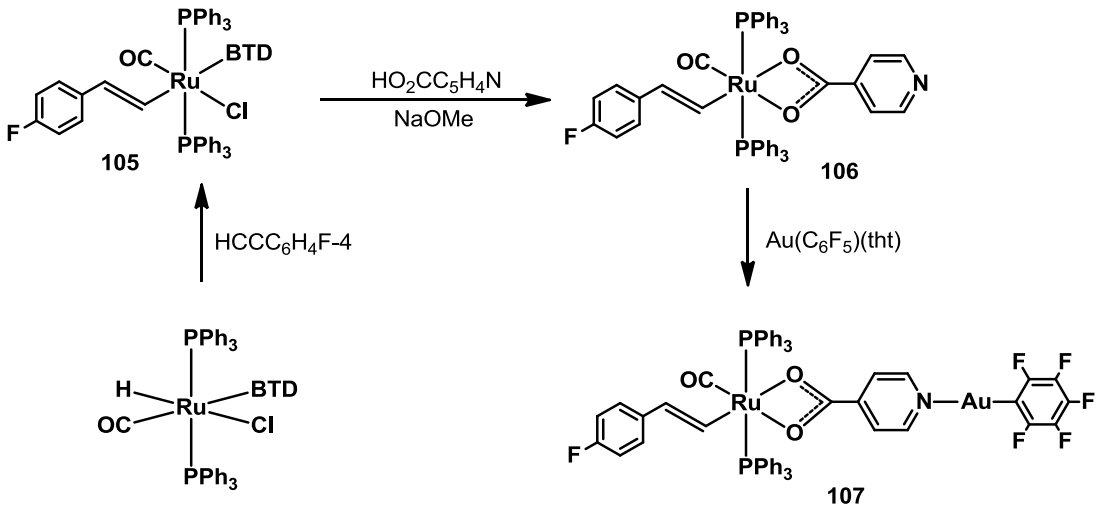

Scheme 21. Formation of a heterobimetallic compound bearing fluorinated ligands.

7.1.1.1. Structural Discussion

The structure of complex **98** is based on a distorted octahedral arrangement with *cis*-angles at the metal centre in the range 58.47(4) – 111.43(5)°, the smallest of which is the O(1)–Ru–O(3) angle. The Ru–O(1) and Ru–O(3) distances of 2.3050(10) and 2.1804(10) Å, respectively, are not equal and indicate the superior *trans* influence of the vinyl ligand, causing an elongation of the Ru–O(1) bond. The ruthenium vinyl precursor used to produce compound **98** was formed by insertion of an alkyne into a Ru-H bond, a process which typically occurs regiospecifically to yield the *E*-isomer.[114, 120] This is reflected in the observed regiochemistry at the double bond of the vinyl ligand in the structure of **98**. The C(10)–C(19) distance of 1.352(2) Å is typical for a double bond between carbon atoms, while the C(11)–C(12) [1.205(2) Å] distance is within the usual range for triple bonds.[150] Otherwise the structural data associated with the vinyl ligand are unremarkable and compare well with related complexes such as [Ru(C(C≡CPh)=CHPh)(O_2CFc)(CS)(PPh_3)$_2$].[178]

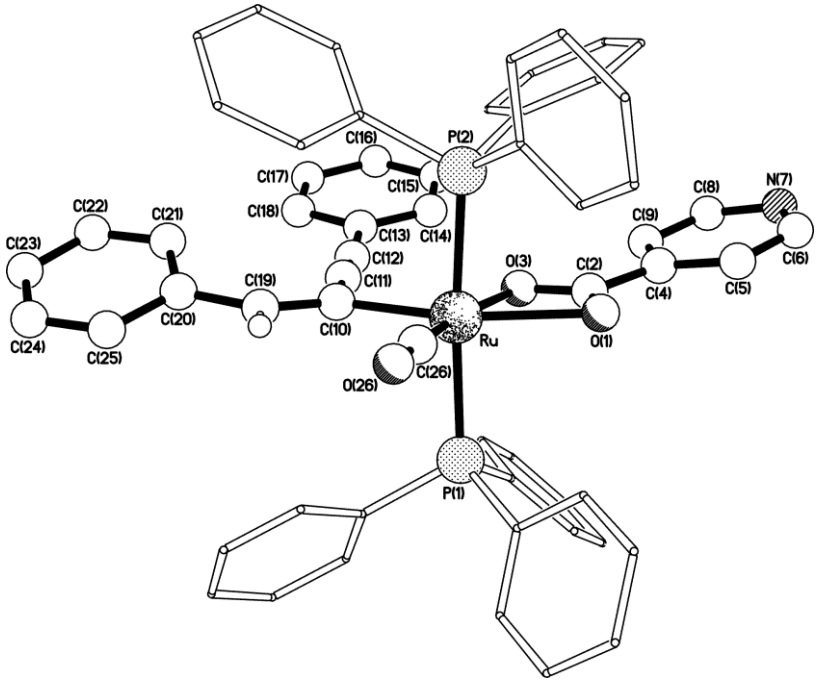

Figure 57. Molecular structure of [Ru(C(C≡CPh)=CHPh)($O_2CC_5H_4N$)(CO)(PPh_3)$_2$] (**98**). Selected bond distances (Å) and angles (°): Ru–C(26) 1.8144(14), Ru–C(10) 2.0618(14), Ru–O(3) 2.1804(10), Ru-O(1) 2.3050(10), Ru–P(1) 2.3683(4), Ru–P(2) 2.3758(4), O(1)–C(2) 1.2620(17), C(2)–O(3) 1.2647(17), C(10)–C(19) 1.352(2), C(10)–C(11) 1.427(2), C(11)–C(12) 1.205(2), C(26)–O(26) 1.1582(17), O(3)–Ru-O(1) 58.47(4), C(19)–C(10)–Ru 130.56(11), P(1)–Ru–P(2) 175.240(13), C(12)–C(11)–C(10) 176.69(16), O(1)–C(2)–O(3) 120.46(13).

7.1.2. Cyanobenzoate complexes

In order to broaden the investigation of multimetallic complexes based on oxygen and nitrogen donor ligands, the reactivity of the related 4-cyanobenzoic acid ligand was also explored. While structurally similar to isonicotinic acid, the nitrogen donor of the nitrile group is separate from the aromatic system and this can have subtle effects on the reactivity observed. The compounds [Ru(CR^1=CHR^2)(κ^2-$O_2CC_6H_4CN$-4)(CO)(PPh_3)$_2$] (R^1 = H, R^2 = C_6H_4Me-4 **108**; R^1 = C≡CPh, R^2 = Ph **109**; R^1 = H, R^2 = C_6H_4F-4 **110**) were all prepared from the appropriate vinyl precursors, [Ru(CR^1=CHR^2)Cl(CO)(BTD)(PPh_3)$_2$], in a similar procedure to that employed in the preparation of **97**, **98** and **106** (Scheme 22). In the ^{1}H NMR spectrum of compound **108**, the coordinated 4-cyanobenzoate ligand gave rise to an AB system at 6.42 and 6.79 ppm, showing a mutual coupling of 8.0 Hz. Similar features were observed in **109** and **110**.

Treatment with [Au(C_6F_5)(tht)] led to the formation of [Ru(CR^1=CHR^2){κ^2-$O_2CC_6H_4$($CNAuC_6F_5$)-4}(CO)(PPh_3)$_2$] (R^1 = H, R^2 = C_6H_4Me-4 **111**; R^1 = C≡CPh, R^2 = Ph **112**; R^1 = H, R^2 = C_6H_4F-4 **113**). Initial experiments were carried out to form **111** and **112**. Apart from a shift in

the resonance attributed to the aromatic protons closest to the nitrile group, little spectroscopic change was observed. However, elemental analysis data and the observation of diagnostic fragments in the mass spectra supported the formulations. Again, the fluorine 'tag' allowed the reaction to be confirmed spectroscopically for compound **113**. The expected ratio of resonances was seen in the ^{19}F NMR spectrum at very similar chemical shifts to those found for **107**.

While the methodology described above is useful, it becomes more powerful when it can be employed commencing from either end of the molecule. Thus, the reaction of 4-cyanobenzoic acid and [Au(C_6F_5)(tht)] was investigated. A colourless solid was obtained which displayed shifted resonances in the ^1H NMR spectrum for the *N*-coordinated isonicotinic acid ligand. No change in the ν_{OCO} absorption was observed in the infrared spectrum compared to the features displayed by the free ligand. On the basis of these data and the mass spectrum, which displayed a molecular ion at *m/z* 513, the product was formulated as [Au(C_6F_5)($NCC_6H_4CO_2H$-4)] (**114**). This was then used to convert [Ru(CH=CHC_6H_4F-4)Cl(CO)(BTD)(PPh_3)$_2$] into [Ru(CH=CHC_6H_4F-4){κ^2-$O_2CC_6H_4$($CNAuC_6F_5$)-4}(CO)(PPh_3)$_2$] (**113**) in the presence of NaOMe. This second, alternative route to **113** illustrated the flexibility of the approach employed, in which the coordinated donor is selective for the first metal introduced (*Scheme 22*).

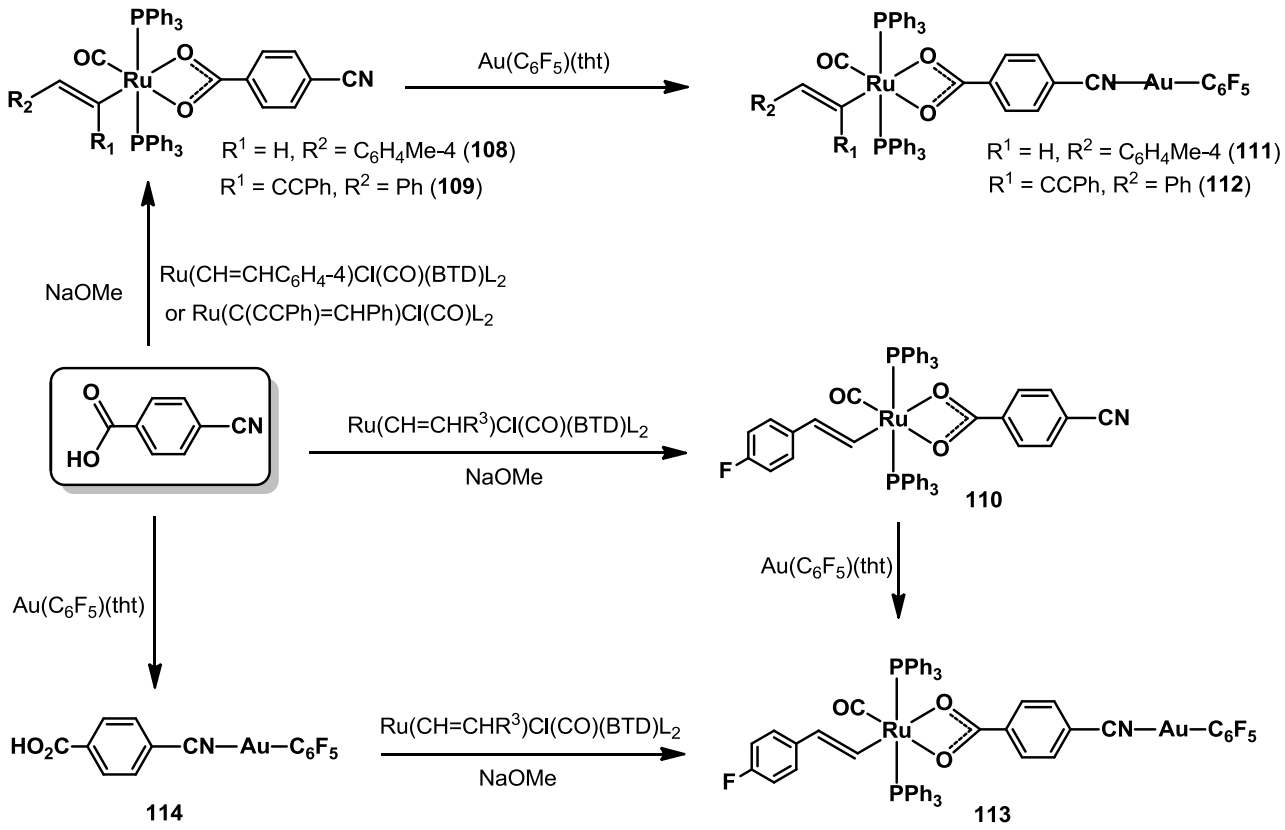

Scheme 22. Formation of bimetallic compounds and the illustration of two routes to the same heterobimetallic compound. $R^3 = C_6H_4F$-4, L = PPh_3.

7.2. Pentametallic complexes

7.2.1. Rhodium complexes

A recent report[103] described a new variation on the standard reaction of pyridine with rhodium chloride, in which $RhCl_3 \cdot 3H_2O$ reacts with isonicotinic acid to give $[RhCl_2(NC_5H_4CO_2)(NC_5H_4CO_2H)_3]Cl$. Following this protocol, the aforementioned compound was treated with saturated sodium hydroxide solution to yield $[RhCl_2(NC_5H_4CO_2)(NC_5H_4CO_2Na)_3]$, which boasts four carboxylate units. Treatment of a methanol solution of this compound with four equivalents of $[Ru(CH=CHC_6H_4Me\text{-}4)Cl(CO)(BTD)(PPh_3)_2]$ yielded $[RhCl_2\{NC_5H_4CO_2(Ru(CH=CHC_6H_4Me\text{-}4)(CO)(PPh_3)_2\}_4]Cl$ (**115**, *Scheme 23*). Evidence for the presence of the ruthenium vinyl units was provided by a diagnostic doublet of triplets (shifted relative

to the precursor) at 7.77 ppm in the ^{1}H NMR spectrum for the Hα proton, while the C_5H_4N unit gave rise to doublet resonances at 6.35 and 8.32 ppm. These chemical shift values are very close to those observed for **97**, which is identical to the termini formed in the reaction to yield **115**. Good agreement of elemental analysis with calculated values indicated successful coordination of all four ruthenium units, although no clear molecular ion was observed in the FAB mass spectrum (+ve mode).

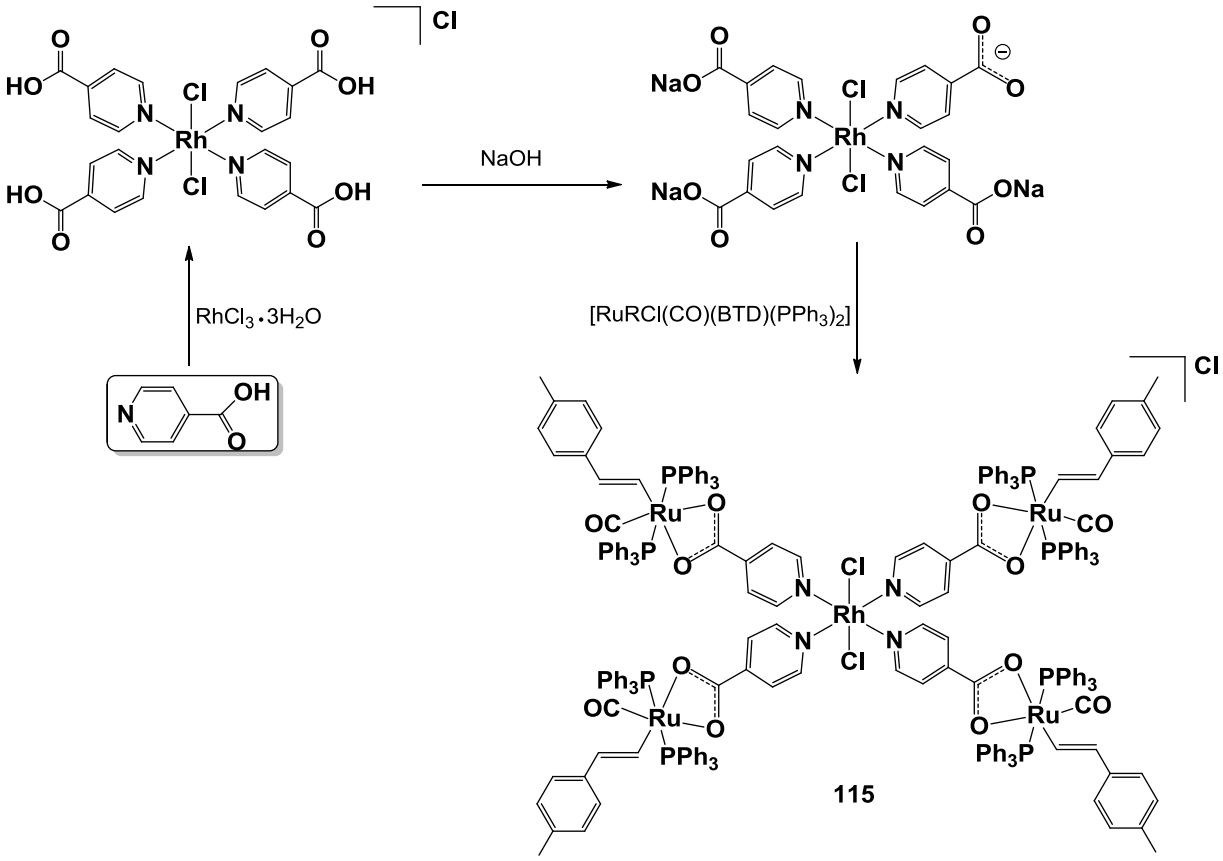

Scheme 23. Formation of a pentametallic compound based on a rhodium core.

R = $CH{=}CHC_6H_4Me$-4

Although the reaction to form **115** proved successful, the product was prone to loss of triphenylphosphine (observed as the oxide in the ^{31}P NMR spectrum). Therefore, a building unit with extended linkers was prepared from the reaction of rhodium trichloride and 4-(4-pyridyl)benzoic acid under the same conditions used to generate $[RhCl_2(NC_5H_4CO_2)(NC_5H_4CO_2Na)_3]$. The compounds, $[RhCl_2\{NC_5H_4(C_6H_4CO_2H)\text{-}4\}_4]Cl$ (**116**) and $[RhCl_2\{NC_5H_4(C_6H_4CO_2)\text{-}4\}\{NC_5H_4(C_6H_4CO_2Na)\text{-}4\}_3]$ (**117**), shown in *Scheme 24*, were isolated and characterised in the usual manner. The 4-(4-pyridyl)benzoate ligand in **117** gave rise to four resonances between 7.90 and 8.80 ppm in the ^{1}H NMR spectrum. Reaction of **117** with *cis*-$[RuCl_2(dppm)_2]$ in the presence of excess NH_4PF_6 led to formation of $[RhCl_2\{NC_5H_4(C_6H_4CO_2Ru(dppm)_2)\text{-}4\}_4](PF_6)_5$ (**118**), as shown in *Scheme 24*.

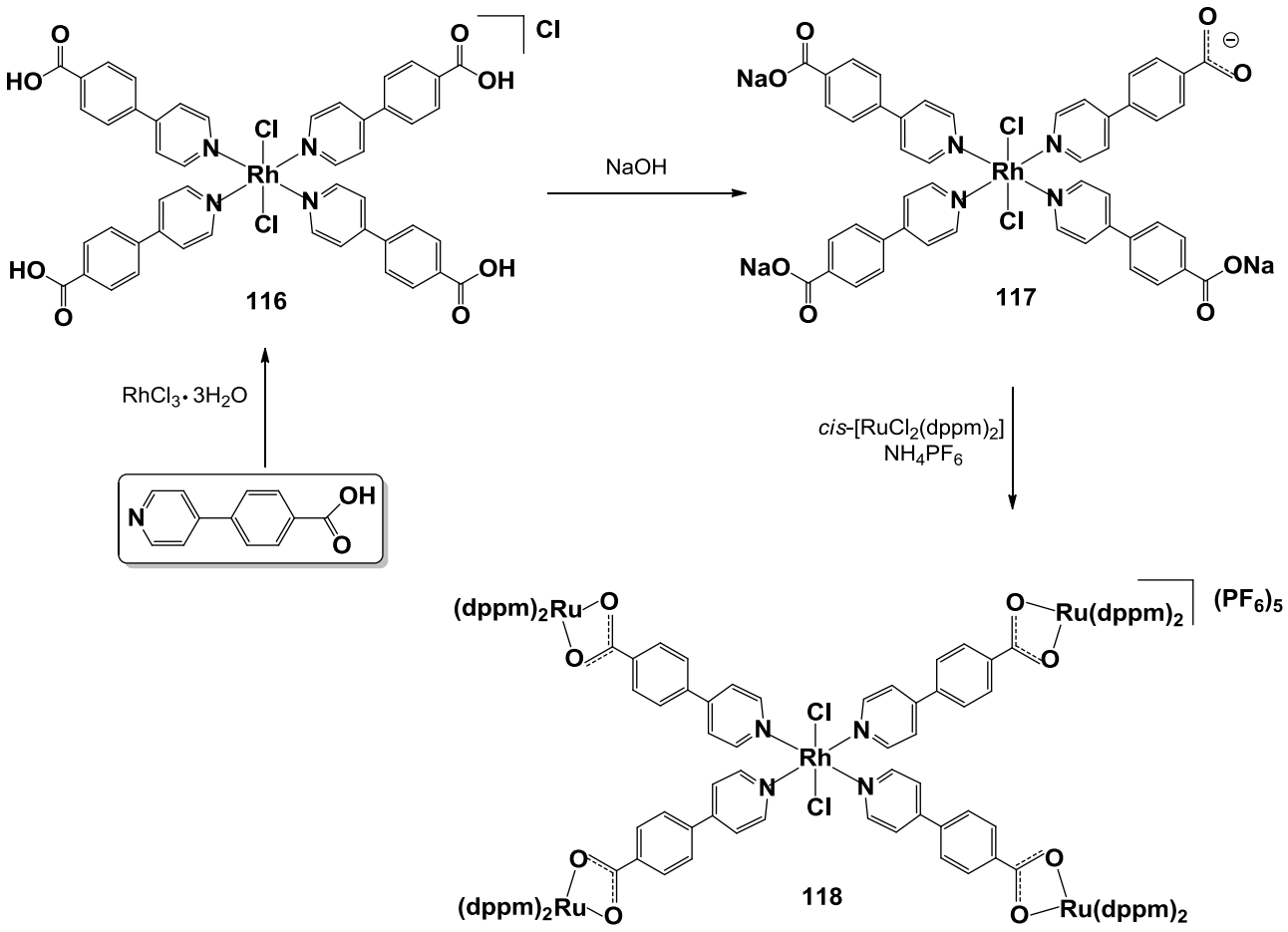

Scheme 24. Pentametallic compounds based on an extended rhodium core.

In addition to similar resonances for the $[O_2CC_6H_4C_5H_4N]^-$ ligand in the ^{1}H NMR spectrum of $[RhCl_2\{NC_5H_4(C_6H_4CO_2Ru(dppm)_2)\text{-}4\}_4](PF_6)_5$ (**118**), characteristic features were observed for the methylene protons of the dppm ligands at 4.03 and 4.75 ppm. The presence of all four ruthenium-phosphine units was confirmed by analytical data.

7.2.2. Palladium porphyrin complexes

In addition to their applications in fields as diverse as catalysis[186, 187] and photodynamic therapy,[188] metalloporphyrins have also been employed as versatile building blocks for more complex systems. Their use as motifs in MOF design has been explored in a number of reports,[189-191] which have illustrated the potential of using peripheral functional groups to build complexity into the system in a controlled manner. The palladium-centred tetraphenylporphyrin, [(Pd-TPP)(*p*-$CO_2H)_4$],[40, 192] has performed this role in a number of recent reports with the carboxylate termini playing a key role in creating porous materials with dirhodium paddlewheel units[193] and ones based on nodes of cobalt[194] and zinc[194, 195] ions. However, despite this activity in the area, no examples exist of non-homoleptic termini (i.e., with co-ligands), or with ruthenium units.

Thus, in order to explore this versatile metalloporphyrin core, [(Pd-TPP)(*p*-$CO_2H)_4$] (*Scheme 25*)[40, 192] was employed as the basis of pentametallic systems. Reaction of *cis*-[$RuCl_2(dppm)_2$] with the metalloporphyrin, in the presence of NaOMe and NH_4PF_6 yielded [(Pd-TPP){*p*-$CO_2Ru(dppm)_2\}_4$]$(PF_6)_4$ (**119**). The orange product was isolated in 74% yield and characterised initially based on the distinctive resonances in the ^{1}H NMR spectrum. Three resonances were observed for the porphyrin at 8.97 (singlet), 8.32 (doublet, J_{AB} = 7.8 Hz) and 8.17 (multiplet, coincident with a C_6H_5 resonance) ppm. The former was attributed to the pyrrole protons and the latter were assigned to the *ortho*/*meta* system for the carboxyphenyl substituents. These features integrated correctly with typical peaks for the methylene protons of the dppm ligands (4.07 and 4.74 ppm). In the solid state infrared spectrum, an intense ν_{OCO} absorption was observed at 1519 cm^{-1}.

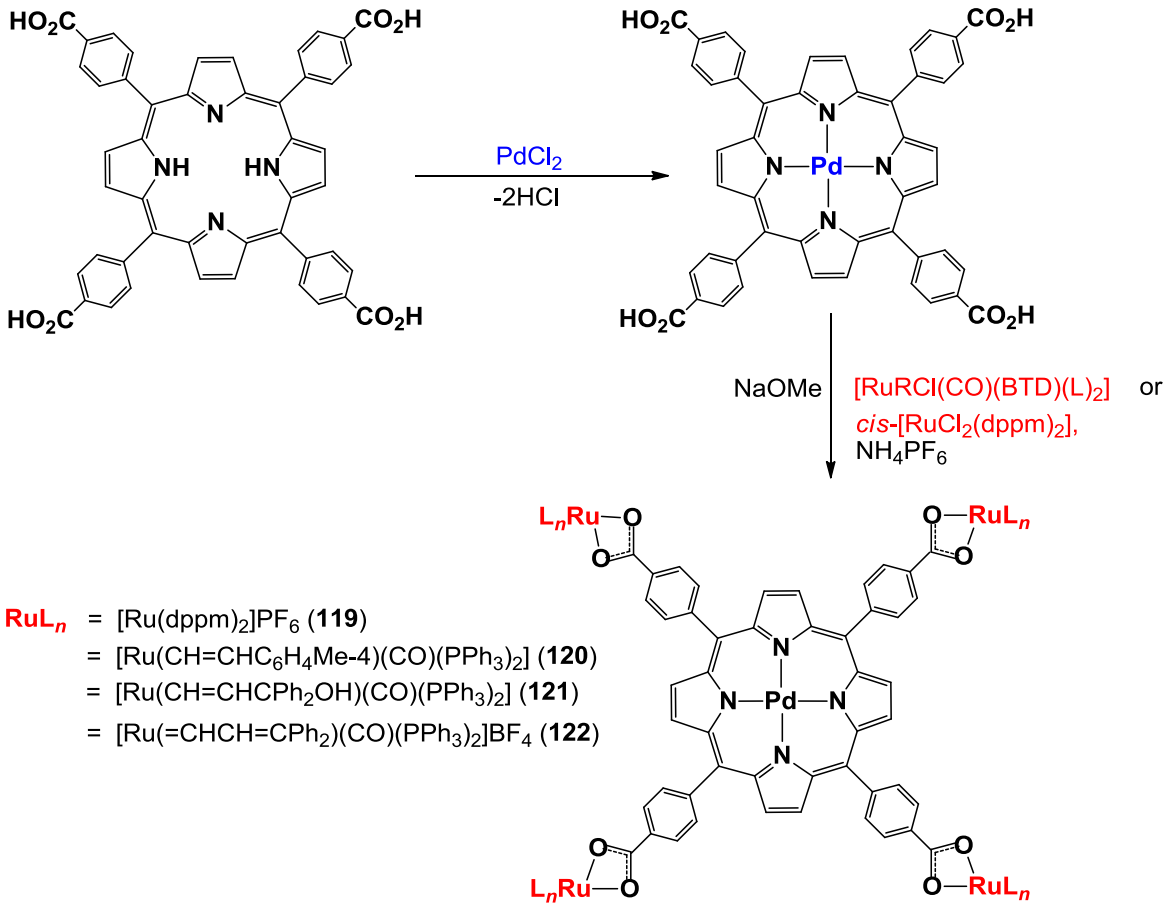

Scheme 25. Formation of a pentametallic compound based on a palladium-porphyrin core; R = CH=CHC$_6$H$_4$Me-4, CH=CHCPh$_2$, L = PPh$_3$, BTD = 2,1,3-benzothiadiazole.

More diverse functionality was introduced into the system through the reaction of [(Pd-TPP)(*p*-CO$_2$H)$_4$] with four equivalents of [Ru(CH=CHC$_6$H$_4$Me-4)Cl(CO)(BTD)(PPh$_3$)$_2$] in the presence of excess base. The product, [(Pd-TPP){*p*-CO$_2$Ru(CH=CHC$_6$H$_4$Me-4)(CO)(PPh$_3$)$_2$}$_4$] (**120**), shown in *Scheme 25* gave rise to distinctive resonances in the ^{1}H NMR spectrum for the tolylvinyl ligand at 2.27 (Me), 6.67 (Hβ), 6.97, 7.10 (AB, C$_6$H$_4$) and 8.57 (Hα) ppm. The lowest field resonance of these was observed as a doublet of triplets (J_{HH} = 15.3 Hz, J_{HP} = 2.7 Hz) assigned to the Hα protons, with the fine structure indicating the retention of mutually *trans* phosphine ligands on the metal units. Intense absorptions were observed at 1919 cm^{-1} (ν_{CO}) and 1508 cm^{-1} (ν_{OCO}) in the solid state infrared spectrum. The overall formulation was confirmed by good agreement of elemental analysis with calculated values.

The γ-hydroxyvinyl compound [(Pd-TPP){*p*-CO$_2$Ru(CH=CHCPh$_2$OH)(CO)(PPh$_3$)$_2$}$_4$] (**121**) was prepared in a similar fashion. Dehydration of this pentametallic complex with HBF$_4$ led to formation of the vinylcarbene compound [(Pd-TPP){*p*-CO$_2$Ru(=CHCH=CPh$_2$)(CO)(PPh$_3$)$_2$}$_4$](BF$_4$)$_4$

(**122**). A broad resonance at 14.94 ppm was assigned to the carbenic proton, based on similar complexes bearing the same ligand,[105] while the Hβ proton was obscured by the features of the C_6H_5 units. The remaining peaks were similar to those found for compounds **119** - **121**. This result illustrates that, not only can such metallo-porphyrins be used as a scaffold for additional of metal units, but that further functionalisation can be performed subsequently.

Electrochemistry

The highly conjugated nature of the pentametallic assemblies prepared in this section led to a brief investigation of their electrochemical properties (measured by Dr. K. B. Holt at UCL). The complex [(Pd-TPP){*p*-CO_2Ru(CH=CHC_6H_4Me-4)(CO)$(PPh_3)_2$}$_4$] (**120**) was chosen for investigation and the degree of interaction between the metal centres probed by cyclic voltammogram (CV). The CV for the pentametallic complex shows a reversible redox couple centred at E = 0.21 V versus ferrocene (Fc / Fc^+), followed by irreversible oxidation at E = 0.77 V versus ferrocene, is observed (*Fig. 58*). The behaviour at lower potential is very similar to that observed for the dinuclear ruthenium complex, [{Ru(CH=CHC_6H_4Me-4)(CO)$(PPh_3)_2$}$_2$($S_2COCH_2C_6H_4CH_2OCS_2$)],[110] and shows that the ruthenium centres are not perturbed by presence of the palladium porphyrin unit. The reversible redox couple corresponds to Ru(II)/Ru(III) electron transfer and is highly reversible and well-behaved over a range of scan rates, indicating the complex is very stable towards electron transfer. The irreversible peak at ca. 0.8 V can also be attributed to further oxidation of the ruthenium units, as this peak was also observed for the dinuclear complex[110]; however the monometallic starting material, [(Pd-TPP)(*p*-$CO_2H)_4$] (in tetrahydrofuran), also undergoes a reversible one electron oxidation at 0.81 V (vs Fc/Fc^+). Thus the rather ill-defined peak at 0.8 V in *Figure 58* is likely a superposition of this secondary irreversible oxidation of the Ru units and the oxidation of the Pd moiety. In principle the peak currents for the Ru centres should be larger than that for the Pd centre by a factor consistent with 4 electron transfer for the 4 Ru centres to 1 electron for the Pd centre. However the superposition of the Pd oxidation with further oxidation of the Ru centres does not allow such a ratio to be determined for this system. Consistent with observations for the dinuclear Ru complex, no evidence can be seen from voltammetry for electronic communication between the Ru centres and electron transfer appears to take place at the four centres simultaneously.

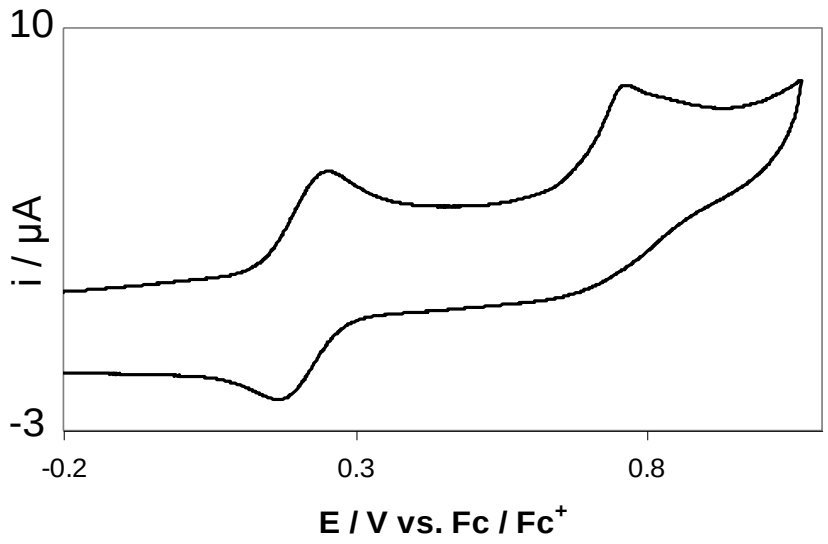

Figure 58. CV for complex [(Pd-TPP){*p*-$CO_2Ru(CH{=}CHC_6H_4Me$-4)$(CO)(PPh_3)_2\}_4$] (**120**); conditions: 0.25 mM in 0.1 M $TBAPF_6$/ DCM, 100 mV/s, glassy carbon electrode.

7.3. Functionalised silver nanoparticles

With the utility of these nitrogen-oxygen mixed-donor ligands in the formation of multimetallic compounds now clear, it was decided to explore this approach for the surface functionalisation of silver nanoparticles. It has been shown that such colloids are readily stabilised by nitrogen donor groups such (poly)pyridines.[196, 197] The commercially available linkers discussed here would thus, potentially, allow straightforward attachment of metal units to the surface of these materials. Due to the robust nature of the dppm ligands (e.g., in the presence of borohydride), [Ru(κ^2-$O_2CC_5H_4N$)$(dppm)_2$]PF_6 (**101**) was chosen as a surface unit. The analogous 4-pyridylbenzoate compound, [Ru{κ^2-$O_2CC_6H_4(C_5H_4N)$-4}$(dppm)_2$]PF_6 (**123**) was also prepared.

Reaction of $AgNO_3$ with sodium borohydride in the presence of [Ru(κ^2-$O_2CC_5H_4N$)$(dppm)_2$]PF_6 (**101**) or [Ru{κ^2-$O_2CC_6H_4(C_5H_4N)$-4}$(dppm)_2$]PF_6 (**123**) gave the silver nanoparticles, Ag@[$NC_5H_4\{CO_2Ru(dppm)_2\}$-4]$PF_6$ (**NP7**) and Ag@[$NC_5H_4\{C_6H_4CO_2Ru(dppm)_2\}$-4]$PF_6$ (**NP8**) as black solids after centrifuging and exhaustive washing to remove excess borohydride (water) and unbound surface units (acetone) (*Scheme 26*).

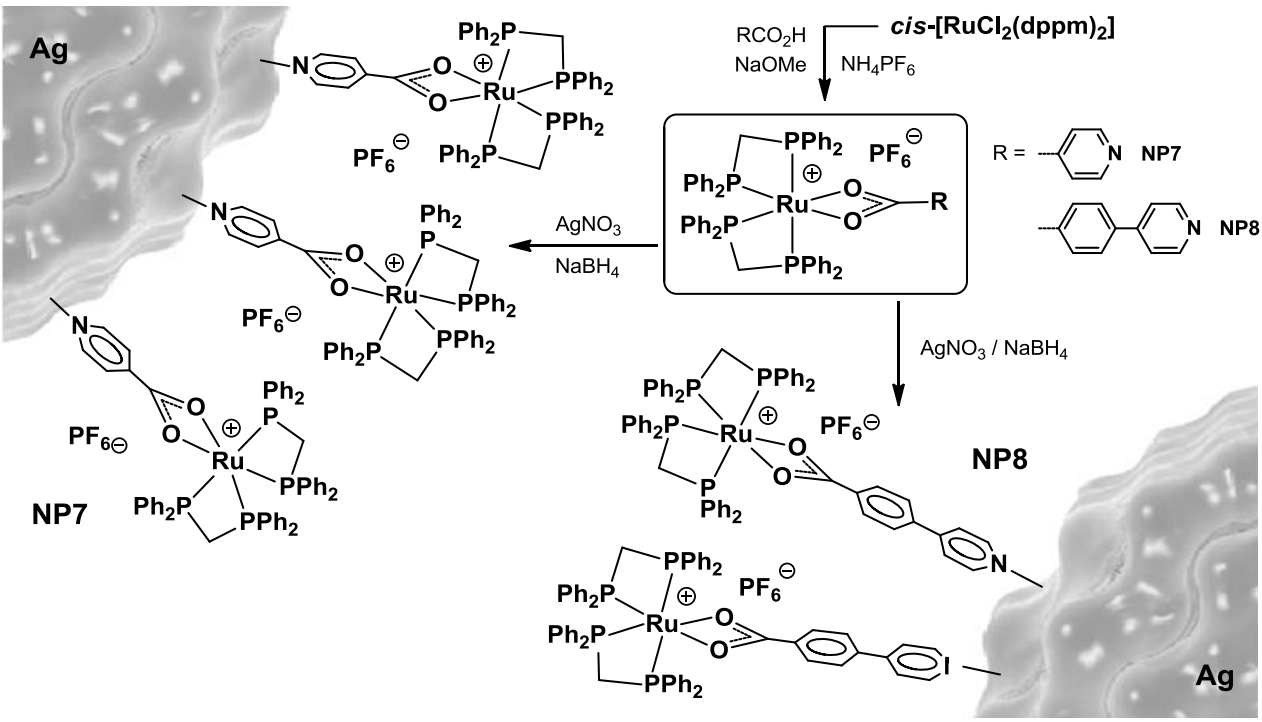

Scheme 26. Functionalisation of silver nanoparticles with ruthenium surface units.

Both **NP7** and **NP8** proved insoluble in common deuterated laboratory solvents so NMR analysis could not be obtained. However, solid state infrared spectra showed the presence of characteristic bands for the ruthenium-phosphine surface units. Transmission electron microscopy (TEM) was used to determine the average diameter of the nanoparticles (*Fig. 59*) and this revealed the sizes of **NP7** to be 19.0 (± 4.1) nm and **NP8** to be 12.8 (± 3.3) nm.

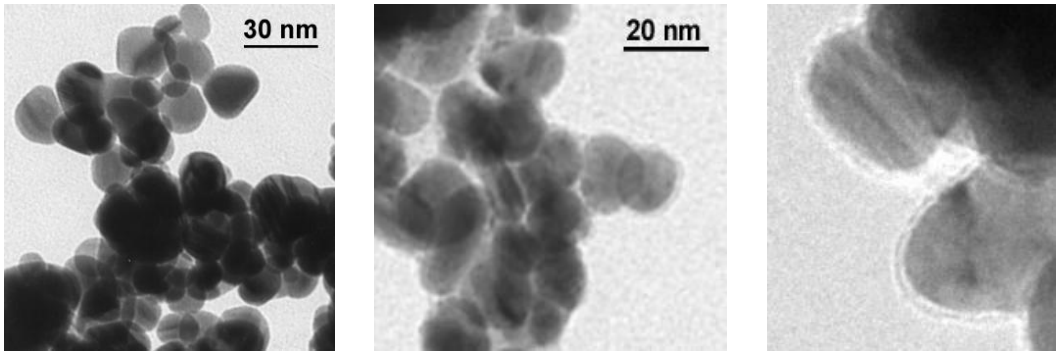

Fig. 59. TEM images of **NP7** (left), **NP8** (middle) and **NP7** (right) in higher resolution

Closer investigation of the images (*Fig. 59, right*), revealed a surface layer, which was analysed by Energy Dispersive X-ray spectroscopy (EDX) to contain both ruthenium and phosphorus (in addition to silver), confirming the presence of the ruthenium-phosphine surface units.

7.4. Summary

The synthesis of a range of new bi-, tri and penta- metallic compounds has been presented. The bifunctional ligands, isonicotinic acid and 4-cyanobenzoic acid were employed in their deprotonated forms to generate versatile ruthenium complexes which could then be used as precursors for the addition of further metals (from groups 10 and 11). Through the differing affinities of the donors for the metal centres employed, heterobimetallic and heterotrimetallic complexes were synthesised. This approach illustrates the way that these simple, commercially available linkers can be used to generate multimetallic compounds. The metal units used here for building blocks were chosen primarily for their spectroscopic and synthetic properties, however, they provide a proof of concept which can be expanded to include metals tailored for particular applications. Furthermore, the metal complexes generated from such mixed-donor ligands, have been shown to functionalise the surface of silver nanoparticles, generating colloids 'decorated' with metal units.

Pentametallic compounds based on a rhodium core, with an extended pyridyl benzoic acid framework, have also been synthesised. The rhodium 4-pyridylbenzoate compound (and the rhodium isonicotinate analogue) can undergo complexation at the carboxylate termini of the linkers with ruthenium vinyl units, to produce extended pentametallic structures. In addition, metalloporphyrins have also been utilised as versatile building blocks for more complex architectures. The palladium-porphyrin, [(Pd-TPP)(*p*-$CO_2H)_4$] has been shown to function as a scaffold for additional metal units containing vinyl co-ligands, generating pentametallic compounds in a similar manner. Moreover, upon dehydration, the γ-hydroxyvinyl analogue has been shown to undergo transformation to generate a pentametallic compound with vinylcarbene units, indicating the potential for further functionalisation.

Chapter 8: Conclusion

8. Chapter 8: Conclusion

The work presented in this thesis describes the preparation of new 'smart' dithiocarbamate complexes by manipulation of the functionality on the dithiocarbamate backbone using cheap and commercially available amines. These complexes can then be used as a starting point for further chemistry as their robust nature has been demonstrated by protonation studies and ring-closing metathesis reactions performed on a range of amine- and diallyl- terminated dithiocarbamate complexes, respectively.

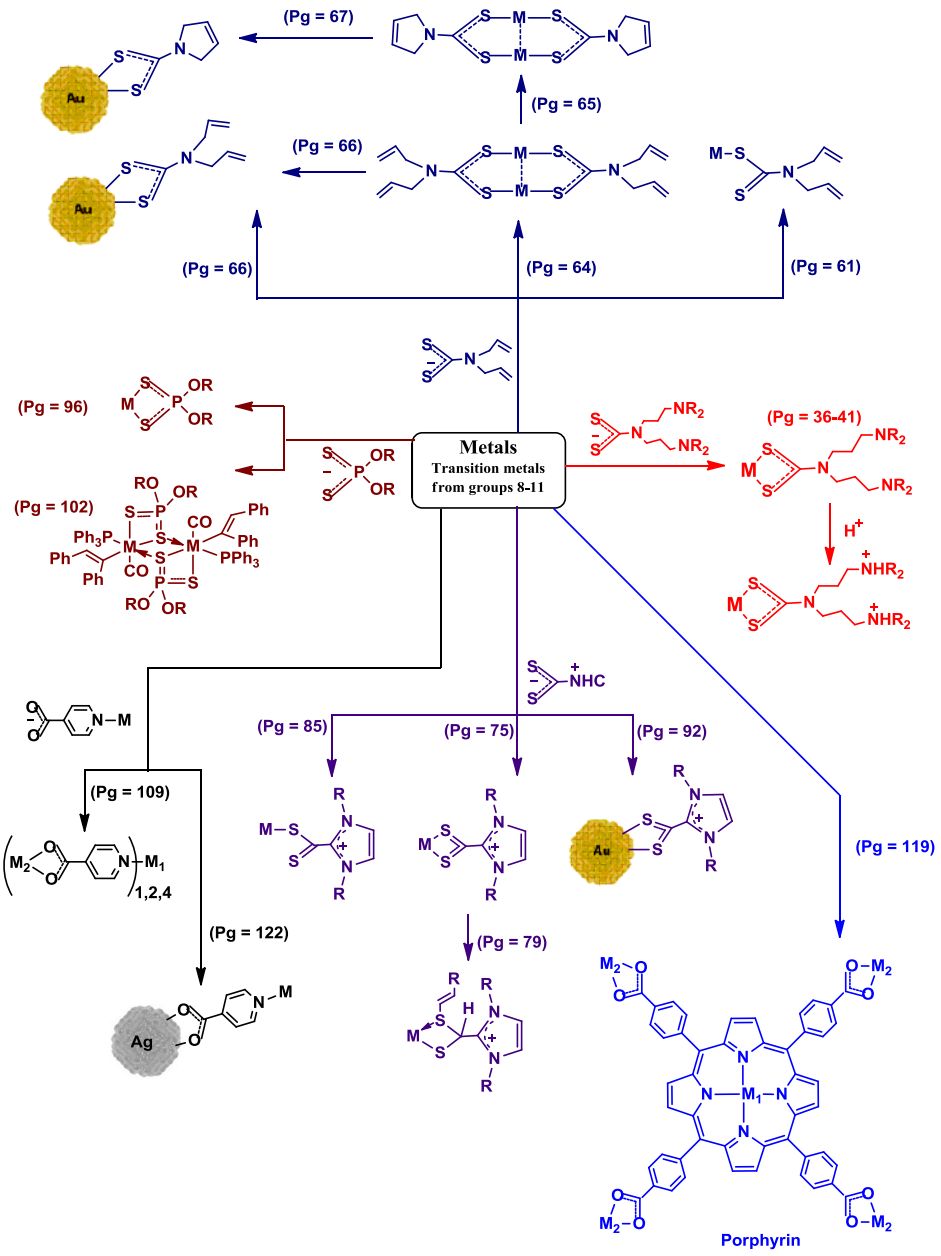

Figure 60. Summary of some of the complexes, assemblies and nanomaterials discussed in this thesis.

The work on dithiocarboxylate ligands expands the underexplored coordination chemistry of this related class of ligand. The first examples of gold(I) complexes of dithiocarboxylate ligands, derived from NHCs, offering additional tuneability due to the R groups on the imidazolium ring have been prepared. The NHC•CS_2 zwitterions have been shown to act as excellent donors for a range of mono- and bimetallic gold complexes with phosphine, carbene and isonitrile co-ligands. This study also reports the synthesis and characterisation of ruthenium-alkenyl complexes with these ligands and evidence of a remarkable rearrangement caused by their steric effect has also been provided.

Having generated the NHC•CS_2 and diallyl DTC ligands, their potential as surface units on gold nanoparticles has been explored. This can be achieved either directly or through molecular precursors.

The possibilities afforded by the sulphur-derivatives of dialkyldithiophosphates in the realm of coordination chemistry has been investigated and this provides a comparison to other members of the 1,1-dithio ligand family. Generally, the reactivity of the ethyldithiophosphate ligand has been shown to be similar to the other dithio analogues, however the ruthenium enynyl compounds isolated have been shown to display different behaviour, generating monophosphine species rather than the expected bis(phosphine) product. Furthermore, the sulphur chelate of the dialkyldithophosphate ligand exhibits greater hemilabile behaviour compared to other 1,1-dithio ligands, allowing synthesis of ruthenium vinyl and acetylide species from [RuH{κ^2-$S_2P(OEt)_2$}$(CO)(PPh_3)_2$]. For the first time dialkyldithiophosphate complexes bearing vinyl, enynyl and thioacyl ligands have been synthesised.

In addition, the $[SP(O)(OEt)_2]^-$ ligand has also been investigated in order to compare its coordination chemistry with its symmetrical dithio analogue.

Complexes based on oxygen and nitrogen donors have been discussed with particular emphasis on multimetallic systems. The use of appropriate bridging ligands such as isonicotinic acid, has allowed the bonding of certain metal ions preferentially to either end of the ligand and has proven to be a successful strategy in building hetero-multimetallic frameworks. Through the differing affinities of the oxygen or nitrogen donors for the metal centres employed, hetero- bimetallic, trimetallic and pentametallic complexes have been synthesised. This approach illustrates how simple, commercially available linkers can be used to generate multimetallic compounds.

The methodology has also been extended to the surface functionalisation of nanoparticles and, for the first, time silver nanoparticles covered with isonicotinate metal complexes have been prepared. This demonstrates that metal units can be introduced to the surface of nanoparticles in a facile manner. If these metal units are tailored for specific applications (catalysis, sensing), this methodology could be exploited to prepare new functional materials.

9: Experimental Details

9. Experimental Details

General Comments

All experiments were carried out under aerobic conditions while the metathesis reactions were conducted under nitrogen using degassed dichloromethane. The majority of the complexes appear indefinitely stable towards the atmosphere in solution or in the solid state. Decomposition to gold colloid was occasionally observed by some of the gold complexes, indicated by a purple colouration.

The complexes $[RuHCl(CO)(BTD)(PPh_3)_2]$,[198] $[Ru(CH=CHBu^t)Cl(CO)(BTD)(PPh_3)_2]$, $[Ru(CH=CHC_6H_4Me\text{-}4)Cl(BTD)(CO)(PPh_3)_2]$, $[Ru(CH=CHCPh_2OH)Cl(BTD)(CO)(PPh_3)_2]$ and $[Os(CH=CHC_6H_4Me\text{-}4)Cl(BTD)(CO)(PPh_3)_2]$ were prepared using the literature route[119], substituting 2,1,3-benzoselanadiazole (BSD) for the for the commercially available 2,1,3-benzothiadiazole (BTD) ligand. The enynyl compounds $[Ru(C(C{\equiv}CPh){=}CHPh)Cl(CO)(PPh_3)_2]$,[199] $[Os(C(C{\equiv}CPh){=}CHPh)Cl(CO)(BTD)(PPh_3)_2]$[162] and $[Ru(C(C{\equiv}CBu^t){=}CHBu^t)Cl(CO)(PPh_3)_2]$[181] were prepared as described elsewhere. *cis*-$[RuCl_2(dppm)_2]$,[200] $[MCl_2(dppf)]$ (M = Ni,[201] Pd,[202] Pt[203]), $[NiCl_2(dppp)]$,[204] $[Pd(C,N\text{-}C_6H_4NCH_2Me_2)Cl]_2$,[205] and $[Ru(=CHPh)Cl_2(SIMes)(PCy_3)]$[24], IPr•$CS_2$,[27] ICy•$CS_2$,[27] IMes•$CS_2$,[27] and IDip•$CS_2$[27] and $[Ru(CPh=CHPh)Cl(CA)(PPh_3)_2]$ (A = O,[115] S[178]) were synthesised as described in the indicated reports. The following gold complexes were prepared as described elsewhere: $[AuCl(PR_3)]$, (R = Me,[206] Cy,[207] Ph[208]), $[dppf(AuCl)_2]$,[209] $[dppm(AuCl)_2]$,[210] $[dppa(AuCl)_2]$,[208] [AuCl(tht)],[211] $[AuCl(CN^tBu)]$,[212] [AuCl(IDip)].[169]

Solutions (4.0 mmol) of the ligands, $KS_2CN(CH_2CH_2CH_2NMe_2)_2$,[107, 108] $KS_2CN(CH_2CH_2NEt_2)_2$,[107, 108] $KS_2CN(CH_2CH_2OMe)_2$[213] and $KS_2CN(CH_2CH{=}CH_2)_2$[107, 108] were prepared in water unless otherwise stated by literature methods. Ammonium diethyldithiophosphate was obtained from Fisher Scientific and potassium diethylthiophosphate was purchased from Sigma-Aldrich. Reagents and solvents were used as received from commercial sources. Petroleum ether refers to the fraction boiling at 40-60°.

Electrospray (ES) and Fast Atom Bombardment (FAB) mass data were obtained using Micromass LCT Premier and Autospec Q instruments, respectively. Infrared data were obtained using a Perkin-Elmer Spectrum 100 FT-IR spectrometer and characteristic triphenylphosphine-associated infrared data are not reported. NMR spectroscopy was performed at 25 °C using Varian Mercury 300 and Bruker AV400 spectrometers in $CDCl_3$ unless otherwise indicated. All coupling constants are in Hertz. Resonances in the ^{31}P NMR spectrum due to the hexafluorophosphate counteranion were observed in all cases but are not included below. Elemental analysis data were obtained from London Metropolitan University. The procedures given provide materials of sufficient purity for synthetic and spectroscopic purposes.

9.1. Experimental details for Chapter 3: Transition metal dithiocarbamate (DTC) complexes of group 8 and 10 metals

Experimental for amine and methoxy-terminated DTC complexes

Reactions with cis-[$RuCl_2(dppm)_2$]

A solution of *cis*-[$RuCl_2(dppm)_2$] (80 mg, 0.085 mmol) in dichloromethane (20 mL) was treated with two equivalents of the dithiocarbamate ligand and NH_4PF_6 (28 mg, 0.172 mmol) in methanol (10 mL) and stirred for 30 mins. All solvent was removed and the residue dissolved in the minimum volume of dichloromethane and filtered through diatomaceous earth (celite). Ethanol (10 mL) was added and the solvent volume reduced (rotary evaporation) until precipitation was complete. The product was washed with ethanol (10 mL) and petroleum ether (10 mL). The product was dried under vacuum.

Reactions of alkenyl complexes with $KS_2CN(CH_2CH_2CH_2NMe_2)_2$

A solution of $KS_2CN(CH_2CH_2CH_2NMe_2)_2$ in water was prepared by a literature procedure[108, 124] and 0.129 mmol was added to a dichloromethane-methanol (10mL : 10 mL) solution of the metal alkenyl complex. The reaction was stirred for one hour. Reduction in solvent volume (rotary evaporator) led to precipitation of the product. This was washed with water (5 mL), ethanol (10 mL) and petroleum ether (10 mL). The product was dried under vacuum.

Reactions of alkenyl complexes with $KS_2CN(CH_2CH_2NEt_2)_2$

A solution of $KS_2CN(CH_2CH_2NEt_2)_2$ in methanol was prepared by a literature procedure[108] and 0.132 mmol was added to a dichloromethane-methanol (10mL : 10 mL) solution of the metal alkenyl complex. The reaction was stirred for one hour. Reduction in solvent volume (rotary evaporator) led to precipitation of the product. This was washed with water (5 mL), ethanol (10 mL) and petroleum ether (10 mL). The product was dried under vacuum.

Reactions of alkenyl complexes with $KS_2CN(CH_2CH_2OMe)_2$

A solution of $KS_2CN(CH_2CH_2OMe)_2$ in water was prepared by a literature procedure[213] and 0.132 mmol was added to an acetone solution (20 mL) of the metal alkenyl complex. The reaction was stirred for one hour. All solvent was removed and diethyl ether (20 mL) added and the crude product triturated ultrasonically. The pale yellow precipitate was filtered and washed with water (5 mL) and diethyl ether (10 mL). The product was dried under vacuum.

[Ru{$S_2CN(CH_2CH_2CH_2NMe_2)_2$}$(dppm)_2$]$PF_6$ (1)

Reaction of two equivalents of $KS_2CN(CH_2CH_2CH_2NMe_2)_2$ with *cis*-[$RuCl_2(dppm)_2$] (80 mg, 0.085 mmol) gave 88.8 mg of colourless product (82 %). IR (solid state): 1504, 1358, 1309, 1258, 1231, 878, 833 (ν_{PF}) cm^{-1}. ^{31}P NMR (CD_2Cl_2): -15.5, -2.1 (t^v x 2, dppm, J_{PP} = 34.1 Hz) ppm. ^1H NMR (CD_2Cl_2): 1.32, 1.40 (m x 2, 2 x 2H, $NCH_2CH_2CH_2N$); 1.87 (m, 4H, CH_2NMe_2); 1.95 (s x 2, 12H, NMe_2); 3.12, 3.64 (m x 2, 2 x 2H, CH_2NCS_2); 4.42, 4.97 (m x 2, 2 x 2H, PCH_2P); 6.37, 6.77, 6.95, 7.07, 7.17, 7.25, 7.56 (m x 7, 40H, C_6H_5) ppm. MS (ES +ve) *m/z* (abundance) = 1132 (100) $[M]^+$. Analysis: Calculated for $C_{61}H_{68}F_6N_3P_5RuS_2$ (M_w = 1277.27): C 57.4%, H 5.4%, N 3.3%; Found: C 57.3%, H 5.2%, N 3.2%.

[Ru{$S_2CN(CH_2CH_2NEt_2)_2$}$(dppm)_2$]PF_6 (2)

Reaction of two equivalents of $KS_2CN(CH_2CH_2NEt_2)_2$ with *cis*-[$RuCl_2(dppm)_2$] (80 mg, 0.085 mmol) gave 70 mg of colourless product (63 %). IR (solid state): 1454 (ν_{CN}), 1382, 1356, 1311, 1246, 1173, 879, 835 (ν_{PF}) cm^{-1}. ^{31}P NMR ($CDCl_3$): -18.5, -6.0 (t^v x 2, dppm, J_{PP} = 34.1 Hz) ppm. ^1H NMR ($CDCl_3$): 1.05 (t, 12H, NCH_2CH_3, J_{HH} = 7.1 Hz); 2.40 (m, 4H, CH_2NEt_2); 2.57 (q, 8H, NCH_2CH_3, J_{HH} = 7.1 Hz); 3.28, 3.81 (m x 2, 2 x 2H, CH_2NCS_2); 4.63, 4.99 (m x 2, 2 x 2H, PCH_2P); 6.54, 6.96, 7.04, 7.19, 7.26, 7.36, 7.61 (m x 7, 40H, C_6H_5) ppm. MS (ES +ve) *m/z* (abundance) = 1160 (100) $[M]^+$. Analysis: Calculated for $C_{63}H_{72}F_6N_3P_5RuS_2$ (M_w = 1305.33): C 58.0%, H 5.6%, N 3.2%; Found: C 57.8%, H 5.5%, N 3.1%.

[Ru{$S_2CN(CH_2CH_2OMe)_2$}$(dppm)_2$]PF_6 (3)

Reaction of two equivalents of $KS_2CN(CH_2CH_2OMe)_2$ with *cis*-[$RuCl_2(dppm)_2$] (80 mg, 0.085 mmol) gave 90.7 mg of colourless product (87 %). IR (solid state): 1424, 1359, 1310, 1284, 1243, 1194, 1116, 975, 920, 831 (ν_{PF}) cm^{-1}. ^{31}P NMR (CD_2Cl_2): -18.6, -5.2 (t^v x 2, dppm, J_{PP} = 34.3 Hz) ppm. ^1H NMR (CD_2Cl_2): 3.38 (s, 6H, OCH_3); 3.51 (m, 4H, CH_2OMe); 3.79 (m, 4H, CH_2NCS_2); 4.48, 4.95 (m x 2, 2 x 2H, PCH_2P); 6.48, 6.99, 7.10, 7.32, 7.41, 7.49, 7.69 (m x 7, 40H, C_6H_5) ppm. MS (ES +ve) *m/z* (abundance) = 1078 (100) $[M]^+$. Analysis: Calculated for $C_{57}H_{58}F_6NO_2P_5RuS_2$ (M_w = 1223.14): C 56.0%, H 4.8%, N 1.2%; Found: C 55.9%, H 4.7%, N 1.1%.

[Ru{$S_2CN(CH_2CH_2NHEt_2)_2$}$(dppm)_2$]$(PF_6)(O_2CCF_3)_2$ (4)

A solution of [Ru{$S_2CN(CH_2CH_2NEt_2)_2$}$(dppm)_2$](PF_6) (**2**) (40 mg, 0.031 mmol) in dichloromethane (10 mL) was treated with 2 equivalents of trifluoroacetic acid in dichloromethane (0.8 mL) and stirred for 5 mins. All solvent was removed (rotary evaporator) and the crude product triturated ultrasonically in diethyl ether (20 mL) to give a yellow product. This washed with diethyl ether (10 mL) and dried to yield 37.8 mg of product (82 %). IR (solid state): 1670 ($\nu_{C=O}$), 1310, 1241, 1198, 1177, 1127, 1096,

833 (ν_{PF}) cm^{-1}. ^{31}P NMR ($CDCl_3$): -5.7, -17.5 (t^v x 2, dppm, J_{PP} = 34.4 Hz) ppm. ^{1}H NMR ($CDCl_3$): 1.29 (s(br), 12H, NCH_2CH_3); 2.66, 3.00 (m x 2, 2 x 2H, CH_2NEt_2); 3.14 (s(br), 8H, NCH_2CH_3); 3.65, 4.40 (m x 2, 2 x 2H, CH_2NCS_2); 4.45, 4.93 (m x 2, 2 x 2H, PCH_2P); 6.46, 6.95, 7.12, 7.22-7.42, 7.60 (m x 5, 40H, C_6H_5) ppm. MS (ES +ve) *m/z* (abundance) = 1160 (100) $[M]^+$. Analysis: Calculated for $C_{67}H_{74}F_{12}N_3O_4P_5RuS_2$ (M_w = 1533.37): C 52.5%, H 4.9%, N 2.7%; Found: C 52.4%, H 4.9%, N 2.7%.

[Ru(CH=CH^{t}Bu){$S_2CN(CH_2CH_2CH_2NMe_2)_2$}(CO)($PPh_3$)$_2$] (**5**)

[Ru(CH=CH^{t}Bu)Cl(CO)(BTD)(PPh_3)$_2$] (100 mg, 0.110 mmol) gave 66 mg of pale yellow product (60 %). IR (solid state): 1905(ν_{CO}), 1572, 1457 (ν_{CN}), 1369, 1354, 1257, 1211, 1174, 1034, 981, 937 cm^{-1}. ^{31}P NMR ($CDCl_3$): 39.5 (s, PPh_3) ppm. ^{13}C NMR (CD_2Cl_2): 207.3 (t, CO, J_{CP} = 15.9 Hz); 206.1 (s, CS_2); 141.9 (t, Cβ, J_{CP} = 3.5 Hz); 135.0 (t^v, *o/m*-C_6H_5, J_{CP} = 5.2 Hz); 134.7 (t, *ipso*-C_6H_5, J_{CP} = 20.9 Hz); 134.2 (t, Cα, J_{CP} = 12.5 Hz); 129.2 (s, *p*-C_6H_5); 127.6 (t^v, *o/m*-C_6H_5, J_{CP} = 4.5 Hz); 57.1, 56.9 (s x 2, NCH_2); 48.3, 47.5 (s x 2, NCH_2), 45.5 (s, NMe_2); 35.7 (s, CMe_3); 29.7 (s, ^{t}Bu-Me); 25.2, 24.9 (s x 2, CCH_2C) ppm. ^{1}H NMR ($CDCl_3$): 0.40 (s, 9H, ^{t}Bu); 1.09, 1.36 (m x 2, 2 x 2H, $NCH_2CH_2CH_2N$); 1.97 (t, 2H, CH_2NMe_2; J_{HH} = 6.9 Hz); 2.07 (t, 2H, CH_2NMe_2; J_{HH} = 7.1 Hz); 2.12, 2.14 (s x 2, 2 x 6H, NMe_2); 2.79, 3.19 (m x 2, 2 x 2H, CH_2NCS_2); 4.60 (dt, 1H, Hβ, J_{HH} = 16.4 Hz; J_{HP} = 1.8 Hz); 6.30 (dt, 1H, Hα, J_{HH} = 16.4 Hz, J_{HP} = 2.7 Hz); 7.27 – 7.31, 7.55 – 7.60 (m x 2, 30H, C_6H_5) ppm. MS (ES +ve) *m/z* (abundance) = 1000 (74) $[M]^+$; 738 (85) $[M - PPh_3]^+$. Analysis: Calculated for $C_{54}H_{65}N_3OP_2RuS_2$ (M_w = 999.26): C 64.9%, H 6.6%, N 4.2%; Found: C 65.0%, H 6.6%, N 4.1%.

[Ru(CH=CHC_6H_4Me-4){$S_2CN(CH_2CH_2CH_2NMe_2)_2$}(CO)($PPh_3$)$_2$] (**6**)

[Ru(CH=CHC_6H_4Me-4)Cl(CO)(BTD)(PPh_3)$_2$] (100 mg, 0.106 mmol) gave 69 mg of pale yellow product (63 %). IR (solid state): 1905 (ν_{CO}), 1540, 1500, 1462 (ν_{CN}), 1416, 1367, 1349, 1296, 1258, 1039, 830 cm^{-1}. ^{31}P NMR ($CDCl_3$): 39.2 (s, PPh_3) ppm. ^{1}H NMR ($CDCl_3$): 1.23, 1.33 (m x 2, 2 x 2H, $NCH_2CH_2CH_2N$); 2.05 (m, 4H, CH_2NMe_2); 2.12, 2.16 (s x 2, 2 x 6H, NMe_2); 2.24 (s, 3H, CCH_3); 2.94, 3.20 (m x 2, 2 x 2H, CH_2NCS_2); 5.55 (d, 1H, Hβ, J_{HH} = 16.8 Hz); 6.39, 6.83 (AB, 4H, C_6H_4, J_{AB} = 8.0 Hz); 7.27 – 7.34, 7.53-7.58 (m x 2, 30H, C_6H_5); 7.72 (dt, 1H, Hα, J_{HH} = 16.8 Hz, J_{HP} = 3.3 Hz) ppm. MS (ES +ve) *m/z* (abundance) = 1034 (68) $[M]^+$; 772 (69) $[M - PPh_3]^+$. Analysis: Calculated for $C_{57}H_{63}N_3OP_2RuS_2$ (M_w = 1033.28): C 66.3%, H 6.2%, N 4.1%; Found: C 66.2%, H 6.1%, N 3.9%.

[Ru(CH=CHCPh_2OH){$S_2CN(CH_2CH_2CH_2NMe_2)_2$}(CO)($PPh_3$)$_2$] (**7**)

[Ru(CH=CHCPh_2OH)Cl(CO)(BTD)(PPh_3)$_2$] (100 mg, 0.097 mmol) gave 51.2 mg of pale yellow product (47 %). IR (solid state): 1913 (ν_{CO}), 1552, 1447(ν_{CN}), 1374, 1313, 1257(ν_{SCS}), 1236, 990, 892, 837 cm^{-1}. ^{31}P NMR ($CDCl_3$): 39.9 (s, PPh_3) ppm. ^{1}H NMR ($CDCl_3$): 1.09, 1.29 (m x 2, 2 x 2H,

$NCH_2C\mathit{H}_2CH_2N$); 1.99 (t, 2H, CH_2NMe_2; J_{HH} = 6.9 Hz); 2.04 (t, 2H, CH_2NMe_2; J_{HH} = 7.0 Hz); 2.11, 2.15 (s x 2, 2 x 6H, NMe_2); 2.60 (s(br), 1H, OH); 2.77, 3.09 (m x 2, 2 x 2H, CH_2NCS_2); 5.51 (d, 1H, Hβ, J_{HH} = 16.6 Hz); 6.83 (m, 4H, CC_6H_5); 6.96 (dt, 1H, Hα, J_{HH} = 16.6 Hz); 7.13 (m, 6H, CC_6H_5); 7.27 – 7.52 (m, 30H, PC_6H_5) ppm. MS (ES +ve) *m/z* (abundance) = 1126 (3) $[M]^+$; 1108 (68) $[M - OH_2]^+$; 846 (40) $[M - OH_2 - PPh_3]^+$. Analysis: Calculated for $C_{63}H_{67}N_3OP_2RuS_2$ (M_w = 1125.38): C 67.2%, H 6.0%, N 3.7%; Found: C 67.3%, H 6.1%, N 3.8%.

[Ru(C(C≡C^{t}Bu)=CH^{t}Bu){$S_2CN(CH_2CH_2CH_2NMe_2)_2$}(CO)($PPh_3$)$_2$] (**8**)

[Ru(C(C≡C^{t}Bu)=CH^{t}Bu)Cl(CO)(PPh_3)$_2$] (100 mg, 0117 mmol) gave 17 mg of pale yellow product (13 %). Product was soluble in methanol resulting in low yield. A further crop was obtained by ultrasonic trituration in diethylether. IR (solid state): 2221 ($\nu_{C\equiv C}$), 1911 (ν_{CO}), 1574, 1785, 1459 (ν_{CN}), 1387, 1356, 1259, 915, 843, 825 cm^{-1}. ^{31}P NMR ($CDCl_3$): 38.2 (s, PPh_3) ppm. ^{1}H NMR ($CDCl_3$): 0.60 (s, 9H, ^{t}Bu); 1.22 (m, 4H, $NCH_2C\mathit{H}_2CH_2N$); 1.33 (s, 9H, ^{t}Bu); 2.02 (m, 4H, $NCH_2C\mathit{H}_2CH_2N$); 2.10, 2.14 (s x 2, 2 x 6H, NMe_2); 2.87, 2.98 (m x 2, 2 x 2H, CH_2NCS_2); 5.19 (s, 1H, Hβ); 7.24 – 7.36, 7.59 (m x 2, 30H, C_6H_5) ppm. MS (ES +ve) *m/z* (abundance) = 1080 (42) $[M]^+$; 818 (95) $[M - PPh_3]^+$. Analysis: Calculated for $C_{60}H_{73}N_3OP_2RuS_2$ (M_w = 1079.39): C 66.8%, H 6.8%, N 3.9%; Found: C 66.7%, H 6.7%, N 4.0%.

[Os(CH=CHC_6H_4Me-4){$S_2CN(CH_2CH_2CH_2NMe_2)_2$}(CO)($PPh_3$)$_2$] (**9**)

[Os(CH=CHC_6H_4Me-4)Cl(CO)(BTD)(PPh_3)$_2$] (20 mg, 0.019 mmol) gave 7 mg (Est.) of pale yellow product (33 %). The product was found to be partially soluble in ethanol and a further crop was obtained by ultrasonic trituration in diethylether. IR (solid state): 1894 (ν_{CO}), 1638, 1364, 1228, 1118 cm^{-1}. ^{31}P NMR ($CDCl_3$): 7.4 (s, PPh_3) ppm. ^{1}H NMR ($CDCl_3$): 1.21, 1.35 (m x 2, 2 x 2H, $NCH_2C\mathit{H}_2CH_2N$); 2.02 (t, 2H, CH_2NMe_2; J_{HH} = 7.5 Hz); 2.06 (t, 2H, CH_2NMe_2; J_{HH} = 7.3 Hz); 2.09, 2.15 (s x 2, 2 x 6H, NMe_2); 2.23 (s, 3H, CCH_3); 2.82, 3.11 (m x 2, 2 x 2H, CH_2NCS_2); 5.49 (d, 1H, Hβ, J_{HH} = 17.1 Hz); 6.38, 6.83 (AB, 4H, C_6H_4, J_{AB} = 8.0 Hz); 7.27 – 7.33, 7.53 – 7.59 (m x 2, 30H, C_6H_5); 8.34 (dt, 1H, Hα, J_{HH} = 17.1 Hz, J_{HP} = 2.5 Hz) ppm. MS (ES +ve) *m/z* (abundance) = 1124 (98) $[M]^+$; 862 (39) $[M - PPh_3]^+$. Analysis: Calculated for $C_{57}H_{63}N_3OOsP_2S_2$ (M_w = 1122.44): C 61.0%, H 5.7%, N 3.7%; Found: C 59.0%, H 5.6%, N 3.7%.

[Ru(CH=CH^{t}Bu){$S_2CN(CH_2CH_2NEt_2)_2$}(CO)(PPh_3)$_2$] (**10**)

[Ru(CH=CH^{t}Bu)Cl(CO)(BTD)(PPh_3)$_2$] (100 mg, 0.110 mmol) gave 59.8 mg of pale yellow product (53 %). IR (solid state): 1898 (ν_{CO}), 1573, 1384, 1372, 1285, 1228, 1176, 984, 914 cm^{-1}. ^{31}P NMR ($CDCl_3$): 39.5 (s, PPh_3) ppm. ^{1}H NMR ($CDCl_3$): 0.38 (s, 9H, ^{t}Bu); 0.95 (m, 12H, $NCH_2C\mathit{H}_3$); 1.93, 2.21 (m x 2, 2 x 2H, CH_2NEt_2); 2.43 (m, 8H, $NC\mathit{H}_2CH_3$); 2.83, 3.28 (m x 2, 2 x 2H, CH_2NCS_2); 4.59

(d, 1H, Hβ, J_{HH} = 16.4 Hz); 6.28 (dt, 1H, Hα, J_{HH} = 16.4 Hz, J_{HP} = 2.7 Hz); 7.29 – 7.34, 7.55 – 7.59 (m x 2, 30H, C_6H_5) ppm. MS (ES +ve) *m/z* (abundance) = 1028 (100) $[M]^+$; 766 (60) $[M - PPh_3]^+$. Analysis: Calculated for $C_{56}H_{69}N_3OP_2RuS_2$ (M_w = 1027.32): C 65.5%, H 6.8%, N 4.1%; Found: C 65.3%, H 6.8%, N 4.0%.

[Ru(CH=CHC$_6$H$_4$Me-4){S$_2$CN(CH$_2$CH$_2$NEt$_2$)$_2$}(CO)(PPh$_3$)$_2$] (11)

[Ru(CH=CHC$_6$H$_4$Me-4)Cl(CO)(BTD)(PPh$_3$)$_2$] (100 mg, 0.106 mmol) gave 73 mg of pale yellow product (65 %). IR (solid state): 1906(ν_{CO}), 1543, 1455(ν_{CN}), 1384, 1282, 1230, 1204, 1177, 969.6, 832.1 cm^{-1}. ^{31}P NMR ($CDCl_3$): 39.3 (s, PPh_3) ppm. ^{1}H NMR ($CDCl_3$): 0.94, 0.98 (t x 2, 2 x 6H, NCH$_2$C*H$_3$*, J_{HH} = 7.1 Hz); 2.07, 2.17 (m x 2, 2 x 2H, CH_2NEt_2); 2.24 (s, 3H, CCH_3); 2.43 (m, 8H, NC*H$_2$*CH$_3$); 2.98, 3.27 (m x 2, 2 x 2H, CH_2NCS_2); 5.53 (d, 1H, Hβ, J_{HH} = 16.6 Hz); 6.37, 6.83 (AB, 4H, C_6H_4, J_{AB} = 8.0 Hz); 7.27 – 7.34, 7.53 – 7.57 (m x 2, 30H, C_6H_5); 7.70 (dt, 1H, Hα, J_{HH} = 16.7 Hz, J_{HP} = 3.3 Hz) ppm. MS (ES +ve) *m/z* (abundance) = 1062 (100) $[M]^+$; 917 (6) [M – CO – alkenyl]$^+$; 800 (55) $[M - PPh_3]^+$. Analysis: Calculated for $C_{59}H_{67}N_3OP_2RuS_2$ (M_w = 1061.33): C 66.8%, H 6.4%, N 4.0%; Found: C 66.7%, H 6.2%, N 4.0%.

[Ru(CH=CHCPh$_2$OH){S$_2$CN(CH$_2$CH$_2$NEt$_2$)$_2$}(CO)(PPh$_3$)$_2$] (12)

[Ru(CH=CHCPh$_2$OH)Cl(CO)(BTD)(PPh$_3$)$_2$] (100 mg, 0.097 mmol) gave 34 mg of pale yellow product (30 %). The product was found to be partially soluble in ethanol and a further crop was obtained by ultrasonic trituration in diethylether. IR (solid state): 1914 (ν_{CO}), 1550, 1446 (ν_{CN}), 1387, 1235, 1174, 988, 850 cm^{-1}. ^{31}P NMR ($CDCl_3$): 40.2 (s, PPh_3) ppm. ^{1}H NMR ($CDCl_3$): 0.94, 0.98 (t x 2, 2 x 6H, NCH$_2$C*H$_3$*, J_{HH} = 7.1 Hz); 1.93, 2.16 (m x 2, 2 x 2H, CH_2NEt_2); 2.44 (m, 8H, NC*H$_2$*CH$_3$); 2.81, 3.18 (m x 2, 2 x 2H, CH_2NCS_2); 5.51 (d, 1H, Hβ, J_{HH} = 16.6 Hz); 6.82 – 6.86 (m, 4H, PC_6H_5); 6.97 (dt, 1H, Hα, J_{HH} = 16.6 Hz, J_{HP} = 2.5 Hz); 7.08 – 7.15 (m, 6H, PC_6H_5); 7.28 – 7.38, 7.47 – 7.52 (m x 2, 30H, PC_6H_5) ppm. MS (ES +ve) *m/z* (abundance) = 1154 (12) $[M]^+$; 1136 (46) $[M - OH_2]^+$; 874 (47) $[M - OH_2 - PPh_3]^+$. Analysis: Calculated for $C_{65}H_{71}N_3OP_2RuS_2$ (M_w = 1153.43): C 67.7%, H 6.2%, N 3.6%; Found: C 67.8%, H 6.1%, N 3.5%.

[Ru(C(C≡C^{t}Bu)=CH^{t}Bu){S$_2$CN(CH$_2$CH$_2$NEt$_2$)$_2$}(CO)(PPh$_3$)$_2$] (13)

[Ru(C(C≡C^{t}Bu)=CH^{t}Bu)Cl(CO)(PPh$_3$)$_2$] (100 mg, 0117 mmol) gave 60.3 mg of pale yellow product (47 %). IR (solid state): 2164 ($\nu_{C\equiv C}$), 1912 (ν_{CO}), 1547, 1420, 1384, 1354, 1257, 1202, 1174, 916, 844, 826 cm^{-1}. ^{31}P NMR ($CDCl_3$): 38.0 (s, PPh_3) ppm. ^{1}H NMR ($CDCl_3$): 0.60 (s, 9H, ^{t}Bu); 0.92, 0.98 (t x 2, 2 x 6H, NCH$_2$C*H$_3$*, J_{HH} = 7.0 Hz); 1.32 (s, 9H, ^{t}Bu); 2.04 (m, 4H, CH_2NEt_2); 2.44 (m, 8H, NC*H$_2$*CH$_3$); 2.97, 3.04 (m x 2, 2 x 2H, CH_2NCS_2); 5.22 (s, 1H, Hβ); 7.24 – 7.35, 7.58 (m x 2, 30H,

C_6H_5) ppm. MS (ES +ve) *m/z* (abundance) = 1108 (100) $[M]^+$; 846 (70) $[M - PPh_3]^+$; 817 (46) $[M - PPh_3]^+$. Analysis: Calculated for $C_{62}H_{77}N_3OP_2RuS_2$ (M_w = 1107.44): C 67.2%, H 7.0%, N 3.8%; Found: C 67.4%, H 7.0%, N 3.7%.

[Os(CH=CHC$_6$H$_4$Me-4){S$_2$CN(CH$_2$CH$_2$NEt$_2$)$_2$}(CO)(PPh$_3$)$_2$] (**14**)

[Os(CH=CHC$_6$H$_4$Me-4)Cl(CO)(BTD)(PPh$_3$)$_2$] (20 mg, 0.019 mmol) gave 14 mg of pale yellow product (66 %). IR (solid state): 1893 (ν_{CO}), 1495, 1453 (ν_{CN}), 1384, 1350, 1282, 1242, 974, 831 cm^{-1}. ^{31}P NMR ($CDCl_3$): 7.4 (s, PPh_3) ppm. ^1H NMR ($CDCl_3$): 0.93, 0.97 (t x 2, 2 x 6H, NCH_2CH_3, J_{HH} = 7.1 Hz); 2.08, 2.21 (m x 2, 2 x 2H, CH_2NEt_2); 2.23 (s, 3H, CCH_3); 2.43 (m, 8H, NCH_2CH_3); 2.86, 3.19 (m x 2, 2 x 2H, CH_2NCS_2); 5.50 (d, 1H, Hβ, J_{HH} = 17.1 Hz); 6.38, 6.83 (AB, 4H, C_6H_4, J_{AB} = 7.9 Hz); 7.29 – 7.31, 7.55 – 7.57 (m x 2, 30H, C_6H_5); 8.33 (dt, 1H, Hα, J_{HH} = 17.1 Hz, J_{HP} = 2.4 Hz) ppm. MS (ES +ve) *m/z* (abundance) = 1152 (100) $[M]^+$; 1007 (4) $[M - CO - alkenyl]^+$; 890 (8) $[M - PPh_3]^+$. Analysis: Calculated for $C_{59}H_{67}N_3OOsP_2S_2$ (M_w = 1150.49): C 61.6%, H 5.9%, N 3.7%; Found: C 61.7%, H 5.8%, N 3.6%.

[Ru(CH=CHBu^t){S$_2$CN(CH$_2$CH$_2$OMe)$_2$}(CO)(PPh$_3$)$_2$] (**15**)

Reaction of 1.2 equivalents of $KS_2CN(CH_2CH_2OMe)_2$ with [Ru(CH=CH^{t}Bu)Cl(CO)(BTD)(PPh$_3$)$_2$] (100 mg, 0.110 mmol) gave 99 mg of pale yellow product (95 %). IR (solid state): 1896 (ν_{CO}), 1711, 1414, 1359, 1273, 1222, 1194, 1109, 913 cm^{-1}. ^{31}P NMR ($CDCl_3$): 39.7 (s, PPh_3) ppm. ^1H NMR ($CDCl_3$): 0.41 (s, 9H, Bu^t); 2.85 (t, 2H, CH_2, J_{HH} = 5.9 Hz); 3.07 (t, 2H, CH_2, J_{HH} = 5.9 Hz); 3.18 (t, 2H, CH_2, J_{HH} = 6.0 Hz); 3.19, 3.20 (s x 2, 2 x 3H, OCH_3); 3.48 (t, 2H, CH_2, J_{HH} = 5.9 Hz); 4.56 (dt, 1H, Hβ, J_{HH} = 16.4 Hz, J_{HP} = 1.6 Hz); 6.31 (dt, 1H, Hα, J_{HH} = 16.4 Hz, J_{HP} = 2.6 Hz); 7.29 – 7.33, 7.56 – 7.61 (m x 2, 30H, C_6H_5) ppm. MS (ES +ve) *m/z* (abundance) = 968 (61) $[M + Na]^+$; 945 (3) $[M]^+$. Analysis: Calculated for $C_{50}H_{55}NO_3P_2RuS_2$ (M_w = 945.13): C 63.5%, H 5.9%, N 1.5%; Found: C 63.5%, H 5.8%, N 1.6%.

[Ru(CH=CHC$_6$H$_4$Me-4){S$_2$CN(CH$_2$CH$_2$OMe)$_2$}(CO)(PPh$_3$)$_2$] (**16**)

Reaction of 1.2 equivalents of $KS_2CN(CH_2CH_2OMe)_2$ with [Ru(CH=CHC$_6$H$_4$Me-4)Cl(CO)(BTD)(PPh$_3$)$_2$] (100 mg, 0.106 mmol) gave 83 mg of pale yellow product (80 %). IR (solid state): 1907 (ν_{CO}), 1712, 1541, 1506, 1413, 1361, 1274, 1179, 1110, 969, 829 cm^{-1}. ^{31}P NMR ($CDCl_3$): 39.3 (s, PPh_3) ppm. ^1H NMR ($CDCl_3$): 2.25 (s, 3H, CCH_3); 3.00 (t, 2H, CH_2, J_{HH} = 5.8 Hz); 3.14 (t, 2H, CH_2, J_{HH} = 5.7 Hz); 3.19, 3.24 (s x 2, 2 x 3H, OCH_3); 3.24 (t, 2H, CH_2, J_{HH} = 5.9 Hz); 3.50 (t, 2H, CH_2, J_{HH} = 5.7 Hz); 5.53 (d, 1H, Hβ, J_{HH} = 16.8 Hz); 6.43, 6.85 (AB, 4H, C_6H_4, J_{AB} = 7.9 Hz); 7.29 – 7.36, 7.55 – 7.59 (m x 2, 30H, C_6H_5); 7.72 (dt, 1H, Hα, J_{HH} = 16.8 Hz, J_{HP} = 3.2 Hz) ppm. MS (ES +ve) *m/z* (abundance) = 1002 (20) $[M + Na]^+$, 1002 (9) $[M]^+$, 862 (39) $[M - alkenyl]^+$.

Analysis: Calculated for $C_{53}H_{53}NO_3P_2RuS_2$ (M_w = 979.14): C 65.0%, H 5.5%, N 1.4%; Found: C 65.1%, H 6.1%, N 1.7%.

[Ru(C(C≡C^{t}Bu)=CH^{t}Bu){$S_2CN(CH_2CH_2OMe)_2$}(CO)(PPh_3)$_2$] (**17**)

Reaction of 1.2 equivalents of $KS_2CN(CH_2CH_2OMe)_2$ with [Ru(C(C≡C^{t}Bu)=CH^{t}Bu)Cl(CO)(PPh_3)$_2$] (100 mg, 0.117 mmol) gave 83 mg of pale yellow product (69 %). IR (solid state): 2166 ($\nu_{C\equiv C}$), 1911 (ν_{CO}), 1413, 1387, 1356, 1305, 1275, 1260, 1232, 1195, 1111, 964 cm^{-1}. ^{31}P NMR ($CDCl_3$): 38.3 (s, PPh_3) ppm. ^{1}H NMR ($CDCl_3$): 0.61 (s, 9H, Bu^t); 3.01, 3.13 (m x 2, 2 x 4H, CH_2); 1.31 (s, 9H, Bu^t); 3.19, 3.22 (s x 2, 2 x 3H, OCH_3); 5.19 (s, 1H, Hβ); 7.26 – 7.36, 7.59 (m x 2, 30H, C_6H_5) ppm. MS (ES +ve) *m/z* (abundance) = 1048 (19) [M + Na]$^+$; 1026 (22) [M]$^+$. Analysis: Calculated for $C_{56}H_{63}NO_3P_2RuS_2$ (M_w = 1025.25): C 65.6%, H 6.2%, N 1.4%; Found: C 65.7%, H 6.3%, N 1.5%.

[Ru(CH=CH^{t}Bu){$S_2CN(CH_2CH_2CH_2NHMe_2)_2$}(CO)($PPh_3$)$_2$]($O_2CCF_3$)$_2$ (**18**)

A solution of [Ru(CH=CH^{t}Bu){$S_2CN(CH_2CH_2CH_2NMe_2)_2$}(CO)($PPh_3$)$_2$] (40 mg, 0.040 mmol) in dichloromethane (10 mL) was treated with 2 equivalents of trifluoroacetic acid in dichloromethane (1 mL) and stirred for 5 mins. All solvent was removed (rotary evaporator) and the crude product triturated ultrasonically in diethyl ether (20 mL) to give a pale yellow product. This washed with diethyl ether (10 mL) and dried to yield 37.3 mg of product (76 %). IR (solid state): 1915 (ν_{CO}), 1674 ($\nu_{C=O}$), 1412, 1385, 1366, 1307, 1286, 1256, 1236, 1197, 1170, 1125, 1091, 1029, 999, 969, 951, 829 cm^{-1}. ^{31}P NMR ($CDCl_3$): 39.2 (s, PPh_3) ppm. ^{1}H NMR ($CDCl_3$): 0.41 (s, 9H, ^{t}Bu); 1.42, 1.73 (m x 2, 2 x 2H, $NCH_2CH_2CH_2N$); 2.66, 2.72 (s x 2, 2 x 6H, NMe_2); 2.80, 2.88 (m x 2, 2 x 2H, CH_2NMe_2); 3.28, 3.51 (m x 2, 2 x 2H, CH_2NCS_2); 4.60 (dt, 1H, Hβ, J_{HH} = 16.4 Hz; J_{HP} = 1.6 Hz); 6.31 (dt, 1H, Hα, J_{HH} = 16.4 Hz, J_{HP} = 2.7 Hz); 7.32 – 7.36, 7.52 – 7.57 (m x 2, 30H, C_6H_5) ppm. MS (ES +ve) *m/z* (abundance) = 1000 (95) [M]$^+$; 738 (75) [M – PPh_3]$^+$. Analysis: Calculated for $C_{58}H_{67}F_6N_3O_5P_2RuS_2$ (M_w = 1227.31): C 56.8%, H 5.5%, N 3.4%; Found: C 56.8%, H 5.7%, N 3.3%.

[Ru(=CHCH=CPh$_2$){$S_2CN(CH_2CH_2CH_2NHMe_2)_2$}(CO)($PPh_3$)$_2$]($O_2CCF_3$)$_3$ (**19**)

A solution of [Ru(CH=CHCPh$_2$OH){$S_2CN(CH_2CH_2CH_2NMe_2)_2$}(CO)($PPh_3$)$_2$] (20 mg, 0.018 mmol) in dichloromethane (10 mL) was treated with excess trifluoroacetic acid (3 drops) in dichloromethane (1 mL) and stirred for 5 mins leading to a deep red colour. All solvent was removed (rotary evaporator) and the crude product triturated ultrasonically in petroleum ether (20 mL) to give a dark red product. This washed with petroleum ether (10 mL) and dried to yield 18 mg of product (69 %). IR (solid state): 1952 (ν_{CO}), 1782, 1739, 1673 ($\nu_{C=O}$), 1600, 1575, 1384, 1309, 1174, 1127, 938, 830, 798 cm^{-1}. ^{31}P NMR ($CDCl_3$): 32.0 (s, PPh_3) ppm. ^{1}H NMR ($CDCl_3$): 1.41 (m, 2 x 2H, $NCH_2CH_2CH_2N$); 2.80, 2.83 (s x 2, 2 x 6H, NMe_2); 2.98 (m, 4H + 4H, CH_2NMe_2 + CH_2NCS_2); 6.14

(d, 2H, ortho-CC_6H_5, J_{HH} = 7.0 Hz); 7.11 (m, 4H, CC_6H_5); 7.29 – 7.85 (m, 30H + 4H, PC_6H_5 + CC_6H_5); 8.10 (d, 1H, Hβ, J_{HH} = 14.0 Hz); 11.83 (s(br), 2H, $NHMe_2$); 14.68 (d, 1H, Hα, J_{HH} = 14.0 Hz) ppm. MS (FAB +ve) *m/z* (abundance) = 1108 (16) $[M]^+$, 916 (40) [M - alkenylcarbene]$^+$, 846 (100) $[M - PPh_3]^+$. Analysis: Calculated for $C_{69}H_{68}F_9N_3O_7P_2RuS_2 \cdot 3CH_2Cl_2$ (M_w = 1449.43): C 50.7%, H 4.4%, N 2.5%; Found: C 51.2%, H 4.1%, N 2.5%.

Experimental for diallyl DTC complexes

$[Ru\{S_2CN(CH_2CH=CH_2)_2\}(dppm)_2]PF_6$ (20)

A solution of *cis*-$[RuCl_2(dppm)_2]$ (200 mg, 0.213 mmol) in acetone (20 mL) and dichloromethane (10 mL) was treated with two equivalents of the dithiocarbamate ligand and NH_4PF_6 (69 mg, 0.423 mmol) in water (5 mL) and the reaction stirred for 30 mins. All solvent was removed and the residue dissolved in the minimum volume of dichloromethane and filtered through diatomaceous earth (Celite) to remove KCl and excess ligand. All solvent was again removed and diethyl ether (30 mL) added and the solid triturated ultrasonically. The pale yellow product was washed with water (10 mL), diethyl ether (10 mL) and dried under vacuum. Yield: 175 (69 %). IR (solid state): 1482, 1435, 1414, 1244, 1098, 999, 928, 833 (ν_{PF}), 739, 727, 694 cm^{-1}. ^{31}P NMR (CD_2Cl_2): -18.4, -5.3 (t x 2, dppm, J_{HH} = 34.3 Hz). ^1H NMR (CD_2Cl_2): 4.09 (m, 4H, NCH_2); 4.50, 4.94 (m x 2, 2 x 2H, PCH_2P); 5.24 (d, 2H, $=CH^A$, J_{HH} = 17.0 Hz); 5.31 (d, 2H, $=CH^B$, J_{HH} = 10.1 Hz); 5.61 (m, 2H, $=CH^C$); 6.49, 6.99, 7.11, 7.27 - 7.51, 7.71 (m x 5, 40H, C_6H_5) ppm. MS (ES +ve) *m/z* (abundance) = 1042 (100) $[M]^+$. Analysis: Calculated for $C_{53}H_{49}NOP_2RuS_2$ (M_w = 1187.11): C 57.7%, H 4.6%, N 1.2%; Found: C 57.7%, H 4.5%, N 1.1%.

Reactions of alkenyl complexes with $KS_2CN(CH_2CH=CH_2)_2$

A fresh solution of $KS_2CN(CH_2CH=CH_2)_2$ in water was prepared by a literature procedure[9] and 0.132 mmol was added to a solution of the metal alkenyl complex in acetone and dichloromethane (20 mL : 10 mL). The reaction was stirred for 20 mins. All solvent was removed and the crude product dissolved in dichloromethane (15 mL) and filtered through diatomaceous earth (Celite) to remove KCl and excess ligand. All solvent was again removed and diethyl ether (20 mL) added and the crude product triturated ultrasonically. The pale yellow precipitate was filtered and washed with water (5 mL) and diethyl ether (10 mL). The product was dried under vacuum.

$[Ru(CH=CHBu^t)\{S_2CN(CH_2CH=CH_2)_2\}(CO)(PPh_3)_2]$ (21)

$[Ru(CH=CHBu^t)Cl(CO)(BTD)(PPh_3)_2]$ (100 mg, 0.110 mmol) gave 63 mg of pale yellow product (63 %). IR (solid state): 1901 (ν_{CO}), 1642, 1479, 1410, 1358, 1227, 982, 916 cm^{-1}. ^{31}P NMR ($CDCl_3$): 39.7

(s, PPh_3). ^1H NMR ($CDCl_3$): 0.39 (s, 9H, CCH_3); 3.31 (d, 2H, NCH_2, J_{HH} = 6.2 Hz); 3.79 (d, 2H, NCH_2, J_{HH} = 6.0 Hz); 4.58 (dt, 1H, Hβ, J_{HH} = 16.4 Hz, J_{HP} = 1.8 Hz); 4.74 (d, 1H, $=CH^A$, J_{HH} = 17.0 Hz); 4.87 (d, 1H, $=CH^A$, J_{HH} = 17.1 Hz); 5.01 (d, 2H, $=CH^B$, J_{HH} = 10.2 Hz); 5.37 (m, 2H, $=CH^C$); 6.29 (dt, 1H, Hα, J_{HH} = 16.4 Hz, J_{HP} = 2.7 Hz); 7.29 – 7.36, 7.56-7.61 (m x 2, 30H, C_6H_5) ppm. MS (ES +ve) *m/z* (abundance) = 909 (71) $[M]^+$; 826 (58) $[M - alkenyl]^+$. Analysis: Calculated for $C_{50}H_{51}NOP_2RuS_2$ (M_w = 909.10): C 66.1%, H 5.7%, N 1.5%; Found: C 65.9%, H 5.6%, N 1.6%.

$[Ru(CH=CHC_6H_4Me\text{-}4)\{S_2CN(CH_2CH=CH_2)_2\}(CO)(PPh_3)_2]$ (22)

$[Ru(CH=CHC_6H_4Me\text{-}4)Cl(CO)(BTD)(PPh_3)_2]$ (100 mg, 0.106 mmol) gave 61 mg of pale yellow product (61 %). IR (solid state): 1094 (ν_{CO}), 1710, 1643, 1548, 1410, 1277, 1230, 1127, 981, 968, 935, 920, 827 cm^{-1}. ^{31}P NMR ($CDCl_3$): 39.3 (s, PPh_3). ^1H NMR ($CDCl_3$): 2.24 (s, 3H, CCH_3); 3.53 (d, 2H, NCH_2, J_{HH} = 5.3 Hz); 3.80 (d, 2H, NCH_2, J_{HH} = 6.0 Hz); 4.81 (d, 1H, $=CH^A$, J_{HH} = 17.1 Hz); 4.86 (d, 1H, $=CH^A$, J_{HH} = 17.4 Hz); 5.00 (d, 2H, $=CH^B$, J_{HH} = 10.2 Hz); 5.25 (m, 2H, $=CH^C$); 5.53 (d, 1H, Hβ, J_{HH} = 16.7 Hz); 6.38, 6.83 (AB, 4H, C_6H_4, J_{AB} = 8.0 Hz); 7.28 – 7.36, 7.55-7.59 (m x 2, 30H, C_6H_5); 7.71 (dt, 1H, Hα, J_{HH} = 16.7 Hz, J_{HP} = 3.2 Hz) ppm. MS (ES +ve) *m/z* (abundance) = 943 (5) $[M]^+$; 826 (32) $[M - alkenyl]^+$. Analysis: Calculated for $C_{53}H_{49}NOP_2RuS_2$ (M_w = 943.11): C 67.5%, H 5.2%, N 1.5%; Found: C 67.4%, H 5.2%, N 1.6%.

$[Ru(C(C{\equiv}CBu^t){=}CHBu^t)\{S_2CN(CH_2CH=CH_2)_2\}(CO)(PPh_3)_2]$ (23)

$[Ru(C(C{\equiv}CBu^t){=}CHBu^t)Cl(CO)(PPh_3)_2]$ (100 mg, 0.117 mmol) gave 32 mg of pale yellow product (28 %). IR (solid state): 2162 ($\nu_{C\equiv C}$), 1921 (ν_{CO}), 1640, 1464, 1410, 1356, 1228, 1186, 992, 920, 828 cm^{-1}. IR (solution): X cm^{-1}. ^{31}P NMR ($CDCl_3$): 38.3 (s, PPh_3). ^1H NMR ($CDCl_3$): 0.61 (s, 9H, Bu^t); 1.59 (s, 9H, Bu^t); 3.48 (m, 2H, NCH_2); 3.59 (d, 2H, NCH_2, J_{HH} = 6.2 Hz); 4.81 (d, 1H, $=CH^A$, J_{HH} = 17.0 Hz); 4.86 (d, 1H, $=CH^A$, J_{HH} = 17.0 Hz); 4.98 (d, 2H, $=CH^B$, J_{HH} = 10.1 Hz); 5.17 (m, 2H, $=CH^C$); 5.22 (s, 1H, Hβ); 7.26 – 7.36, 7.60 (m x 2, 30H, C_6H_5) ppm. MS (ES +ve) *m/z* (abundance) = 990 (32) $[M]^+$; 826 (20) $[M - alkenyl]^+$. Analysis: Calculated for $C_{56}H_{59}NOP_2RuS_2{\cdot}3.25CH_2Cl_2$ (M_w = 989.22): C 56.2%, H 5.2%, N 1.1%; Found: C 56.0%, H 4.8%, N 1.5%.

$[Ni\{S_2CN(CH_2CH=CH_2)_2\}(dppp)]PF_6$ (24)

A solution of $[NiCl_2(dppp)]$ (200 mg, 0.369 mmol) in acetone (20 mL) and dichloromethane (10 mL) was treated with 1.5 equivalents of $KS_2CN(CH_2CH=CH_2)_2$ and NH_4PF_6 (120 mg, 0.736 mmol) in water (5 mL) and the reaction stirred for 30 mins. All solvent was removed and the residue dissolved in the minimum volume of dichloromethane and filtered through diatomaceous earth (Celite) to remove KCl, excess NH_4PF_6 and ligand. All solvent was again removed and petroleum ether (30 mL) added and the solid triturated ultrasonically. The orange product was washed with water (10 mL), petroleum ether (10 mL) and dried under vacuum. Yield: 212 mg (73 %). IR (solid state): 1515, 1435,

1418, 1242, 1177, 1100, 971, 938, 824 (ν_{PF}), 742, 691 cm^{-1}. ^{31}P NMR ($CDCl_3$): 12.8 (s, dppp). ^{1}H NMR ($CDCl_3$): 2.18 (m, 2H, dppp-CH_2); 2.68 (m, 4H, dppp-PCH_2); 4.15 (d, 4H, NCH_2, J_{HH} = 6.2 Hz); 5.23 (d, 2H, =CH^A, J_{HH} = 17.1 Hz); 5.33 (d, 2H, =CH^B, J_{HH} = 10.2 Hz); 5.67 (m, 2H, =CH^C); 7.40 – 7.62 (m, 20H, C_6H_5) ppm. MS (ES +ve) *m/z* (abundance) = 642 (100) $[M]^+$. Analysis: Calculated for $C_{34}H_{36}F_6NNiP_3S_2$ (M_w = 788.39): C 51.8%, H 4.6%, N 1.8%; Found: C 52.0%, H 4.7%, N 1.8%.

$[Ni\{S_2CN(CH_2CH=CH_2)_2\}(dppf)]PF_6$ (25)

A solution of $[NiCl_2(dppf)]$ (100 mg, 0.146 mmol) in acetone (20 mL) and dichloromethane (10 mL) was treated with 1.5 equivalents of $KS_2CN(CH_2CH=CH_2)_2$ and NH_4PF_6 (48 mg, 0.295 mmol) in water (5 mL) and the reaction stirred for 30 mins. All solvent was removed and the residue dissolved in the minimum volume of dichloromethane and filtered through diatomaceous earth (Celite) to remove KCl, excess NH_4PF_6 and ligand. All solvent was again removed and petroleum ether (30 mL) added and the solid triturated ultrasonically. The orange product was washed with water (10 mL), petroleum ether (10 mL) and dried under vacuum. Yield: 130 mg (96 %). IR (solid state): 1528, 1500, 1481, 1434, 1240, 1164, 1094, 1025, 976, 932, 830 (ν_{PF}), 742, 697 cm^{-1}. ^{31}P NMR (d^6-acetone): 31.1 (s, dppp). ^{1}H NMR (d^6-acetone): 4.25 (d, 4H, NCH_2, J_{HH} = 6.0 Hz); 4.59, 4.69 (s(br) x 2, 2 x 4H, C_5H_4); 5.23 (d, 2H, =CH^A, J_{HH} = 17.2 Hz); 5.29 (d, 2H, =CH^B, J_{HH} = 10.0 Hz); 5.73 (m, 2H, =CH^C); 7.35 – 7.96 (m, 20H, C_6H_5) ppm. MS (ES +ve) *m/z* (abundance) = 785 (100) $[M]^+$. Analysis: Calculated for $C_{41}H_{38}F_6FeNNiP_3S_2$ (M_w = 930.33): C 52.9%, H 4.1%, N 1.5%; Found: C 52.8%, H 4.0%, N 1.5%.

$[Pd\{S_2CN(CH_2CH=CH_2)_2\}(dppf)]PF_6$ (26)

A solution of $[PdCl_2(dppf)]$ (50 mg, 0.068 mmol) in acetone (20 mL) and dichloromethane (10 mL) was treated with 1.5 equivalents of $KS_2CN(CH_2CH=CH_2)_2$ and NH_4PF_6 (22.4 mg, 0.137 mmol) in water (5 mL) and the reaction stirred for 30 mins. All solvent was removed and the residue dissolved in the minimum volume of dichloromethane and filtered through diatomaceous earth (Celite) to remove KCl, excess NH_4PF_6 and ligand. All solvent was again removed and petroleum ether (30 mL) added and the solid triturated ultrasonically. The orange product was washed with water (10 mL), petroleum ether (10 mL) and dried under vacuum. Yield: 60 mg (90 %). IR (solid state): 1522, 1482, 1436, 1309, 1243, 1168, 1096, 997, 984, 830 (ν_{PF}), 757, 742, 698 cm^{-1}. ^{31}P NMR (d^6-acetone): 32.3 (dppp). ^{1}H NMR (d^6-acetone): 4.33 (d, 4H, NCH_2, J_{HH} = 6.0 Hz); 4.59, 4.74 (s(br) x 2, 2 x 4H, C_5H_4); 5.27 (d, 2H, =CH^A, J_{HH} = 17.2 Hz); 5.31 (d, 2H, =CH^B, J_{HH} = 10.5 Hz); 5.77 (m, 2H, =CH^C); 7.59 – 7.82 (m, 20H, C_6H_5) ppm. MS (ES +ve) *m/z* (abundance) = 832 (100) $[M]^+$. Analysis: Calculated for $C_{41}H_{38}F_6FeNP_3S_2$ (M_w = 978.06): C 50.3%, H 3.9%, N 1.4%; Found: C 50.4%, H 4.0%, N 1.5%.

$[Pt\{S_2CN(CH_2CH=CH_2)_2\}(dppf)]PF_6$ (27)

A solution of [$PtCl_2$(dppf)] (100 mg, 0.122 mmol) in acetone (20 mL) and dichloromethane (10 mL) was treated with 1.5 equivalents of $KS_2CN(CH_2CH{=}CH_2)_2$ and NH_4PF_6 (40 mg, 0.245 mmol) in water (5 mL) and the reaction stirred for 30 mins. All solvent was removed and the residue dissolved in the minimum volume of dichloromethane and filtered through diatomaceous earth (Celite) to remove KCl, excess NH_4PF_6 and ligand. All solvent was again removed and petroleum ether (30 mL) added and the solid triturated ultrasonically. The orange product was washed with water (10 mL), petroleum ether (10 mL) and dried under vacuum. Yield: 125 mg (96 %). IR (solid state): 1528, 1483, 1436, 1411, 1245, 1194, 1168, 1098, 1026, 997, 942, 829 (ν_{PF}), 757, 699, 690 cm^{-1}. ^{31}P NMR ($CDCl_3$): 15.9 (dppf, J_{PtP} = 3367 Hz). ^{1}H NMR ($CDCl_3$): 4.11 (d, 4H, NCH_2, J_{HH} = 6.2 Hz); 4.41, 4.60 (s(br) x 2, 2 x 4H, C_5H_4); 5.24 (d, 2H, $=CH^A$, J_{HH} = 17.1 Hz); 5.34 (d, 2H, $=CH^B$, J_{HH} = 10.0 Hz); 5.67 (m, 2H, $=CH^C$); 7.49 – 7.69 (m, 20H, C_6H_5) ppm. MS (ES +ve) *m/z* (abundance) = 921 (100) $[M]^+$. Analysis: Calculated for $C_{41}H_{38}F_6FeNP_3PtS_2$ (M_w = 1066.71): C 46.2%, H 3.6%, N 1.3%; Found: C 46.0%, H 3.6%, N 1.3%.

[Pd(*C,N*-$CH_2C_6H_4NMe_2$){$S_2CN(CH_2CH{=}CH_2)_2$}] (**28**)

A solution of [Pd(*C,N*-$CH_2C_6H_4NMe_2$)Cl]$_2$ (200 mg, 0.362 mmol) in acetone (20 mL) and dichloromethane (10 mL) was treated with 3 equivalents of $KS_2CN(CH_2CH{=}CH_2)_2$ and the reaction stirred for 30 mins. All solvent was removed and the residue dissolved in the minimum volume of dichloromethane and filtered through diatomaceous earth (Celite) to remove KCl and excess ligand. All solvent was again removed and petroleum ether (30 mL) added and the solid triturated ultrasonically. The orange product was washed with water (10 mL), petroleum ether (10 mL) and dried under vacuum. Yield: 258 mg (86 %). IR (solid state): 1488, 1407, 1343, 1329, 1280, 1249, 1177, 1139, 1112, 1044, 1022, 992, 973, 926, 870, 852, 750 cm^{-1}. ^{1}H NMR ($CDCl_3$): 2.93 (s, 6H, NMe_2); 4.02 (s, 2H, CH_2Pd); 4.43 (m, 4H, NCH_2); 5.26 (d, 2H, $=CH^B$, J_{HH} = 10.2 Hz); 5.29 - 5.34 (m, 2H, $=CH^A$); 5.84 (m, 2H, $=CH^C$); 6.94 - 7.05 (m, 4H, C_6H_4) ppm. MS (ES +ve) *m/z* (abundance) = 413 (100) $[M]^+$. Analysis: Calculated for $C_{16}H_{22}N_2PdS_2$ (M_w = 412.91): C 46.5%, H 5.4%, N 6.8%; Found: C 46.5%, H 5.3%, N 6.8%.

Experimental for methylallyl DTC complexes

[Ru{$S_2CN(CH_2CH{=}CH_2)Me$}$(dppm)_2$]PF_6 (**29**)

A solution of $KS_2CN(CH_2CH{=}CH_2)Me$ in water was prepared by a literature procedure and a solution of *cis*-[$RuCl_2(dppm)_2$] (300 mg, 0.319 mmol) in acetone (20 mL) and dichloromethane (10 mL) was treated with two equivalents of this dithiocarbamate ligand and NH_4PF_6 (104 mg, 0.638 mmol) in water (5 mL) and the reaction was stirred for 30 mins. All solvent was removed and the residue

dissolved in the minimum volume of dichloromethane and filtered through diatomaceous earth (Celite) to remove KCl and excess ligand. All solvent was again removed and diethyl ether (30 mL) added and the solid triturated ultrasonically. The pale yellow product was washed with water (10 mL), diethyl ether (10 mL) and dried under vacuum. Yield: 350 mg (95 %). IR (solid state): 1483, 1434, 1398, 1096, 998, 928, 831 (ν_{PF}), 740, 723, 693, 666, 616 cm^{-1}. ^{31}P NMR ($CDCl_3$): -18.8, -5.4 (t x 2, dppm, J_{HH} = 34.1 Hz). ^{1}H NMR ($CDCl_3$): 2.93 (s, 3H, NMe); 4.06 (m, 2H, NCH_2); 4.60, 4.96 (m x 2, 2 x 2H, PCH_2P); 5.25, (d, 1H, $=CH^A$, J_{HAHC} = 31.9 Hz, J_{HAHB} = 1.2 Hz); 5.30 (d, 1H, $=CH^B$, J_{HBHC} = 25.2 Hz, J_{HBHA} = 0.8 Hz); 5.58 (m, 1H, $=CH^C$); 6.53, 6.96, 7.10, 7.18 - 7.41, 7.65 (m x 5, 40H, C_6H_5) ppm. MS (ES +ve) *m/z* (abundance) = 1016 (100) $[M]^+$. Analysis: Calculated for $C_{55}H_{52}F_6NP_5RuS_2$ (M_w = 1161.12): C 56.9%, H 4.5%, N 1.2%; Found: C 56.7%, H 4.5%, N 1.3%.

$[Ru(CH=CHC_6H_4Me\text{-}4)\{S_2CN(CH_2CH=CH_2)Me\}(CO)(PPh_3)_2]$ (30)

1.5 equivalents of the $KS_2CN(CH_2CH=CH_2)Me$ ligand was added to a solution of $[Ru(CH=CHC_6H_4Me\text{-}4)Cl(CO)(BTD)(PPh_3)_2$ (300 mg, 0.319 mmol) in acetone and dichloromethane (20 mL : 10 mL). The reaction was stirred for 20 mins. All solvent was removed and the crude product dissolved in dichloromethane (15 mL) and filtered through diatomaceous earth (Celite) to remove KCl and excess ligand. All solvent was again removed and diethyl ether (20 mL) added and the crude product triturated ultrasonically. The pale yellow precipitate was filtered and washed with water (5 mL) and diethyl ether (10 mL). The product was dried under vacuum. Yield: 202 mg (70 %). IR (solid state): 1906 (ν_{CO}), 1570, 1538, 1479, 1431, 1389, 1267, 1212, 1185, 1145, 967, 831 cm^{-1}. ^{31}P NMR ($CDCl_3$): 39.5 (s, PPh_3). ^{1}H NMR ($CDCl_3$): 2.24 (s, 6H, CCH_3); 2.40, 2.60 (s x 2, 2 x 3H, NMe -isomers A+B); 3.48, 3.78 (d x 2, 2 x 2H, NCH_2 -isomers A+B, J_{HH} = 5.9 Hz); 4.82, 4.85 (d x 2, 2 x 1H, $=CH^A$ -isomers A+B, J_{HAHC} = 16.7 Hz, J_{HAHB} = unresolved); 5.01 (dd, 2 x 1H, $=CH^B$ -isomers A+B, J_{HBHC} = 11.3 Hz, J_{HBHA} = 1.2 Hz); 5.24, 5.32 (m x 2, 2 x 1H, $=CH^C$ -isomers A+B); 5.60 (d, 2H, Hβ-isomers A+B, J_{HH} = 16.6 Hz); 6.42, 6.83 (AB, 8H, C_6H_4, J_{AB} = 7.9 Hz); 7.29 – 7.35, 7.56-7.60 (m x 2, 60H, C_6H_5); 7.73 (m, 2H, Hα-isomers A+B) ppm. MS (ES +ve) *m/z* (abundance) = 917 (5) $[M]^+$; 800 (22) $[M - alkenyl]^+$. Analysis: Calculated for $C_{51}H_{47}NOP_2RuS_2$ (M_w = 917.16): C 66.8%, H 5.2%, N 1.5%; Found: C 66.7%, H 5.1%, N 1.6%.

$[Ni\{S_2CN(CH_2CH=CH_2)Me\}(dppp)]PF_6$ (31)

A solution of $[NiCl_2(dppp)]$ (300 mg, 0.556 mmol) in acetone (20 mL) and dichloromethane (10 mL) was treated with 1.5 equivalents of $KS_2CN(CH_2CH=CH_2)Me$ and NH_4PF_6 (181 mg, 1.110 mmol) in water (5 mL) and the reaction stirred for 30 mins. All solvent was removed and the residue dissolved in the minimum volume of dichloromethane and filtered through diatomaceous earth (Celite) to remove KCl, excess NH_4PF_6 and ligand. All solvent was again removed and petroleum ether (30 mL) added and the solid triturated ultrasonically. The orange product was washed with water (10 mL),

petroleum ether (10 mL) and dried under vacuum. Yield: 295 mg (70 %). IR (solid state): 1538, 1435, 1403, 1367, 1215, 1100, 973, 833(ν_{PF}), 746, 693, 665, cm^{-1}. ^{31}P NMR ($CDCl_3$): 12.9 (s, dppp). ^{1}H NMR ($CDCl_3$): 2.17 (m, 2H, dppp-CH_2); 2.67 (m, 4H, dppp-PCH_2); 3.12 (s, 3H, NMe); 4.18 (d, 2H, NCH_2, J_{HH} = 6.2 Hz); 5.30 (m, 2H, $=CH^{A,B}$); 5.65 (m, 1H, $=CH^{C}$); 7.40 – 7.63 (m, 20H, C_6H_5) ppm. MS (ES +ve) *m/z* (abundance) = 616 (100) $[M]^+$. Analysis: Calculated for $C_{32}H_{34}F_6NNiP_3S_2$ (M_w = 761.06): C 50.4%, H 4.5%, N 1.8%; Found: C 50.4%, H 4.6%, N 1.9%.

[Ni{$S_2CN(CH_2CH=CH_2)Me$}$_2$] (**32**)

A solution of [$NiCl_2.6H_2O$] (200 mg, 0.848 mmol) in acetone (20 mL) and dichloromethane (10 mL) was treated with 3 equivalents of $KS_2CN(CH_2CH=CH_2)Me$ and the reaction stirred for 30 mins. All solvent was removed and the residue dissolved in the minimum volume of dichloromethane and filtered through diatomaceous earth (Celite) to remove excess ligand. All solvent was again removed and petroleum ether (30 mL) added and the solid triturated ultrasonically. The dark green product was washed with water (10 mL), petroleum ether (10 mL) and dried under vacuum. Yield: 237 mg (88 %). IR (solid state): 1641, 1515, 1382, 1252, 1209, 1143, 1075, 987, 929, 679 cm^{-1}. ^{1}H NMR ($CDCl_3$): 3.14 (s, 6H, NMe); 4.20 (d, 4H, NCH_2, J_{HH} = 4.8 Hz); 5.30 (m, 4H, $=CH^{A,B}$); 5.77 (m, 2H, $=CH^{C}$) ppm. MS (ES +ve) *m/z* (abundance) = 351 (20) $[M]^+$. Analysis: Calculated for $C_{10}H_{16}N_2NiS_4$ (M_w = 351.20): C 34.2%, H 4.6%, N 8.0%; Found: C 34.3%, H 4.5%, N 7.9%.

[Au{$S_2CN(CH_2CH=CH_2)Me$}(PPh_3)] (**33**)

A solution of [$AuCl(PPh_3)$] (300 mg, 0.605 mmol) in acetone (20 mL) and dichloromethane (10 mL) was treated with 1.5 equivalents of $KS_2CN(CH_2CH=CH_2)Me$ and the reaction stirred for 30 mins. All solvent was removed and the residue dissolved in the minimum volume of dichloromethane and filtered through diatomaceous earth (Celite) to remove KCl and excess ligand. All solvent was again removed and petroleum ether (30 mL) added and the solid triturated ultrasonically. The yellow product was washed with water (10 mL), petroleum ether (10 mL) and dried under vacuum. Yield: 231 mg (63 %). IR (solid state): 1584, 1475, 1434, 1379, 1261, 1205, 1098, 975, 910, 745, 990 cm^{-1}. ^{31}P NMR ($CDCl_3$): 36.2 (s, PPh_3). ^{1}H NMR ($CDCl_3$): 3.45 (s, 3H, NMe); 4.62 (d, 2H, NCH_2, J_{HH} = 5.8 Hz); 5.26, 5.29 (m x 2, 2 x 1H, $=CH^{A,B}$); 5.96 (m, 1H, $=CH^{C}$); 7.44 – 7.53, 7.61 – 7.66 (m x 2, 15H, C_6H_5) ppm. MS (ES +ve) *m/z* (abundance) = 606 (10) $[M]^+$. Analysis: Calculated for $C_{23}H_{23}AuNPS_2$ (M_w = 605.07): C 45.6%, H 3.8%, N 2.3%; Found: C 45.6%, H 3.8%, N 2.3%.

NMR Data of literature complexes

[Ni{$S_2CN(CH_2CH=CH_2)_2$}$_2$] (**34**)

Prepared using the literature procedure.[8] ^{1}H NMR ($CDCl_3$): 4.19 (d, 8H, NCH_2, J_{HH} = 5.6 Hz); 5.25 (d, 4H, $=CH^{A}$, J_{HH} = 17.1 Hz); 5.31 (d, 4H, $=CH^{B}$, J_{HH} = 10.1 Hz); 5.76 (m, 4H, $=CH^{C}$) ppm.

[Co{$S_2CN(CH_2CH=CH_2)_2$}$_3$] (**35**)

Prepared using the literature procedure.[9] ^{1}H NMR ($CDCl_3$): 4.19, 4.44 (dd x 2, 2 x 6H, NCH_2, J_{HH} = 15.0, 5.1 Hz); 5.25 – 5.29 (m, 12H, $=CH^{A/B}$); 5.82 (m, 6H, $=CH^{C}$) ppm.

Experimental for pyrroline-DTC complexes

Preparation of $KS_2CNC_4H_6$

An aqueous solution (30 mL) of 3-pyrroline (40 mg, 0.579 mmol) and KOH (32.5 mg, 0.579 mmol) was stirred for 10 mins and then treated with carbon disulphide (52.8 mg, 0.693 mmol). After stirring for a further 40 mins, the solution was used for the additions to the metal complexes.

$[Ni(S_2CNC_4H_6)_2]$ (36)

a) Compound **34** (40 mg, 0.099 mmol) and $[Ru(=CHPh)Cl_2(IMes)(PCy_3)]$ (8.4 mg, 0.010 mmol) were dissolved in dry, degassed dichloromethane (20 mL) and stirred for 2 hours. All solvent was then removed and the residue triturated in diethylether (20 mL) to yield a green/brown product, which was washed with diethylether (20 mL) and dried under vacuum. Yield: 28 mg (81 %). **b)** $Ni(OAc)_2$ (20 mg, 0.113 mmol) was dissolved in dichloromethane (10 mL) and acetone (20 mL) and treated with an aqueous solution of $KS_2CNC_4H_6$ (0.170 mmol). The reaction was stirred for one hour and all solvent removed. The crude product was dissolved in dichloromethane and filtered through diatomaceous earth (Celite) to remove KCl and excess ligand. All solvent was again removed and ultrasonic trituration in diethylether (20 mL) used to obtain a green/brown product. Yield: 30 mg (77 %). IR (solid state): 1625, 1497, 1434, 1351, 1326, 1187, 995, 930, 895, 755 cm^{-1}. ^{1}H NMR ($CDCl_3$): 4.36 (s, 8H, NCH_2); 5.91 (s, 4H, HC=CH) ppm. MS (ES +ve) *m/z* (abundance) = 696 (100) $2[M]^+$. Analysis: Calculated for $C_{10}H_{12}N_2NiS_4$ (M_w = 347.17): C 34.6%, H 3.5%, N 8.1%; Found: C 34.8%, H 3.5%, N 8.0%.

$[Pd(C,N\text{-}CH_2C_6H_4NMe_2)(S_2CNC_4H_6)]$ (37)

a) Compound **28** (40 mg, 0.097 mmol) and $[Ru(=CHPh)Cl_2(IMes)(PCy_3)]$ (4.1 mg, 0.005 mmol) were dissolved in dry, degassed dichloromethane (20 mL) and stirred for 2 hours. All solvent was then removed and the residue triturated in diethyl ether (20 mL) to yield a pale brown product, which was washed with petroleum ether (20 mL) and dried under vacuum. Yield: 26 mg (70 %). **b)** The same procedure as for **36** was employed using $[Pd(C,N\text{-}CH_2C_6H_4NMe_2)Cl]_2$ (20 mg, 0.036 mmol) and $KS_2CNC_4H_6$ (0.109 mmol) with trituration in petroleum ether (20 mL) to yield a pale brown product. Yield: 19 mg (69 %). IR (solid state): 1577, 1501, 1449, 1354, 1188, 1105, 1045, 1027, 989, 929, 869, 849, 737 cm^{-1}. ^{1}H NMR ($CDCl_3$): 2.94 (s, 6H, NMe_2); 4.03 (s, 2H, CH_2Pd); 4.56 (d, 4H, NCH_2, J_{HH} = 13.5 Hz); 5.97 (m, 2H, HC=CH); 6.94 - 7.04 (m, 4H, C_6H_4) ppm. MS (ES +ve) *m/z* (abundance) =

385 (100) $[M]^+$. Analysis: Calculated for $C_{14}H_{18}N_2PdS_2$ (M_w = 384.86): C 43.7%, H 4.7%, N 7.3%; Found: C 43.8%, H 4.7%, N 7.2%.

$[Co(S_2CNC_4H_6)_3]$ (38)

$[Co(O_2CMe)_2]\cdot 4H_2O$ (100 mg, 0.401 mmol) was dissolved in water (20 mL) and treated with an aqueous solution of $KS_2CNC_4H_6$ (1.606 mmol). The reaction was stirred for three hours and all solvent removed. The crude product was dissolved in dichloromethane and filtered through diatomaceous earth (Celite). All solvent was again removed and ultrasonic trituration in diethylether (20 mL) used to obtain a green product. Yield: 192 mg (97 %). IR (solid state): 1572, 1475, 1428, 1351, 1193, 1171, 1102, 1008, 990, 930, 761 cm^{-1}. ^1H NMR ($CDCl_3$): 4.48 (s(br), 12H, NCH_2); 5.91 (s(br), 6H, HC=CH) ppm. MS (ES +ve) *m/z* (abundance) = 1005 (65) $[2M + Na]^+$, 514 (4) $[M + Na]^+$. Analysis: Calculated for $C_{15}H_{18}CoN_3S_6$ (M_w = 491.65): C 36.6%, H 3.7%, N 8.6%; Found: C 36.6%, H 3.7%, N 8.5%.

$[Ni(S_2CNC_4H_6)(dppp)]PF_6$ (39)

a) Compound **24** (40 mg, 0.051 mmol) and $[Ru(=CHPh)Cl_2(IMes)(PCy_3)]$ (4.3 mg, 0.005 mmol) were dissolved in dry, degassed dichloromethane (20 mL) and stirred for 24 hours. All solvent was then removed and the residue triturated in diethyl ether (20 mL) to yield a green/brown product, which was washed with diethylether (20 mL) and dried under vacuum. Yield: 26 mg (67 %). **b)** $NiCl_2$(dppp) (20 mg, 0.037 mmol) was dissolved in dichloromethane (10 mL) and acetone (20 mL) and treated with an aqueous solution of $KS_2CNC_4H_6$ (0.056 mmol) followed by NH_4PF_6 (12 mg, 0.074 mmol) in water (0.5 mL). The reaction was stirred for one hour and all solvent removed. The crude product was dissolved in dichloromethane and filtered through diatomaceous earth (Celite) to remove KCl and excess ligand. All solvent was again removed and ultrasonic trituration in diethylether (20 mL) used to obtain a green/brown product. Yield: 26 mg (92 %). IR (solid state): 1631, 1522, 1485, 1452, 1435, 1355, 1264, 1184, 1160, 1100, 998, 972, 931, 831 (ν_{PF}) cm^{-1}. ^{31}P NMR ($CDCl_3$): 12.5 (s, dppp). ^1H NMR ($CDCl_3$): 2.19 (m, 2H, dppp-CCH_2C); 2.70 (m, 4H, dppp-PCH_2); 4.33 (s(br), 4H, NCH_2); 5.89 (s, 2H, HC=CH); 7.43 – 7.63 (m, 20H, C_6H_5) ppm. MS (ES +ve) *m/z* (abundance) = 614 (100) $[M]^+$. Analysis: Calculated for $C_{32}H_{32}F_6NNiP_3S_2$ (M_w = 760.34): C 50.6%, H 4.2%, N 1.8%; Found: C 50.7%, H 4.3%, N 1.9%.

$[Ru(S_2CNC_4H_6)(dppm)_2]PF_6$ (40)

a) Compound **20** (40 mg, 0.034 mmol) and $[Ru(=CHPh)Cl_2(IMes)(PCy_3)]$ (2.9 mg, 0.003 mmol) were dissolved in dry, degassed dichloromethane (20 mL) and stirred for 24 hours. All solvent was then removed and the residue triturated in diethyl ether (20 mL) to yield a colourless product, which was washed with diethylether (20 mL) and dried under vacuum. Yield: 34 mg (86 %). **b)** The same procedure as for **39** was employed using *cis*-$[RuCl_2(dppm)_2]$ (20 mg, 0.021 mmol), $KS_2CNC_4H_6$

(0.032 mmol) and NH_4PF_6 (7 mg, 0.043 mmol) to yield a colourless product. Yield: 19 mg (78 %). IR (solid state): 1477, 1449, 1434, 1355, 1312, 1190, 1097, 1028, 999, 932, 835 (ν_{PF}) cm^{-1}. ^{31}P NMR (d^6-acetone): -19.5, -3.9 (t^v x 2, dppm, J_{HH} = 34.5 Hz). ^1H NMR (d^6-acetone): 3.91, 4.36 (d x 2, 2 x 2H, NCH_2, J_{HH} = 14.9 Hz); 4.74, 4.35 (m x 2, 2 x 2H, PCH_2P); 5.96 (s, 2H, HC=CH); 6.71, 7.02, 7.20 – 7.39, 7.42 – 7.59, 7.90 (m x 5, 40H, C_6H_5) ppm. MS (ES +ve) *m/z* (abundance) = 1014 (100) $[M]^+$. Analysis: Calculated for $C_{55}H_{50}F_6NP_5RuS_2$ (M_w = 1159.05): C 57.0%, H 4.4%, N 1.2%; Found: C 57.0%, H 4.3%, N 1.2%.

$[Pt(S_2CNC_4H_6)(dppf)]PF_6$ (41)

a) Compound **27** (40 mg, 0.038 mmol) and $[Ru(=CHPh)Cl_2(IMes)(PCy_3)]$ (3.2 mg, 0.004 mmol) were dissolved in dry, degassed dichloromethane (20 mL) and stirred for 24 hours. All solvent was then removed and the residue triturated in diethyl ether (20 mL) to yield a yellow product, which was washed with diethylether (20 mL) and dried under vacuum. Yield: 35 mg (89 %). **b)** The same procedure as for **39** was employed using $[PtCl_2(dppf)]$ (20 mg, 0.024 mmol), $KS_2CNC_4H_6$ (0.036 mmol) and NH_4PF_6 (8 mg, 0.049 mmol) to yield a yellow product. Yield: 22 mg (88 %). IR (solid state): 1632, 1523, 1482, 1453, 1436, 1354, 1307, 1265, 1169, 1098, 1035, 998, 929, 830 (ν_{PF}) cm^{-1}. ^{31}P NMR ($CDCl_3$): 15.9 (s, dppf, J_{PtP} = 3374 Hz). ^1H NMR ($CDCl_3$): 4.42 (s, 4H + 4H, C_5H_4 + NCH_2); 4.61 (s, 4H, C_5H_4); 5.93 (s, 2H, HC=CH); 7.50 – 7.71 (m, 20H, C_6H_5) ppm. MS (ES +ve) *m/z* (abundance) = 893 (100) $[M]^+$. Analysis: Calculated for $C_{39}H_{34}F_6FeNP_3PtS_2$ (M_w = 1038.66): C 45.1%, H 3.3%, N 1.4%; Found: C 45.0%, H 3.4%, N 1.3%.

$[Ru(CH=CHC_6H_4Me\text{-}4)(S_2CNC_4H_6)(CO)(PPh_3)_2]$ (42)

a) Compound **22** (40 mg, 0.042 mmol) and $[Ru(=CHPh)Cl_2(IMes)(PCy_3)]$ (3.6 mg, 0.004 mmol) were dissolved in dry, degassed dichloromethane (20 mL) and stirred for 24 hours. All solvent was then removed and the residue triturated in diethyl ether (20 mL) to yield a colourless product, which was washed with diethylether (20 mL) and dried under vacuum. Yield: 34 mg (88 %). **b)** The same procedure as for **39** was employed using $[Ru(CH=CHC_6H_4Me\text{-}4)Cl(CO)(BTD)(CO)(PPh_3)_2]$ (20 mg, 0.021 mmol) and $KS_2CNC_4H_6$ (0.032 mmol) to yield a colourless product. Yield: 10 mg (52 %). IR (solid state): 1912 (ν_{CO}), 1477, 1355, 1266, 1185, 1032, 933, 851, 832 cm^{-1}. ^{31}P NMR ($CDCl_3$): 39.5 (s, PPh_3). ^1H NMR ($CDCl_3$): 2.25 (s, 3H, CCH_3); 3.50, 3.77 (s(br) x 2, 2 x 2H, NCH_2); 5.58 (d, 1H, Hβ, J_{HH} = 16.7 Hz); 5.62 (s, 2H, HC=CH); 6.45, 6.84 (AB, 4H, C_6H_4, J_{AB} = 7.9 Hz); 7.28 – 7.33, 7.57-7.62 (m x 2, 30H, C_6H_5); 7.77 (dt, 1H, Hα, J_{HH} = 16.7 Hz, J_{HP} = 3.2 Hz) ppm. MS (ES +ve) *m/z* (abundance) = 915 (8) $[M]^+$; 798 (62) [M – alkenyl]$^+$. Analysis: Calculated for $C_{51}H_{45}NOP_2RuS_2{\cdot}CH_2Cl_2$ (M_w = 999.99): C 62.5%, H 4.7%, N 1.4%; Found: C 62.7%, H 4.7%, N 1.7%.

9.2. Experimental details for Chapter 4: Gold(I) dithiocarbamate complexes

Experimental for gold diallyl- and pyrroline-DTC complexes

Preparation of $KS_2CN(CH_2CH=CH_2)_2$

Diallylamine (1.00 mL, 6.371 mmol) and CS_2 (0.42 mL, 6.984 mmol) were stirred in the presence of KOH (393 mg, 7.004 mmol) for 40 minutes. Assuming complete conversion, this solution was used (in slight excess) for the subsequent additions to the metal precursors.

$[(Ph_3P)Au\{S_2CN(CH_2CH=CH_2)_2\}]$ (43)

A solution of $[AuCl(PPh_3)]$ (300 mg, 0.605 mmol) in acetone (20 mL) and dichloromethane (10 mL) was treated with 1.5 equivalents of $KS_2CN(CH_2CH=CH_2)_2$ in water (5 mL) and the reaction stirred for 30 mins. All solvent was removed and the residue dissolved in the minimum volume of dichloromethane and filtered through diatomaceous earth (Celite) to remove KCl and excess ligand. All solvent was again removed and petroleum ether (30 mL) added and the solid triturated ultrasonically. The yellow product was washed with water (10 mL), petroleum ether (10 mL) and dried under vacuum. Yield: 369 mg (95 %). IR (solid state): 1644, 1467, 1399, 1354, 1291, 1277, 1221, 1174, 978, 943, 906 cm^{-1}. ^{31}P NMR ($CDCl_3$): 36.3 (s, PPh_3). ^{1}H NMR ($CDCl_3$): 4.59 (m, 4H, NCH_2); 5.25 (m, 4H, $=CH^{A,B}$); 5.98 (m, 2H, $=CH^{C}$); 7.44 – 7.53, 7.61 – 7.67 (m x 2, 15H, C_6H_5) ppm. MS (ES +ve) *m/z* (abundance) = 632 (22) $[M]^+$. Analysis: Calculated for $C_{25}H_{25}AuNPS_2$ (M_w = 631.55): C 47.6%, H 4.0%, N 2.2%; Found: C 47.6%, H 4.1%, N 2.3%.

$[(Cy_3P)Au\{S_2CN(CH_2CH=CH_2)_2\}]$ (44)

A solution of $[AuCl(PCy_3)]$ (60 mg, 0.117 mmol) in dichloromethane (10 mL) and methanol (5 mL) was treated with 1.1 equivalents of $KS_2CN(CH_2CH=CH_2)_2$ in water (5 mL) and the reaction stirred for 1 h. All solvent was removed and the residue dissolved in the minimum volume of dichloromethane and filtered through diatomaceous earth (Celite) to remove KCl and excess ligand. All solvent was again removed and diethyl ether (20 mL) added and the solid triturated ultrasonically. The bright yellow product was washed with petroleum ether (10 mL) and dried under vacuum. Yield: 55 mg (72 %). IR (solid state): 3077, 3014, 2920, 2849, 1739, 1641, 1465, 1447, 1423, 1389, 1347, 1331, 1222, 1174, 1141, 1114, 1098, 1074, 1045, 996, 971, 931, 911, 888, 852, 820, 790, 755, 739, 691, 641 cm^{-1}. ^{31}P NMR (d^6-acetone): 56.0 (s, PCy_3). ^{1}H NMR (d^6-acetone): 1.10 – 1.88, 2.20 (m x 2, 30H + 3H, PCy_3); 4.54 (d, 4H, NCH_2, J_{HH} = 5.8 Hz); 5.22 (dd, 2H, $=CH^{B}$, J_{HBHC} = 8.8 Hz, J_{HBHA} = 1.4 Hz); 5.25 (dd, 2H, $=CH^{A}$, J_{HAHC} = 15.9 Hz, J_{HAHB} = 1.4 Hz); 5.97 (m, 2H, $=CH^{C}$) ppm. MS (FAB +ve) *m/z*

(abundance) = 650 (53) $[M]^+$; 477 (100). Analysis: Calculated for $C_{25}H_{43}AuNPS_2$ (M_w = 649.22): C 46.2%, H 6.7%, N 2.2%; Found: C 46.0%, H 6.8%, N 2.1%.

$[(Me_3P)Au\{S_2CN(CH_2CH=CH_2)_2\}]$ (**45**)

A solution of $[AuCl(PMe_3)]$ (40 mg, 0.130 mmol) in dichloromethane (10 mL) and methanol (5 mL) was treated with 1.1 equivalents of $KS_2CN(CH_2CH=CH_2)_2$ in water (5 mL) and the reaction stirred for 1 h. All solvent was removed and the residue dissolved in the minimum volume of dichloromethane and filtered through diatomaceous earth (Celite) to remove KCl and excess ligand. All solvent was again removed and the oil was triturated ultrasonically with ethanol (20 mL). The bright yellow product was washed with petroleum ether (10 mL) and dried under vacuum. Low yield is due to high solubility in ethanol. Yield: 37 mg (64 %). IR (solid state): 3071, 2974, 2899, 2031, 1639, 1460, 1415, 1391, 1352, 1333, 1280, 1221, 1171, 1122, 1064, 957, 942, 925, 899, 857, 744, 677, 641 cm^{-1}. ^{31}P NMR (d^6-acetone): - 6.3 (s, PMe_3). ^1H NMR (d^6-acetone): 1.65 (d, 9H, PMe_3, J_{HP} = 11.0 Hz); 4.54 (d, 4H, NCH_2, J_{HH} = 5.7 Hz); 5.19 (dd, 2H, $=CH^B$, J_{HBHC} = 10.1 Hz, J_{HBHA} = 1.3 Hz); 5.21 (dd, 2H, $=CH^A$, J_{HAHC} = 17.2 Hz, J_{HAHB} = 1.5 Hz); 5.94 (m, 2H, $=CH^C$) ppm. MS (FAB +ve) *m/z* (abundance) = 446 (42) $[M]^+$. Analysis: Calculated for $C_{10}H_{19}AuNPS_2$ (M_w = 445.04): C 27.0%, H 4.3%, N 3.2%; Found: C 27.1%, H 4.2%, N 3.1%.

$[(^tBuNC)Au\{S_2CN(CH_2CH=CH_2)_2\}]$ (**46**)

A solution of $[AuCl(^tBuNC)]$ (60 mg, 0.190 mmol) in dichloromethane (10 mL) and methanol (5 mL) was treated with 1.1 equivalents of $KS_2CN(CH_2CH=CH_2)_2$ in water (5 mL) and the reaction stirred for 1 h. All solvent was removed and the residue dissolved in the benzene (150 mL) and filtered through diatomaceous earth (Celite) to remove KCl and excess ligand. All solvent was again removed and diethyl ether (20 mL) added and the solid triturated ultrasonically. The bright orange product was washed with petroleum ether (10 mL) and dried under vacuum. Yield: 64 mg (74 %). IR (solid state): 3082, 3015, 2982, 2895, 2700, 2203 (ν_{CN}), 1968, 1874, 1641, 1468, 1396, 1344, 1329, 1289, 1269, 1218, 1162, 1115, 1067, 968, 931, 905, 854, 689, 628 cm^{-1}. ^1H NMR (C_6D_6): 0.53 (s, 9H, ^tBu); 4.15 (d, 4H, NCH_2, J_{HH} = 5.7 Hz); 4.90 (dd, 2H, $=CH^A$, J_{HAHC} = 17.1 Hz, J_{HAHB} = 1.3 Hz); 4.99 (dd, 2H, $=CH^B$, J_{HBHC} = 10.2 Hz, J_{HBHA} = 1.2 Hz); 5.58 (m, 2H, $=CH^C$) ppm. MS (FAB +ve) *m/z* (abundance) = 369 (2) $[M - {}^tBuCN]^+$. Analysis: Calculated for $C_{12}H_{19}AuN_2S_2$ (M_w = 452.07): C 31.9%, H 4.2%, N 6.2%; Found: C 32.1%, 4.5%, N 6.4%.

$[(IDip)Au\{S_2CN(CH_2CH=CH_2)_2\}]$ (**47**)

A solution of [AuCl(IDip)] (60 mg, 0.097 mmol) in dichloromethane (10 mL) and acetone (5 mL) was treated with 1.1 equivalents of $KS_2CN(CH_2CH=CH_2)_2$ in water (5 mL) and the reaction stirred for 1 h. All solvent was removed and the residue dissolved in dichloromethane (10 mL) and filtered through diatomaceous earth (Celite) to remove KCl and excess ligand. All solvent was again removed

and petroleum ether (20 mL) added and the solid triturated ultrasonically. The yellow product was washed with petroleum ether (10 mL) and dried under vacuum. Yield: 52 mg (71 %). IR (solid state): 1387, 1350, 1331, 1277, 1216, 1177, 1108, 1061, 996, 972, 926, 803, 758, 745 cm^{-1}. ^{1}H NMR (d^6-acetone): 1.25, 1.41 (d x 2, 2 x 12H, Me_{IDip}, J_{HH} = 6.9 Hz); 2.74 (sept, 4H, $CHMe_{IDip}$, J_{HH} = 6.9 Hz); 4.36 (d, 4H, NCH_2, J_{HH} = 6.9 Hz), 5.08 (d, 2H, $=CH^B$, J_{HBHC} = 7.6 Hz), 5.09 (d, 2H, $=CH^A$, J_{HAHC} = 17.9 Hz), 5.80 (m, 2H, $=CH^C$), 7.38 (d, 4H, *m*-C_6H_3, J_{HH} = 7.8 Hz), 7.53 (t, 2H, *p*-C_6H_3, J_{HH} = 7.8 Hz), 7.77 (s, 2H, HC=CH) ppm. MS (FAB +ve) *m/z* (abundance) = 758 (23) $[M]^+$. Analysis: Calculated for $C_{34}H_{46}AuN_3S_2$ (M_w = 757.85): C 53.9%, H 6.1%, N 5.6%; Found: C 53.9%, H 6.1%, N 5.5%.

[(dppa){$AuS_2CN(CH_2CH=CH_2)_2$}$_2$] (**48**)

A solution of [dppa$(AuCl)_2$] (60 mg, 0.070 mmol) in dichloromethane (10 mL) and methanol (5 mL) was treated with 2.2 equivalents of $KS_2CN(CH_2CH=CH_2)_2$ in water (5 mL) and the reaction stirred for 1 h. All solvent was removed and the residue dissolved in the minimum volume of dichloromethane and filtered through diatomaceous earth (Celite) to remove KCl and excess ligand. All solvent was again removed and diethyl ether (20 mL) added and the solid triturated ultrasonically. The bright yellow product was washed with petroleum ether (10 mL) and dried under vacuum. Yield: 62 mg (78 %). IR (solid state): 3055, 2897, 1640, 1572, 1462, 1435, 1397, 1346, 1332, 1291, 1221, 1173, 1118, 1069, 1028, 978, 919, 830, 742, 688, 643, 617 cm^{-1}. ^{31}P NMR (d^6-acetone): -11.9 (s, dppa). ^{1}H NMR (d^6-acetone): 4.54 (d, 8H, NCH_2, J_{HH} = 5.8 Hz); 5.27 (dd, 4H, $=CH^B$, J_{HBHC} = 10.1 Hz, J_{HBHA} = 1.3 Hz); 5.30 (dd, 4H, $=CH^A$, J_{HAHC} = 17.1 Hz, J_{HAHB} = 1.5 Hz); 5.99 (m, 4H, $=CH^C$); 7.50 – 7.58 (m, 20H, PPh_2) ppm. MS (FAB +ve) *m/z* (abundance) = 1133 (1) $[M]^+$; 960 (100). Analysis: Calculated for $C_{40}H_{40}Au_2N_2P_2S_4$ (M_w = 1132.90): C 42.4%, H 3.6%, N 2.5%; Found: C 42.6%, H 3.4%, N 2.4%.

[(dppf){$AuS_2CN(CH_2CH=CH_2)_2$}$_2$] (**49**)

A solution of [Au_2Cl_2(dppf)] (60 mg, 0.059 mmol) in dichloromethane (10 mL) and methanol (5 mL) was treated with 2.2 equivalents of $KS_2CN(CH_2CH=CH_2)_2$ in water (5 mL) and the reaction stirred for 1 h. All solvent was removed and the residue dissolved in the minimum volume of dichloromethane and filtered through diatomaceous earth (Celite) to remove KCl and excess ligand. All solvent was again removed and diethyl ether (20 mL) added and the solid triturated ultrasonically. The pale yellow product was washed with petroleum ether (10 mL) and dried under vacuum. Yield: 61 mg (80 %). IR (solid state): 3066, 3009, 2977, 2904, 1970, 1640, 1587, 1454, 1434, 1389, 1353, 1333, 1309, 1280, 1217, 1173, 1102, 1070, 1039, 998, 972, 922, 833, 742, 689, 635cm^{-1}. ^{31}P NMR (d^6-acetone): 30.1 (s, dppf). ^{1}H NMR (d^6-acetone): 4.49 (m, 4H, C_5H_4); 4.57 (d, 8H, NCH_2, J_{HH} = 5.8 Hz); 4.92 (m, 4H, C_5H_4); 5.25 (dd, 4H, $=CH^B$, J_{HBHC} = 10.3 Hz, J_{HBHA} = 1.3 Hz); 5.28 (dd, 4H, $=CH^A$, J_{HAHC} = 17.2 Hz, J_{HAHB} = 1.5 Hz); 5.99 (m, 4H, $=CH^C$); 7.52 – 7.74 (m, 20H, PPh_2) ppm. MS (FAB +ve) *m/z* (abundance) = 1120 (38) $[M - DTC]^+$. Analysis: Calculated for $C_{48}H_{48}Au_2FeN_2P_2S_4$ (M_w = 1292.90): C 44.6%, H 3.7%, N 2.2%; Found: C 44.5%, H 3.6%, N 2.3%.

[(dppm)Au_2{$S_2CN(CH_2CH=CH_2)_2$}]OTf (50)

[(dppm)$(AuCl)_2$] (50 mg, 0.059 mmol) and silver triflate (30.3 mg, 0.118 mmol) were dissolved in dry tetrahydrofuran (10 mL). The reaction was stirred in the dark for 45 min at 0 C and then the solution was filtered into an mixture containing the aqueous solution of the diallyl ligand (0.34 mL, 0.065 mmol) and acetone (10 mL). Stirring was continued for 1 hr at 0 °C and then all solvent removed. The crude product was dissolved in dichloromethane (30 mL) and filtered through Celite. All solvent was again removed and the residue triturated ultrasonically in diethyl ether (10 mL) to give a pale yellow product. Yield: 63 mg (97 %). IR (solid state): 3058, 2939, 2991, 1636, 1482, 1436, 1408, 1333, 1255, 1225, 1155, 1100, 1029, 995, 962, 933, 848, 782, 740, 726, 688, 634 cm^{-1}. ^{31}P NMR (d^6-acetone): 33.88 (s, dppm). ^1H NMR (d^6-acetone): 4.70 (d, 4H, NCH_2, J_{HH} = 5.7 Hz); 4.74 (m, 2H, PCH_2P, J_{HP} = unresolved); 5.38 (d, 2H, $=CH^B$, J_{HBHC} = 10.1 Hz); 5.39 (d, 2H, $=CH^A$, J_{HAHC} = 18.0 Hz); 6.05 (m, 2H, $=CH^C$); 7.43 – 7.56, 7.85 – 7.87 (m x 2, 15H, PPh_2) ppm. MS (FAB +ve) *m/z* (abundance) = 950 (20) $[M]^+$. Analysis: Calculated for $C_{33}H_{32}Au_2F_3NO_3P_2S_3$ (M_w = 1099.03): C 36.0%, H 2.9%, N 1.3%; Found: C 36.1%, H 2.9%, N 1.2%.

[Au_2{$S_2CN(CH_2CH=CH_2)_2$}$_2$] (51)

A solution of [AuCl(tht)] (100 mg, 0.312 mmol) in dichloromethane (10 mL) and methanol (5 mL) was treated with one equivalent of $KS_2CN(CH_2CH=CH_2)_2$ (0.312 mmol) in water (1.6 mL) and the reaction stirred for 1 h. All solvent was removed and the residue dissolved in the minimum volume of dichloromethane and filtered through diatomaceous earth (Celite) to remove KCl and excess ligand. All solvent was again removed and diethyl ether (30 mL) added and the solid triturated ultrasonically. The yellow product was washed with petroleum ether (10 mL) and dried under vacuum. Yield: 140 mg (61 %). IR (solid state): 1640, 1468, 1398, 1346, 1329, 1290, 1269, 1221, 1164, 1121, 1067, 971, 934, 907, 855, 683 cm^{-1}. ^1H NMR (d^6-benzene): 4.13 (d, 8H, NCH_2, J_{HH} = 5.6 Hz); 4.90 (d, 4H, $=CH^A$, J_{HH} = 17.1 Hz); 4.97 (d, 4H, $=CH^B$, J_{HH} = 10.2 Hz); 5.53 – 5.63 (m, 4H, $=CH^C$) ppm. MS (ES +ve) *m/z* (abundance) = 739 (36) $[M]^+$, 541 (99) $[M - Au]^+$. Analysis: Calculated for $C_{14}H_{20}Au_2N_2S_4$ (M_w = 738): C 22.8%, H 2.7%, N 3.8%; Found: C 22.9%, H 2.6%, N 3.6%.

[$(Ph_3P)Au(S_2CNC_4H_6)_2$] (52)

A solution of [AuCl(PPh_3)] (200 mg, 0.404 mmol) in dichloromethane (20 mL) and acetone (20 mL) was treated with 1.5 equivalents of $KS_2CNC_4H_6$ [generated from 3-pyrroline and CS_2 in the presence of KOH] in water (4 mL) and the reaction stirred for 30 mins. All solvent was removed and the residue dissolved in the minimum volume of dichloromethane and filtered through diatomaceous earth (Celite) to remove KCl and excess ligand. All solvent was again removed and diethyl ether (30 mL) added and the solid triturated ultrasonically. The pale orange product was washed with petroleum ether (10 mL), and dried under vacuum. Yield: 205 mg (84%). IR (solid state): 1481, 1454, 1436, 1400, 1353, 1310, 1288, 1194, 1099, 1071, 1027, 998, 935, 877, 846, 796, 782, 748, 710, 690, 662

cm^{-1}. ^{31}P NMR (d^6-acetone): 34.1 (s, PPh_3). ^1H NMR (d^6-acetone) 4.49 (s, 4H, NCH_2); 5.96 (s, 4H, CH=CH); 7.57 – 7.73 (m, 15H, C_6H_5) ppm. MS (ES +ve) *m/z* (abundance) = 604 (16) $[M]^+$. Analysis: Calculated for $C_{23}H_{21}AuNPS_2$ (M_w = 603.5): C 45.8%, H 3.5%, N 2.3%; Found: C 45.8%, H 3.4%, N 2.4%.

$[Au_2(S_2CNC_4H_6)_2]$ (**53**)

a) A solution of [AuCl(tht)] (50 mg, 0.156 mmol) in dichloromethane (10 mL) and methanol (10 mL) was treated with one equivalent of $KS_2CNC_4H_6$ (0.156 mmol) in water (11.4 mL) and the reaction stirred for 1 h. All solvent was removed and benzene (100 mL) added to dissolve the relatively insoluble material and the solid triturated ultrasonically. The bright orange solid was filtered and washed with water to remove KCl and excess ligand and dried under vacuum. Yield: 88 mg (83 %). **b)** Compound **51** (50 mg, 0.068 mmol) and [Ru(=CHPh)Cl_2(SIMes)(PCy_3)] (5.8 mg, 0.007 mmol) were dissolved in dry, degassed dichloromethane (30 mL),and this solution was stirred for 2 h. All solvent was then removed, and the residue was triturated in diethyl ether (10 mL) to yield a bright orange product, which was dried under vacuum. Yield: 33 mg (71%). IR (solid state): 3083, 2900, 2847, 1413, 1352, 1318, 1291, 1264, 1225, 1174, 1002, 938, 741, 661 cm^{-1}. ^1H NMR (DMSO): 4.52 (s, 8H, NCH_2); 6.00 (s, 4H, CH=CH) ppm. MS (ES +ve) *m/z* (abundance) = 680 (2) $[M]^+$, 485 (100) $[M – Au]^+$. Analysis: Calculated for $C_{10}H_{12}Au_2N_2S_4$ (M_w = 682.4): C 17.6%, H 1.8%, N 4.1%; Found: C 17.7%, H 1.7%, N 4.0%.

Experimental for functionalised gold nanoparticles

$Au@S_2CN(CH_2CH=CH_2)_2$ (**NP1**)

An acetone solution (25 mL) of **51** (6 mg, 0.008 mmol) was treated with an aqueous solution (2 mL) of sodium borohydride (3 mg, 0.079 mmol) causing an instant darkening and precipitation of the product. The product was separated by centrifugation and washed repeatedly with water to give a fine black solid. IR (solid state): 1638, 1454, 1385, 1346, 1330, 1290, 1266, 1213, 1166, 1125, 1068, 971, 923, 908, 873, 697 cm^{-1}. ^1H NMR (d^6-benzene): 4.06 (d, 4H, NCH_2, J_{HH} = 5.8 Hz); 4.94 (dd, 2H, $=CH^A$, J_{HAHC} = 17.1 Hz, J_{HAHB} = 1.3 Hz); 4.99 (dd, 2H, $=CH^B$, J_{HBHC} = 10.2 Hz, J_{HBHA} = 1.3 Hz); 5.53 (m, 2H, $=CH^C$) ppm.

$Au@S_2CNC_4H_6$ (**NP2**)

An acetone solution (25 mL) of **53** (10 mg, 0.015 mmol) was warmed gently with a heat gun, causing an instant darkening and precipitation of the product. The product was separated by centrifugation and washed repeatedly with water to give a fine black solid. IR (solid state): 1420, 1339, 1257, 1129,

1079, 993, 936, 877, 809, 705 cm^{-1}. ^1H NMR (d^6-acetone): 4.36 (s, 8H, NCH_2); 6.88 (s, 4H, CH=CH) ppm.

Au@$S_2CN(CH_2CH=CH_2)_2$ (NP3)

An aqueous solution (100 mL) of $HAuCl_4$ (200 mg, 0.589 mmol) was heated to reflux, and sodium citrate (692 mg, 2.354 mmol) in water (70 mL) was added, causing a darkening of the colour. The reaction was stirred at reflux for 10min and then for a further 15 min at room temperature. A solution of $KS_2CN(CH_2CH=CH_2)_2$ (1.766 mmol) in water (6.22 mL) was added dropwise and the reaction stirred for a further 3 h. The resulting suspension was left to stand and the supernatant decanted, and the solid was washed with water (100 mL) to remove excess sodium citrate and ligand. The black solid was dried under vacuum. IR (solid state): 1676, 1484, 1417, 1348, 1242, 1144, 1038, 941, 760, 648 cm^{-1}. ^1H NMR (d^6-acetone): 4.52 (m, 4H, NCH_2); 5.34 (m, 4H, $=CH^A$ + $=CH^B$); 5.92 (m, 2H, $=CH^C$) ppm.

Au@$S_2CNC_4H_6$ (NP4)

An aqueous solution (100 mL) of $HAuCl_4$ (200 mg, 0.589 mmol) was heated to reflux, and sodium citrate (692 mg, 2.354 mmol) in water (70 mL) was added, causing a darkening of the colour. The reaction was stirred at reflux for 10min and then for a further 15 min at room temperature. A solution of $KS_2CNC_4H_6$ (1.766 mmol) in water (8.40 mL) was added dropwise and the reaction stirred for a further 3 h. The resulting suspension was left to stand and the supernatant decanted, and the solid was washed with water (100 mL) to remove excess sodium citrate and ligand. The black solid was dried under vacuum. IR (solid state): 1420, 1339, 1464, 1374, 1345, 1166, 987, 923, 838, 718, 652 cm^{-1}. ^1H NMR (d^6-acetone): 4.60, 4.78 (s x2, 4H, NCH_2); 6.09 (s, 2H, CH=CH) ppm.

9.3. Experimental details for Chapter 5: Dithiocarboxylate complexes

Experimental for ruthenium and osmium dithiocarboxylate complexes

[Ru(CH=CHBu^t)(κ^2-S$_2$C•IPr)(CO)(PPh$_3$)$_2$]PF$_6$ (54)

A solution of [Ru(CH=CHBu^t)Cl(CO)(BTD)(PPh$_3$)$_2$] (80 mg, 0.088 mmol) in dichloromethane (10 mL) was treated with a solution of IPr•CS$_2$ (22 mg, 0.096 mmol) in dichloromethane (5 mL) and a solution of NH_4PF_6 (29 mg, 0.178 mmol) in methanol (5 mL). The reaction mixture was stirred for 40 min before all solvents were removed. The residue was dissolved in dichloromethane (10 mL) and filtered through Celite to remove NH_4Cl and excess NH_4PF_6. Ethanol (20 mL) was added and the solvent volume was reduced to precipitate a purple-black solid. This crude product was filtered, washed with ethanol (10 mL) and hexane (10 mL), and dried to afford the title compound. Yield: 57 mg (58 %). IR (nujol/KBr): 1932 $\nu_{(CO)}$, 1567, 1311, 1254, 1211, 1039, 941, 841 $\nu_{(PF)}$ cm^{-1}. ^{31}P NMR ($CDCl_3$): 37.5 ppm (s, PPh_3). ^{1}H NMR ($CDCl_3$): 0.42 (s, 9H, Bu^t); 1.15 (d, 12H, $NCCH_3$, J_{HH} = 6.7 Hz); 3.49 (hept, 2H, $NCHMe_2$, J_{HH} = 6.7 Hz); 4.76 (dt, 1H, Hβ, J_{HH} = 16.5 Hz, J_{HP} = 2.4 Hz); 6.27 (dt, 1H, Hα, J_{HH} = 16.5 Hz, J_{HP} = 4.3 Hz); 7.29 (s, 2H, HC=CH); 7.37–7.50 (m, 30H, C_6H_5) ppm. MS (ES +ve) *m/z* (abundance): 965 (100) [M]$^+$. Analysis: Calculated for $C_{53}H_{57}F_6N_2OP_3RuS_2$ (M_w = 110.1): C 57.3%, H 5.2%, N 2.5%; Found: C 57.3%, H 5.2%, N 2.4%.

[Ru(CH=CHC$_6$H$_4$Me-4)(κ^2-S$_2$C•IPr)(CO)(PPh$_3$)$_2$]PF$_6$ (55)

A solution of [Ru(CH=CHC$_6$H$_4$Me-4)Cl(CO)(BTD)(PPh$_3$)$_2$] (80 mg, 0.085 mmol) in dichloromethane (10 mL) was treated with a solution of IPr•CS$_2$ (21 mg, 0.092 mmol) in dichloromethane (5 mL). On addition of NH_4PF_6 (27 mg, 0.166 mmol) in methanol (5 mL), a green colouration appeared. The reaction mixture was stirred for 40 min before all solvents were removed. The residue was dissolved in dichloromethane (10 mL) and filtered through Celite to remove NH_4Cl and excess NH_4PF_6. Ethanol (20 mL) was added and the solvent volume reduced to precipitate a black microcrystalline solid. This crude product was filtered, washed with ethanol (10 mL) and hexane (10 mL), and dried to afford the title compound. Yield: 85 mg (87 %). IR (nujol/KBr): 1935 $\nu_{(CO)}$, 1568, 1544, 1311, 1211, 1039, 840 ν(PF) cm^{-1}. ^{31}P NMR ($CDCl_3$): 38.6 ppm (s, PPh_3). ^{1}H NMR ($CDCl_3$): 1.14, 1.16 (s × 2, 2 × 6H, $NCCH_3$), 2.23 (s, 3H, CH_3), 3.45 (hept, 2H, $NCHMe_2$, J_{HH} = 6.7 Hz), 5.37 (dt, 1H, Hβ, J_{HH} = 14.8 Hz, J_{HP} = 2.1 Hz), 6.21, 6.85 (AB, 4H, C_6H_4, J_{AB} = 8.1 Hz), 7.32 (s, 2H, HC=CH), 7.37–7.52 (m, 30H + 1H, C_6H_5 + Hα) ppm. MS (ES +ve) *m/z* (abundance): 999 (100) [M]$^+$. Analysis: Calculated for $C_{56}H_{55}F_6N_2OP_3RuS_2$ (M_w = 1144.2): C 58.8%, H 4.9%, N 2.5%; Found: C 58.9%, H 4.8%, N 2.4%.

[Ru(C(C≡CPh)=CHPh)(κ^2-S_2C•IPr)(CO)(PPh_3)$_2$]PF_6 (56)

A solution of [Ru(C(C≡CPh)=CHPh)Cl(CO)(PPh_3)$_2$] (80 mg, 0.090 mmol) in dichloromethane (10 mL) was treated with a solution of IPr•CS_2 (23 mg, 0.101 mmol) in dichloromethane (5 mL). On addition of NH_4PF_6 (29 mg, 0.178 mmol) in methanol (5 mL), a green colouration appeared. The reaction mixture was stirred for 40 min before all solvents were removed. The residue was dissolved in dichloromethane (10 mL) and filtered through Celite to remove NH_4Cl and excess NH_4PF_6. Ethanol (20 mL) was added and the solvent volume reduced to precipitate a dark green solid. This crude product was filtered, washed with ethanol (10 mL) and hexane (10 mL), and dried to afford the title compound. Yield: 99 mg (89 %). IR (nujol/KBr): 2146 ν($_{C≡C}$), 1935 ν(CO), 1593, 1564, 1309, 1210, 1037, 940, 838 ν($_{PF}$) cm^{-1}. ^{31}P NMR ($CDCl_3$): 37.4 ppm (s, PPh_3). ^{1}H NMR ($CDCl_3$): 1.13, 1.15 (s × 2, 2 × 6H, $NCCH_3$), 3.52 (hept, 2H, $NCHMe_2$, J_{HH} = 6.7 Hz); 5.76 (s, 1H, Hβ); 6.92 (d, 2H, *ortho*-CC_6H_5, J_{HH} = 7.0 Hz); 7.03 (t, 1H, *para*-CC_6H_5, J_{HH} = 7.1 Hz); 7.08 (t, *meta*-CC_6H_5, 2H, J_{HH} = 7.1 Hz); 7.26–7.40, 7.54–7.60 (m × 2, 30H + 5H + 2H, PC_6H_5 + CC_6H_5 + HC=CH) ppm. MS (ES +ve) *m/z* (abundance): 1085 (100) [M]$^+$. Analysis: Calculated for $C_{63}H_{57}F_6N_2OP_3RuS_2$ (M_w = 1230.3): C 61.5%, H 4.7%, N 2.3%; Found: C 61.5%, H 4.6%, N 2.3%.

[Ru(CH=CHC_6H_4Me-4)(k^2-S_2C•ICy)(CO)(PPh_3)$_2$]PF_6 (57)

A solution of [Ru(CH=CHC_6H_4Me-4)Cl(CO)(BTD)(PPh_3)$_2$] (100 mg, 0.106 mmol) in dichloromethane (10 mL) was treated with a solution of ICy•CS_2 (36 mg, 0.117 mmol) in dichloromethane (5 mL). On addition of NH_4PF_6 (35 mg, 0.212 mmol) in methanol (5 mL), a green colouration appeared. The reaction mixture was stirred for 1 h before all solvents were removed. The residue was dissolved in dichloromethane (10 mL) and filtered through Celite to remove NH_4Cl and excess NH_4PF_6. Ethanol (20 mL) was added and the solvent volume reduced to precipitate a pale green solid. This crude product was filtered, washed with ethanol (10 mL) and hexane (10 mL), and dried to afford the title compound. Yield: 78 mg (60%). IR (nujol/KBr): 1933 ν($_{CO}$), 1710, 1571, 1506, 1308, 1277, 1251, 1191, 1048, 941, 841 ν($_{PF}$) cm^{-1}. ^{31}P NMR ($CDCl_3$): 38.2 ppm (s, PPh_3). ^{1}H NMR ($CDCl_3$): 0.85–1.01, 1.45–1.64, 1.74–1.87 (m × 3, 6H + 6H + 8H, Cy); 2.23 (s, 3H, CH_3); 4.32 (m, 2H, NCH^{Cy}); 5.67 (dt, 1H, Hβ, J_{HH} = 16.7 Hz, J_{HP} = 2.4 Hz); 6.30, 6.86 (AB, 4H, C_6H_4, J_{AB} = 7.9 Hz); 7.35–7.52 (m, 30H + 2H, C_6H_5 + HC=CH); 7.56 (dt, 1H, Hα, J_{HH} = 16.8 Hz, J_{HP} = 4.1 Hz) ppm. ^{13}C NMR: 206.1 (t, CS, J_{PC} = 4.7 Hz), 205.2 (t, CO, J_{PC} = 15.2 Hz), 145.4 (t, Cα, J_{PC} = 15.3 Hz), 141.6 (t, CN_2, J_{PC} = 2.5 Hz), 138.5 (t, Cβ, J_{PC} = 5.3 Hz), 138.2 (t, tolyl-C_1, J_{PC} = 5.3 Hz), 134.7 (s, CMe), 134.3 (virtual t, *o/m*-C_6H_5, J_{PC} = 5.3 Hz), 133.4 (virtual t, *ipso*-C_6H_5, J_{PC} = 22.4 Hz), 130.7 (s, *p*-C_6H_5), 128.9 (s, tolyl-$C_{2,6}$), 128.7 (virtual t, *o/m*-C_6H_5, J_{PC} = 5.3 Hz), 125.0 (s, tolyl-$C_{3,5}$), 120.0 (s, NC_2H_2N), 59.3 (s, Cy-C_1), 34.1 (s, Cy-$C_{2,6}$), 25.5 (s, Cy-$C_{3,5}$), 24.5 (s, Cy-C_4), 21.1 (s, CH_3) ppm. MS (ES +ve) *m/z* (abundance): 1079 (100) [M]$^+$. Analysis: Calculated for $C_{62}H_{63}F_6N_2OP_3RuS_2$ (M_w = 1224.3): C 60.8%, H 5.2%, N 2.3%; Found: C 60.9%, H 5.3%, N 2.3%.

[Ru(C(C≡CPh)=CHPh)(κ^2-S_2C•ICy)(CO)(PPh_3)$_2$]PF_6 (58)

A solution of [Ru(C(C≡CPh)=CHPh)Cl(CO)(PPh_3)$_2$] (100 mg, 0.112 mmol) in dichloromethane (10 mL) was treated with a solution of ICy•CS_2 (38 mg, 0.123 mmol) in dichloromethane (5 mL). On addition of NH_4PF_6 (37 mg, 0.227 mmol) in methanol (5 mL), a green colouration appeared. The reaction mixture was stirred for 1 h before all solvents were removed. The residue was dissolved in dichloromethane (10 mL) and filtered through Celite to remove NH_4Cl and excess NH_4PF_6. Ethanol (20 mL) was added and the solvent volume reduced to precipitate a pale green solid. This crude product was filtered, washed with ethanol (10 mL) and hexane (10 mL), and dried to afford the title compound. A second crop of product was obtained by evaporating the solvent from the filtrate and triturating the residue in diethyl ether. Yield: 89 mg (61 %). IR (nujol/KBr): 2143 ν($_{C≡C}$), 1941 ν($_{CO}$), 1593, 1562, 1307, 1250, 1189, 1049, 940, 915, 839 ν($_{PF}$) cm^{-1}. ^{31}P NMR ($CDCl_3$): 36.2 ppm (s, PPh_3). ^{1}H NMR ($CDCl_3$): 0.77–0.90, 1.49–1.65, 1.70–1.80 (m × 3, 20H, Cy); 4.32 (m, 2H, NCH^{Cy}); 6.03 (t, 1H, Hβ, J_{HP} = 2.1 Hz); 7.09 (s, 2H, HC=CH); 7.19–7.55 (m, 40H, C_6H_5) ppm. MS (ES +ve) *m/z* (abundance): 1165 (100) [M]$^+$. Analysis: Calculated for $C_{69}H_{65}F_6N_2OP_3RuS_2$ (M_w = 1310.4: C 63.2%, H 5.0%, N 2.1%; Found: C 63.3%, H 5.1%, N 2.2%.

[Ru(CH=CHBu^t)(κ^2-S_2C•IMes)(CO)(PPh_3)$_2$]PF_6 (59)

A solution of [Ru(CH=CHBu^t)Cl(CO)(BTD)(PPh_3)$_2$] (65 mg, 0.072 mmol) and IMes•CS_2 (27 mg, 0.071 mmol) in dichloromethane (20 mL) was treated with NH_4PF_6 (23 mg, 0.141 mmol) in methanol (5 mL) causing a green colouration to appear. The reaction mixture was stirred for 1 h before all solvents were removed. The residue was dissolved in dichloromethane (10 mL) and filtered through Celite to remove NH_4Cl and excess NH_4PF_6. All solvents were again removed. Hexane (20 mL) was added and the solid triturated ultrasonically to yield a green-black solid. This crude product was filtered, washed with hexane (20 mL), and dried to afford the title compound. Yield: 86 mg (95 %). IR (nujol/KBr): 1930 ν($_{CO}$), 1606, 1552, 1308, 1231, 968, 839 ν($_{PF}$) cm^{-1}. ^{31}P NMR ($CDCl_3$): 38.7 ppm (s, PPh_3). ^{1}H NMR ($CDCl_3$): 0.02 (s, 9H, Bu^t); 1.38 (s, 12H, *o*-CH_3); 2.30 (s, 6H, *p*-CH_3); 4.28 (dt, 1H, Hβ, J_{HH} = 16.4 Hz, J_{HP} = 2.7 Hz); 5.80 (dt, 1H, Hα, J_{HH} = 16.4 Hz, J_{HP} = 4.3 Hz); 6.79 (s, 4H, *m*-CH); 6.91–7.22 (m, 30H + 2H, C_6H_5 + HC=CH) ppm. MS (ES +ve) *m/z* (abundance): 1117 (100) [M]$^+$. Analysis: Calculated for $C_{65}H_{65}F_6N_2OP_3RuS_2$ (M_w = 1262.3): C 61.9%, H 5.2%, N 2.2%; Found: C 61.9%, H 5.2%, N 2.1%.

[Ru(CH=CHC_6H_4Me-4)(κ^2-S_2C•IMes)(CO)(PPh_3)$_2$]PF_6 (60)

A solution of [Ru(CH=CHC_6H_4Me-4)Cl(CO)(BTD)(PPh_3)$_2$] (100 mg, 0.106 mmol) in dichloromethane (10 mL) was treated with a solution of IMes•CS_2 (44 mg, 0.117 mmol) in dichloromethane (5 mL). On addition of NH_4PF_6 (35 mg, 0.212 mmol) in methanol (5 mL), a green

colouration appeared. The reaction mixture was stirred for 1 h before all solvents were removed. The residue was dissolved in dichloromethane (10 mL) and filtered through Celite to remove NH_4Cl and excess NH_4PF_6. Ethanol (20 mL) was added and the solvent volume reduced to precipitate a pale green solid. This crude product was filtered, washed with ethanol (10 mL) and hexane (10 mL), and dried to afford the title compound. A second crop of product was obtained by evaporating the solvent from the filtrate and triturating the residue in diethyl ether. Yield: 106 mg (77%). IR (nujol/KBr): 1934 $\nu_{(CO)}$, 1606, 1552, 1310, 1230, 1185, 840 $\nu_{(PF)}$ cm^{-1}. ^{31}P NMR ($CDCl_3$): 40.1 ppm (s, PPh_3). ^1H NMR ($CDCl_3$): 1.53 (s, 12H, *o*-CH_3); 2.29 (s, 3H, tolyl-CH_3); 2.46 (s, 6H, *p*-CH_3); 5.05 (dt, 1H, Hβ, J_{HH} = 17.0 Hz, J_{HP} = 2.0 Hz); 5.84, 6.66 (AB, 4H, C_6H_4, J_{AB} = 7.7 Hz); 6.94 (s, 4H, *m*-CH); 6.91–7.36 (m, 30H + 2H + 1H, C_6H_5 + HC=CH + Hα) ppm. MS (ES +ve) *m/z* (abundance): 1151 (100) $[M]^+$. Analysis: Calculated for $C_{68}H_{63}F_6N_2OP_3RuS_2$ (M_w = 1296.4): C 63.0%, H 4.9%, N 2.2%; Found: C 63.1%, H 4.9%, N 2.3%.

[Ru(C(C≡CPh)=CHPh)(κ^2-S_2C•IMes)(CO)(PPh_3)$_2$]PF_6 (61)

A solution of [Ru(C(C≡CPh)=CHPh)Cl(CO)(PPh_3)$_2$] (65 mg, 0.073 mmol) and IMes•CS_2 (28 mg, 0.074 mmol) in dichloromethane (20 mL) was treated with NH_4PF_6 (24 mg, 0.147 mmol) in methanol (5 mL) causing a green colouration to appear. The reaction mixture was stirred for 1 h before all solvents were removed. The residue was dissolved in dichloromethane (10 mL) and filtered through Celite to remove NH_4Cl and excess NH_4PF_6. The solvent was again removed. Diethyl ether (20 mL) was added and the solid triturated ultrasonically to give a green solid. This crude product was filtered, washed with diethyl ether (10 mL), and dried to afford the title compound. Yield: 81 mg (80 %). IR (nujol/KBr): 2146 $\nu_{(C\equiv C)}$, 1937, 1924 $\nu_{(CO)}$, 1593, 1552, 1309, 1228, 1121, 908, 838 $\nu_{(PF)}$ cm^{-1}. ^{31}P NMR ($CDCl_3$): 36.4 ppm (s, PPh_3). ^1H NMR ($CDCl_3$): 1.56 (s, 12H, *o*-CH_3); 2.41 (s, 6H, *p*-CH_3); 5.65 (t, 1H, Hβ, J_{HP} = 2.5 Hz); 6.90 (s, 4H, *m*-CH); 6.97–7.50 (m, 40H + 2H, C_6H_5 + HC=CH) ppm. MS (ES +ve) *m/z*: 1237 $[M]^+$. Analysis: Calculated for $C_{75}H_{65}F_6N_2OP_3RuS_2$ (Mw = 1382.4): C 65.2%, H 4.7%, N 2.0%; Found: C 65.1%, H 4.6%, N 2.1%.

[Os(CH=CHC_6H_4Me-4)(κ^2-S_2C•IMes)(CO)(PPh_3)$_2$]PF_6 (62)

A solution of [Os(CH=CHC_6H_4Me-4)Cl(CO)(BTD)(PPh_3)$_2$] (70 mg, 0.068 mmol) in dichloromethane (10 mL) was treated with a solution of IMes•CS_2 (28 mg, 0.074 mmol) in dichloromethane (5 mL). On addition of NH_4PF_6 (22 mg, 0.135 mmol) in methanol (5 mL), a green colouration appeared. The reaction mixture was stirred for 1 h before all solvents were removed. The residue was dissolved in dichloromethane (10 mL) and filtered through Celite to remove NH_4Cl and excess NH_4PF_6. Hexane (20 mL) was added and the solid was triturated ultrasonically to yield a dark green solid. This crude product was filtered, washed with hexane (10 mL), and dried to afford the title compound. Yield: 76 mg (81 %). IR (nujol/KBr): 1919 $\nu_{(CO)}$, 1607, 1552, 1309, 1230, 1208, 840 $\nu_{(PF)}$ cm^{-1}. ^{31}P NMR

($CDCl_3$): 10.0 ppm (s, PPh_3). ^{1}H NMR ($CDCl_3$): 1.54 (s, 12H, *o*-CH_3); 2.09 (s, 3H, tolyl-CH_3); 2.47 (s, 6H, *p*-CH_3); 4.98 (dt, 1H, Hβ, J_{HH} = 17.3 Hz, J_{HP} = 3.0 Hz); 5.83, 6.65 (AB, 4H, C_6H_4, J_{AB} = 8.1 Hz); 6.96 (s, 4H, *m*-CH); 7.04–7.56 (m, 30H + 2H, C_6H_5 + HC=CH); 7.73 (dt, 1H, Hα, J_{HH} = 17.2 Hz, J_{HP} = 4.2 Hz) ppm. MS (ES +ve) *m/z* (abundance): 1241 (100) $[M]^+$. Analysis: Calculated for $C_{68}H_{63}F_6N_2OOsP_3S_2$ (M_w = 1385.5): C 59.0%, H 4.6%, N 2.0%; Found: C 59.1%, H 4.7%, N 2.1%.

[Os(C(C≡CPh)=CHPh)(κ^2-S_2C•IMes)(CO)(PPh_3)$_2$]PF_6 (63)

A solution of [Os(C(C≡CPh)=CHPh)Cl(CO)(BTD)(PPh_3)$_2$] (47 mg, 0.042 mmol) in dichloromethane (10 mL) was treated with a solution of IMes•CS_2 (18 mg, 0.048 mmol) in dichloromethane (5 mL) and a solution of NH_4PF_6 (14 mg, 0.086 mmol) in methanol (5 mL). The reaction mixture was heated for 10 min and then stirred for 1 h before all solvents were removed. The residue was dissolved in dichloromethane (10 mL) and filtered through Celite to remove NH_4Cl and excess NH_4PF_6. Diethyl ether (20 mL) was added and the solid triturated ultrasonically to give a brown solid. This crude product was filtered, washed with diethyl ether (10 mL), and dried to afford the title compound. Yield: 57 mg (92 %). Recrystallisation was performed by slow diffusion of diethyl ether into a chloroform solution of the complex. IR (nujol/KBr): 2143 ν($_{C≡C}$), 1923 ν($_{CO}$), 1607, 1594, 1552, 1310, 1230, 838 ν($_{PF}$) cm^{-1}. ^{31}P NMR ($CDCl_3$): 5.7 ppm (s, PPh_3). ^{1}H NMR ($CDCl_3$): 1.48 (s, 12H, *o*-CH_3); 2.21 (s, 3H, tolyl-CH_3); 2.32 (s, 6H, *p*-CH_3); 6.48 (s, 1H, Hβ); 6.82 (br s, 4H, *m*-CH); 6.91–7.59 (m, 40H + 2H, C_6H_5 + HC=CH) ppm. MS (ES +ve) *m/z*: 1327 $[M]^+$. Analysis: Calculated for $C_{75}H_{65}F_6N_2OOsP_3S_2{\cdot}2(CHCl_3)$ (Mw = 1710.4): C 54.1% H 4.0%, N 1.6%; Found: C 54.1%, H 4.4%, N 1.9%.

[Ru{κ^2-SC(H)S(CH=CHC_6H_4Me-4)•IDip)}Cl(CO)(PPh_3)$_2$]PF_6 (64)

A solution of [Ru(CH=CHC_6H_4Me-4)Cl(CO)(BTD)(PPh_3)$_2$] (50 mg, 0.053 mmol) in dichloromethane (10 mL) was treated with a solution of IDip•CS_2 (25 mg, 0.054 mmol) in dichloromethane (5 mL). After addition of NH_4PF_6 (17 mg, 0.104 mmol) in methanol (5 mL), the reaction mixture was stirred for 2 h before all solvents were removed. The residue was dissolved in dichloromethane (10 mL) and filtered through Celite to remove NH_4Cl and excess NH_4PF_6. Ethanol (20 mL) was added and the solvent volume reduced to precipitate a pale brown solid. This crude product was filtered, washed with ethanol (10 mL) and hexane (10 mL), and dried to afford the title compound. Yield: 45 mg (60 %). IR (nujol/KBr): 1962 ν($_{CO}$), 1556, 1511, 1388, 1367, 1326, 1274, 1183, 835 ν($_{PF}$) cm^{-1}. ^{31}P NMR (500 MHz, CD_2Cl_2): 26.7, 37.1 ppm (d × 2, PPh_3, J_{PP} = 20.1 Hz). ^{1}H NMR (500 MHz, CD_2Cl_2): 1.05 (d, 6H, aryl-CH_3, J_{HH} = 6.7 Hz); 1.07 (d, 6H, aryl-CH_3, J_{HH} = 7.0 Hz); 1.13 (d, 6H, aryl-CH_3, J_{HH} = 7.0 Hz); 1.33 (d, 6H, aryl-CH_3, J_{HH} = 6.7 Hz); 2.34 (s, 3H, tolyl-CH_3); 2.35, 2.46 (hept × 2, 2 × 2H, $CHMe_2$, J_{HH} = 6.7 Hz); 5.04 (d, 1H, =CHtolyl, J_{HH} = 15.8 Hz); 6.37 (s, 1H, CHS_2); 6.89 (d, 2H, C_6H_4, J_{AB} = 8.1 Hz); 6.99–7.06, 7.10–7.15, 7.24–7.29, 7.34–7.36 (m × 4, 30H + 2H + 2H + 1H, C_6H_5 + *m*-

C_6H_3 + C_6H_4 + SCH=C); 7.43 (s, 2H, HC=CH); 7.52 (dd, 2H, *m*-C_6H_3, J_{HH} = 7.9 Hz, 1.2 Hz); 7.72 (t, 2H, *p*-C_6H_3, J_{HH} = 7.9 Hz) ppm. ^{13}C NMR (500 MHz, CD_2Cl_2): 198.1 (t, CO, J_{PC} = 12.9 Hz), 147.6 (t, NCN, J_{PC} = 2.9 Hz), 146.0, 145.9 (s × 2, *o*-C_6H_3), 140.8 (tolyl-C4), 139.5 (s, SC=*C*), 134.7 (d, *o*-PC_6H_5, J_{PC} = 10.5 Hz), 134.6 (d, *o*-PC_6H_5, J_{PC} = 9.5 Hz), 133.5 (d, *ipso*-PC_6H_5, J_{PC} = 47.7 Hz), 132.9 (s, *p*-C_6H_3), 132.4 (d, *ipso*-PC_6H_5, J_{PC} = 40.1 Hz), 131.8 (s, *ipso*-C_6H_4), 130.6 (d, *p*-PC_6H_5, J_{PC} = 2.8 Hz), 130.5 (d, *p*-PC_6H_5, J_{PC} = 1.9 Hz), 130.0, 130.6 (s, *ipso*-C_6H_3), 129.8 (s, *m*-C_6H_4), 128.7 (d, *m*-PC_6H_5, J_{PC} = 9.5 Hz), 128.1 (d, *m*-PC_6H_5, J_{PC} = 10.5 Hz), 127.8 (s, *o*-C_6H_4), 125.9 (s, HC=CH), 125.4, 125.0 (s × 2, *m*-C_6H_3), 113.7 (S*C*=C), 59.5 (S_2CH), 30.4, 30.1 (s × 2, $CHMe_2$), 26.3, 26.2, 23.2, 22.3 (s × 4, Pr^i-CH_3), 21.6 (s, tolyl-CH_3) ppm. MS (ES +ve) *m/z* (abundance): 1271 (100) $[M]^+$, 1236 (68) $[M–Cl]^+$. Analysis: Calculated for $C_{74}H_{76}ClF_6N_2OP_3RuS_2$ (Mw = 1417.0): C 62.7%, H 5.4%, N 2.0%; Found: C 62.4%, H 5.2%, N 1.9%.

[Ru{κ^2-SC(H)S(CH=CHC$_6$H$_4$Me-4)•IMes)}Cl(CO)(PPh$_3$)$_2$]PF$_6$ (65)

A solution of [Ru(CH=CHC$_6$H$_4$Me-4)Cl(CO)(BTD)(PPh$_3$)$_2$] (100 mg, 0.106 mmol) in dichloromethane (10 mL) was treated with a solution of IMes•CS_2 (44 mg, 0.116 mmol) in dichloromethane (5 mL). After addition of NH_4PF_6 (81 mg, 0.213 mmol) in methanol (5 mL), the reaction mixture was stirred for 18 h before all solvents were removed. The residue was dissolved in dichloromethane (10 mL) and filtered through Celite to remove NH_4Cl and excess NH_4PF_6. All solvent was removed and hexane (20 mL) added. Ultrasonic trituration led to a pale brown solid, which was filtered, washed with hexane (10 mL), and dried to afford the title compound. Yield: 122 mg (86%). IR (neat): 1958 ν$_{(CO)}$, 1605, 1553, 1462, 1434, 1381, 1231, 1185, 970, 834 ν$_{(PF)}$, 744, 693 cm^{-1}. ^{31}P NMR (CD_2Cl_2): 28.1, 37.9 ppm (d × 2, PPh_3, J_{PP} = 19.1 Hz). ^{1}H NMR (CD_2Cl_2): 2.02, 2.16 (s × 2, 2 x 6H, *o*-CH_3); 2.41 (s, 3H, tolyl-CH_3); 2.48 (s, 6H, *p*-CH_3); 5.41 (d, 1H, =CHtolyl, J_{HH} = 15.7 Hz); 6.28 (s, 1H, CHS_2); 6.91 (d, 1H, SCH=C, J_{HH} = 15.7 Hz); 6.96 (d, 2H, C_6H_4, J_{AB} = 8.1 Hz); 7.04–7.25, 7.36–7.42 (m × 2, 30H + 2H, C_6H_5 + C_6H_4); 7.37 (s, 4H, meta-C_6H_2); 7.39 (s, 2H, HC=CH) ppm. MS (ES +ve) *m/z* (abundance): 1187 (5) $[M]^+$, 1151 (100) $[M – Cl]^+$. Analysis: Calculated for $C_{68}H_{64}ClF_6N_2OP_3RuS_2$ (Mw = 1332.8): C 61.3%, H 4.8%, N 2.1%; Found: C 61.5%, H 4.7%, N 2.4%.

Experimental for gold(I) NHC•CS_2 complexes

[(Ph$_3$P)Au(S$_2$C•IPr)]PF$_6$ (66)

A dichloromethane solution (10 mL) of [AuCl(PPh_3)] (40 mg, 0.081 mmol) was treated with a solution of IPr•CS_2 (19 mg, 0.083 mmol) in dichloromethane (5 mL). On addition of NH_4PF_6 (26 mg, 0.160 mmol) in methanol (5 mL), a purple colouration appeared. The reaction was stirred for 1 hr and

then all solvent removed. The crude product was dissolved in dichloromethane (10 mL) and filtered through Celite to remove NH_4Cl and excess NH_4PF_6. Hexane (15 mL) was added and the crude product triturated ultrasonically to give a brown solid. This was filtered and washed with hexane (10 mL) and dried. Yield: 49 mg (73 %). IR (nujol/KBr): 1566, 1311, 1209, 1055, 839 $\nu_{(PF)}$ cm^{-1}. ^{31}P NMR($CDCl_3$): 36.0 ppm (s, PPh_3). ^1H NMR ($CDCl_3$): 1.55 (d, 12H, CH_3, J_{HH} = 6.8 Hz), 4.87 (sept., 2H, $CHMe_2$, J_{HH} = 6.8 Hz); 7.36 (s, 2H, HC=CH); 7.54-7.66 (m, 15H, C_6H_5) ppm. MS (ES +ve) *m/z* (abundance): 687 (100) $[M]^+$. Analysis: Calculated for $C_{28}H_{31}AuF_6N_2P_2S_2$ (M_w = 832.6): C 40.4%, H 3.8%, N 3.4%; Found: C 40.3%, H 3.8%, N 3.4%.

$[(Ph_3P)Au(S_2C•IMes)]PF_6$ (67)

A dichloromethane solution (10 mL) of [$AuCl(PPh_3)$] (45 mg, 0.091 mmol) was treated with a solution of IMes•CS_2 (38 mg, 0.100 mmol) in dichloromethane (5 mL). On addition of NH_4PF_6 (30 mg, 0.184mmol) in methanol (5 mL), a green colouration appeared. The reaction was stirred for 1 hr and then all solvent removed. The crude product was dissolved in dichloromethane (10 mL) and filtered through Celite to remove NH_4Cl and excess NH_4PF_6. Pentane (15 mL) was added and the solid triturated ultrasonically to give a pale green solid. This was filtered and washed with pentane (10 mL) and dried. Yield: 75 mg (84 %). IR (nujol/KBr): 1722, 1566, 1311, 1209, 1055, 839 $\nu_{(PF)}$ cm^{-1}. ^{31}P NMR ($CDCl_3$): 35.1 ppm (s, PPh_3). ^1H NMR ($CDCl_3$): 2.25 (s, 12H, ortho-CH_3); 2.37 (s, 6H, para-CH_3); 7.08 (s, 4H, meta-C_6H_2); 7.41 (s, 2H, HC=CH); 7.45 - 7.60 (m, 15H, C_6H_5) ppm. MS (ES +ve) *m/z* (abundance): 839 (100) $[M]^+$. Analysis: Calculated for $C_{40}H_{39}AuF_6N_2P_2S_2$ (M_w = 984.8); Found: C 48.9, H 4.1, N 2.9%. C 48.8, H 4.0, N 2.9%.

$[(Ph_3P)Au(S_2C•IDip)]PF_6$ (68)

A dichloromethane solution (10 mL) of [$AuCl(PPh_3)$] (50 mg, 0.101 mmol) was treated with a solution of IDip•CS_2 (47 mg, 0.101 mmol) in dichloromethane (5 mL). On addition of NH_4PF_6 (33 mg, 0.203 mmol) in methanol (5 mL), a green colouration appeared. The reaction was stirred for 1 hr and then all solvent removed. The crude product was dissolved in dichloromethane (10 mL) and filtered through Celite to remove NH_4Cl and excess NH_4PF_6. Pentane (15 mL) was added and the crude product triturated ultrasonically to give a green solid. This was filtered and washed with pentane (10 mL) and dried. Yield: 62 mg (58 %). A purple colouration was observed in the solid state indicating the formation of gold colloid. IR (nujol/KBr): 1711, 1587, 1554, 1327, 1275, 1212, 1101, 1070, 839 $\nu_{(PF)}$ cm^{-1}. ^{31}P NMR ($CDCl_3$): 35.4 ppm (s, PPh_3). ^1H NMR ($CDCl_3$): 1.24 (d, 12H, CH_3, J_{HH} = 7.1 Hz); 1.36 (d, 12H, CH_3, J_{HH} = 6.7 Hz); 2.66 (sept., 4H, $CHMe_2$, J_{HH} = 6.8 Hz); 7.38-7.63 (m, 15H + 6H + 2H, C_6H_5 + C_6H_3 + HC=CH) ppm. MS (ES +ve) *m/z* (abundance): 923 (100) $[M]^+$. Analysis: Calculated for $C_{46}H_{51}AuF_6N_2P_2S_2$ (M_w = 1069.0): C 51.7%, H 4.8%, N 2.6%; Found: C 51.7%, H 4.8%, N 2.6%.

[(Cy_3P)Au(S_2C•IMes)]PF_6 (69)

A dichloromethane solution (10 mL) of [AuCl(PCy_3)] (40 mg, 0.078 mmol) was treated with a solution of IMes•CS_2 (31 mg, 0.082 mmol) in dichloromethane (5 mL). On addition of NH_4PF_6 (25 mg, 0.153 mmol) in methanol (5 mL), a green colouration appeared. The reaction was stirred for 1 hr and then all solvent removed. The crude product was dissolved in dichloromethane (10 mL) and filtered through Celite to remove NH_4Cl and excess NH_4PF_6. Ethanol (15 mL) was added and the solvent volume reduced until precipitation of the green solid was complete. This was filtered and washed with ethanol (10 mL), pentane (10 mL) and dried. Yield: 59 mg (75 %). IR (nujol/KBr): 1712, 1607, 1557, 1300, 1230, 1170, 1114, 1069, 1041, 1005, 839 $\nu_{(PF)}$ cm^{-1}. ^{31}P NMR ($CDCl_3$): 56.7 ppm (s, PCy_3). ^1H NMR ($CDCl_3$): 1.24-1.45, 1.71-1.91, 1.96-2.08 (m x 3, 33H, Cy); 2.24 (s, 12H, ortho-CH_3); 2.39 (s, 6H, para-CH_3); 7.08 (s, 4H, meta-C_6H_2); 7.36 (s, 2H, HC=CH) ppm. MS (ES +ve) *m/z* (abundance): 858 (100) $[M]^+$. Analysis: Calculated for $C_{40}H_{57}AuF_6N_2P_2S_2$ (M_w = 1003.0): C 47.9%, H 5.7%, N 2.8%; Found: C 48.0%, H 5.6%, N 2.8%

[(Me_3P)Au(S_2C•IMes)]PF_6 (70)

A dichloromethane solution (10 mL) of [AuCl(PMe_3)] (30 mg, 0.097 mmol) was treated with a solution of IMes•CS_2 (41 mg, 0.108 mmol) in dichloromethane (5 mL). On addition of NH_4PF_6 (32 mg, 0.196 mmol) in methanol (5 mL), a green colouration appeared. The reaction was stirred for 30 mins and then all solvent removed. The crude solid was dissolved in dichloromethane (10 mL) and filtered through diatomaceous earth (Celite) to remove NH_4Cl and excess NH_4PF_6. All solvent was again removed and the green product triturated ultrasonically in diethylether (20 mL). This was filtered and washed with diethylether (15 mL) and dried. Yield: 65 mg (84 %). IR (solid): 1608, 1558, 1486, 1465, 1420, 1381, 1293, 1115, 1065, 1006, 958, 828 $\nu_{(PF)}$ cm^{-1}. ^{31}P NMR ($CDCl_3$): -4.1 ppm (s, PMe_3). ^1H NMR ($CDCl_3$): 1.58 (d, 9H, CH_3, J_{HP} = 11.2 Hz); 2.27 (s, 12H, ortho-CH_3); 2.42 (s, 6H, para-CH_3); 7.11 (s, 4H, meta-C_6H_2); 7.38 (s, 2H, HC=CH) ppm. MS (FAB +ve) *m/z* (abundance): 653 (95) $[M]^+$. Analysis: Calculated for $C_{25}H_{33}AuF_6N_2P_2S_2$ (M_w = 798.6): C 37.6%, H 4.2%, N 3.5%; Found: C 37.5%, H 4.3%, N 3.4%.

[(^{t}BuNC)Au(S_2C•IMes)]PF_6 (71)

A dichloromethane solution (10 mL) of [AuCl($CNBu^t$)] (30 mg, 0.095 mmol) was treated with a solution of IMes•CS_2 (38 mg, 0.100 mmol) in dichloromethane (5 mL). On addition of NH_4PF_6 (31 mg, 0.190 mmol) in methanol (5 mL), a green colouration appeared. The reaction was stirred for 1 hr and then all solvent removed. The crude product was dissolved in dichloromethane (10 mL) and filtered through Celite to remove NH_4Cl and excess NH_4PF_6. All solvent was again removed and the crude solid triturated ultrasonically in diethyl ether (20 mL). The green product was filtered, washed with diethyl ether (10 mL) and dried. Yield: 71 mg (93 %). IR (nujol/KBr): 2258, 2234 $\nu_{(CN)}$, 1607,

1557, 1309, 1232, 1193, 1116, 1070, 1037, 1005, 931, 839 $\nu_{(PF)}$ cm^{-1}. ^1H NMR ($CDCl_3$): 1.54 (s, 9H, Bu^t); 2.21 (s, 12H, ortho-CH_3); 2.38 (s, 6H, para-CH_3); 7.07 (s, 4H, meta-C_6H_2); 7.40 (s, 2H, HC=CH) ppm. MS (ES +ve) *m/z* (abundance): 660 (62) $[M]^+$. Analysis: Calculated for $C_{27}H_{33}AuF_6N_3PS_2$ (M_w = 805.6): C 40.4%, H 4.1%, N 5.2%; Found: C 40.3%, H 4.1%, N 5.2%.

[(IDip)Au(S_2C•IPr)]PF_6 (72)

A dichloromethane solution (10 mL) of [AuCl(IDip)] (50 mg, 0.081 mmol) was treated with a solution of IPr•CS_2 (20 mg, 0.088 mmol) in dichloromethane (5 mL). On addition of NH_4PF_6 (27 mg, 0.166 mmol) in methanol (5 mL), a purple colouration appeared. The reaction was stirred for 30 mins and then all solvent removed. The crude product was dissolved in dichloromethane (10 mL) and filtered through diatomaceous earth (Celite) to remove NH_4Cl and excess NH_4PF_6. All solvent was again removed and the pale purple product triturated ultrasonically in diethylether (20 mL). This was filtered and washed with diethylether (15 mL) and dried. Yield: 55 mg (71 %). IR (solid): 1597, 1563, 1475, 1422, 185, 1365, 1354, 1330, 1256, 1207, 1181, 1137, 1092, 1062, 876, 832 $\nu_{(PF)}$ cm^{-1}. ^1H NMR ($CDCl_3$): 1.31, 1.38 (d x 2, 2 x 12H, Me_{IDip}, J_{HH} = 6.9 Hz); 1.46 (d, 12H, Me_{IPr}, J_{HH} = 6.7 Hz); 2.68 (sept., 4H, $CHMe_{IDip}$, J_{HH} = 6.9 Hz); 4.62 (s(br), 2H, $CHMe_{IPr}$); 7.24 (s, 2H, $HC=CH_{IDip}$); 7.38 (s, 2H, $HC=CH_{IPr}$); 7.40 (d, 4H, meta-C_6H_3, J_{HH} = 7.8 Hz); 7.62 (t, 2H, para-C_6H_3, J_{HH} = 7.8 Hz) ppm. MS (FAB +ve) *m/z* (abundance): 813 (100) $[M]^+$, 585 (12) $[M - S_2C{\cdot}IPr]^+$. Analysis: Calculated for $C_{37}H_{52}AuF_6N_4PS_2$ (Mw = 958.9): C 46.3%, H 5.5%, N 5.8%: Found: C 46.2%, H 5.4%, N 5.8%.

[(IDip)Au(S_2C•IMes)]PF_6 (73)

A dichloromethane solution (10 mL) of [AuCl(IDip)] (50 mg, 0.081 mmol) was treated with a solution of IMes•CS_2 (34 mg, 0.089 mmol) in dichloromethane (5 mL). On addition of NH_4PF_6 (26 mg, 0.160 mmol) in methanol (5 mL), a green colouration appeared. The reaction was stirred for 30 mins and then all solvent removed. The crude product was dissolved in dichloromethane (10 mL) and filtered through diatomaceous earth (Celite) to remove NH_4Cl and excess NH_4PF_6. All solvent was again removed and the pale green product triturated ultrasonically in diethylether (20 mL). This was filtered and washed with diethylether (15 mL) and dried. Yield: 69 mg (87 %). IR (solid): 1608, 1558, 1486, 1462, 1421, 1384, 1365, 1330, 1230, 1183, 1117, 1071, 1007, 932, 835 $\nu_{(PF)}$, 760 cm^{-1}. ^1H NMR ($CDCl_3$): 1.15, 1.23 (d x 2, 2 x 12H, Me_{IDip}, J_{HH} = 6.9 Hz); 2.12 (s, 12H, ortho-$C_6H_2Me_2$); 2.12 (s, 6H, para-$C_6H_2Me_2$); 2.47 (sept., 4H, $CHMe_{IDip}$, J_{HH} = 6.9 Hz); 7.02 (s(br), 4H, $HC=CH_{IDip/IMes}$); 7.28 (d, 4H, meta-C_6H_3, J_{HH} = 7.8 Hz); 7.29 (s, 4H, meta-C_6H_2); 7.54 (t, 2H, para-C_6H_3, J_{HH} = 7.8 Hz) ppm. MS (FAB +ve) *m/z* (abundance): 965 (100) $[M]^+$, 585 (9) $[M - S_2C{\cdot}IMes]^+$. Analysis: Calcuated for $C_{49}H_{60}AuF_6N_4PS_2$ (M_w = 1111.1): C 53.0%, H 5.4%, N 5.0%; Found: C 52.9%, H 5.5%, N 4.9%.

[(dppb){Au(S_2C•IMes)}$_2$](PF_6)$_2$ (74)

A dichloromethane solution (10 mL) of [(dppb)($AuCl$)$_2$] (25 mg, 0.028 mmol) was treated with a solution of IMes•CS_2 (21 mg, 0.055 mmol) in dichloromethane (5 mL). On addition of NH_4PF_6 (14 mg, 0.086 mmol) in methanol (5 mL), a green colouration appeared. The reaction was stirred for 40 mins and then all solvent removed. The crude product was dissolved in dichloromethane (10 mL) and filtered through Celite to remove NH_4Cl and excess NH_4PF_6. Diethyl ether (20 mL) was added and the solid triturated ultrasonically to give a green solid. This was filtered and washed with diethyl ether (10 mL) and dried. Yield: 46 mg (88 %). IR (nujol/KBr): 1607, 1556, 1308, 1231, 1157, 1104, 1068, 1005, 931, 839 $\nu_{(PF)}$ cm^{-1}. ^{31}P NMR ($CDCl_3$): 31.9 ppm (s, dppb). ^1H NMR ($CDCl_3$): 1.62, 2.37 (m x 2, 8H, CH_2); 2.24 (s, 24H, ortho-CH_3); 2.31 (s, 12H, para-CH_3); 7.02 (s, 8H, meta-C_6H_2); 7.39 (s, 4H, HC=CH); 7.41 - 7.56 (m, 20H, C_6H_5) ppm. MS (FAB +ve) *m/z* (abundance): 1727 (5) $[M + PF_6]^+$. Analysis: Calculated for $C_{72}H_{76}Au_2F_{12}N_4P_4S_4$ (M_w = 1871.5): C 46.2%, H 4.1%, N 3.0%; Found: C 46.2%, H 4.1%, N 3.1%

[(dppf){Au(S_2C•IMes)}$_2$](PF_6)$_2$ (75)

A dichloromethane solution (10 mL) of [(dppf)($AuCl$)$_2$] (50 mg, 0.049 mmol) was treated with a solution of IMes•CS_2 (37.4 mg, 0.098 mmol) in dichloromethane (10 mL). Addition of NH_4PF_6 (24 mg, 0.147 mmol) in methanol (5 mL) resulted in a green colouration. The reaction was stirred for 1 hour and then all solvent removed. The crude product was dissolved in dichloromethane (10 mL) and filtered through Celite to remove NH_4Cl and excess NH_4PF_6. The solvent was again removed and the crude solid triturated ultrasonically in diethyl ether (20 mL) to yield a green solid. This was filtered and washed with diethyl ether (10 mL) and dried. Yield: 88 mg (90 %). IR (nujol/KBr): 1612, 1563, 1484, 1438, 1380, 1313, 1231, 1173, 1103, 1066, 1032, 1007, 828 $\nu_{(PF)}$ cm^{-1}. ^{31}P NMR ($CDCl_3$): 29.9 ppm (s, dppf). ^1H NMR ($CDCl_3$): 2.26 (s, 24H, ortho-CH_3); 2.28 (s, 12H, para-CH_3); 4.23, 4.38 (s x 2, 2 x 4H, C_5H_4); 6.99 (s, 8H, meta-C_6H_2); 7.39 - 7.60 (m, 20H + 4H, C_6H_5 + HC=CH) ppm. MS (FAB +ve) *m/z* (abundance): 1854 (3) $[M + PF_6]^+$, 1328 (42) $[M - IMesCS_2]^+$. Analysis: Calculated for $C_{78}H_{76}Au_2F_{12}FeN_4P_4S_4$ (M_w = 1999.4): C 46.9%, H 3.8%, N 2.8%; Found: C 47.0% H 3.9%, N 2.8%.

[(dppm){Au_2(S_2C•IMes)}](PF_6)$_2$ (76)

A dichloromethane solution (10 mL) of [(dppm)($AuCl$)$_2$] (34 mg, 0.040 mmol) was treated with a solution of IMes•CS_2 (16 mg, 0.042 mmol) in dichloromethane (5 mL). Addition of NH_4PF_6 (15 mg, 0.092 mmol) in methanol (5 mL) resulted in a green colouration. The reaction was stirred for 40 mins and then all solvent removed. The crude product was dissolved in dichloromethane (10 mL) and filtered through Celite to remove NH_4Cl and excess NH_4PF_6. Ethanol (15 mL) was added and the solvent volume reduced to precipitate an olive green solid. This was filtered and washed with cold ethanol (10 mL), hexane (10 mL) and dried. A further crop could be obtained by removing all solvent

and triturating the solid in diethyl ether (20 mL). Yield: 49 mg (85 %). IR (nujol/KBr): 1606, 1555, 1308, 1230, 1156, 1101, 1068, 1000, 931, 838 $\nu_{(PF)}$ cm^{-1}. ^{31}P NMR ($CDCl_3$): 28.4 ppm (s, dppm). ^{1}H NMR ($CDCl_3$): 2.28 (s(br), 12H, ortho-CH_3); 2.34 (s, 6H, para-CH_3); 3.72 (t, 2H, CH_2, J_{HP} = 12.3 Hz); 7.08 (s, 4H, meta-C_6H_2); 7.29-7.63 (m, 20H + 2H, C_6H_5 + HC=CH) ppm. MS (ES +ve) *m/z* (abundance): 1158 (28) $[M]^+$. Analysis: Calculated for $C_{47}H_{46}Au_2F_{12}N_2P_4S_2$ (M_w = 1448.8): C 39.0%, H 3.2%, N 1.9%; Found: C 38.9%, H 3.0%, N 1.8%.

$[Au_2(S_2C•IPr)_2](PF_6)_2$ (77)

[AuCl(tht)] (17.5 mg, 0.055 mmol) and IPr•CS_2 (13 mg, 0.057 mmol) were dissolved in dichloromethane (15 mL) and a methanolic solution (10 mL) of NH_4PF_6 (18 mg, 0.110 mmol) was added. The reaction was stirred for 1 hr and then all solvent removed. The crude product was dissolved in dichloromethane (10 mL) and filtered through Celite to remove NH_4Cl and excess NH_4PF_6. Ethanol (20 mL) was added and the solvent volume reduced until precipitation of the red-brown product was complete. This was filtered and washed with ethanol (10 mL), hexane (10 mL) and dried. Yield: 37 mg (59 %). IR (nujol/KBr): 1566, 1317, 1260, 1210, 1180, 1138, 1060, 841 $\nu_{(PF)}$ cm^{-1}. ^{1}H NMR ($CDCl_3$): 1.59 (d, CH_3, 24H, J_{HH} = 6.8 Hz); 4.96 (sept., 4H, $CHMe_2$, J_{HH} = 6.8 Hz); 7.45 (s, 4H, HC=CH) ppm. MS (FAB +ve) *m/z* (abundance): 850 (52) $[M]^+$, 653 (78) $[M - Au]^+$. Analysis: Calculated for $C_{20}H_{32}Au_2F_{12}N_4P_2S_4$ (M_w = 1140.6): C 21.1%, H 2.8%, N 4.9%; Found: C 21.2%, H 2.9%, N 4.7%.

$[Au_2(S_2C•IMes)_2](PF_6)_2$ (78)

A dichloromethane solution (10 mL) of [AuCl(tht)] (32 mg, 0.100 mmol) was treated with a solution of IMes•CS_2 (38 mg, 0.100 mmol) in dichloromethane (5 mL) and NH_4PF_6 (35 mg, 0.215 mmol) in methanol (5 mL). The reaction was stirred for 1 hr and then all solvent removed. The crude product was dissolved in dichloromethane (10 mL) and filtered through Celite to remove NH_4Cl and excess NH_4PF_6. Diethyl ether (15 mL) was added and the solid triturated ultrasonically to give a dark brown solid. This was filtered and washed with diethyl ether (10 mL) and dried. Yield: 68 mg (47 %). IR (nujol/KBr): 1606, 1554, 1307, 1231, 1170, 1117, 1070, 931, 837 $\nu_{(PF)}$ cm^{-1}. ^{1}H NMR ($CDCl_3$): 2.16 (s, 24H, ortho-CH_3); 2.36 (s, 12H, para-CH_3); 7.05 (s, 8H, meta-C_6H_2); 7.53 (s, 4H, HC=CH) ppm. MS (FAB +ve) *m/z* (abundance): 1155 (21) $[M]^+$. Analyis: Calculated for $C_{44}H_{48}Au_2F_{12}N_4P_2S_4$ (M_w = 1445.0): C 36.6%, H 3.4%, N 3.9%; Found: C 36.7%, H 3.5%, N 4.0%.

$[Au_2(S_2C•IDip)_2](PF_6)_2$ (79)

[AuCl(tht)] (9.6 mg, 0.030 mmol) and IDip•CS_2 (14 mg, 0.030 mmol) were dissolved in dichloromethane (15 mL) and a methanolic solution (10 mL) of NH_4PF_6 (21 mg, 0.129 mmol) was added. The reaction was stirred for 1 hr and then all solvent removed. The crude product was

dissolved in dichloromethane (10 mL) and filtered through Celite to remove NH_4Cl and excess NH_4PF_6. Ethanol (20 mL) was added and the solvent volume reduced until precipitation of the orange-red product was complete. This was filtered and washed with ethanol (10 mL), hexane (10 mL) and dried. Yield: 26 mg (54 %). IR (nujol/KBr): 1555, 1212, 1154, 1072, 844 $\nu_{(PF)}$ cm^{-1}. ^1H NMR ($CDCl_3$): 1.19, 1.29 (d x 2, 48H, CH_3, J_{HH} = 6.7 Hz); 2.52 (s(br), 8H, $CHMe_2$); 7.35 (d, 8H, meta-C_6H_3, J_{HH} = 8.0 Hz); 7.46 (s(br), 4H, HC=CH); 7.59 (t, 4H, para-C_6H_3, J_{HH} = 8.0 Hz) ppm. MS (FAB +ve) *m/z* (abundance): 1322 (27) $[M]^+$, 1125 (100) $[M - Au]^+$. Analysis: Calculated for $C_{56}H_{72}Au_2F_{12}N_4P_2S_4$ (M_w = 1613.3): C 41.7%, H 4.5%, N 3.5%; Found: C 42.0%, H 4.6%, N 3.7%.

Experimental for functionalised gold nanoparticles

Au@(S_2C•IMes)^{Citrate} (NP5)

An aqueous solution (30 mL) of $HAuCl_4$ (10.8 mg, 0.032 mmol) was heated to reflux and sodium citrate (38 mg, 0.129 mmol) in water (5 mL) was added, causing a darkening of the colour. The reaction was stirred at reflux for 10 minutes and then for a further 15 mins at room temperature. A dichloromethane-methanol (5:10 mL) solution of IMes•CS_2 (30 mg, 0.079 mmol) was added dropwise and the reaction stirred for a further 2 hours. The resulting suspension was left to stand and the supernatant decanted and the solid washed with water (30 mL) to remove excess sodium citrate and cold dichloromethane (20 mL) to remove excess ligand. The dichloromethane washings yielded 16 mg of IMes•CS_2 indicating that only 14 mg (0.037 mmol) had been required in the surface functionalization of the nanoparticles (1:1 Au:ligand ratio). The black solid was dried under vacuum. IR: 1607, 1563, 1486 $\nu_{(NCN)}$, 1459, 1378, 1222, 1165, 1104, 1049 $\nu_{(SCS)}$, 931, 865 cm^{-1}. ^1H NMR (d^6-acetone): 2.30 (s, 6H, para-CH_3); 2.38 (s, 12H, ortho-CH_3); 7.04 (s, 4H, meta-C_6H_2); 7.60 (s, 2H, HC=CH) ppm.

Au@(S_2C•IMes)^{Brust} (NP6)

An aqueous solution (10 mL) of $HAuCl_4$ (17 mg, 0.050 mmol) and tetraoctylammonium bromide (109.4 mg, 0.200 mmol) in chloroform (15 mL) were stirred rapidly together for 15 mins until phase transfer had been completed. The lower organic layer was cooled to 4 °C and treated with IMes•CS_2 (28.5 mg, 0.075 mmol) as a dichloromethane solution (5 mL). The reaction was stirred for 10 mins and then sodium borohydride (38 mg, 1.005 mmol) was added rapidly leading do a darkening of solution. After 2 hours stirring below 10 °C, the organic layer was separated and washed with water (3 x 10 mL). The volume was concentrated to ca. 5 mL and ethanol (20 mL) added to precipitate the crude black solid. Centrifugation allowed the solvent to be decanted, leaving a black product, which was dried under vacuum. Excess ligand was removed by dissolving the material in warm acetonitrile

and cooling the solution overnight at -20 °C and removing the crystalline material. IR: 1604, 1562, 1486 $\nu_{(NCN)}$, 1459, 1447, 1378, 1223, 1166, 1105, 1051 $\nu_{(SCS)}$, 930, 868 cm^{-1}. ^{1}H NMR (d^{6}-acetone): 2.31 (s, 6H, para-CH_3); 2.38 (s, 12H, ortho-CH_3); 7.03 (s, 4H, meta-C_6H_2); 7.59 (s, 2H, HC=CH) ppm.

9.4. Experimental details for Chapter 6: Dialkyldithiophosphate complexes

Experimental for dialkyldithiophosphate complexes

[Ru(CH=CHC$_6$H$_4$Me-4){κ^2-S$_2$P(OEt)$_2$}(CO)(PPh$_3$)$_2$] (80)

a) [Ru(CH=CHC$_6$H$_4$Me-4)Cl(CO)(BTD)(PPh$_3$)$_2$] (200 mg, 0.212 mmol) and (NH$_4$)[S$_2$P(OEt)$_2$] (47 mg, 0.233 mmol) were dissolved in dichloromethane (20 mL) and ethanol (10 mL). The reaction mixture was stirred for 1 hour. Rotary evaporation to a solvent volume of approximately 10 mL led to precipitation of the yellow product. This was washed with ethanol (10 mL) and petroleum ether (10 mL) and dried. Yield: 147 mg (72 %). b) [RuH{κ^2-S$_2$P(OEt)$_2$}(CO)(PPh$_3$)$_2$] (40 mg, 0.049 mmol) and HC≡C$_6$H$_4$Me-4 (11.3 mg, 0.097 mmol) were dissolved in dichloromethane (10 mL). The reaction mixture was stirred for 1 hour. Rotary evaporation of solvent led to precipitation of the yellow product, which was washed and dried as above. Yield: 33 mg (70 %). IR: 1916 ν($_{CO}$), 1514, 1186, 1015, 947, 789, 770, 671 cm^{-1}. ^{31}P NMR (CD$_2$Cl$_2$): 32.7 (s, PPh$_3$); 94.8 (s, S$_2$P) ppm. ^{1}H NMR (CD$_2$Cl$_2$): 0.89 (t, 6H, OCCH$_3$, J_{HH} = 7.1 Hz); 2.22 (s, 3H, tolyl-CH$_3$); 2.93, 3.18 (m x 2, 4H, OCH$_2$); 5.25 (d, 1H, Hβ, J_{HH} = 16.9 Hz); 6.17, 6.82 (AB, 4H, C$_6$H$_4$, J_{AB} = 8.0 Hz); 7.34 – 7.56 (m, 30H, C$_6$H$_5$); 7.48 (dt, 1H, Hα, J_{HH} = 16.9 Hz, J_{HP} = 4.1 Hz) ppm. ^{13}C NMR (CD$_2$Cl$_2$): 205.3 (t, CO, J_{PC} = 14.9 Hz), 147.4 (t, Cα, J_{PC} = 14.0 Hz), 138.7 (s, tolyl-C$_1$), 135.4 (t^v, o/m-PC$_6$H$_5$, J_{PC} = 5.0 Hz), 135.1 (s(br), Cβ), 133.4 (t^v, ipso-PC$_6$H$_5$, J_{PC} = 20.6 Hz), 133.4 (s, tolyl-C$_4$), 129.7 (s, p-PC$_6$H$_5$), 126.6 (s, tolyl-C$_{2,6}$), 127.8 (t^v, o/m-PC$_6$H$_5$, J_{PC} = 4.3 Hz), 124.6 (s, tolyl-C$_{2,6}$), 61.7 (d, OCH$_2$, J_{PC} = 7.4 Hz), 20.9 (d, tolyl-CH$_3$), 15.7 (d, OCH$_2$, J_{PC} = 8.8 Hz) ppm. MS (ES +ve) *m/z* (abundance): 955 (3) [M]$^+$. Analysis: Calculated for C$_{50}$H$_{49}$O$_3$P$_3$RuS$_2$ (M$_w$ = 956.0): C 62.8%, H 5.2 %; Found: C 59.0%, H 4.5%.

[Ru(CH=CHBu^t){κ^2-S$_2$P(OEt)$_2$}(CO)(PPh$_3$)$_2$] (81)

[Ru(CH=CHBu^t)Cl(CO)(BTD)(PPh$_3$)$_2$] (100 mg, 0.110 mmol) and (NH$_4$)[S$_2$P(OEt)$_2$] (25 mg, 0.121 mmol) were dissolved in dichloromethane (20 mL) and ethanol (10 mL). The reaction mixture was stirred for 1 hour. Rotary evaporation of solvent led to precipitation of an orange solid, which was then dissolved in dichloromethane (5 mL). This was then passed through celite, and treated with ethanol (10 mL). Rotarty evaporation to a solvent volume of approximately 10 mL led to precipitation of the orange solid. This was then washed with ethanol (10 mL) and petroleum ether (10 mL) and dried. Yield: 55 mg (47 %). IR: 1940 ν($_{CO}$), 1480, 1433, 1094, 693 cm^{-1}. ^{31}P NMR (CD$_2$Cl$_2$): 31.4 (s, PPh$_3$, 2P), 95.5 (s, S$_2$P) ppm. ^{1}H NMR (CD$_2$Cl$_2$: 0.36 (s, 9H, Bu^t); 0.85 (t, 6H, OCCH$_3$, J_{HH} = 7.0 Hz); 3.01 (m, 4H, OCH$_2$); 4.61 (d, 1H, Hβ, J_{HH} = 16.1 Hz); 6.08 (dt, 1H, Hα, J_{HH} = 16.1 Hz, J_{HP} = 3.6 Hz);

7.32 – 7.69 (m, 30H, C_6H_5) ppm. MS (FAB +ve) *m/z* (abundance): 922 (1) $[M]^+$, 660 (7) $[M - PPh_3]^+$. Analysis: Calculated for $C_{47}H_{51}O_3P_3RuS_2$ (M_w = 922.0): C 61.2%, H 5.6 %; Found: C 61.2%, H 5.5%.

[RuH{κ^2-$S_2P(OEt)_2$}(CO)(PPh_3)$_2$] (**82**)

[RuHCl(CO)(BTD)(PPh_3)$_2$] (150 mg, 0.182 mmol) and (NH_4)[$S_2P(OEt)_2$] (40.6 mg, 0.200 mmol) were dissolved in dichloromethane (20 mL) and ethanol (10 mL). The reaction mixture was stirred for 60 min. Rotary evaporation to a solvent volume of approximately 10 mL led to precipitation of the green product. This was washed with ethanol (10 mL) and petroleum ether (10 mL) and dried. Yield: 106 mg (70 %). IR: 1948 ν($_{Ru-H}$), 1922 ν($_{CO}$), 1389, 1185, 1035, 1015, 945, 649 cm^{-1}. ^{31}P NMR (CD_2Cl_2): 41.8 (s, PPh_3), 94.5 (s, S_2P) ppm. ^{1}H NMR (CD_2Cl_2): – 11.87 (t, 1H, RuH, J_{HP} = 24.0 Hz), 0.87 (t, 6H, $OCCH_3$, J_{HH} = 8.0 Hz); 3.00 – 3.15 (m, 4H, OCH_2); 7.40 – 7.73 (m, 30H, C_6H_5) ppm. MS (FAB +ve) *m/z* (abundance): 839 (5) $[M]^+$. Analysis: Calculated for $C_{41}H_{41}O_3P_3RuS_2$ (M_w = 839.9): C 58.6%, H 4.9 %; Found: C 58.7%, H 4.8%.

[Ru{CH=CH(*n*-C_4H_9){{κ^2-$S_2P(OEt)_2$}(CO)(PPh_3)$_2$] (**83**)

[RuH{κ^2-$S_2P(OEt)_2$}(CO)(PPh_3)$_2$] (**82**) (50 mg, 0.060 mmol) and 1-hexyne (10 mg, 0.122 mmol) were dissolved in dichloromethane (20 mL). The reaction mixture was stirred for 40 min, revealing a colour change from green to yellow. Rotary evaporation of all solvent, and further recrystallisation with dichloromethane (10 mL) and ethanol (10 mL) led to precipitation of the yellow product. This was washed with ethanol (10 mL) and petroleum ether (10 mL) and dried. Yield: 38 mg (69 %). IR: 1914 ν($_{CO}$), 1572, 1387, 1185, 1017, 942, 770, 670 cm^{-1}. ^{31}P NMR (CD_2Cl_2): 32.4 (s, PPh_3), 95.1 (s, S_2P) ppm. ^{1}H NMR (CD_2Cl_2): 0.73 – 1.60 (m, 9H, $(CH_2)_3CH_3$); 0.88 (t, 6H, $OCCH_3$, J_{HH} = 7.1 Hz); 2.96, 3.14 (m x 2, 4H, OCH_2); 4.37 (m, 1H, Hβ); 6.13 (dt, 1H, Hα, J_{HH} = 15.9 Hz, J_{HP} unresolved); 7.27 – 7.68 (m, 30H, PC_6H_5) ppm. MS (FAB +ve) *m/z* (abundance): 938 (1) $[M]^+$, 660 (100) $[M - PPh_3]^+$. Analysis: Calculated for $C_{47}H_{51}O_3P_3RuS_2$ (M_w = 922.0): C 61.2%, H 5.6 %; Found: C 61.1%, H 5.5%.

[Ru{CH=CHCH_2OSi(Bu^t)Me_2}{κ^2-$S_2P(OEt)_2$}(CO)(PPh_3)$_2$] (**84**)

[RuH{κ^2-$S_2P(OEt)_2$}(CO)(PPh_3)$_2$] (**82**) (50 mg, 0.060 mmol) and HC≡CCH_2OSi(Bu^t)Me_2 (15 mg, 0.088 mmol) were dissolved in dichloromethane (20 mL). The reaction mixture was stirred for 20 min, revealing a colour change from green to yellow. Rotary evaporation of all solvent, and further recrystallisation with dichloromethane (10 mL) and methanol (10 mL) led to precipitation of the yellow product. This was washed with methanol (10 mL) and petroleum ether (10 mL) and dried. Yield: 33 mg (55 %). IR: 1913 ν($_{CO}$), 1572, 1388, 1249, 1187, 1019, 945, 835, 773, 666 cm^{-1}. ^{31}P NMR (CD_2Cl_2): 32.4 (s, PPh_3), 95.1 (s, S_2P) ppm. ^{1}H NMR (CD_2Cl_2): 0.09 (s, 6H, SiMe); 0.86 (s, 9H, SiBu^t); 0.88 (t, 6H, $OCCH_3$, J_{HH} = 7.1 Hz); 2.96, 3.14 (m x 2, 4H, OCH_2); 3.44 (d, 2H, OCH_2, J_{HH} =

5.2 Hz); 4.53 (m, 1H, Hβ); 6.51 (d, 1H, Hα, J_{HH} = 15.8 Hz); 7.34 – 7.62 (m x 2, 30H, PC_6H_5) ppm. MS (FAB +ve) *m/z* (abundance): 1009 (1) $[M]^+$, 748 (89) $[M - PPh_3]^+$. Analysis: Calculated for $C_{50}H_{59}O_4P_3RuS_2Si$ (M_w = 1010.2): C 59.5%, H 5.9 %; Found: C 60.5%, H 6.0%.

[Ru(CH=CHCO$_2$Me){κ^2-S$_2$P(OEt)$_2$}(CO)(PPh$_3$)$_2$] (**85**)

[RuH{κ^2-$S_2P(OEt)_2$}(CO)(PPh_3)$_2$] (**82**) (50 mg, 0.060 mmol) and HC≡CCO_2Me (8 mg, 0.095 mmol) were dissolved in dichloromethane (20 mL). The reaction mixture was stirred for 40 min. Rotary evaporation of all solvent, and further recrystallisation with dichloromethane (10 mL) and methanol (10 mL) led to precipitation of the olive green product. This was washed with methanol (10 mL) and petroleum ether (10 mL) and dried. Yield: 36 mg (65 %). IR: 1923 ν($_{CO}$), 1674 ν($_{C-O}$), 1535, 1389, 1247, 1015, 946, 786, 771, 743 cm^{-1}. ^{31}P NMR (CD_2Cl_2): 31.3 (s, PPh_3), 94.5 (s, S_2P) ppm. ^{1}H NMR (CD_2Cl_2): 0.88 (t, 6H, $OCCH_3$, J_{HH} = 7.0 Hz); 2.93, 3.12 (m x 2, 4H, OCH_2); 3.35 (s, 3H, Me); 5.03 (d, 1H, Hβ, J_{HH} = 16.6 Hz); 7.32 – 7.60 (m, 30H, PC_6H_5); 9.16 (dt, 1H, Hα, J_{HH} = 16.6 Hz, J_{HP} = 3.2 Hz) ppm. MS (FAB +ve) *m/z* (abundance): 924 (2) $[M]^+$, 739 (4) $[M - S_2P(OEt)_2]^+$, 634 (100) $[M - CO - PPh_3]^+$. Analysis: Calculated for $C_{45}H_{45}O_5P_3RuS_2$ (M_w = 924.1): C 58.5%, H 4.9 %; Found: C 58.6%, H 5.0%.

[Ru(CH=CHFc){κ^2-S$_2$P(OEt)$_2$}(CO)(PPh$_3$)$_2$] (**86**)

[RuH{κ^2-$S_2P(OEt)_2$}(CO)(PPh_3)$_2$] (**82**) (50 mg, 0.060 mmol) and HC≡CFc (19 mg, 0.091 mmol) were dissolved in dichloromethane (20 mL). The reaction mixture was stirred for 40 min, revealing a colour change from green to dark yellow. Rotary evaporation of all solvent, and further recrystallisation with dichloromethane (10 mL) and methanol (10 mL) led to precipitation of the yellow product. This was washed with methanol (10 mL) and petroleum ether (10 mL) and dried. Yield: 25 mg (40 %). IR: 1917 ν($_{CO}$), 1560, 1387, 1187, 1016, 945, 781, 663 cm^{-1}. ^{31}P NMR (CD_2Cl_2): 32.1 (s, PPh_3), 94.7 (s, S_2P) ppm. ^{1}H NMR (CD_2Cl_2): 0.91 (t, 6H, $OCCH_3$, J_{HH} = 7.1 Hz); 2.95, 3.18 (m x 2, 4H, OCH_2); 3.39, 3.84 (t^v x 2, 2 x 2H, C_5H_4, J_{HH} = 1.7 Hz); 3.88 (s, 5H, C_5H_5); 5.06 (d, 1H, Hβ, J_{HH} = 16.4 Hz); 6.93 (dt, 1H, Hα, J_{HH} = 16.4 Hz, J_{HP} = 3.8 Hz); 7.39 – 7.62 (m, 30H, PC_6H_5) ppm. MS (FAB +ve) *m/z* (abundance): 839 (7) $[M - CO - S_2P(OEt)_2]^+$, 788 (8) $[M - PPh_3]^+$. Analysis: Calculated for $C_{53}H_{51}FeO_3P_3RuS_2$ (M_w = 1050.0): C 60.6%, H 4.9 %; Found: C 60.5%, H 4.8%.

[Ru(CH=CHCPh$_2$OH){κ^2-S$_2$P(OEt)$_2$}(CO)(PPh$_3$)$_2$] (**87**)

[RuH{κ^2-$S_2P(OEt)_2$}(CO)(PPh_3)$_2$] (**82**) (100 mg, 0.119 mmol) and HC≡CCPh_2OH (25 mg, 0.119 mmol) were dissolved in dichloromethane (20 mL). The reaction mixture was stirred for 90 min, revealing a colour change from green to yellow. Rotary evaporation of all solvent, and further recrystallisation with dichloromethane (10 mL) and ethanol (10 mL) led to precipitation of the yellow product. This was washed with ethanol (10 mL) and petroleum ether (10 mL) and dried. Yield: 95 mg

(78 %). IR: 1929 $\nu_{(CO)}$, 1158, 1088, 941, 778 cm^{-1}. ^{31}P NMR (CD_2Cl_2): 30.8 (s, PPh_3), 95.0 (s, S_2P) ppm. ^{1}H NMR (CD_2Cl_2): 0.87 (t, 6H, $OCCH_3$, J_{HH} = 7.1 Hz); 0.92 (s, 1H, CPh_2OH); 2.86, 3.14 (m x 2, 4H, OCH_2); 5.40 (d, 1H, Hβ, J_{HH} = 16.4 Hz); 6.81 – 7.11 (m, 10H, CC_6H_5); 7.32 – 7.48 (m, 30H, PC_6H_5); 6.87 (dt, 1H, Hα, partially obscured) ppm. MS (FAB +ve) *m/z* (abundance): 1047 (1) $[M]^+$, 786 (23) $[M - PPh_3]^+$. Analysis: Calculated for $C_{56}H_{53}O_4P_3RuS_2$ (M_w = 1048.1): C 64.2%, H 5.1 %; Found: C 64.1%, H 5.0%.

[Ru{CH=CH(HO)C_6H_{10}}{κ^2-$S_2P(OEt)_2$}(CO)(PPh_3)$_2$] (**88**)

[RuH{κ^2-$S_2P(OEt)_2$}(CO)(PPh_3)$_2$] (**82**) (100 mg, 0.119 mmol) and HC≡C(HO)C_6H_{10} (32 mg, 0.235 mmol) were dissolved in dichloromethane (20 mL) and stirred for 15 min. Rotary evaporation of all solvent, and trituration in petroleum ether (10 mL) led to precipitation of the yellow product. This was washed with petroleum ether (10 mL) and dried. Yield: 71 mg (62 %). IR: 3571 ν(O-H), 1925 $\nu_{(CO)}$, 1571, 1313, 1020, 944, 659 cm^{-1}. ^{31}P NMR (CD_2Cl_2): 31.6 (s, PPh_3), 95.3 (s, S_2P) ppm. ^{1}H NMR (CD_2Cl_2): 0.78 – 1.34 (m, 10H, Cy); 0.87 (t, 6H, $OCCH_3$, J_{HH} = 7.0 Hz); 1.61 (s, 1H, OH); 2.90 – 3.12 (m x 2, 4H, OCH_2); 4.79 (d, 1H, Hβ, J_{HH} = 16.4 Hz); 6.58 (d, 1H, Hα, J_{HH} = 16.4 Hz); 7.38 – 7.58 (m, 30H, PC_6H_5) ppm. MS (FAB +ve) *m/z* (abundance): 702 (12) $[M - PPh_3]^+$, 685 (15) $[M - OH - PPh_3]^+$, 656 (15) $[M - CO - OH - PPh_3]^+$. Analysis: Calculated for $C_{49}H_{53}O_4P_3RuS_2$ (M_w = 964.1): C 61.1%, H 5.5 %; Found: C 61.2%, H 5.6%.

[Ru(C≡CC_6H_4Me-4){κ^2-$S_2P(OEt)_2$}(CO)(PPh_3)$_2$] (**89**)

a) [RuH{κ^2-$S_2P(OEt)_2$}(CO)(PPh_3)$_2$] (**82**) (40 mg, 0.049 mmol) and HC≡CC_6H_4Me-4 (11.3 mg, 0.097 mmol) were dissolved in dichloromethane (10 mL). The reaction mixture was stirred for 3 hours. Rotary evaporation of solvent led to precipitation of the yellow product. This was recrystalised in dichloromethane (10 mL) and methanol (10 mL) and then washed with methanol (10 mL) and petroleum ether (10 mL) before drying. Yield: 5 mg (11 %). **b)** [Ru(CH=CHC_6H_4Me-4){κ^2-$S_2P(OEt)_2$}(CO)(PPh_3)$_2$] (**85**) (50 mg, 0.052 mmol) and HC≡CC_6H_4Me-4 (12 mg, 0.103 mmol) were dissolved in dichloromethane (10 mL) and methanol (5 mL). The reaction mixture was stirred for 40 min. Rotary evaporation to a solvent volume of approximately 5 mL led to precipitation of the yellow product. This was washed with methanol (10 mL) and petroleum ether (10 mL) and dried. Yield: 47 mg (95 %). IR: 2105 $\nu_{(C\equiv C)}$, 1936 $\nu_{(CO)}$, 1502, 1018, 947, 816, 786, 765, 675 cm^{-1}. ^{31}P NMR (CD_2Cl_2): 30.5 (s, PPh_3), 94.7 (s, S_2P) ppm. ^{1}H NMR (CD_2Cl_2): 0.93 (t, 6H, $OCCH_3$, J_{HH} = 7.1 Hz); 2.23 (s, 3H, tolyl-CH_3); 3.01 – 3.18 (m, 4H, OCH_2); 6.44, 6.83 (AB, 4H, C_6H_4, J_{AB} = 7.8 Hz); 7.36 – 7.87 (m, 30H, C_6H_5) ppm. ^{13}C: 204.4 (t, CO, J_{PC} = 15.6 Hz), 135.7 (t^v, o/m-PC_6H_5, J_{PC} = 5.0 Hz), 134.2 (s, tolyl-C_4), 133.6 (t^v, ipso-PC_6H_5, J_{PC} = 4.4 Hz), 130.4 (s, tolyl-$C_{2,6}$), 129.8 (s, p-PC_6H_5), 128.5 (s, tolyl-$C_{2,6}$), 127.7 (t^v, o/m-PC_6H_5, J_{PC} = X Hz), 126.4 (s, tolyl-C_1), 115.8 (s, Cβ), 108.1 (t, Cα, J_{PC} = 21.0 Hz), 62.0 (d, OCH_2, J_{PC} = 7.5 Hz), 21.2 (d, tolyl-CH_3), 15.7 (d, OCH_2, J_{PC} = 8.4 Hz) ppm. MS

(FAB +ve) *m/z* (abundance): 954 (2) $[M]^+$, 926 (12) $[M - CO]^+$, 692 (58) $[M - PPh_3]^+$. Analysis: Calculated for $C_{51}H_{47}O_3P_3RuS_2$ (M_w = 966.0): C 63.4%, H 4.9 %; Found: C 63.1%, H 4.9 %.

[Ru(C≡CBu^t){κ^2-S$_2$P(OEt)$_2$}(CO)(PPh$_3$)$_2$] (**90**)

[Ru(CH=CHC$_6$H$_4$Me-4){κ^2-S$_2$P(OEt)$_2$}(CO)(PPh$_3$)$_2$] (**85**) (50 mg, 0.052 mmol) and HC≡CBu^t (13 mg, 0.158 mmol) were dissolved in tetrahydrofuran (20 mL) and heated at reflux for 2 hours. After cooling to room temperature, all solvent was removed from mixture by rotary evaporation, and the solid dissolved in dichloromethane (10 mL). Ethanol (10 mL) was added and subsequent rotary evaporation led to precipitation of the yellow product. This was washed with ethanol (10 mL) and petroleum ether (10 mL) and dried. Yield: 32 mg (67 %). IR: 2113 ν(C≡C), 1943 ν(CO), 1249, 1013, 949, 791, 660 cm^{-1}. ^{31}P NMR (CD_2Cl_2): 30.4 (s, PPh_3), 94.9 (s, S_2P) ppm. ^{1}H NMR (CD_2Cl_2): 0.76 (s, 9H, Bu^t); 0.93 (t, 6H, $OCCH_3$, J_{HH} = 7.1 Hz); 3.06 – 3.15 (m, 4H, OCH_2); 7.36 – 7.90 (m, 30H, C_6H_5) ppm. MS (ES +ve) m/z (abundance): 839 (6) $[M - \text{acetylide}]^+$. Analysis: Calculated for $C_{47}H_{49}O_3P_3RuS_2$ (M_w = 920.0): C 61.4%, H 5.4 %; Found: C 61.1%, H 5.3%.

[RuCl{κ^2-S$_2$P(OEt)$_2$}(CO)(PPh$_3$)$_2$] (**91**)

a) The reaction between [Ru(CH=CHC$_6$H$_4$Me-4){κ^2-S$_2$P(OEt)$_2$}(CO)(PPh$_3$)$_2$] (**85**) (50 mg, 0.052 mmol) and HC≡CBu^t (20 mg, 0.243 mmol) in 1,2-dichloroethane (20 mL) formed a white sideproduct in low yield. Spectroscopic analysis helped clarify its formulation as [RuCl{κ^2-S$_2$P(OEt)$_2$}(CO)(PPh$_3$)$_2$]. **b)** [RuH{κ^2-S$_2$P(OEt)$_2$}(CO)(PPh$_3$)$_2$] (**85**) (50 mg, 0.060 mmol) and *N*-chlorosuccinimide (16 mg, 0.119 mmol) were dissolved in dichloromethane (10 mL) and methanol (5 mL). The reaction mixture was stirred for 40 min. Removal of the solvent and trituration in diethylether (5 mL) led to isolation of a colourless product. Yield: 46 mg (88 %). IR: 1965 ν(CO), 1089, 1011, 951, 774, 745, 649 cm^{-1}. ^{31}P NMR (CD_2Cl_2): 36.8 (s, PPh_3), 103.6 (s, S_2P) ppm. ^{1}H NMR (CD_2Cl_2): 1.31 (t, 6H, $OCCH_3$, J_{HH} = 7.2 Hz); 4.11, 4.29 (m x 2, 4H, OCH_2); 7.24 – 7.54 (m, 30H, C_6H_5) ppm. MS (FAB +ve) *m/z* (abundance): 874 (2) $[M]^+$, 839 (63) $[M - Cl]^+$. Analysis: Calculated for $C_{41}H_{40}ClO_3P_3RuS_2$ (M_w = 874.3): C 56.3%, H 4.6 %; Found: C 56.0%, H 4.3%.

[Ru(η^3-PhC≡C-C=CHPh){κ^2-S$_2$P(OEt)$_2$}(CO)(PPh$_3$)]$_2$ (**92**)

[Ru(C(C≡CPh)=CHPh)Cl(CO)(PPh$_3$)$_2$] (100 mg, 0.112 mmol) and (NH$_4$)[S$_2$P(OEt)$_2$] (25 mg, 0.123 mmol) were dissolved in dichloromethane (20 mL) and ethanol (10 mL). The reaction mixture was stirred for 1 hour, showing a colour change from orange to yellow. Rotary evaporation to a solvent volume of approximately 10 mL led to precipitation of the bright yellow product. This was washed with ethanol (10 mL) and petroleum ether (10 mL) and dried. Yield: 26 mg (23 %). IR: 1921 ν(CO), 1191, 1019, 950, 862, 664 cm^{-1}. ^{31}P NMR (CD_2Cl_2): 52.5 (s, PPh_3), 100.5 (s, S_2P) ppm. ^{1}H NMR (CD_2Cl_2): 1.31 (t, 6H, $OCCH_3$, J_{HH} = 7.1 Hz); 4.04 – 4.12 (m, 4H, OCH_2); 6.39 (s, 1H, Hβ); 7.13 –

7.72 (m, 50H, C_6H_5) ppm. MS (ES +ve) *m/z* (abundance): 780 (12) $[Ru(C(C{\equiv}CPh){=}CHPh)\{S_2P(OEt)_2\}(CO)(PPh_3)]^+$. Analysis: Calculated for $C_{39}H_{36}O_3P_2RuS_2$ (M_w = 779.9): C 60.1%, H 4.7 %; Found: C 59.8%, H 4.4%.

$[Ru(CPh{=}CHPh)\{\mu,\kappa^1,\kappa^2\text{-}S_2P(OEt)_2\}(CO)(PPh_3)]_2$ (93)

$[Ru(CPh{=}CHPh)Cl(CO)(PPh_3)_2]$ (100 mg, 0.115 mmol) and $(NH_4)[S_2P(OEt)_2]$ (26 mg, 0.127 mmol) were dissolved in dichloromethane (10 mL) and methanol (15 mL). The reaction mixture was stirred for 1 hour. Rotary evaporation to a solvent volume of approximately 10 mL led to precipitation of the pale brown product. This was washed with methanol (10 mL) and petroleum ether (10 mL) and dried. Yield: 46 mg (53 %). IR: 1965 $\nu_{(CO)}$, 1163, 1089, 1011, 950, 796, 745, 651 cm^{-1}. ^{31}P NMR (CD_2Cl_2): 36.9 (s, PPh_3), 103.6 (s, S_2P) ppm. ^1H NMR (CD_2Cl_2): 1.33 (t, 6H, $OCCH_3$, J_{HH} = 7.1 Hz); 4.11, 4.29 (m x 2, 4H, OCH_2); 6.71 (s, 1H, Hβ); 7.24 – 7.55 (m, 25H, C_6H_5) ppm. MS (FAB +ve) *m/z* (abundance): not diagnostic. Analysis: Calculated for $C_{74}H_{72}O_6P_4Ru_2S_4$ (M_w = 1511.7): C 58.8%, H 4.8 %; Found: C 58.6%, H 4.7%.

$[Ru(CPh{=}CHPh)\{\mu,\kappa^1,\kappa^2\text{-}S_2P(OEt)_2\}(CS)(PPh_3)]_2$ (94)

$[Ru(CPh{=}CHPh)Cl(CS)(PPh_3)_2]$ (55 mg, 0.062 mmol) and $(NH_4)[S_2P(OEt)_2]$ (14 mg, 0.068 mmol) were dissolved in dichloromethane (10 mL) and methanol (15 mL). The reaction mixture was stirred for 20 min. Rotary evaporation to a solvent volume of approximately 10 mL led to precipitation of the orange product. This was washed with methanol (10 mL) and petroleum ether (10 mL) and dried. Yield: 37 mg (77 %). IR: 1594, 1280 $\nu_{(CS)}$, 1386, 1280, 1187, 1014, 945, 840, 779, 706, 645 cm^{-1}. ^{31}P NMR (CD_2Cl_2): 45.6 (s, PPh_3), 99.4 (s, S_2P) ppm. ^1H NMR (CD_2Cl_2): 1.46 (t, 6H, $OCCH_3$, J_{HH} = 6.8 Hz); 4.26 – 4.33 (m x 2, 4H, OCH_2); 6.81 (s, 1H, CPh=CHPh); 6.87 – 7.47 (m, 25H, C_6H_5) ppm. MS (ES +ve) *m/z* (abundance): 772 (14) $[Ru(CPh{=}CHPh)\{S_2P(OEt)_2\}(CS)(PPh_3)]^+$. Analysis: Calculated for $C_{74}H_{72}O_4P_4Ru_2S_6$ (M_w = 1543.8): C 57.6%, H 4.7 %; Found: C 57.8%, H 4.6%.

$[Ru(\eta^2\text{-}SCCPh{=}CHPh)\{\kappa^2\text{-}S_2P(OEt)_2\}(CO)(PPh_3)]$ (95)

Carbon monoxide gas was bubbled through a yellow solution of $[Ru(CPh{=}CHPh)\{\kappa^2\text{-}S_2P(OEt)_2\}(CS)(PPh_3)]$ (**94**) (40 mg, 0.052 mmol) in dichloromethane, resulting in a red colour change. All solvent was removed and the residue triturated in petroleum ether (10 mL) to yield a red solid. This was washed with petroleum ether (10 mL) and dried. Yield: 39 mg (94 %) . IR: 1910 $\nu_{(CO)}$, 1584, 1567, 1385, 1256 $\nu_{(C\text{-}S)}$, 1205, 1144, 1014, 956, 816, 791, 639 cm^{-1}. ^{31}P NMR (CD_2Cl_2): 49.7 (s, PPh_3) 102.7 (s, S_2P) ppm. ^1H NMR (CD_2Cl_2): 1.40 (t, 6H, $OCCH_3$, J_{HH} = 7.0 Hz); 4.13 – 4.31 (m, 4H, OCH_2); 6.77 – 7.67 (m, 25H, C_6H_5); 7.94 (s, 1H, CPh=CHPh) ppm. MS (FAB +ve) *m/z* (abundance): 801 (28) $[M]^+$, 772 (100) $[M - CO]^+$. Analysis: Calculated for $C_{38}H_{36}O_3P_2RuS_3$ (M_w = 800.0): C 57.1%, H 4.5 %; Found: C 57.2%, H 4.4%.

[Ru(CH=CHC$_6$H$_4$Me-4){κ^2-SOP(OEt)$_2$}(CO)(PPh$_3$)$_2$] (**96**)

[Ru(CH=CHC$_6$H$_4$Me-4)Cl(CO)(BTD)(PPh$_3$)$_2$] (100 mg, 0.106 mmol) and K[SOP(OEt)$_2$] (24 mg, 0.115 mmol) were dissolved in dichloromethane (20 mL) and ethanol (10 mL). The reaction mixture was stirred for 1 hour. Rotary evaporation to a solvent volume of approximately 10 mL led to precipitation of the yellow product. This was washed with ethanol (10 mL) and petroleum ether (10 mL) and dried. Yield: 86 mg (86 %). IR: 1927 ν($_{CO}$), 1029, 968, 949, 786, 649 cm^{-1}. ^{31}P NMR (CD$_2$Cl$_2$): 29.7 (s, PPh$_3$), 48.8 (s, S$_2$P) ppm. ^{1}H NMR (CD$_2$Cl$_2$): 0.75 (t, 6H, OCCH$_3$, J_{HH} = 7.1 Hz); 2.16 (s, 3H, tolyl-CH$_3$); 3.11 – 3.21 (m, 4H, OCH$_2$); 5.88 (d, 1H, Hβ, J_{HH} = 16.2 Hz); 6.31, 6.78 (AB, 4H, C$_6$H$_4$, J_{AB} = 7.9 Hz); 7.27 – 7.70 (m, 30H, C$_6$H$_5$) ppm. MS (ES +ve) *m/z* (abundance): 939 (1) [M]$^+$, 678 (100) [M – PPh$_3$]$^+$. Analysis: Calculated for C$_{50}$H$_{49}$O$_4$P$_3$RuS (M$_w$ = 940.0): C 63.9%, H 5.2 %; Found: C 64.1%, H 5.2%.

9.5. Experimental details for Chapter 7: Multimetallic complexes based on nitrogen-oxygen mixed-donor ligands

Experimental for bi- and trimetallic complexes

[Ru(CH=CHC$_6$H$_4$Me-4)(κ^2-O$_2$CC$_5$H$_4$N)(CO)(PPh$_3$)$_2$] (97)

A solution of [Ru(CH=CHC$_6$H$_4$Me-4)Cl(BTD)(CO)(PPh$_3$)$_2$] (200 mg, 0.212 mmol) in dichloromethane (40 mL) was treated with a methanolic solution (30 mL) of isonicotinic acid (29 mg, 0.234 mmol) and sodium methoxide (23 mg, 0.424 mmol). The reaction mixture was allowed to stir for 1 h at room temperature. The solvent volume was slowly reduced on a rotary evaporator resulting in the precipitation of an orange-yellow solid. This was filtered, washed with petroleum ether (10 mL) and dried under vacuum. Yield: 156 mg (82 %). IR (solid state): 1912 (ν_{CO}), 1515 (ν_{OCO}), 1480, 1185, 865, 745 cm^{-1}. ^{31}P NMR (CDCl$_3$): 38.1 (s, PPh$_3$) ppm. ^{1}H NMR (CDCl$_3$): 2.24 (s, 3H, CCH$_3$); 5.36 (d, 1H, Hβ, J_{HH} = 15.3 Hz); 6.33 (d, 2H, C*H*$_2$CH$_2$N, J_{HH} = 5.6 Hz); 6.83, 6.88 (AB, 4H, C$_6$H$_4$, J_{AB} = 7.9 Hz), 7.28 – 7.48 (m, 30H, C$_6$H$_5$), 7.76 (dt, 1H, Hα, J_{HH} = 15.3 J_{HP} = 2.6 Hz); 8.31 (d, 2H, CH$_2$C*H*$_2$N, J_{HH} = 5.6 Hz) ppm. MS (ES +ve) *m/z* (abundance) = 893 (9) [M]$^+$. Analysis: Calculated for C$_{52}$H$_{43}$NO$_3$P$_2$Ru (M$_w$ = 893.2): C 69.9%, H 4.9%, N 1.6%; Found: C 70.0%, H 4.8%, N 1.5%.

[Ru(C(C≡CPh)=CHPh)(κ^2-O$_2$CC$_5$H$_4$N)(CO)(PPh$_3$)$_2$] (98)

A solution of [Ru(C(C≡CPh)=CHPh)Cl(CO)(PPh$_3$)$_2$] (100 mg, 0.112 mmol) in dichloromethane (10 mL) was treated with a solution of isonicotinic acid (15 mg, 0.123 mmol) and sodium methoxide (7 mg, 0.123 mmol) in methanol (20 mL). The reaction mixture was stirred for 1 h at room temperature. The solvent volume was slowly reduced on a rotary evaporator resulting in the precipitation of a yellow solid. This was filtered, washed with petroleum ether (10 mL) and dried under vacuum. Yield: 71 mg (65 %). IR (solid state): 2159 ($\nu_{C\equiv C}$), 1914 (ν_{CO}), 1740, 1516 (ν_{OCO}), 1480, 1370, 1311, 1218, 1094, 867, 610 cm^{-1}. ^{31}P NMR (CDCl$_3$): 38.1 (s, PPh$_3$) ppm. ^{1}H NMR (CDCl$_3$): 5.72 (s(br), 1H, Hβ); 6.87 – 7.56 (m, 30H + 10H + 2H, PC$_6$H$_5$ + C$_6$H$_5$ + C*H*$_2$CH$_2$N); 8.31 (d, 2H, CH$_2$C*H*$_2$N, J_{HH} = 5.6 Hz) ppm. MS (ES +ve) *m/z* (abundance) = 980 (2) [M]$^+$; 857 (6) [M – O$_2$CC$_5$H$_4$N]$^+$. Analysis: Calculated for C$_{59}$H$_{44}$NO$_3$P$_2$Ru (M$_w$ = 979.2): C 72.3%, H 4.6%, N 1.4%; Found: C 72.4%, H 4.7%, N 1.4%.

[Os(CH=CHC$_6$H$_4$Me-4)(κ^2-O$_2$CC$_5$H$_4$N)(CO)(PPh$_3$)$_2$] (99)

A solution of [Os(CH=CHC$_6$H$_4$Me-4)Cl(BTD)(CO)(PPh$_3$)$_2$] (100 mg, 0.097 mmol) in dichloromethane (40 mL) was treated with a methanolic solution (20 mL) of isonicotinic acid (13 mg, 0.110 mmol) and sodium methoxide (10 mg, 0.194 mmol). The reaction mixture stirred for 3 h at

room temperature. All solvent was removed and the red product triturated ultrasonically in water (10mL). This was filtered, washed with hexane (10mL) and dried under vacuum. Yield: 86 mg (91 %). IR (solid state): 1900 (ν_{CO}), 1547 (ν_{OCO}), 1508, 1482, 1245, 1187, 1030, 874, 616 cm^{-1}. ^{31}P NMR (d_6-acetone): 19.1 (s, PPh_3) ppm. ^{1}H NMR (d_6-acetone): 2.16 (s, 3H, CCH_3); 5.81 (d, 1H, Hβ, J_{HH} = 15.7 Hz); 6.40, 6.76 (AB, 4H, C_6H_4, J_{AB} = 7.9 Hz); 6.89 (d, 2H, CH_2CH_2N, J_{HH} = 5.9 Hz); 7.39 – 7.54 (m, 30H, C_6H_5), 8.12 (dt, 1H, Hα, J_{HH} = 15.8 J_{HP} = 2.1 Hz); 8.37 (d, 2H, CH_2CH_2N, J_{HH} = 5.9 Hz) ppm. MS (ES +ve) *m/z* (abundance) = 984 (100) $[M]^+$; 862 (5) $[M - O_2CC_5H_4N]^+$. Analysis: Calculated for $C_{52}H_{43}NO_3OsP_2 \cdot CH_2Cl_2$ (M_w = 1067.2): C 59.7%, H 4.3%, N 1.3%; Found: C 59.3%, H 4.0%, N 1.0%.

[{Ru(C(C≡CPh)=CHPh)(CO)(PPh_3)$_2$(κ^2-$O_2CC_5H_4N$)}$_2$Ag]OTf (100)

A dichloromethane solution (40 mL) of Ru(C(C≡CPh)=CHPh)($O_2CC_5H_4N$)(CO)(PPh_3)$_2$] **(98)** (50 mg, 0.051 mmol) and silver triflate (7 mg, 0.026 mmol) was allowed to stir for 2 h at room temperature. All solvent was removed and the product triturated ultrasonically in petroleum ether (10mL). The dark yellow solid was filtered and dried under vacuum. Yield: 33 mg (58 %). IR (solid state): 2178 ($\nu_{C\equiv C}$), 1925 (ν_{CO}), 1523 (ν_{OCO}), 1483, 1289, 1230, 1157, 869, 635 cm^{-1}. ^{31}P NMR (d_6-acetone): 38.5 (s, PPh_3) ppm. ^{1}H NMR (d_6-acetone): 6.1 (s(br), 2H, Hβ); 6.95 – 7.62 (m, 60H + 10H + 10H + 4H, C_6H_5 + CH_2CH_2N); 8.44 (d, 4H, CH_2CH_2N, J_{HH} = 5.8 Hz) ppm. MS (FAB +ve) *m/z* (abundance) = 1234 (28) [M – Ru(PPh_3)$_2$CO($O_2CC_5H_4N$ + CF_3SO_3]$^+$; 1086 (37) [M – Ru(PPh_3)$_2$CO($O_2CC_5H_4N$)]$^+$. Analysis: Calculated for $C_{119}H_{90}AgF_3N_2O_9P_4Ru_2S \cdot 3CH_2Cl_2$ (M_w = 2469.8): C 59.3%, H 3.9%, N 1.1%; Found: C 59.3%, H 4.0%, N 0.9%.

[Ru(κ^2-$O_2CC_5H_4N$)(dppm)$_2$]PF_6 (101)

A solution of *cis*-[$RuCl_2$(dppm)$_2$] (331 mg, 0.352 mmol) in dichloromethane (50 mL) was treated with a solution of isonicotinic acid (48 mg, 0.387 mmol), sodium methoxide (38 mg, 0.708 mmol) and ammonium hexafluorophosphate (114 mg, 0.704 mmol) in methanol (25 mL). The reaction mixture was allowed to stir for 1 h at room temperature. All solvent was removed and the crude product dissolved in dichloromethane (10 mL) and filtered through diatomaceous earth (Celite) to remove NaCl, NaOMe and excess ligand. Ethanol (20 mL) was then added and the solvent volume was slowly reduced on a rotary evaporator resulting in the precipitation of yellow solid. This was filtered, washed with petroleum ether (10 mL) and dried under vacuum. Yield: 314 mg (79 %). IR (solid state): 1513 (ν_{OCO}), 1484, 1096, 833 (ν_{PF}), 734 cm^{-1}. ^{31}P NMR ($CDCl_3$): -11.8, 8.8 (t x 2, dppm, J_{pp} = 39.1 Hz) ppm. ^{1}H NMR ($CDCl_3$): 4.15, 4.80 (m x 2, 2 x 2H, PCH_2P); 6.25, 7.01, 7.29, 7.49, 7.60, 7.75 (m x 6, 40H, C_6H_5); 7.41 (d, 2H, CH_2CH_2N, J_{HH} = 5.9 Hz); 8.73 (d, 2H, CH_2CH_2N, J_{HH} = 5.6 Hz) ppm. ^{13}C NMR (CD_2Cl_2, 400 MHz): 180.3 (s, CO_2), 150.6 (s, $C_{2,6}$-benzoate), 139.5 (s, C_4-benzoate), 128.8 – 134.0 (m x 11, C_6H_5), 121.9 (s, $C_{3,5}$-benzoate), 43.4 (t, PCH_2P, J_{PC} = 13.1 Hz) ppm. MS (ES

+ve) *m/z* (abundance) = 992 (100) $[M]^+$. Analysis: Calculated for $C_{56}H_{48}F_6NO_2P_5Ru$ (M_w = 1137.1): C 59.1%, H 4.3%, N 1.2%; Found: C 59.2%, H 4.2%, N 1.2%.

$[\{Ru(dppm)_2(\kappa^2\text{-}O_2CC_5H_4N)\}_2Ag](PF_6)_2(OTf)$ (102)

A dichloromethane solution (40 mL) of $[Ru(dppm)_2(O_2CC_5H_4N)]PF_6$ (**101**) (50 mg, 0.044 mmol) and silver triflate (6 mg, 0.022 mmol) was allowed to stir for 2 h at room temperature. All solvent was removed and the product triturated ultrasonically in diethyl ether (10mL). The dark yellow crystalline solid was filtered and dried under vacuum. Yield: 42 mg (75 %). IR (solid state): 1511 (ν_{OCO}), 1484, 1158, 1096, 1028, 833 (ν_{PF}, 731, 636 cm^{-1}. ^{31}P NMR (d_6-acetone): -12.3, 9.3 (2 x 2, dppm, J_{pp} = 39.3 Hz) ppm. ^1H NMR (d_6-acetone): 4.29, 5.14 (m x 2, 2 x 4H, PCH_2P); 6.40, 7.09, 7.23, 7.33, 7.67, 7.57, 7.79, 8.00 (m x 8, 80H, C_6H_5); 7.71 (d, 4H, CH_2CH_2N, J_{HH} = 6.0 Hz); 8.87 (d, 4H, CH_2CH_2N, J_{HH} = 6.0 Hz) ppm. MS (FAB +ve) *m/z* (abundance) = 992 (100) $[Ru(dppm)_2(O_2CC_5H_4N)]^+$. Analysis: Calculated for $C_{113}H_{96}AgF_{15}N_2O_7P_{10}Ru_2S$ (M_w = 2530.1): C 53.7%, H 3.8%, N 1.1%; Found: C 53.7%, H 3.9%, N 1.1%.

$[\{Ru(dppm)_2(\kappa^2\text{-}O_2CC_5H_4N)\}_2PdCl_2](PF_6)_2$ (103)

A chloroform (10mL) and methanol (10 mL) solution of $[Ru(dppm)_2(O_2CC_5H_4N)]PF_6$ (**101**) (50 mg, 0.043 mmol) and $PdCl_2$ (4 mg, 0.022 mmol) was allowed to stir at reflux for 3 h. All solvent was removed and the grey/yellow solid was triturated with diethylether (10 mL) and filtered. Yield: 53 mg (98 %). IR (solid state): 1517 (ν_{OCO}), 1484, 1313, 833 (ν_{PF}, 773, 730, 713 cm^{-1}. ^{31}P NMR ($CDCl_3$): -11.6, 9.1 (t x 2, dppm, J_{pp} = 38.9 Hz) ppm. ^1H NMR ($CDCl_3$): 4.23, 4.77 (m x 2, 2 x 4H, PCH_2P); 6.27, 7.03, 7.38, 7.56, 7.74 (m x 5, 80H, C_6H_5); 7.36 (d, 4H, CH_2CH_2N, J_{HH} = 6.5 Hz); 8.94 (d, 4H, CH_2CH_2N, J_{HH} = 6.5 Hz) ppm. MS (FAB +ve) *m/z* (abundance) = 2306 (8) $[M]^+$, 992 (100) $[Ru(dppm)_2(O_2CC_5H_4N)]^+$. Analysis: Calculated for $C_{112}H_{96}Cl_2F_{12}N_2O_4P_{10}PdRu_2$ (M_w = 2450.1): C 54.9%, H 4.0%, N 1.1%; Found: C 54.5%, H 3.6%, N 1.0%.

$[\{Ru(dppm)_2(\kappa^2\text{-}O_2CC_5H_4N)\}_2PtCl_2](PF_6)_2$ (104)

A chloroform (10mL) and ethanol (20 mL) solution of $[Ru(dppm)_2(O_2CC_5H_4N)]PF_6$ **(101)** (50 mg, 0.044 mmol) and K_2PtCl_4 (9 mg, 0.022 mmol) was allowed to stir at reflux for 3 h and then overnight at room temperature. All solvent was removed and dichloromethane (10mL) and ethanol (20 mL) was added and the solvent volume was slowly reduced on a rotary evaporator resulting in the precipitation of a red/orange solid. This was filtered and dried under vacuum. Yield: 31 mg (55 %). IR (solid state): 1511 (ν_{OCO}), 1484, 1313, 836 (ν_{PF}, 774, 732 cm^{-1}. ^{31}P NMR ($CDCl_3$): -11.7, 8.8 (t x 2, dppm, J_{pp} = 39.2 Hz) ppm. ^1H NMR ($CDCl_3$): 4.15, 4.76 (m x 2, 2 x 4H, PCH_2P); 6.25, 7.01, 7.34, 7.60, 7.75 (m x 5, 80H + 4H, C_6H_5 + CH_2CH_2N); 8.73 (m, 4H, CH_2CH_2N) ppm. MS (FAB +ve) *m/z* (abundance) = 2248 (4) $[M]^+$, 992 (100) $[Ru(dppm)_2(O_2CC_5H_4N)]^+$. Analysis: Calculated for

$C_{112}H_{96}Cl_2F_{12}N_2O_4P_{10}PtRu_2$ (M_w = 2539.2): C 52.9%, H 3.8%, N 1.1%; Found: C 53.1%, H 3.7%, N 1.0%.

[Ru(CH=CHC$_6$H$_4$F-4)Cl(CO)(BTD)(PPh$_3$)$_2$] (105)

A solution of [RuHCl(BTD)(CO)(PPh$_3$)$_2$] (437 mg, 0.528 mmol) in dichloromethane (30 mL) was treated with a methanolic solution (15 mL) of 1-ethynyl-4-fluorobenzene (0.09 mL, 0.792 mmol) and BTD (72 mg, 0.528 mmol). The reaction mixture was allowed to stir for 0.5 h at room temperature. The solvent volume was slowly reduced on a rotary evaporator resulting in the precipitation of an orange solid. This was filtered, washed with petroleum ether (10 mL) and dried under vacuum. Yield: 443 mg (89 %). IR (solid state): 1914 (ν_{CO}), 1502, 1480, 1220, 1184, 924, 874, 841 cm^{-1}. ^{31}P NMR (CD_2Cl_2): 26.5 (s, PPh_3) ppm. ^{1}H NMR (CD_2Cl_2): 5.80 (d, 1H, Hβ, J_{HH} = 16.2 Hz); 6.85 (m, 4H, C_6H_4F); 7.95 (m, 2H, BTD); 8.59 (dt, 1H, Hα, J_{HH} = 16.2 J_{HP} = 3.0 Hz) ppm. ^{19}F NMR (CD_2Cl_2): -120.1 (s, 1F, CF) ppm. MS (ES +ve) *m/z* (abundance) = 810 (10) [M – BTD]$^+$. Analysis: Calculated for $C_{51}H_{40}ClFN_2OP_2RuS$ (M_w = 946.4): C 64.7%, H 4.3%, N 3.0%; Found: C 64.8%, H 4.2%, N 2.6%.

[Ru(CH=CHC$_6$H$_4$F-4)(κ^2-O$_2$CC$_5$H$_4$N)(CO)(PPh$_3$)$_2$] (106)

A solution of [Ru(CH=CHC$_6$H$_4$F-4)Cl(BTD)(CO)(PPh$_3$)$_2$] (**105**, 100 mg, 0.106 mmol) in dichloromethane (30 mL) was treated with a methanolic solution (15 mL) of isonicotinic acid (14 mg, 0.116 mmol) and sodium methoxide (6 mg, 0.116 mmol). The reaction mixture was allowed to stir for 0.5 h at room temperature. The solvent volume was slowly reduced on a rotary evaporator resulting in the precipitation of a yellow solid. This was filtered, washed with petroleum ether (10 mL) and dried under vacuum. Yield: 59 mg (62 %). IR (solid state): 1916 (ν_{CO}), 1571, 1520 (ν_{OCO}), 1502, 1481, 1218, 1183, 1028, 952, 840, 767, 604 cm^{-1}. ^{31}P NMR (CD_2Cl_2): 38.1 (s, PPh_3) ppm. ^{1}H NMR (CD_2Cl_2): 5.86 (d, 1H, Hβ, J_{HH} = 15.6 Hz); 6.43, 6.72 (m x 2, 2 x 2H, C_6H_4F); 6.89 (d, 2H, C*H*$_2$CH$_2$N, J_{HH} = 5.0 Hz), 7.04 –7.69 (m, 30H, C_6H_5); 7.81 (dt, 1H, Hα, J_{HH} = 15.3 J_{HP} = 2.6 Hz); 8.31 (d, 2H, CH$_2$C*H*$_2$N, J_{HH} = 5.8 Hz) ppm. ^{19}F NMR (CD_2Cl_2): -121.4 (s, 1F, CF) ppm; MS (ES +ve) *m/z* (abundance) = 371 (3) [M – (PPh$_3$)$_2$]$^+$; 343 (3) [M – CO(PPh$_3$)$_2$]$^+$. Analysis: Calculated for $C_{51}H_{40}FNO_3P_2Ru$ (M_w = 896.9): C 68.3%, H 4.5%, N 1.6%; Found: C 68.2%, H 4.4%, N 1.5%.

[Ru(CH=CHC$_6$H$_4$F-4){κ^2-O$_2$CC$_5$H$_4$N(AuC$_6$F$_5$)}(CO)(PPh$_3$)$_2$] (107)

A solution of [Ru(CH=CHC$_6$H$_4$F-4)(κ^2-O$_2$CC$_5$H$_4$N)(CO)(PPh$_3$)$_2$] (**106**, 60 mg, 0.067 mmol) in dichloromethane (25 mL) was treated with [Au(tht)C$_6$F$_5$] (28 mg, 0.061 mmol) dissolved in dichloromethane (10 mL). The reaction mixture was stirred for 1 h at room temperature. The solvent volume was slowly reduced on a rotary evaporator resulting in the precipitation of a brown solid. This was filtered, and then washed with petroleum ether (10 mL). Yield: 40 mg (70 %). IR (solid

state): 1925 (ν_{CO}), 1743, 1501 (ν_{OCO}), 1482, 1451, 1221, 1057, 952, 869, 841 cm^{-1}. ^{31}P NMR (CD_2Cl_2): 38.0 (s, PPh_3) ppm. ^{1}H NMR (CD_2Cl_2): 5.87 (d, 1H, Hβ, J_{HH} = 15.4 Hz); 6.43, 6.72 (m x 2, 2 x 2H, C_6H_4F); 6.89 (d, 2H, CH_2CH_2N, J_{HH} = 5.8 Hz); 6.96 – 7.68 (m, 30H, C_6H_5); 7.83 (dt, 1H, Hα, J_{HH} = 4.30 J_{HP} = 2.6 Hz); 8.31 (d, 2H, CH_2CH_2N, J_{HH} = 5.8 Hz) ppm. ^{19}F NMR (CD_2Cl_2): -163.1 (m, 2F, *m*-C_6F_5), -159.3 (t, 1F, *p*-C_6F_5, J_{FF} = 20.0 Hz); -121.2 (s, 1F, C_6H_4F); -116.5 (m, 2F, *o*-C_6F_5) ppm: MS (FAB +ve) *m/z* (abundance) = 897 (38) $[M - AuC_6F_5]^+$; 774 (4) $[M - O_2CC_5H_4N(AuC_6F_5)]^+$. Analysis: Calculated for $C_{57}H_{40}AuF_6NO_3P_2Ru$ (M_w = 1260.9): C 54.3%, H 3.2%, N 1.1%; Found: C 54.2%, H 3.3%, N 1.1%.

[Ru(CH=CHC$_6$H$_4$Me-4)(κ^2-O$_2$CC$_6$H$_4$CN)(CO)(PPh$_3$)$_2$] (108)

A solution of [Ru(CH=CHC$_6$H$_4$Me-4)Cl(BTD)(CO)(PPh$_3$)$_2$] (100 mg, 0.106 mmol) in dichloromethane (30 mL) was treated with a methanolic solution (15 mL) of cyanobenzoic acid (17 mg, 0.117 mmol) and sodium methoxide (11 mg, 0.212 mmol). The reaction mixture was stirred for 1.5 h at room temperature. The solvent volume was slowly reduced on a rotary evaporator resulting in the precipitation of a yellow solid. This was filtered, and then washed with petroleum ether (10 mL) Yield: 77 mg (79 %). IR (solid state): 2229 (ν_{CN}), 1916 (ν_{CO}), 1579, 1518 (ν_{OCO}), 1482, 1184, 964, 863, 606 cm^{-1}. ^{31}P NMR (*d*$_6$-acetone): 37.8 (s, PPh_3) ppm. ^{1}H NMR (*d*$_6$-acetone): 2.17 (s, 3H, CCH_3); 5.99 (d, 1H, Hβ, J_{HH} = 15.3 Hz); 6.42, 6.79 (AB, 4H, C_6H_4, J_{AB} = 8.0 Hz); 7.27 (d, 2H, CH_2CH_2CN, J_{HH} = 8.4 Hz); 7.37 – 7.60 (m, 30H + 2H, C_6H_5, CH_2CH_2CN), 7.85 (dt, 1H, Hα, J_{HH} = 15.3 J_{HP} = 2.7 Hz) ppm. MS (ES +ve) *m/z* (abundance) = 890 (3) $[M - CN]^+$; 814 (55) $[M - C_6H_4CN]^+$; 771 (2) $[M - O_2CC_6H_4CN]^+$. Analysis: Calculated for $C_{54}H_{43}NO_3P_2Ru$ (M_w = 916.9): C 70.7%, H 4.7%, N 1.5%; Found: C 70.9%, H 4.8%, N 1.5%.

[Ru(C(C≡CPh)=CHPh)(κ^2-O$_2$CC$_6$H$_4$CN)(CO)(PPh$_3$)$_2$] (109)

A solution of [Ru(C(C≡CPh)=CHPh)Cl(CO)(PPh$_3$)$_2$] (100 mg, 0.112 mmol) in dichloromethane (30 mL) was treated with a solution of cyanobenzoic acid (18 mg, 0.123 mmol) and sodium methoxide (7 mg, 0.123 mmol) in methanol (15 mL). The reaction mixture was allowed to stir for 1 h at room temperature. The solvent volume was slowly reduced on a rotary evaporator resulting in the precipitation of a yellow solid. This was filtered, and then washed with petroleum ether (10 mL). Yield: 66 mg (59 %). IR (solid state): 2227 (ν_{CN}), 1917 (ν_{CO}), 1579, 1522 (ν_{OCO}), 1483, 1186, 1028, 913, 864, 774, 750, 608 cm^{-1}. ^{31}P NMR (*d*$_6$-acetone): 37.8 (s, PPh_3) ppm. ^{1}H NMR (*d*$_6$-acetone): 6.13 (s(br), 1H, Hβ); 6.92 – 7.73 (m, 30H + 10H + 4H, PC_6H_5 + C_6H_5 + C_6H_4CN) ppm. MS (ES +ve) *m/z* (abundance) = 1004 (12) $[M]^+$; 898 (100) $[M - CCPh]^+$ 857 (13) $[M - O_2CC_6H_4CN]^+$. Analysis: Calculated for $C_{61}H_{45}NO_3P_2Ru$ (M_w = 1003.03): C 73.0%, H 4.5%, N 1.4%; Found: C 73.2%, H 4.4%, N 1.3%.

[Ru(CH=CHC$_6$H$_4$F-4)(κ^2-O$_2$CC$_6$H$_4$CN)(CO)(PPh$_3$)$_2$] (110)

A solution of [Ru(CH=CHC$_6$H$_4$F-4)Cl(BTD)(CO)(PPh$_3$)$_2$] (**105**, 100 mg, 0.106 mmol) in dichloromethane (30 mL) was treated with a methanolic solution (15 mL) of cyanobenzoic acid (17 mg, 0.117 mmol) and sodium methoxide (11 mg, 0.211 mmol). The reaction mixture was allowed to stir for 0.5 h at room temperature. The solvent volume was slowly reduced on a rotary evaporator resulting in the precipitation of a yellow solid. This was filtered, and then washed with petroleum ether (10 mL) Yield: 80 mg (82 %). IR (solid state): 2230 (ν_{CN}), 1914 (ν_{CO}), 1740, 1520 (ν_{OCO}), 1502, 1481, 1222, 1184, 948, 865, 838, 774, 608 cm^{-1}. ^{31}P NMR (d_6-acetone): 38.0 (s, PPh$_3$) ppm. ^{1}H NMR (d_6-acetone): 5.97 (d, 1H, Hβ, J_{HH} = 15.4 Hz); 6.49, 6.73 (m x 2, 2 x 2H, C$_6$H$_4$F); 7.27 (d, 2H, C*H*$_2$CH$_2$CN, J_{HH} = 8.4 Hz); 7.37 – 7.60 (m, 30H + 2H, C$_6$H$_5$, CH$_2$C*H*$_2$CN); 7.86 (d, 1H, Hα, J_{HH} = 15.4 J_{HP} = 2.5 Hz) ppm. ^{19}F NMR (d_6-acetone): -121.8 (s, CF) ppm. MS (ES +ve) *m/z* (abundance) = 818 (54) [M – C$_6$H$_4$CN]$^+$. Analysis: Calculated for C$_{53}$H$_{40}$FNO$_3$P$_2$Ru (M$_w$ = 920.9): C 69.1%, H 4.4%, N 1.5%; Found: C 69.0%, H 4.5%, N 1.5%.

[Ru(CH=CHC$_6$H$_4$Me-4){κ^2-O$_2$CC$_6$H$_4$CN(AuC$_6$F$_5$)}(CO)(PPh$_3$)$_2$] (111)

A solution of [Ru(CH=CHC$_6$H$_4$Me-4)(κ^2-O$_2$CC$_6$H$_4$CN)(CO)(PPh$_3$)$_2$] (**108**, 60 mg, 0.065 mmol) in dichloromethane (15 mL) was treated with [Au(tht)C$_6$F$_5$] (27 mg, 0.059 mmol) dissolved in dichloromethane (10 mL). The reaction mixture was allowed to stir for 1h at room temperature. The solvent volume was slowly reduced on a rotary evaporator to 5 mL resulting in the precipitation of a brown/orange solid. This was filtered, and then washed with petroleum ether (10 mL). Yield: 19 mg (30 %). IR (solid state): 1924 (ν_{CO}), 1598, 1550 (ν_{OCO}), 1498, 1449, 1187, 1051, 951, 863, 778 cm^{-1}. ^{31}P NMR (d_6-acetone): 37.8 (s, PPh$_3$) ppm. ^{1}H NMR (d_6-acetone): 2.17 (s, 3H, CCH$_3$); 5.98 (d, 1H, Hβ, J_{HH} = 15.3 Hz); 6.42, 6.79 (AB, 4H, C$_6$H$_4$, J_{AB} = 8.0 Hz); 7.27 (d, 2H, C*H*$_2$CH$_2$CN, J_{HH} = 8.4 Hz); 7.35 – 7.87 (m, 30H + 2H, C$_6$H$_5$, CH$_2$C*H*$_2$CN); 7.85 (dt, 1H, Hα, J_{HH} = 15.3 J_{HP} = 2.7 Hz) ppm. ^{19}F NMR (d_6-acetone): -165.4 (t, 2F, *m*-C$_6$F$_5$, J_{FF} = 20.6 Hz); -164.6 (t, 1F, *p*-C$_6$F$_5$, J_{FF} = 20.5 Hz); -115.8 (d, 2F, *o*-C$_6$F$_5$, J_{FF} = 22.9) ppm. MS (FAB +ve) *m/z* (abundance) = 1164 (2) [M – vinylTol]$^+$; 917 (8) [M – AuC$_6$F$_5$]$^+$; 771 (11) [M – O$_2$CC$_6$H$_4$CN(AuC$_6$F$_5$)]$^+$. Analysis: Calculated for C$_{60}$H$_{43}$AuF$_5$NO$_3$P$_2$Ru (M$_w$ = 1280.96): C 56.3%, H 3.4%, N 1.1%; Found: C 56.4%, H 3.1%, N 1.1%.

[Ru(C(C≡CPh)=CHPh){κ^2-O$_2$CC$_6$H$_4$CN(AuC$_6$F$_5$)}(CO)(PPh$_3$)$_2$] (112)

A solution of [Ru(C(C≡CPh)=CHPh)(κ^2-O$_2$CC$_6$H$_4$CN)(CO)(PPh$_3$)$_2$] (**109**, 60 mg, 0.059 mmol) in dichloromethane (15 mL) was treated with [Au(tht)C$_6$F$_5$] (24 mg, 0.054 mmol) dissolved in dichloromethane (10 mL). The reaction mixture was allowed to stir for 1 h at room temperature. The solvent volume was slowly reduced on a rotary evaporator to 5 mL, resulting in the precipitation of a yellow solid. This was filtered, and then washed with petroleum ether (10 mL). Yield: 23 mg (31%). IR (solid state): 2249 (ν_{CN}), 1975, 1923 (ν_{CO}), 1596 (ν_{OCO}), 1494, 1450, 1188, 1053, 951, 864, 778 cm^{-1}. ^{31}P NMR (d_6-acetone): 37.8 (s, PPh$_3$) ppm. ^{1}H NMR (d_6-acetone): 6.13 (s(br), 1H, Hβ); 6.93 –

7.75 (m, 30H + 10H + 4H, PC_6H_5, C_6H_5, C_6H_4CN) ppm. ^{19}F NMR (d_6-acetone): -165.4 (t, 2F, *m*-C_6F_5, J_{FF} = 19.5 Hz); -164.6 (t, 1F, *p*-C_6F_5, J_{FF} = 20.6 Hz); -115.7 (d, 2F, *o*-C_6F_5, J_{FF} = 20.6 Hz) ppm. MS (FAB +ve) *m/z* (abundance) = 1003 (5) $[M - AuC_6F_5]^+$; 857 (53) $[M - O_2CC_6H_4CN(AuC_6F_5)]^+$. Analysis: Calculated for $C_{67}H_{45}AuF_5NO_3P_2Ru$ (M_w = 1367.06): C 58.9%, H 3.3%, N 1.0%; Found: C 59.1%, H 3.1%, N 1.0%.

[Ru(CH=CHC$_6$H$_4$F-4){κ^2-O$_2$CC$_6$H$_4$CN(AuC$_6$F$_5$)-4}(CO)(PPh$_3$)$_2$] (113)

(a) A solution of [Ru(CH=CHC$_6$H$_4$F-4)(κ^2-O$_2$CC$_6$H$_4$CN)(CO)(PPh$_3$)$_2$] (**110**, 60 mg, 0.065 mmol) in dichloromethane (25 mL) was treated with [Au(tht)C_6F_5] (27 mg, 0.059 mmol) dissolved in dichloromethane (10 mL) The reaction mixture was allowed to stir for 1 h at room temperature. The solvent volume was slowly reduced on a rotary evaporator resulting in the precipitation of a yellow/grey solid. This was filtered, and then washed with petroleum ether (10 mL). (b) A solution of [$C_6F_5AuNCC_6H_4CO_2H$] (**114**, 30 mg, 0.058 mmol) in dichloromethane (25 mL) was treated with sodium methoxide (6 mg, 0.106 mmol) and a methanolic solution of [Ru(CH=CHC$_6$H$_4$F-4)Cl(CO)(BTD)(PPh$_3$)$_2$] (**105**, 51 mg, 0.053 mmol). The reaction mixture was allowed to stir for 1 h at room temperature. The solvent volume was slowly reduced on a rotary evaporator resulting in the precipitation of a yellow/grey solid. This was filtered, and then washed with petroleum ether (10 mL). Yield: 60 mg (88 %). IR (solid state): 2250 (ν_{CN}), 1967, 1922 (ν_{CO}), 1596, 1557, 1500 (ν_{OCO}), 1482, 1450, 1220, 1187, 1094, 1051, 951, 864, 775 cm^{-1}. ^{31}P NMR (d_6-acetone): 38.0 (s, PPh_3) ppm. ^1H NMR (d_6-acetone): 5.97 (d, 1H, Hβ, J_{HH} = 15.3 Hz); 6.49, 6.73 (m x 2, 2 x 2H, C_6H_4F); 7.27 (d, 2H, C*H*$_2$CH$_2$CN, J_{HH} = 8.3 Hz); 7.37 – 7.80 (m, 30H, C_6H_5); 7.86 (d, 1H, Hα, J_{HH} = 15.3 J_{HP} = 2.6 Hz); 8.08 (m, 2H, CH$_2$C*H*$_2$CN) ppm. ^{19}F NMR (d_6-acetone): -165.4 (t, 2F, *m*-C_6F_5, J_{FF} = 19.5 Hz); -164.6 (t, 1F, *p*-C_6F_5, J_{FF} = 19.4 Hz); -121.8 (s, 1F, C_6H_4F); -115.8 (d, 2F, *o*-C_6F_5, J_{FF} = 22.9 Hz) ppm. MS (FAB +ve) *m/z* (abundance) = 921 (13) $[M - AuC_6F_5]^+$; 775 (12) $[M - O_2CC_6H_4CN(AuC_6F_5)]^+$; 733 (3) $[M - CO(PPh_3)_2]^+$. Analysis: Calculated for $C_{59}H_{40}AuF_6NO_3P_2Ru$ (M_w = 1284.9): C 55.2%, H 3.1%, N 1.1%; Found: C 56.1%, H 3.5%, N 1.0%.

[(HO$_2$CC$_6$H$_4$CN)Au(C$_6$F$_5$)] (114)

A solution of [Au(tht)C_6F_5] (50 mg, 0.111 mmol) in dichloromethane (25 mL) was treated with a methanolic solution (15 mL) of cyanobenzoic acid (16 mg, 0.111 mmol). The reaction mixture was allowed to stir for 1 h at room temperature and the solvent volume was slowly reduced on a rotary evaporator resulting in the precipitation of a grey solid. This was filtered, washed with petroleum ether (10 mL) Yield: 32 mg (57 %). IR (solid state): 2278, 2236 (ν_{CN}), 1698, 1615, 1555, 1504 (ν_{OCO}), 1461, 1398, 1288, 1064, 1017, 957, 863, 807, 771, 644 cm^{-1}. ^1H NMR (d_6-acetone): 7.93 (d, 2H, C*H*$_2$CH$_2$CN, J_{HH} = 8.1 Hz); 8.23 (d, 2H, CH$_2$C*H*$_2$CN, J_{HH} = 8.1 Hz). ^{19}F NMR (d_6-acetone): -165.6 (t, 2F, *m*-C_6F_5, J_{FF} = 19.6 Hz); -164.1 (t, 1F, *p*-C_6F_5, J_{FF} = 19.5 Hz); -115.8 (d, 2F, *o*-C_6F_5, J_{FF} = 21.7 Hz)

ppm. MS (FAB +ve) *m/z* (abundance) = 513 (3) $[M]^+$; 466 (5) $[M - CO_2H]^+$; 369 (4) $[M - NCC_6H_4CO_2H]^+$; 347 (4) $[M - C_6F_5]^+$. Analysis: Calculated for $C_{14}H_5AuF_5NO_2$ (M_w = 511.0): C 32.9%, H 1.0%, N 2.7%; Found: C 32.1%, H 0.9%, N 2.8%.

Experimental for pentametallic complexes

$[RhCl_2\{NC_5H_4CO_2(Ru(CH=CHC_6H_4Me\text{-}4)(CO)(PPh_3)_2\}_4]Cl$ (115)

A solution of $[Ru(CH=CHC_6H_4Me\text{-}4)Cl(BTD)(CO)(PPh_3)_2]$ (50 mg, 0.053 mmol) in dichloromethane (10 mL) and acetone (10 mL) was treated with a solution of $RhCl_2(O_2CC_5H_4N)(NaO_2CC_5H_4N)_3$ (12 mg, 0.016 mmol) in water (5 mL) and acetone (15 mL). The reaction mixture was allowed to stir for 1 h at room temperature. All solvent was removed and the crude product dissolved in dichloromethane (10 mL) and filtered through diatomaceous earth (Celite) to remove NaCl. Ethanol (20 mL) was added and the solvent volume was slowly reduced on a rotary evaporator resulting in the precipitation of a fine yellow solid. This was filtered, washed with petroleum ether (10 mL) and dried under vacuum. Yield: 32 mg (53 %). IR (solid state): 1916 (ν_{CO}), 1576, 1519 (ν_{OCO}), 1481, 1185, 999, 867, 604 cm^{-1}. ^{31}P NMR ($CDCl_3$): 38.1 (s, PPh_3) ppm. ^1H NMR ($CDCl_3$): 2.25 (s(br), 12H, CCH_3); 5.90 (d, 4H, Hβ, J_{HH} = 15.6 Hz); 6.42 (d, 8H, CH_2CH_2N, J_{HH} = 7.2 Hz); 6.85 (d, 8H, C_6H_4, J_{HH} = 7.7 Hz); 6.90 (d, 8H, C_6H_4, J_{HH} = unresolved); 7.27 – 7.52 (m, 120H, C_6H_5); 7.77 (dt(br), 4H, Hα, J_{HH} = 15.1 J_{HP} = unresolved); 8.32 (s(br), 8H, CH_2CH_2N) ppm. MS FAB (+ve), MALDI (+ve) not diagnostic. Analysis: Calculated for $C_{208}H_{172}Cl_3N_4O_{12}P_8RhRu_4$ (M_w = 3780.9): C 66.1%, H 4.6%, N 1.5%; Found: C 66.2%, H 4.4%, N 1.4%.

$[RhCl_2\{NC_5H_4(C_6H_4CO_2H)\text{-}4\}_4]Cl$ (116)

An ethanolic suspension (10 mL) of pyridylbenzoic acid (200 mg, 1.004 mmol) was added to a solution of $RhCl_3{\cdot}3H_2O$ (64 mg, 0.243 mmol) in 0.25 M hydrochloroic acid (10 mL). The mixture was heated to boiling with vigorous stirring. After the pyridylbenzoic acid was dissolved, the red solution rapidly turned yellow and a fine precipitate formed. Reflux was continued for further 5 min, then the mixture was cooled to ambient temperature. Sodium hydroxide solution (0.1 M) was added until the system reached pH 4.5, thus increasing the yield of the product. The pale yellow-pink solid was collected and washed with hot water (5mL) and acetone (5 mL). Yield: 207 mg (84 %). IR (solid state): 1917, 1691, 1605, 1522 (ν_{OCO}), 1405, 1115, 1068, 1004, 826, 767, 656 cm^{-1}. ^1H NMR (CD_2Cl_2): 7.60 (dd, 8H, CH_2CH_2N, J_{HH} = 4.5, J_{RhH} = 1.8 Hz); 7.81, 8.21 (d x 2, 2 x 8H, C_6H_4, J_{HH} = 8.6 Hz); 8.72 (dd, 8H, CH_2CH_2N, J_{HH} = 4.5 Hz J_{RhH} = 1.9 Hz); 11.12 (s, 4H, OH); ppm. MS (FAB +ve) *m/z* (abundance) = 200 (23) $[NC_5H_4C_6H_4CO_2H]^+$. MS (FAB -ve) *m/z* (abundance) = 199 (33)

$[NC_5H_4C_6H_4CO_2]^-$. Analysis: Calculated for $C_{48}H_{36}Cl_3N_4O_8Rh$ (M_w = 1006.1): C 57.3%, H 3.6%, N 5.6%; Found: C 57.3%, H 3.7%, N 5.5%.

$[RhCl_2\{NC_5H_4(C_6H_4CO_2)-4\}\{NC_5H_4(C_6H_4CO_2Na)-4\}_3]$ (117)

A saturated solution of NaOH was added to $[RhCl_2\{NC_5H_4(C_6H_4CO_2H)-4\}_4]Cl$ (**116**, 170mg, 0.169 mmol) until complete dissolution of the solid phase (molar ratio Rh : NaOH = 1 : 3). The obtained yellow solution was evaporated until all solvent was removed and the product was triturated ultrasonically in acetone (10 mL). The yellow-brown solid was filtered, washed with ice-cold water (5 mL) and acetone (5 mL) and dried under vacuum. Yield: 99 mg (57 %). IR (solid state): 1593, 1550 (ν_{OCO}), 1378, 1222, 1186, 1070, 1005, 833, 777, 736, 700 cm^{-1}. ^1H NMR (d_6-dmso): 7.90 (dd(br), 8H, CH_2CH$_2$N, J_{HH} = 5.7 Hz J_{RhH} = unresolved); 7.95, 8.16 (d(br) x 2, 2 x 8H, C_6H_4, J_{HH} = 8.1 Hz); 8.80 (dd(br), 8H, CH$_2$CH_2N, J_{HH} = 5.7 Hz J_{RhH} = unresolved) ppm. MS (FAB -ve) *m/z* (abundance) = 765 (2) $[M - 2Cl - NC_5H_4(C_6H_4CO_2]^-$. Analysis: Calculated for $C_{48}H_{32}Cl_2N_4Na_3O_8Rh$ (M_w = 1035.6): C 55.7%, H 3.1%, N 5.4%; Found: C 60.1%, H 3.3%, N 5.3%.

$[RhCl_2\{NC_5H_4(C_6H_4CO_2Ru(dppm)_2)-4\}_4](PF_6)_5$ (118)

A solution of *cis*-$[RuCl_2(dppm)_2]$ (100 mg, 0.106 mmol) in chloroform (30 mL) was treated with a solution of $[RhCl_2\{NC_5H_4(C_6H_4CO_2)-4\}\{NC_5H_4(C_6H_4CO_2Na)-4\}_3]$ (**117**, 28 mg, 0.027 mmol) in water (5 mL) and then with a solution of ammonium hexafluorophosphate (6 mg, 0.106 mmol) in ethanol (10 mL). The reaction mixture was refluxed for 15 min. All solvent was removed and the crude product dissolved in dichloromethane (10 mL) and filtered through diatomaceous earth (Celite) to remove NaCl. All solvent was removed again and dissolved in ethanol (10 mL) and then filtered through diatomaceous earth (Celite) to remove other impurities. The crystalline black product was recrystallised from dichloromethane/petroleum ether solution. Yield: 123 mg (88 %). IR (solid state): 1604, 1557 (ν_{OCO}), 1483, 1362, 1187, 867 (ν_{PF}), 831, 778, 731, 616 cm^{-1}. ^{31}P NMR (CD_2Cl_2): -11.8, 9.1 (t x 2, dppm, J_{PP} = 39.2 Hz) ppm. ^1H NMR (CD_2Cl_2): 4.03, 4.75 (m x 2, 2 x 8H, PCH_2P); 6.52 – 7.92 (m, 160H + 16H + 8H, C_6H_5 + C_6H_4 + CH_2CH$_2$N); 8.25 (s(br), 8H, CH$_2$CH_2N) ppm. MS (MALDI +ve) *m/z* (abundance) = not diagnostic. Analysis: Calculated for $C_{248}H_{208}Cl_2F_{30}N_4O_8P_{21}RhRu_4$ (M_w = 5170.5): C 57.6%, H 4.1%, N 1.1%; Found: C 57.7%, H 4.2%, N 1.1%.

$[(Pd$-TPP$)\{p$-$CO_2Ru(dppm)_2\}_4](PF_6)_4$ (119)

A solution of *cis*-$[RuCl_2(dppm)_2]$ (100 mg, 0.106 mmol) in dichloromethane (100 mL) was treated with a solution of 5,10,15,20-Tetrakis(4-carboxyphenyl)porphyrin-Pd(II) (24 mg, 0.027 mmol), sodium methoxide (9 mg, 0.160 mmol) and ammonium hexafluorophosphate (22 mg, 0.133 mmol) in methanol (50 mL). The reaction mixture was stirred for 48 hr at room temperature. All solvent was

removed and the crude product dissolved in dichloromethane (10 mL) and filtered through diatomaceous earth (Celite) to remove NaCl, NaOMe and excess ligand. Methanol (20 mL) was then added and the solvent volume was slowly reduced on a rotary evaporator resulting in the precipitation of a bright orange/red solid. This was filtered, washed with methanol (10 mL) and petroleum ether (10 mL) and dried under vacuum. Yield: 98 mg (74 %). IR (solid state): 1607, 1584, 1519 (ν_{OCO}), 1484, 1430, 1095, 1012, 836 (ν_{PF}), 774, 732, 694, 616 cm^{-1}. ^{31}P NMR (CD_2Cl_2): -11.6, 9.0 (t x 2, dppm, J_{PP} = 39.0 Hz) ppm. ^{1}H NMR (CD_2Cl_2): 4.07, 4.74 (m x 2, 2 x 8H, PC*H*$_2$P); 7.04 – 7.91 (m, 160H, C_6H_5); 8.17 (m, 8H, C_6H_4); 8.32 (d, 8H, C_6H_4, J_{HH} = 7.8 Hz); 8.97 (s, 8H, NC_4H_2) ppm. MS (MALDI +ve) not diagnostic. Analysis: Calculated for $C_{248}H_{200}F_{24}N_4O_8P_{20}PdRu_4$ (M_w = 4950.4): C 60.2%, H 4.1%, N 1.1%; Found: C 60.1%, H 3.9%, N 1.2%.

[(Pd-TPP){*p*-CO_2Ru(CH=CHC_6H_4Me-4)(CO)(PPh_3)$_2$}$_4$] (120)

A solution of [Ru(CH=CHC_6H_4Me-4)Cl(BTD)(CO)(PPh_3)$_2$] (100 mg, 0.106 mmol) in dichloromethane (40 mL) was treated with a methanolic solution (20 mL) of 5,10,15,20-Tetrakis(4-carboxyphenyl)porphyrin-Pd(II) (24 mg, 0.027 mmol) and sodium methoxide (9 mg, 0.159 mmol). The reaction mixture was allowed to stir overnight at room temperature. The solvent volume was slowly reduced on a rotary evaporator resulting in the precipitation of red solid. This was filtered, washed with methanol (10 mL) and petroleum ether (10 mL) and dried under vacuum. Yield: 69 mg (64 %). IR (solid state): 1919 (ν_{CO}), 1508(ν_{OCO}), 1481, 1352, 1314, 1181, 1012, 796 cm^{-1}. ^{31}P NMR (d_6-benzene): 39.1 (s, PPh_3) ppm. ^{1}H NMR (d_6-benzene): 2.27 (s, 12H, CCH_3); 6.67 (d, 4H, Hβ, J_{HH} = 15.0 Hz); 6.97, 7.10 (d, 16H, AB, J_{AB} = 8.1 Hz); 7.16 – 7.48 (m, 120H, C_6H_5); 7.94 (d, 8H, C_6H_4, J_{HH} = 8.1 Hz); 8.05 (m, 8H, C_6H_4); 8.57 (dt, 4H, Hα, J_{HH} = 15.3 J_{HP} = 2.7 Hz); 8.90 (s, 8H, NC_4H_2) ppm. MS (MALDI +ve) not diagnostic. Analysis: Calculated for $C_{232}H_{180}N_4O_{12}P_8PdRu_4{\cdot}6CH_2Cl_2$ (M_w = 4484.1): C 63.8%, H 4.3%, N 1.3%; Found: C 64.1 %, H 3.9 %, N 1.4 %.

[(Pd-TPP){*p*-CO_2Ru(CH=$CHCPh_2OH$)(CO)(PPh_3)$_2$}$_4$] (121)

A solution of [Ru(CH=$CHCPh_2OH$Cl(BTD)(CO)(PPh_3)$_2$] (100 mg, 0.097 mmol) in dichloromethane (100 mL) was treated with a solution of 5,10,15,20-Tetrakis(4-carboxyphenyl)porphyrin-Pd(II) (22 mg, 0.024 mmol), sodium methoxide (8 mg, 0.145 mmol) in methanol (20 mL). The reaction mixture was allowed to stir overnight at room temperature. The solvent volume was slowly reduced on a rotary evaporator resulting in the precipitation of a brick red solid. This was filtered, washed with methanol (10 mL) and petroleum ether (10 mL) and dried under vacuum. Yield: 42 mg (40 %). IR (solid state): 1919 (ν_{CO}), 1587, 1512 (ν_{OCO}), 1482, 1391, 1352, 1312, 1181, 1013, 796, 773 cm^{-1}. ^{31}P NMR (CD_2Cl_2): 38.7 (s, PPh_3) ppm. ^{1}H NMR (CD_2Cl_2): 1.03 (s, 4H, OH); 5.99 (d, 4H, Hβ, J_{HH} = 15.3 Hz); 6.84 (m, 16H, C_6H_5); 7.08 (d, 4H, Hα, J_{HH} = 15.3 Hz); 7.18 (m, 16H + 8H, C_6H_5 + C_6H_5); 7.42 – 7.58 (m, 120H + 8H, PPh_3 + C_6H_4); 7.74 (d, 8H, *o*-C_6H_4, J_{HH} = 8.0 Hz); 8.61 (s, 8H, NC_4H_2). MS

(MALDI +ve): not diagnostic. Analysis: Calculated for $C_{256}H_{196}N_4O_{16}P_8PdRu_4$ (M_w = 4342.8): C 70.8%, H 4.5%, N 1.3%; Found: C 71.1%, H 4.5 %, N 1.5 %.

[(Pd-TPP){*p*-CO_2Ru(=CHCH=CPh_2)(CO)(PPh_3)$_2$}$_4$](BF_4)$_4$ (122)

A suspension of [(Pd-TPP){*p*-CO_2Ru(CH=CHCPh_2OH)(CO)(PPh_3)$_2$}$_4$] (**121**, 18 mg, 0.004 mmol) in diethylether (5 mL) was treated with 5 drops of tetrafluoroboric acid and stirred for 5 mins at room temperature. The orange/red solid was filtered and dried under vacuum. Yield: 17 mg (89 %). IR (solid state): 1968 (ν_{CO}), 1692, 1606, 1497 (ν_{OCO}), 1481, 1227, 1093 (ν_{BF}), 1012, 871, 860, 772, 745, 708 cm^{-1}. ^{31}P NMR (CD_2Cl_2): 34.2 (s, PPh_3) ppm. ^{1}H NMR (CD_2Cl_2): 6.33 (d, 8H, C_6H_5, J_{HH} = 7.8 Hz); 7.31 (d, 8H, C_6H_4, J_{HH} = 7.8 Hz); 7.43 (t, 8H, C_6H_5, J_{HH} = 7.7 Hz); 7.52 – 7.66 (m, 120H + 8H + 8H +4H, PC_6H_5 + CC_6H_5 + CC_6H_4 + Hβ); 7.72 (m, 8H, C_6H_5); 7.91 (d, 8H, CC_6H_4, J_{HH} = 8.1 Hz); 8.66 (s, 8H, NC_4H_2); 14.94 (s(br), 4H, Hα). MS (MALDI +ve) not diagnostic. Analysis: Calculated for $C_{256}H_{192}B_4F_{16}N_4O_{12}P_8PdRu_4$ (M_w = 4622.1): C 66.5%, H 4.2%, N 1.2%; Found: C 66.7%, H 4.2%, N 1.2%.

[Ru{κ^2-$O_2CC_6H_4(C_5H_4N)$-4}$(dppm)_2$]PF_6 (123)

A solution of *cis*-[$RuCl_2(dppm)_2$] (100 mg, 0.106 mmol) in dichloromethane (30 mL) was treated with a solution of pyridylbenzoic acid (23 mg, 0.117 mmol), sodium methoxide (12 mg, 0.213 mmol) and ammonium hexafluorophosphate (35 mg, 0.213 mmol) in methanol (20 mL). The reaction mixture was allowed to stir for 1 h at room temperature. All solvent was removed and the crude product dissolved in dichloromethane (10 mL) and filtered through diatomaceous earth (Celite) to remove NaCl, NaOMe and excess ligand. Ethanol (20 mL) was then added and the solvent volume was slowly reduced on a rotary evaporator resulting in the precipitation of a yellow solid. This was filtered, washed with petroleum ether (10 mL) and dried under vacuum. Yield: 51 mg (40 %). IR (solid state): 1594, 1500 (ν_{OCO}), 1484, 1188, 1096, 832(ν_{PF}), 778, 755, 732, 617 cm^{-1}. ^{31}P NMR (CD_2Cl_2): -11.9, 9.0 (2 x t, dppm, J_{PP} = 39.2 Hz) ppm. ^{1}H NMR (CD_2Cl_2): 3.99, 4.68 (m x 2, 2 x 2H, PCH_2P); 7.01 – 7.85 (m, 40H + 2H + 4H, C_6H_5 + CH_2CH_2N + C_6H_4); 8.75 (d, 2H, CH_2CH_2N, J_{HH} = 5.6 Hz) ppm. MS (FAB +ve) *m/z* (abundance) = 1068 (12) $[M]^+$, 869 (4) $[M - O_2CC_6H_4C_5H_4N]^+$. Analysis: Calculated for $C_{62}H_{52}F_6NO_2P_5Ru$ (M_w = 1213.0): C 61.4%, H 4.3%, N 1.5%; Found: C 61.4%, H 4.3%, N 1.1%.

[Ru(CH=CHC_6H_4Me-4)$(O_2CC_6H_4C_5H_4N)$(CO)(PPh_3)$_2$] (124)

A solution of [Ru(CH=CHC_6H_4Me-4)Cl(BTD)(CO)(PPh_3)$_2$] (100 mg, 0.106 mmol) in dichloromethane (30 mL) was treated with a solution of pyridylbenzoic acid (23 mg, 0.117 mmol) and sodium methoxide (12 mg, 0.213 mmol in methanol (20 mL). The reaction mixture was allowed to stir for 1 h at room temperature. The solvent volume was slowly reduced on a rotary evaporator resulting in the precipitation of a pale yellow solid. This was filtered, washed with petroleum ether

(10 mL) and dried under vacuum. Yield: 100 mg (88 %). IR (solid state): 1917 (ν_{CO}), 1592, 1545, 1507 (ν_{OCO}), 1482, 1184, 864, 823, 775, 747, 606 cm^{-1}. ^{31}P NMR (CD_2Cl_2): 37.7 (s, PPh_3) ppm. ^{1}H NMR (CD_2Cl_2): 2.24 (s, 3H, CCH_3); 5.89 (d, 1H, Hβ, J_{HH} = 15.4 Hz); 6.42, 6.84 (d x 2, 2 x 2H, CC_6H_4Me, J_{AB} = 7.2 Hz); 7.23 (d, 2H, CH_2CH_2N, J_{HH} = 6.8 Hz); 7.36 – 7.52 (m, 30H + 4H, C_6H_5 + C_6H_4); 7.87 (d, 1H, Hα, J_{HH} = 15.1); 8.64 (d(br), 2H, CH_2CH_2N, J_{HH} = unresolved) ppm. ^{13}C NMR (CD_2Cl_2, 400 MHz): 206.9 (t, CO, J_{PC} = 15.4 Hz), 171.1 (s, CO_2), 152.9 (t, Cα, J_{PC} = 11.7 Hz), 150.6 (s, $C_{2,6}$-py), 147.8 (s, C_4-benzoate/ C_4-py/ C_1-py); 140.4 (s, C_4-benzoate/ C_4-py/ C_1-py), 138.5 (s, C_1-tolyl), 134.8 (virtual t, *o/m*-C_6H_5, J_{PC} = 5.6 Hz), 134.3 (s, C_4-tolyl), 133.9 (t (br), Cβ, J_{PC} = unresolved), 133.4 (s, C_4-benzoate/ C_4-py/ C_1-py), 131.7 (t, ipso, J_{PC} = 21.5 Hz), 130.2 (s, *p*-C_6H_5), 129.0 (s, $C_{2,6}$-tolyl), 128.7 (s, $C_{3,5}$-tolyl), 128.4 (virtual t, *o/m*-C_6H_5, J_{PC} = 4.4 Hz), 125.9 (s, $C_{3,5}$-benzoate/ $C_{3,5}$-py/ $C_{2,6}$-py), 124.5 (s, $C_{3,5}$-benzoate/ $C_{3,5}$-py/ $C_{2,6}$-py), 121.8 (s, $C_{3,5}$-benzoate/ $C_{3,5}$-py/ $C_{2,6}$-py), 21.0 (s, Me) ppm. MS (FAB +ve) *m/z* (abundance) = 969 (18) $[M]^+$, 852 (7) $[M - vinyl]^+$, 771 (8) $[M - O_2CC_6H_4C_5H_4N]^+$, 707 (20) $[M - PPh_3]^+$. Analysis: Calculated for $C_{58}H_{47}NO_3P_2Ru$ (M_w = 969.0): C 71.9%, H 4.9%, N 1.5%; Found: C 71.7%, H 5.0%, N 1.4%.

Experimental for silver nanoparticles

Ag@[$NC_5H_4CO_2Ru(dppm)_2$]PF_6 (NP7)

To an acetonitrile solution (15 mL) of $AgNO_3$ (5 mg, 0.030 mmol), [Ru(κ^2-$O_2CC_5H_4N$)$(dppm)_2$]PF_6 (**101**, 45 mg, 0.040 mmol) in acetonitrile (5 mL) was added. Then, an aqueous solution of sodium borohydride (80 µL, 4M) was added dropwise over 10 mins, causing a darkening of the colour. The resulting suspension was stirred for an hour at room temperature and then left to stand. The supernatant was decanted and the solid washed with acetonitrile (10 mL x 2) and then with water (10 mL x 2) to remove excess ruthenium complex and sodium borohydride. The black solid was dried under vacuum. IR (solid state): 1590, 1550 (ν_{OCO}), 1330, 1223, 1134, 1076, 990, 934, 821 (ν_{PF}), 766, 709, 681 cm^{-1}.

Ag@[NC_5H_4{$C_6H_4CO_2Ru(dppm)_2$}-4]PF_6 (NP8)

To an acetonitrile solution (15 mL) of $AgNO_3$ (3 mg, 0.020 mmol), [Ru(κ^2-$O_2CC_6H_4C_5H_4N$)$(dppm)_2$]PF_6 (**123**, 30 mg, 0.030 mmol) in acetonitrile (5 mL) was added. Then, an aqueous solution of sodium borohydride (50 µL, 4M) was added dropwise over 10 mins, causing a darkening of the colour. The resulting suspension was stirred for an hour at room temperature and then left to stand. The supernatant was decanted and the solid washed with acetonitrile (10 mL x 2)

and then with water (10 mL x 2) to remove excess ruthenium complex and sodium borohydride. The black solid was dried under vacuum. IR (solid sate): 1555 (ν_{OCO}), 1361, 1260, 1021, 815 (ν_{PF}) cm^{-1}.

10: Supplementary Information

10. Supplementary Information

10.1. Chapter 3: Transition metal dithiocarbamate (DTC) complexes of group 8 and 10 metals

10.1.1. *Crystal data for compounds* $[Ru\{S_2CN(CH_2CH_2OMe)_2\}(dppm)_2]PF_6$ (3) and $[Ru(CH=CHC_6H_4Me\text{-}4)\{S_2CN(CH_2CH_2OMe)_2\}(CO)(PPh_3)_2]$ (16):

Single crystals of complexes **3** and **16** were grown by slow diffusion of ethanol into a dichloromethane solution of each complex.

Crystal data for **3**: $[C_{57}H_{58}NO_2P_4RuS_2](PF_6)$, M = 1223.08, monoclinic, $P2_1/c$ (no. 14), a = 17.3740(3), b = 12.01286(19), c = 26.6409(4) Å, β = 95.1247(14)°, V = 5538.04(15) Å^3, Z = 4, D_c = 1.467 g cm^{-3}, μ(Mo-Kα) = 0.566 mm^{-1}, T = 173 K, pale yellow needles, Oxford Diffraction Xcalibur 3 diffractometer; 12994 independent measured reflections (R_{int} = 0.0300), F^2 refinement, R_1(obs) = 0.0316, wR_2(all) = 0.0721, 9490 independent observed absorption-corrected reflections [$|F_o| > 4\sigma(|F_o|)$, $2\theta_{max}$ = 58°], 705 parameters. CCDC 750274.

Crystal data for **16**: $C_{53}H_{53}NO_3P_2RuS_2 \cdot 0.3CH_2Cl_2$, M = 1004.57, triclinic, $P\bar{1}$ (no. 2), a = 11.9999(3), b = 15.2412(3), c = 15.3608(4) Å, α = 111.203(2), β = 106.398(2), γ = 95.0213(18)°, V = 2455.53(12) Å^3, Z = 2, D_c = 1.359 g cm^{-3}, μ(Cu-Kα) = 4.631 mm^{-1}, T = 173 K, pale yellow platy needles, Oxford Diffraction Xcalibur PX Ultra diffractometer; 9694 independent measured reflections (R_{int} = 0.0248), F^2 refinement, R_1(obs) = 0.0278, wR_2(all) = 0.0713, 8842 independent observed absorption-corrected reflections [$|F_o| > 4\sigma(|F_o|)$, $2\theta_{max}$ = 145°], 629 parameters. CCDC 750275.

10.1.2. *Crystal data for compounds* $[Ru(CH=CHC_6H_4Me\text{-}4)\{S_2CN(CH_2CH=CH_2)_2\}(CO)(PPh_3)_2]$ (22) and $[Ru(CH=CHC_6H_4Me\text{-}4)\{S_2CN(CH_2CH=CH_2)Me\}(CO)(PPh_3)_2]$ (30):

Single crystals of complex **22** were grown by slow diffusion of ethanol into a dichloromethane solution of each complex.

Crystal data for **22**: $[C_{53}H_{49}NOP_2RuS_2] \cdot 2CH_2Cl_2$, M = 1027.99, triclinic, P-1 (no. 2), a = 11.9308(4), b = 13.4909(4), c = 17.5672(5) Å, α = 109.806(3), β = 109.393(3), γ = 93.684(2)°, V = 2459.09(15) Å^3, Z = 2, D_c = 1.388 g cm^{-3}, μ(Cu-Kα) = 5.290 mm^{-1}, T = 173 K, pale yellow needles, Oxford Diffraction Xcalibur PX Ultra diffractometer; 9569 independent measured reflections (R_{int} = 0.0268), F^2 refinement, R_1(obs) = 0.0303, wR_2(all) = 0.0807, 8384 independent observed absorption-corrected reflections [$|F_o| > 4\sigma(|F_o|)$, $2\theta_{max}$ = 145°], 583 parameters. CCDC 768226.

Single crystals of complex **30** were grown by slow diffusion of diethylether into a dichloromethane solution of the compound.

Crystal data for **30**: $[C_{51}H_{47}NOP_2S_2](PF_6)\cdot C_4H_{10}O$, M = 862.50, Triclinic, P-1 (no. 2), a = 12.0925(3), b = 13.2486(3), c = 17.1306(4) Å, α = 91.4086(18), β = 108.979(2), γ = 111.961(2)°, V = 2373.28(11)Å^3, Z = 2, D_c = 1.402 g cm^{-3}, μ(Mo-Kα) = 0.637 mm^{-1}, T = 173 K, yellow blocks, Oxford Diffraction Xcalibur 3 diffractometer; 28715 independent measured reflections (R_{int} = 0.0210), F^2 refinement, R_1(obs) = 0.0320, wR_2(all) = 0.0781, 11961 independent observed absorption-corrected reflections [$|F_o| > 4\sigma(|F_o|)$, $2\theta_{max}$ = 33°], 564 parameters.

10.1.3. *Crystal data for compounds* $[Ni\{S_2CN(CH_2CH{=}CH_2)_2\}(dppp)]PF_6$ (**24**) and $[Ni(S_2CNC_4H_6)(dppp)]PF_6$ (**39**):

Single crystals of complex **24** were grown by slow diffusion of diethylether into a dichloromethane solution of the compound.

Crystal data for **24**: $[C_{34}H_{36}NNiP_2S_2](PF_6)\cdot C_4H_{10}O$, M = 862.50, monoclinic, C2/c (no. 15), a = 21.0143(5), b = 10.6307(3), c = 36.8148(15) Å, β = 97.725(3)°, V = 8149.7(5) Å^3, Z = 8, D_c = 1.406 g cm^{-3}, μ(Mo-Kα) = 0.755 mm^{-1}, T = 173 K, orange blocks, Oxford Diffraction Xcalibur 3 diffractometer; 12382 independent measured reflections (R_{int} = 0.0324), F^2 refinement, R_1(obs) = 0.1071, wR_2(all) = 0.2567, 9319 independent observed absorption-corrected reflections [$|F_o| > 4\sigma(|F_o|)$, $2\theta_{max}$ = 64°], 469 parameters. CCDC 768227.

Single crystals of complex **39** were grown by slow diffusion of ethanol into a chloroform solution of the compound.

	A	B		A	B
Ni(1)–S(1)	2.2158(7)	2.2286(7)	Ni(1)–S(3)	2.2300(7)	2.2277(7)
Ni(1)–P(9)	2.1740(7)	2.1697(7)	Ni(1)–P(13)	2.1654(7)	2.1775(7)
S(1)–C(2)	1.722(3)	1.716(3)	C(2)–N(4)	1.300(3)	1.309(3)
C(2)–S(3)	1.721(3)	1.717(3)	C(6)–C(7)	1.305(5)	1.311(5)
S(1)–Ni(1)–S(3)	79.45(3)	79.21(3)	S(1)–Ni(1)–P(9)	172.64(3)	172.16(3)
S(1)–Ni(1)–P(13)	92.47(3)	93.26(3)	S(3)–Ni(1)–P(9)	93.81(3)	93.01(3)
S(3)–Ni(1)–P(13)	169.03(3)	169.67(3)	P(9)–Ni(1)–P(13)	93.81(3)	94.33(3)
S(1)–C(2)–S(3)	111.22(14)	111.65(15)			

Table 2. Selected bond lengths (Å) and angles (°) for the two crystallographically independent cationic complexes (A and B) present in the crystals of **39**.

$[Ni(S_2CNC_4H_6)(dppp)]PF_6$ (**39**) crystallized with two independent cation:anion pairs (A and B) in the asymmetric unit, complex cation A is shown in *Fig. 35* and complex cation B is shown in *Fig. S1*. The geometry at the nickel centre is distorted square planar with P(13) lying ca. 0.22 Å [0.25 Å] out of the {Ni,S(1),S(3),P(9)} plane, the atoms of which are coplanar to within ca. 0.04 Å [0.01 Å] (the values in square parentheses refer to cation B). One interesting oddity of the two independent cations is that in **39-B** the two Ni–S bonds are the same [2.2286(7) and 2.2277(7) Å], but in **39-A** they are statistically significantly different [2.2158(7) and 2.2300(7) Å]; it is the bond to S(1) that is anomalously short. There is no obvious reason why the bonding should be different between the two independent complexes. The bite angle of the dithiocarbamate ligand, S(1)–Ni(1)–S(3), is 79.45(3)° and 79.21(3)° for the two independent molecules in the structure are close to that of 79.68(7)° for $[Ni(S_2CNC_4H_8NH_2)(dppp)]^{2+}$. The C(6)C(7) distances of 1.305(5) Å and 1.311(5) Å are consistent with the presence of a double bond.

Crystal data for **39**: $[C_{32}H_{32}NNiP_2S_2](PF_6)\cdot 1.75CHCl_3$, M = 969.22, triclinic, P-1 (no. 2), a = 13.7545(4), b = 15.2829(3), c = 20.3044(4) Å, α = 92.0086(14), β = 102.8560(19), γ = 98.9786(18)°, V = 4099.38(17) $Å^3$, Z = 4 (two independent complexes), D_c = 1.570 g cm^{-3}, μ(Mo-Kα) = 1.089 mm^{-1}, T = 173 K, orange prisms, Oxford Diffraction Xcalibur 3 diffractometer; 24642 independent measured reflections (R_{int} = 0.0173), F^2 refinement, R_1(obs) = 0.0381, wR_2(all) = 0.0980, 16353 independent observed absorption-corrected reflections [$|F_o| > 4\sigma(|F_o|)$, $2\theta_{max}$ = 64°], 1064 parameters. CCDC 768228.

All structures were refined using the SHELXTL and SHELX-97 program systems.[214]

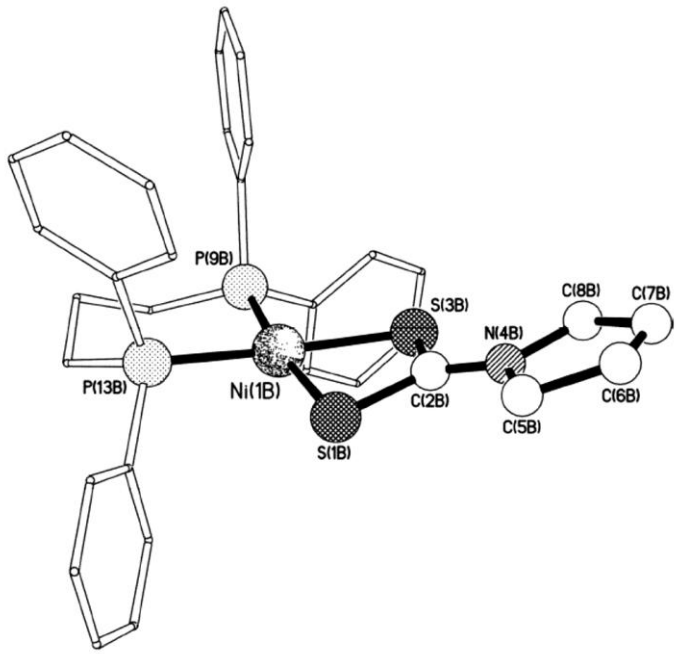

Figure S1. $[Ni(S_2CNC_4H_6)(dppp)]PF_6$ (**39**) complex cation B

10.2. Chapter 4: Gold(I) dithiocarbamate complexes

10.2.1. *Crystal data for compounds* $[(Ph_3P)Au\{S_2CN(CH_2CH{=}CH_2)_2\}]$ (43) *and* $[Au_2\{S_2CN(CH_2CH{=}CH_2)_2\}_2]$ (51):

Crystals of compounds **43** and **51** were grown by vapour diffusion of diethyl ether onto a dichloromethane solution of the complex in each case. Data were collected using an Oxford Diffraction Xcalibur 3 diffractometer, and the structures were refined based on F^2 using the SHELXTL and SHELX-97 program systems.[214]

Crystal data for **43**: $C_{25}H_{25}AuNPS_2$, M = 631.52, monoclinic, $P2_1/c$ (no. 14), a = 12.94805(15), b = 12.83389(14), c = 14.34358(15) Å, β = 91.0548(10)°, V = 2383.12(5) $Å^3$, Z = 4, D_c = 1.760 g cm^{-3}, μ(Mo-Kα) = 6.428 mm^{-1}, T = 173 K, pale yellow blocks, Oxford Diffraction Xcalibur PX Ultra diffractometer; 8080 independent measured reflections (R_{int} = 0.0237), F^2 refinement, R_1(obs) = 0.0180, wR_2(all) = 0.0328, 6131 independent observed absorption-corrected reflections [$|F_o| > 4\sigma(|F_o|)$, $2\theta_{max}$ = 66°], 272 parameters. CCDC 830717.

Crystal data for **51**: $C_{14}H_{20}Au_2N_2S_4$, M = 738.49, tetragonal, $I4_1/a$ (no. 88), a = b = 18.4430(2), c = 22.9755(3) Å, V = 7815.0(2) $Å^3$, Z = 16, D_c = 2.511 g cm^{-3}, μ(Mo-Kα) = 15.425 mm^{-1}, T = 173 K, yellow needles, Oxford Diffraction Xcalibur 3 diffractometer; 6882 independent measured reflections (R_{int} = 0.0376), F^2 refinement, R_1(obs) = 0.0242, wR_2(all) = 0.0494, 5670 independent observed absorption-corrected reflections [$|F_o| > 4\sigma(|F_o|)$, $2\theta_{max}$ = 66°], 209 parameters. CCDC 830718.

10.3. Chapter 5: Dithiocarboxylate complexes

10.3.1. *Crystal data for compounds* $[Ru(CH{=}CHC_6H_4Me\text{-}4)(\kappa^2\text{-}S_2C{\bullet}IPr)(CO)(PPh_3)_2]PF_6$ (55) *and* $[Ru(C(C{\equiv}CPh){=}CHPh)(\kappa^2\text{-}S_2C{\bullet}ICy)(CO)(PPh_3)_2]PF_6$ (58):

Crystals of compounds **55** and **58** were grown by vapour diffusion of diethyl ether into a dichloromethane solution of the complex. Single crystal X-ray data for complex **55** (CCDC 801405) were collected using monochromated Mo-Kα radiation (λ = 0.71073 Å) on an Oxford Diffraction Xcalibur 3 instrument (*Table 3*). The diffractometer was equipped with an Oxford Instruments Cryojet XL liquid nitrogen cooling device and the data were collected at 173 K. A series of ω-scans were performed to collect the unique monoclinic data to a resolution of 0.7 Å. Cell parameters and intensity data for compound **55** were processed using CrysAlis Pro version 1.171.34.36.[215] The

structure was solved by direct methods and refined by full-matrix least-squares based on F^2 using the SHELXTL and SHELX-97 program systems.[214] An analytical numeric absorption correction was applied using a multifaceted crystal model based on expressions derived by Clark and Reid.[216]

Single crystal diffraction data for complex **58** (CCDC 801406) were collected using an Enraf-Nonius KappaCCD diffractometer (Mo-Kα radiation (λ = 0.71073 Å) at 150(2) K equipped with an Oxford Cryosystems Cryostream N_2 open-flow cooling device,[217] and processed using the DENZO-SMN package,[218] including unit cell parameter refinement and inter-frame scaling, which was carried out using SCALEPACK within DENZO-SMN (*Table 3*). The structure was solved using SIR92[219] and refinement was carried out using full-matrix least-squares within the CRYSTALS suite,[220] on *F*. All non-hydrogen atoms were refined with anisotropic displacement parameters, however, vibrational restraints were required to ensure sensible atomic displacement ellipsoids. From examination of the difference Fourier map, it was clear that there were two molecules of diethyl ether. Enlarged ADPs for one of these suggested the possibility of partial occupancy, however, refinement of the occupancy and careful examination of the difference Fourier using MCE[221] suggested that this was not the case. Hydrogen atoms were generally visible in the difference map and their positions and isotropic displacement parameters were treated in the usual manner (refinement using restraints prior to inclusion into the model with riding constraints).[222]

compound	**55**	**58**
chemical formula	$[C_{56}H_{55}N_2OP_2RuS_2](PF_6)$	$[C_{69}H_{65}N_2OP_2RuS_2](PF_6)$
Solvent	1.75 CH_2Cl_2	2 $C_4H_{10}O$
Fw	1292.74	1458.64
T (°C)	–100	–123
space group	$P2_1/c$ (no. 14)	$P2_1/c$ (no. 14)
a (Å)	12.45635(19)	11.6709(2)
b (Å)	37.8723(4)	15.6018(3)
c (Å)	13.4521(2)	39.4957(8)
β (deg)	111.2767(18)	93.1372(8)
V ($Å^3$)	5913.48(16)	7180.9(2)
Z	4	4
D_{calcd} (g cm^{-3})	1.452	1.349
λ (Å)	0.71073	0.71073
μ (mm^{-1})	0.635	0.408
$\rho_{min,max}$	–1.709, 0.731	–0.68, 0.96
R_1(obs)[a]	0.0574	0.0618
wR_2(all)[b]	0.1191	0.0764

[a] $R_1 = \sum||F_o| - |F_c||/\sum|F_o|$. [b] $wR_2 = \{\sum[w(F_o^2 - F_c^2)^2] / \sum[w(F_o^2)^2]\}^{1/2}$; $w^{-1} = \sigma^2(F_o^2) + (aP)^2 + bP$.

Table 3. Crystallographic Data for Compounds **55** and **58**.

10.3.2. *Crystal data for compounds* **[(Ph$_3$P)Au(S$_2$C•IMes)]PF$_6$** (**67**), **[(Ph$_3$P)Au(S$_2$C•IDip)]PF$_6$** (**68**), **[(IDip)Au(S$_2$C•IPr)]PF$_6$** (**72**) and **[(IDip)Au(S$_2$C•IMes)]PF$_6$** (**73**):

Table 4 provides a summary of the crystallographic data for compounds **67**, **68**, **72** and **73**. The data were collected using Oxford Diffraction Xcalibur 3 (**67** and **68**) and PX Ultra (**72** and **73**) diffractometers, and the structures were refined based on F^2 using the SHELXTL and SHELX-97 program systems.[214] The absolute structures of **67** and **68** were determined by a combination of R-factor tests [for 2, $R_1^+ = 0.027$, $R_1^- = 0.070$; for 3, $R_1^+ = 0.021$, $R_1^- = 0.066$] and by use of the Flack parameter [for 2, $x^+ = 0.000(3)$; for 3, $x^+ = 0.0000(18)$]. The absolute structure of **73** was shown to be a partial polar twin by a combination of R-factor tests [$R_1^+ = 0.032$, $R_1^- = 0.041$] and by use of the Flack parameter [$x^+ = 0.319(6)$, $x^- = 0.681(6)$]. CCDC 745830 to 745833.

data	**67**	**68**	**72**	**73**
formula	$[C_{40}H_{39}AuN_2PS_2](PF_6)$	$[C_{46}H_{51}AuN_2PS_2](PF_6)$	$[C_{37}H_{52}AuN_4S_2](PF_6)$	$[C_{49}H_{60}AuN_4S_2](PF_6)$
solvent	$0.55CH_2Cl_2 \cdot 0.45Et_2O$	Et_2O	—	CH_2Cl_2
Fw	1064.82	1143.03	958.88	1195.99
T (°C)	–100	–100	–100	–100
space group	$P2_12_12_1$ (no. 19)	$P2_1$ (no. 4)	$P2_1/n$ (no. 14)	Iba2 (no. 45)
a (Å)	13.11504(16)	10.65689(11)	13.39748(6)	16.89890(8)
b (Å)	13.99608(18)	13.57473(13)	13.32238(6)	31.95473(15)
c (Å)	24.7953(3)	18.59207(17)	23.37032(12)	19.98864(11)
α (deg)	—	—	—	—
β (deg)	—	101.3289(9)	100.4298(5)	—
γ (deg)	—	—	—	—
V (Å^3)	4551.41(10)	2637.21(5)	4102.36(3)	10793.86(9)
Z	4	2	4	8
ρ_{calcd} (g cm^{-3})	1.554	1.439	1.553	1.472

λ (Å)	0.71073	0.71073	1.54184	1.54184
μ (mm^{-1})	3.516	2.986	8.557	7.517
R_1(obs) [a]	0.027	0.021	0.030	0.028
wR_2(all) [b]	0.055	0.033	0.080	0.074

[a] $R_1 = \Sigma||F_o| - |F_c||/\Sigma|F_o|$. [b] $wR_2 = \{\Sigma[w(F_o^2 - F_c^2)^2] / \Sigma[w(F_o^2)^2]\}$

$^{1/2}$; $w^{-1} = \sigma^2(F_o^2) + (aP)^2 + bP$.

Table 4. Crystallographic Data for compounds **67**, **68**, **72** and **73**.

10.4. Chapter 6: Dialkyldithiophosphate complexes

10.4.1. *Crystal data for* [Ru(CH=CHCPh$_2$OH){κ^2-S$_2$P(OEt)$_2$}(CO)(PPh$_3$)$_2$] (87):

Crystals of compound **87** were grown by slow diffusion of ethanol into a dichloromethane solution of the complex. Data were collected using an Oxford Diffraction Xcalibur 3 diffractometer, and the structures were refined based on F^2 using the SHELXTL and SHELX-97 program systems.[214] Crystal data for **87**: $C_{56}H_{53}O_4P_3RuS_2 \cdot CH_2Cl_2$, M = 1133.01, triclinic, P-1 (no. 2), a = 10.4330(3), b = 14.2442(3), c = 18.2189(5) Å, α = 80.194(2), β = 84.401(3), γ = 87.677(2)°, V = 2654.43(12) Å^3, Z = 2, D_c = 1.418 g cm^{-3}, μ(Cu-Kα) = 5.269 mm^{-1}, T = 173 K, pale yellow tablets, Oxford Diffraction Xcalibur PX Ultra diffractometer; 10267 independent measured reflections (R_{int} = 0.0332), F^2 refinement, R_1(obs) = 0.0356, wR_2(all) = 0.0925, 9052 independent observed absorption-corrected reflections [$|F_o| > 4\sigma(|F_o|)$, $2\theta_{max}$ = 145°], 652 parameters. CCDC 834118.

10.4.2. *Signer measurement for* [Ru(η^3-PhC≡C-C=CHPh){κ^2-S$_2$P(OEt)$_2$}(CO)(PPh$_3$)]$_2$ (92):

The Signer apparatus for molecular weight determination:[183, 223]

The apparatus is shown below. Similar masses (10 mg) of the complex to be examined (‘unknown’) and a standard were weighed (to 4 decimal places) and dissolved, separately, in dichloromethane (~2-

3 mL). These solutions were introduced to the separate bulbs of the apparatus and the taps closed. One valve was then attached to the Schlenk line and a very slight vacuum created. The apparatus was placed in a warm place and left undisturbed while the vapour pressures equilibrated through the glass frit connecting the bulbs. To make the measurement, the apparatus was rotated so that the solvent filled the arms, and the heights from the sealed end in both arms were determined. The heights of the solvent in the two arms were proportional to the volume of solution. Readings were taken over a two day period until the measurements stabilised.

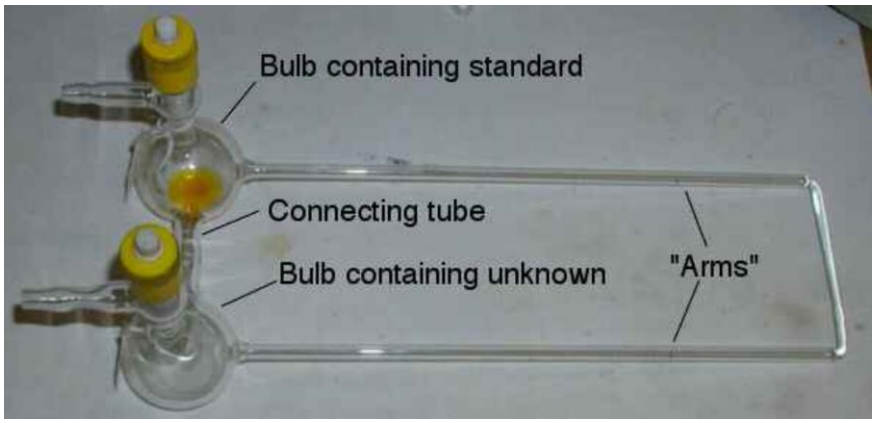

Ferrocene (M_w = 186.03) is typically used as a standard, however, the standard should ideally have a similar molecular weight to the unknown being determined. For this reason, Vaska's complex (M_w =780.25) was used for the determinations in this work. The stability of the standard in CD_2Cl_2 was confirmed by ^{31}P NMR spectroscopy over a period of days.

The molecular weight is then given by:

$$M_x = \frac{(m_x)(M_s)(h_s)}{(m_s)(h_x)}$$

Where:

M_x and M_s are the molar masses of the unknown and of the standard.

m_x and m_s are the masses of the unknown and of the standard used in the experiment.

h_x and h_s are the heights of the unknown and standard solutions in the arms.

10.5. Chapter 7: Multimetallic complexes based on nitrogen-oxygen mixed-donor ligands

10.5.1. *Crystal data for* [Ru(C(C≡CPh)=CHPh)($O_2CC_5H_4N$)(CO)(PPh_3)$_2$] (98):

Crystals of compounds **98** were grown by slow diffusion of ethanol into a dichloromethane solution of the complex. Data were collected using an Oxford Diffraction Xcalibur 3 diffractometer, and the structures were refined based on F^2 using the SHELXTL and SHELX-97 program systems.[214] Crystal data for **103**: $C_{59}H_{45}NO_3P_2Ru$, M = 978.97, monoclinic, $P2_1/n$, a = 18.67558(18), b = 13.24963(15), c = 19.20324(19) Å, α = 90, β = 95.2130(9)°, γ = 90°, V = 4732.08(8) Å^3, Z = 4, D_c = 1.374 mg m^{-3}, μ(Mo-Kα) = 0.447 mm^{-1}, T = 173 K, yellow prisms, Oxford Diffraction Xcalibur 3 Ultra diffractometer; 16065 independent measured reflections (R_{int} = 0.0337), F^2 refinement, R_1(obs) = 0.0493, wR_2(all) = 0.0870, 12963 independent observed absorption-corrected reflections [$|F_o| > 4\sigma(|F_o|)$, $2\theta_{max}$ = 33°], 595 parameters. CCDC 859598.

11: References

11. References

1. G. Hogarth, *Prog. Inorg. Chem.*, 2005, **53**, 71-561.
2. D. Coucouvanis, *Prog. Inorg. Chem.*, 1979, **26**, 301-469.
3. E. R. T. Tiekink and I. Haiduc, in *Prog. Inorg. Chem.*, John Wiley & Sons, Inc., Editon edn., 2005, pp. 127-319.
4. C. G. Young, S. A. Roberts and J. H. Enemark, *Inorg. Chim. Acta*, 1986, **114**, L7-L8.
5. E. J. Fernández, J. M. López-de-Luzuriaga, M. Monge, E. Olmos, M. C. Gimeno, A. Laguna and P. G. Jones, *Inorg. Chem.*, 1998, **37**, 5532-5536.
6. E. J. Fernández, J. M. López-de-Luzuriaga, M. Monge, E. Olmos, A. Laguna, M. D. Villacampa and P. G. Jones, *J. Cluster Sci.*, 2000, **11**, 153-167.
7. J. Stary, *The Solvent Extraction of Metal Chelates*, 1964, 155.
8. G. Schwedt, *Chromatographia*, 1979, **12**, 613-619.
9. P. C. Uden and I. E. Bigley, *Anal. Chim. Acta*, 1977, **94**, 29-34.
10. M. L. Riekkola, *Fin. Chem. Lett.*, 1980, 83-86.
11. M. L. Riekkola, *Mikrochim. Acta*, 1982, **1**, 327-334.
12. http://www.tut.fi/plastics/tyreschool/moduulit/moduuli_4/hypertext_2/2/2_3.html.
13. http://www.inchem.org/documents/jmpr/jmpmono/v070pr12.htm.
14. http://www.inchem.org/documents/pds/pds/pest94_e.htm.
15. V. Milacic, D. Chen, L. Ronconi, K. R. Landis-Piwowar, D. Fregona and Q. P. Dou, *Cancer Res.*, 2006, **66**, 10478-10486.
16. M. M. Jones, L. T. Burka, M. E. Hunter, M. Basinger, G. Campo and A. D. Weaver, *J. Inorg. Nucl. Chem.*, 1980, **42**, 775-778.
17. M. Delépine, *C. R. Chim*, 1907, **144**, 1125.
18. A. M. Bond and R. L. Martin, *Coord. Chem. Rev.*, 1984, **54**, 23-98.
19. J. D. E. T. Wilton-Ely, D. Solanki, E. R. Knight, K. B. Holt, A. L. Thompson and G. Hogarth, *Inorg. Chem.*, 2008, **47**, 9642-9653.
20. E. R. Knight, A. R. Cowley, G. Hogarth and J. D. E. T. Wilton-Ely, *Dalton Trans.*, 2009, 607-609.
21. J. Cookson and P. D. Beer, *Dalton Trans.*, 2007, 1459-1472.
22. A. J. Arduengo, R. L. Harlow and M. Kline, *J. Am. Chem. Soc.*, 1991, **113**, 361-363.
23. J. Huang, E. D. Stevens, S. P. Nolan and J. L. Petersen, *J. Am. Chem. Soc.*, 1999, **121**, 2674-2678.
24. M. Scholl, S. Ding, C. W. Lee and R. H. Grubbs, *Org. Lett.*, 1999, **1**, 953-956.
25. H. G. Raubenheimer and S. Cronje, *Chem. Soc. Rev.*, 2008, **37**, 1998-2011.
26. A. Tudose, A. Demonceau and L. Delaude, *J. Organomet. Chem.*, 2006, **691**, 5356-5365.

27. L. Delaude, A. Demonceau and J. Wouters, *Eur. J. Inorg. Chem.*, 2009, 1882-1891.
28. L. Delaude, X. Sauvage, A. Demonceau and J. Wouters, *Organometallics*, 2009, **28**, 4056-4064.
29. L. L. Borer, J. V. Kong, P. A. Keihl and D. M. Forkey, *Inorg. Chim. Acta*, 1987, **129**, 223-226.
30. V. K. Jain and V. S. Jakkal, *J. Organomet. Chem.*, 1996, **515**, 81-87.
31. W.-H. Leung, K.-K. Lau, Q.-f. Zhang, W.-T. Wong and B. Tang, *Organometallics*, 2000, **19**, 2084-2089.
32. J. Perez, L. Riera, V. Riera, S. Garcia-Granda, E. Garcia-Rodriguez and D. Miguel, *Chem. Commun.*, 2002, 384-385.
33. W. E. van Zyl, J. M. López-de-Luzuriaga, J. P. Fackler Jr and R. J. Staples, *Can. J. Chem.*, 2001, **79**, 896-903.
34. M. M. Rauhut, H. A. Currier and V. P. Wystrach, *J. Org. Chem.*, 1961, **26**, 5133-5135.
35. I. Haiduc, ed. F. Devillanova, RSC Publishing, The Royal Society of Chemistry, London, Editon edn., 2007, vol. Handbook of Chalcogen Chemistry. New Perspectives in Sulfur, Selenium and Tellurium, pp. 593-643.
36. W. Tuszynski, J. Molenda and M. Makowska, *Tribol. Lett.*, 2002, **13**, 103-109.
37. A. I. Busev and M. Ivanyutin, I, *Tr. Kom. Anal. Kh. Akad. Nauk*, 1960, **11**, 172-191.
38. H. Bode and W. Arnswald, *Fresenius J. Anal. Chem.*, 1962, **185**, 179-201.
39. K. Hayashi, Y. Sasaki, S. Tagashira, Y. Murakami and T. Suehiro, *Anal. Sci.*, 1987, **3**, 55-57.
40. A. D. Adler, F. R. Longo, F. Kampas and J. Kim, *J. Inorg. Nucl. Chem.*, 1970, **32**, 2443-2445.
41. G. J. Bridger, S. P. Fricker, M. J. Abrams and I. Mayers, in *U.S. Pat. Appl. Publ*, Editon edn., 2002, vol. US 20020193363 A1 20021219.
42. F. Faraone and V. Marsala, *Inorg. Chim. Acta*, 1976, **17**, 217-220.
43. V. K. Jain, *Transition Met. Chem.*, 1993, **18**, 312-314.
44. P. U. Jain, P. Munshi, M. G. Walawalkar, S. P. Rath, K. K. Rajak and G. K. Lahiri, *Polyhedron*, 2000, **19**, 801-808.
45. S. W. Ng, *Acta Crystallogr. E*, 2002, **58**, m18-m19.
46. E. P. L. Tay, S. L. Kuan, W. K. Leong and L. Y. Goh, *Inorg. Chem.*, 2007, **46**, 1440-1450.
47. A. Deeming, C. Forth and G. Hogarth, *Transition Met. Chem.*, 2006, **31**, 42-45.
48. www.britishmuseum.org.
49. M.-C. Daniel and D. Astruc, *Chem. Rev.*, 2003, **104**, 293-346.
50. D. H. Brown and W. E. Smith, *Chem. Soc. Rev.*, 1980, **9**, 217-240.
51. M. Faraday, *Phil. Trans. R. Soc. Lond.*, 1857, **147**.
52. M. Faraday, ed., *Faraday's Diary*, 1932.
53. J. Turkevich, P. C. Stevenson and J. Hillier, *Discussions of the Faraday Society*, 1951, **11**.

54. G. Frens, *Nature: Physical Science*, 1973, **241**, 20-22.
55. T. Yonezawa and T. Kunitake, *Colloids Surf., A*, 1999, **149**, 193-199.
56. A. Ulman, *Chem. Rev.*, 1996, **96**, 1533-1554.
57. M. Giersig and P. Mulvaney, *Langmuir*, 1993, **9**, 3408-3413.
58. M. Brust, M. Walker, D. Bethell, D. J. Schiffrin and R. Whyman, *J. Chem. Soc., Chem. Commun.*, 1994, 801-802.
59. M. Brust, J. Fink, D. Bethell, D. J. Schiffrin and C. Kiely, *J. Chem. Soc., Chem. Commun.*, 1995, 1655-1656.
60. B. L. V. Prasad, C. M. Sorensen and K. J. Klabunde, *Chem. Soc. Rev.*, 2008, **37**, 1871-1883.
61. M. J. Hostetler, A. C. Templeton and R. W. Murray, *Langmuir*, 1999, **15**, 3782-3789.
62. A. C. Templeton, W. P. Wuelfing and R. W. Murray, *Acc. Chem. Res.*, 1999, **33**, 27-36.
63. T. Nakaya, Y.-J. Li and K. Shibata, *J. Mater. Chem.*, 1996, **6**, 691-697.
64. A. Labande, J. Ruiz and D. Astruc, *J. Am. Chem. Soc.*, 2002, **124**, 1782-1789.
65. M. Bartz, J. Küther, R. Seshadri and W. Tremel, *Angew. Chem. Int. Ed.*, 1998, **37**, 2466-2468.
66. Z. Wang, R. Lévy, D. G. Fernig and M. Brust, *Bioconjugate Chem.*, 2005, **16**, 497-500.
67. T. Belser, M. Stöhr and A. Pfaltz, *J. Am. Chem. Soc.*, 2005, **127**, 8720-8731.
68. A. Labande and D. Astruc, *Chem. Commun.*, 2000, 1007-1008.
69. P. D. Beer, D. P. Cormode and J. J. Davis, *Chem. Commun.*, 2004, 414-415.
70. M. Ito, T. Tsukatani and H. Fujihara, *J. Mater. Chem.*, 2005, **15**, 960-964.
71. B. I. Ipe, K. Yoosaf and K. G. Thomas, *J. Am. Chem. Soc.*, 2006, **128**, 1907-1913.
72. O. Tzhayik, P. Sawant, S. Efrima, E. Kovalev and J. T. Klug, *Langmuir*, 2002, **18**, 3364-3369.
73. L. A. Porter, D. Ji, S. L. Westcott, M. Graupe, R. S. Czernuszewicz, N. J. Halas and T. R. Lee, *Langmuir*, 1998, **14**, 7378-7386.
74. Y. Zhao, W. Pérez-Segarra, Q. Shi and A. Wei, *J. Am. Chem. Soc.*, 2005, **127**, 7328-7329.
75. J. Sharma, R. Chhabra, H. Yan and Y. Liu, *Chem. Commun.*, 2008, 2140-2142.
76. Z. Li, R. Jin, C. A. Mirkin and R. L. Letsinger, *Nucleic Acids Res.*, 2002, **30**, 1558-1562.
77. J. M. Wessels, H.-G. Nothofer, W. E. Ford, F. von Wrochem, F. Scholz, T. Vossmeyer, A. Schroedter, H. Weller and A. Yasuda, *J. Am. Chem. Soc.*, 2004, **126**, 3349-3356.
78. M. S. Vickers, J. Cookson, P. D. Beer, P. T. Bishop and B. Thiebaut, *J. Mater. Chem.*, 2006, **16**, 209-215.
79. E. R. Knight, N. H. Leung, Y. H. Lin, A. R. Cowley, D. J. Watkin, A. L. Thompson, G. Hogarth and J. D. E. T. Wilton-Ely, *Dalton Trans.*, 2009, 3688-3697.
80. H. Arora and R. Mukherjee, *New J. Chem.*, 2010, **34**, 2357-2365.
81. C. Janiak, *Dalton Trans.*, 2003, 2781-2804.
82. H. Li, M. Eddaoudi, M. O'Keeffe and O. M. Yaghi, *Nature*, 1999, **402**, 276-279.
83. J. R. Long and O. M. Yaghi, *Chem. Soc. Rev.*, 2009, **38**, 1213-1214.

84. C. Janiak and J. K. Vieth, *New J. Chem.*, 2010, **34**, 2366-2388.
85. J. Y. Lu and K. A. Runnels, *Inorg. Chem. Commun.*, 2001, **4**, 678-681.
86. J. Sun, L. Weng, Y. Zhou, J. Chen, Z. Chen, Z. Liu and D. Zhao, *Angew. Chem. Int. Ed.*, 2002, **41**, 4471-4473.
87. Y. Kang, Y.-G. Yao, Y.-Y. Qin, J. Zhang, Y.-B. Chen, Z.-J. Li, Y.-H. Wen, J.-K. Cheng and R.-F. Hu, *Chem. Commun.*, 2004, 1046-1047.
88. M. Athar, A. M. Qureshi, M. Najam-ul-haq, G. Li, Z. Shi and S. Feng, *J. Chem. Soc. Pak*, 2012, **34**.
89. M. Koberl, M. Cokoja, W. A. Herrmann and F. E. Kuhn, *Dalton Trans.*, 2011, **40**, 6834-6859.
90. J. Hansen and H. M. L. Davies, *Coord. Chem. Rev.*, 2008, **252**, 545-555.
91. K. Biradha, M. Sarkar and L. Rajput, *Chem. Commun.*, 2006, 4169-4179.
92. W. Yang, X. Lin, A. J. Blake, C. Wilson, P. Hubberstey, N. R. Champness and M. Schröder, *Inorg. Chem.*, 2009, **48**, 11067-11078.
93. B. Chen, N. W. Ockwig, A. R. Millward, D. S. Contreras and O. M. Yaghi, *Angew. Chem. Int. Ed.*, 2005, **44**, 4745-4749.
94. A. R. Millward and O. M. Yaghi, *J. Am. Chem. Soc.*, 2005, **127**, 17998-17999.
95. D. Britt, D. Tranchemontagne and O. M. Yaghi, *Proc. Natl. Acad. Sci. U S A*, 2008, **105**, 11623-11627.
96. H. Wu, W. Zhou and T. Yildirim, *J. Am. Chem. Soc.*, 2009, **131**, 4995-5000.
97. B. Mu, P. M. Schoenecker and K. S. Walton, *J. Physical Chem. C*, 2010, **114**, 6464-6471.
98. S. Herrero, R. Jimenez-Aparicio, J. Perles, J. L. Priego and F. A. Urbanos, *Green Chem.*, 2010, **12**, 965-967.
99. M. Ranocchiari and J. A. van Bokhoven, *PCCP*, 2011, **13**, 6388-6396.
100. A. Pichon and S. L. James, *Cryst. Eng. Comm*, 2008, **10**, 1839-1847.
101. P. Teo, L. L. Koh and T. S. A. Hor, *Inorg. Chem.*, 2008, **47**, 6464-6474.
102. F. Wang, Y.-X. Tan, H. Yang, H.-X. Zhang, Y. Kang and J. Zhang, *Chem. Commun.*, 2011, **47**, 5828-5830.
103. D. Vasil'chenko, A. Venediktov, E. Filatov, I. Baidina, P. Plyusnin and S. Korenev, *Russ. J. Coord. Chem.*, 2011, **37**, 48-56.
104. J. H. Han, B. G. Kim and K. S. Min, *Acta Crystallogr. E*, 2008, **E64**, m366.
105. S. Naeem, E. Ogilvie, A. J. P. White, G. Hogarth and J. D. E. T. Wilton-Ely, *Dalton Trans.*, 2010, **39**, 4080-4089.
106. S. Naeem, A. J. P. White, G. Hogarth and J. D. E. T. Wilton-Ely, *Organometallics*, 2010, **29**, 2547-2556.
107. B. J. McCormick and R. I. Kaplan, *Can. J. Chem.*, 1970, **48**, 1876-1880.
108. G. Hogarth, E.-J. C. R. C. R. Rainford-Brent, S. E. Kabir, I. Richards, J. D. E. T. Wilton-Ely and Q. Zhang, *Inorg. Chim. Acta*, 2009, **362**, 2020-2026.

109. J. D. E. T. Wilton-Ely, D. Solanki and G. Hogarth, *Eur. J. Inorg. Chem.*, 2005, **2005**, 4027-4030.
110. Y. H. Lin, N. H. Leung, K. B. Holt, A. L. Thompson and J. Wilton-Ely, *Dalton Trans.*, 2009, 7891-7901.
111. B. P. Sullivan and T. J. Meyer, *Inorg. Chem.*, 1982, **21**, 1037-1040.
112. A. Dobson, D. S. Moore, S. D. Robinson, M. B. Hursthouse and L. New, *Polyhedron*, 1985, **4**, 1119-1130.
113. P. Bishop, P. Marsh, A. K. Brisdon, B. J. Brisdon and M. F. Mahon, *J. Chem. Soc.-Dalton Trans.*, 1998, 675-682.
114. M. K. Whittlesey, ed., *Comprehensive Organometallic Chemistry III*, Elsevier: Oxford, U.K., 2006.
115. M. R. Torres, A. Vegas, A. Santos and J. Ros, *J. Organomet. Chem.*, 1986, **309**, 169-177.
116. M. R. Torres, A. Vegas, A. Santos and J. Ros, *J. Organomet. Chem.*, 1987, **326**, 413-421.
117. J. C. Cannadine, A. F. Hill, A. J. P. White, D. J. Williams and J. D. E. T. Wilton-Ely, *Organometallics*, 1996, **15**, 5409-5415.
118. G. Jia, W. Wan Fung, R. C. Y. Yeung and H. P. Xia, *J. Organomet. Chem.*, 1997, **539**, 53-59.
119. M. C. J. Harris and A. F. Hill, *Organometallics*, 1991, **10**, 3903-3906.
120. A. F. Hill, ed., *Comprehensive Organometallic Chemistry II*, Pergamon Press, Oxford, UK,, 1995.
121. H. Loumrhari, J. Ros and M. R. Torres, *Polyhedron*, 1991, **10**, 421-427.
122. J. M. Martín-Alvarez, F. Hampel, A. M. Arif and J. A. Gladysz, *Organometallics*, 1999, **18**, 955-957.
123. J. Lokaja, V. Kettmannb, F. Pavelčíkb, V. Vrábela and J. Garaja, *Collect. Czech. Chem. Commun.*, 1982, **47**, 2633-2638.
124. E. Kello, J. Lokaj and V. Vrabel, *Collect. Czech. Chem. Commun.*, 1992, **57**, 332-338.
125. J. Lokaj, F. Pavelčik, V. Kettmann, J. Masaryk, V. Vrábel and J. Garaj, *Acta Crystallogr. B*, 1981, **37**, 926-928.
126. E. Kellöa, V. Kettmannb and J. Garaja, *Collect. Czech. Chem. Commun.*, 1984, **49**, 2210-2221.
127. O. Kazuyuki and K. Shinichi, *J. Photopolym. Sci. Technol.*, 1995, **8**, 365-368.
128. M. J. B and B. J. L, *Synth. React. Inorg. Met.-Org. Nano-met. Chem.*, 1985, **15**, 223-233.
129. K. C. Nicolaou, P. G. Bulger and D. Sarlah, *Angew. Chem. Int. Ed.*, 2005, **44**, 4490-4527.
130. S. J. Connon, M. Rivard, M. Zaja and S. Blechert, *Adv. Synth. Catal.*, 2003, **345**, 572-575.
131. Q. Yang, W.-J. Xiao and Z. Yu, *Org. Lett.*, 2005, **7**, 871-874.
132. D. Fuentes-Alemán, R.-A. Toscano, M. Muñoz-Hernández, M. López-Cardoso, P. G. y. García and R. Cea-Olivares, *J. Organomet. Chem.*, 2008, **693**, 3166-3170.

133. M. J. Macgregor, G. Hogarth, A. L. Thompson and J. D. E. T. Wilton-Ely, *Organometallics*, 2008, **28**, 197-208.
134. S.-Y. Yu, Z.-X. Zhang, E. C.-C. Cheng, Y.-Z. Li, V. W.-W. Yam, H.-P. Huang and R. Zhang, *J. Am. Chem. Soc.*, 2005, **127**, 17994-17995.
135. O. D. Fox, J. Cookson, E. J. S. Wilkinson, M. G. B. Drew, E. J. MacLean, S. J. Teat and P. D. Beer, *J. Am. Chem. Soc.*, 2006, **128**, 6990-7002.
136. J. D. E. T. Wilton-Ely, A. Schier and H. Schmidbaur, *Organometallics*, 2001, **20**, 1895-1897.
137. J. D. E. T. Wilton-Ely, H. Ehlich, A. Schier and H. Schmidbaur, *Helv. Chim. Acta*, 2001, **84**, 3216-3232.
138. J. D. E. T. Wilton-Ely, A. Schier, N. W. Mitzel and H. Schmidbaur, *Inorg. Chem.*, 2001, **40**, 6266-6271.
139. J. D. E. T. Wilton-Ely, A. Schier, N. W. Mitzel, S. Nogai and H. Schmidbaur, *J. Organomet. Chem.*, 2002, **643–644**, 313-323.
140. W. W. Weare, S. M. Reed, M. G. Warner and J. E. Hutchison, *J. Am. Chem. Soc.*, 2000, **122**, 12890-12891.
141. X. Lu, M. S. Yavuz, H.-Y. Tuan, B. A. Korgel and Y. Xia, *J. Am. Chem. Soc.*, 2008, **130**, 8900-8901.
142. J. Vignolle and T. D. Tilley, *Chem. Commun.*, 2009, 7230-7232.
143. T. Selvam and K.-M. Chi, *J. Nanopart. Res.*, 2011, **13**, 1769-1780.
144. D. Cormode, J. Davis and P. Beer, *J. Inorg. Organomet. Polym.*, 2008, **18**, 32-40.
145. E. R. Knight, N. H. Leung, A. L. Thompson, G. Hogarth and J. D. E. T. Wilton-Ely, *Inorg. Chem.*, 2009, **48**, 3866-3874.
146. K. C. Grabar, R. G. Freeman, M. B. Hommer and M. J. Natan, *Anal. Chem.*, 1995, **67**, 735-743.
147. C. Vericat, M. E. Vela, G. Benitez, P. Carro and R. C. Salvarezza, *Chem. Soc. Rev.*, 2010, **39**, 1805-1834.
148. Z. Tang, B. Xu, B. Wu, M. W. Germann and G. Wang, *J. Am. Chem. Soc.*, 2010, **132**, 3367-3374.
149. D. J. Lewis, T. M. Day, J. V. MacPherson and Z. Pikramenou, *Chem. Commun.*, 2006, 1433-1435.
150. F. H. Allen, O. Kennard, D. G. Watson, L. Brammer, A. G. Orpen and R. Taylor, *J. Chem. Soc., Perkin Trans. 2*, 1987, S1-S19.
151. H. Schmidbaur and A. Schier, *Chem. Soc. Rev.*, 2008, **37**, 1931-1951.
152. M. A. Mansour, W. B. Connick, R. J. Lachicotte, H. J. Gysling and R. Eisenberg, *J. Am. Chem. Soc.*, 1998, **120**, 1329-1330.
153. *Based on a search of the Cambridge Structural Database, version 5.32 (May-2011 update).*
154. L. L. Borer, J. Kong and E. Sinn, *Inorg. Chim. Acta*, 1986, **122**, 145-148.

155. S. Naeem, A. L. Thompson, A. J. P. White, L. Delaude and J. D. E. T. Wilton-Ely, *Dalton Trans.*, 2011, **40**, 3737-3747.
156. S. Naeem, A. L. Thompson, L. Delaude and J. D. E. T. Wilton-Ely, *Chem. Eur. J.*, 2010, **16**, 10971-10974.
157. S. Naeem, L. Delaude, A. J. P. White and J. D. E. T. Wilton-Ely, *Inorg. Chem.*, 2010, **49**, 1784-1793.
158. R. B. Bedford and C. S. J. Cazin, *J. Organomet. Chem.*, 2000, **598**, 20-23.
159. Y. H. Lin, N. H. Leung, K. B. Holt, A. L. Thompson and J. D. E. T. Wilton-Ely, *Dalton Trans.*, 2009, 7891-7901.
160. A. C. Hillier, W. J. Sommer, B. S. Yong, J. L. Petersen, L. Cavallo and S. P. Nolan, *Organometallics*, 2003, **22**, 4322-4326.
161. L. Delaude, C. W. Bielawski, D. M. Estes, C. L. Cannon, J. G. Leid, W. J. Youngs, C. M. Crudden and L. Cavallo, *Eur. J. Inorg. Chem.*, 2009, **2009**.
162. A. F. Hill and J. D. E. T. Wilton-Ely, *J. Chem. Soc., Dalton Trans.*, 1998, 3501-3510.
163. J.D.E.T. Wilton-Ely and A. L. Thompson, *Private Communication*.
164. D. J. Cook, K. J. Harlow, A. F. Hill, T. Welton, A. J. P. White and D. J. Williams, *New J. Chem.*, 1998, **22**, 311-314.
165. K. J. Harlow, A. F. Hill, T. Welton, A. J. P. White and D. J. Williams, *Organometallics*, 1998, **17**, 1916-1918.
166. A. L. Hector and A. F. Hill, *J. Organomet. Chem.*, 1993, **447**, C7-C9.
167. F. H. Allen, D. G. Watson, L. Brammer, A. G. Orpen and R. Taylor, eds., *International Tables for Crystallography*, 2006.
168. J. Nakayama, T. Kitahara, Y. Sugihara, A. Sakamoto and A. Ishii, *J. Am. Chem. Soc.*, 2000, **122**, 9120-9126.
169. P. de Frémont, N. M. Scott, E. D. Stevens and S. P. Nolan, *Organometallics*, 2005, **24**, 2411-2418.
170. S. S. Tang, C.-P. Chang, I. J. B. Lin, L.-S. Liou and J.-C. Wang, *Inorg. Chem.*, 1997, **36**, 2294-2300.
171. F. Canales, M. C. Gimeno, P. G. Jones, A. Laguna and C. Sarroca, *Inorg. Chem.*, 1997, **36**, 5206-5211.
172. M. Concepción Gimeno and A. Laguna, *Gold Bull.*, 1999, **32**, 90-95.
173. D. D. Heinrich, J.-C. Wang and J. P. Fackler Jnr, *Acta Crystallogr. C*, 1990, **C46**, 1444–1447.
174. S. Y. Ho and E. R. T. Z. Tiekink, *Z. Kristallogr. - New Cryst. Struct.*, 2004, **219**, 73-74.
175. W. Schneider, A. Bauer and H. Schmidbaur, *Organometallics*, 1996, **15**, 5445-5446.
176. P. Patel, S. Naeem, A. J. P. White and J. D. E. T. Wilton-Ely, *RSC Adv.*, 2012, **2**, 999-1008.
177. A. F. Hill and J. D. E. T. Wilton-Ely, *Organometallics*, 1997, **16**, 4517-4518.

178. A. R. Cowley, A. L. Hector, A. F. Hill, A. J. P. White, D. J. Williams and J. D. E. T. Wilton-Ely, *Organometallics*, 2007, **26**, 6114-6125.
179. X. Liu, Q.-F. Zhang and W.-H. Leung, *J. Coord. Chem.*, 2005, **58**, 1299-1305.
180. A. M. Echavarren, J. Lo´pez, A. Santos and J. Montoya, *J. Organomet. Chem.*, 1991, **414**, 393-400.
181. Y. Wakatsuki, H. Yamazaki, N. Kumegawa, T. Satoh and J. Y. Satoh, *J. Am. Chem. Soc.*, 1991, **113**, 9604-9610.
182. N. W. Alcock, A. F. Hill, R. P. Melling and A. R. Thompsett, *Organometallics*, 1993, **12**, 641-648.
183. E. Clark, *Ind. Eng. Chem. Anal. Ed.*, 1941, **13**, 820-821.
184. J. D. E. T. Wilton-Ely, S. J. Honarkhah, M. Wang, D. A. Tocher and A. M. Z. Slawin, *Dalton Trans.*, 2005, 1930-1939.
185. A. D. Richards and A. Rodger, *Chem. Soc. Rev.*, 2007, **36**, 471-483.
186. H. Lu and X. P. Zhang, *Chem. Soc. Rev.*, 2011, **40**, 1899-1909.
187. C.-M. Che, V. K.-Y. Lo, C.-Y. Zhou and J.-S. Huang, *Chem. Soc. Rev.*, 2011, **40**, 1950-1975.
188. M. Ethirajan, Y. Chen, P. Joshi and R. K. Pandey, *Chem. Soc. Rev.*, 2011, **40**, 340-362.
189. K. S. Suslick, P. Bhyrappa, J. H. Chou, M. E. Kosal, S. Nakagaki, D. W. Smithenry and S. R. Wilson, *Acc. Chem. Res.*, 2005, **38**, 283-291.
190. M. E. Kosal, J.-H. Chou, S. R. Wilson and K. S. Suslick, *Nat. Mater.* , 2002, **1**, 118-121.
191. C. M. Drain, I. Goldberg, I. Sylvain and A. Falber, ed. A. D. Schlüter, Springer Berlin / Heidelberg, Editon edn., 2005, vol. 245, pp. 55-88.
192. S. Lipstman and I. Goldberg, *Acta Crystallogr. C*, 2008, **64**, m53-m57.
193. T. Sato, W. Mori, C. N. Kato, E. Yanaoka, T. Kuribayashi, R. Ohtera and Y. Shiraishi, *J. Catal.*, 2005, **232**, 186-198.
194. E.-Y. Choi, P. M. Barron, R. W. Novotny, H.-T. Son, C. Hu and W. Choe, *Inorg. Chem.*, 2008, **48**, 426-428.
195. O. K. Farha, A. M. Shultz, A. A. Sarjeant, S. T. Nguyen and J. T. Hupp, *J. Am. Chem. Soc.*, 2011, **133**, 5652-5655.
196. C. R. Mayer, E. Dumas and F. Secheresse, *Chem. Commun.*, 2005, 345-347.
197. A. Kaczor, K. Malek and M. Baranska, *J. Physical Chem. C*, 2010, **114**, 3909-3917.
198. N. W. Alcock, A. F. Hill and M. S. Roe, *J. Chem. Soc., Dalton Trans.*, 1990, 1737-1740.
199. A. F. Hill and R. P. Melling, *J. Organomet. Chem.*, 1990, **396**, C22-C24.
200. B. Gómez-Lor, A. Santos, M. Ruiz and Antonio M. Echavarren, *Eur. J. Inorg. Chem.*, 2001, **2001**, 2305-2310.
201. A. W. Rudie, D. W. Lichtenberg, M. L. Katcher and A. Davison, *Inorg. Chem.*, 1978, **17**, 2859-2863.

202. T. Hayashi, M. Konishi, Y. Kobori, M. Kumada, T. Higuchi and K. Hirotsu, *J. Am. Chem. Soc.*, 1984, **106**, 158-163.
203. G. M. Whitesides, J. F. Gaasch and E. R. Stedronsky, *J. Am. Chem. Soc.*, 1972, **94**, 5258-5270.
204. J. A. S. Bomfim, F. P. de Souza, C. A. L. Filgueiras, A. G. de Sousa and M. T. P. Gambardella, *Polyhedron*, 2003, **22**, 1567-1573.
205. A. C. Cope and E. C. Friedrich, *J. Am. Chem. Soc.*, 1968, **90**, 909-913.
206. M. Bruce, E. Horn, J. Matisons and M. Snow, *Aust. J. Chem.*, 1984, **37**, 1163-1170.
207. J. Bailey, *J. Inorg. Nucl. Chem.*, 1973, **35**, 1921-1924.
208. H. Schmidbaur, A. Wohlleben, F. Wagner, O. Orama and G. Huttner, *Chem. Ber.*, 1977, **110**, 1748-1754.
209. D. T. Hill, G. R. Girard, F. L. McCabe, R. K. Johnson, P. D. Stupik, J. H. Zhang, W. M. Reiff and D. S. Eggleston, *Inorg. Chem.*, 1989, **28**, 3529-3533.
210. S. J. Berners-Price and P. J. Sadler, *Inorg. Chem.*, 1986, **25**, 3822-3827.
211. R. Uson, A. Laguna and J. Vicente, *J. Organomet. Chem.*, 1977, **131**, 471-475.
212. D. S. Eggleston, D. F. Chodosh, R. L. Webb and L. L. Davis, *Acta Crystallogr. C*, 1986, **42**, 36-38.
213. G. Hogarth, E.-J. C. R. C. R. Rainford-Brent and I. Richards, *Inorg. Chim. Acta*, 2009, **362**, 1361-1364.
214. *SHELXTL PC, version 5.1, Bruker AXS,Madison, WI, 1997; SHELX-97; G. Sheldrick, Institut Anorg. Chemie, Tammannstr. 4, D37077, Gottingen, Germany, 1998.*
215. O. D. L. CrysAlisPro, Version 1.171.34.36 (release 02- and 08-2010 CrysAlis171.NET) (compiled Aug 2, 13 : 00 : 58).
216. R. C. Clark and J. S. Reid, *Acta Crystallogr. D*, 1995, **51**, 887-897.
217. J. Cosier and A. M. Glazer, *J. Appl. Crystallogr.*, 1986, **19**, 105-107.
218. Z. Otwinowski and W. Minor, in *Methods Enzymol.*, ed. Charles W. Carter, Jr., Academic Press, Editon edn., 1997, vol. Volume 276, pp. 307-326.
219. A. Altomare, G. Cascarano, C. Giacovazzo, A. Guagliardi, M. C. Burla, G. Polidori and M. Camalli, *J. Appl. Crystallogr.*, 1994, **27**, 435.
220. P. W. Betteridge, J. R. Carruthers, R. I. Cooper, K. Prout and D. J. Watkin, *J. Appl. Crystallogr.*, 2003, **36**, 1487.
221. J. Rohlicek and M. Husak, *J. Appl. Crystallogr.*, 2007, **40**, 600-601.
222. R. I. Cooper, A. L. Thompson and D. J. Watkin, *J. Appl. Crystallogr.*, 2010, **43**, 1100-1107.
223. R. Signer, *Liebigs Ann.*, 1930, **478**, 246-266.

12: Abbreviations

12. Abbreviations

ICy	(1,3-dicyclohexyl)imidazolium-2-ylidene
IPr	(1,3-diisopropyl)imidazolium-2-ylidene
IMes	(1,3-dimesityl)imidazolium-2-ylidene
dppf	1,1'-bis(diphenylphosphino)ferrocene
dppm	1,1-Bis(diphenylphosphino)methane
dppa	1,2-bis(diphenylphosphino)acetylene
SIMes	1,3-bis(2,4,6-trimethylphenyl)imidazolium-2-ylidene
IDip	1,3-bis(2,6-diisopropylphenyl)imidazium-2-ylidene
dppp	1,3-bis(diphenylphosphino)propane
dppb	1,4-bis(diphenylphosphino)butane
DBU	1,8-Diazabicyclo[5.4.0]undec-7-ene
p-cymene	1-isopropyl-4-methylbenzene
BTD	2,1,3- benzothiadiazole
OAc	Acetate
bipy	Bipyridine
Cm	Centimetre
COSY	Correlation spectroscopy
DTC	Dithiocarbamate
ESI	Electrospray Ionisation
EDX	Energy Dispersive X-Ray Absorption spectroscopy
FAB	Fast atom bombardment
Fc	Ferrocene
GC	Gas chromatography
Hz	Hertz
HMBC	Heteronuclear multiple-bond correlation spectroscopy
HMQC	Heteronuclear multiple-quantum correlation spectroscopy
HPLC	High-performance liquid chromatography
h	Hour
IR	Infrared
m/z	Mass-to-charge ratio
MHz	Megahertz
MOF	metal-organic framework
Me	Methyl

mg	Milligram
mL	Millilitre
mM	Millimole
min	Minute
NP	Nanoparticle
NHC	N-heterocyclic carbene
NMR	Nuclear Magnetic Resonance
NOESY	Nuclear Overhauser effect spectroscopy
PWC	Paddlewheel complex
Pd-TPP	Palladium tetraphenylporphyrin
ppm	Parts-per-million
ppm	Parts-per-million
(%V_{Bur})	Percentage of buried volume
RCM	Ring-closing metathesis
ROESY	Rotating Frame Nuclear Overhauser effect spectroscopy
SAMs	Self-assembled monolayers
Bu^t	Tertiary butyl
tht	Tetrahydrothiophene
TOAB	Tetraoctylammoniumbromide
TM	Transition metal
TEM	Transmission electron microscopy
TFA	Trifluoroacetic acid
OTf	Trifluoromethanesulfonate